Ion diffusion from Sellafield OPC paste formulations

by

Sandeep Kadam

A thesis submitted in partial fulfilment of the requirements for the degree of

Doctor of Philosophy at the University of Central Lancashire

September 2015

Dedicated in loving memory of Sunita who was a great mum

![uclan University of Central Lancashire]

Student declaration

Concurrent registration for two or more academic awards

I declare that while registered as a candidate for the research degree, I have not been a registered candidate or enrolled student for another award of the University or other academic or professional institution.

Material submitted for another award

I declare that no material contained in the thesis has been used in any other submission for an academic award and is solely my own work.

Signature of Candidate

Sandeep Kadam (M.Sc.)

Type of Award   Doctor of Philosophy

School   School of Forensic and Investigative Sciences

Acknowledgements

First and foremost I would like to extend my deep and sincere gratitude to my supervisory team. Firstly, my Director of Studies, Professor Gary Bond for giving me the opportunity to be a part of UCLan Nuclear Materials Chemistry group to pursue my PhD research, for his constant guidance, encouragement and moral support, I am truly grateful. It has been a distinct privilege to work under the supervision of Professor Harry Eccles. He has been a great inspiration and his critical thinking has contributed tremendously to this project. My sincere thanks also to Professor Glyn Morton for keeping me motivated especially during the challenges of the research process. I could not have imagined a better supervisory team for my PhD research and will always be grateful.

I would like to express my gratitude to the University of Central Lancashire for the award of a research studentship and for providing the research facilities.

Completing a large amount of the sample analysis for this research would not have been possible without the expertise of the technical team. Many thanks to Dr Runjie Moa for BET and SEM/EDAX analysis, Tamar Garcia Sorribes and Jim Donnelly for their assistance in using ICP-MS and Ion Chromatography, Sal Tracey for chemicals and materials required for the experiments.

Thanks also goes to Research Student Registry office, particularly Professor Mike Holmes, Fiona Mair and Clare Altham for their help and support, especially during my time at Westlakes campus in Cumbria. My special thanks to Maddy Buckley (former head of the "I") for being my mentor, encouraging me to engage

Abstract

The disposal of nuclear waste is highly regulated and the disposal option will be dependent on the radionuclide content of the waste. The encapsulation of nuclear waste to prevent migration of radionuclides into the environment and as a safe means of long term storage and disposal can be achieved using ordinary Portland cement (OPC) and various additives such as blast furnace slag (BFS) or pulverised fly ash (PFA). Treated radioactive wastes in this manner are characterised by good thermal, chemical, physical stability and compressive strength. In addition the alkaline chemistry of concrete renders most radionuclides highly insoluble. The ultimate destination of some of these encapsulated wastes is in a Deep Geological Facility (GDF), where for many years the wastes will remain inert to their environment. In the longer-term the environmental conditions will change and the inertness of these waste forms could be affected from the seepage of water into the facility along with microbial activity. The diffusivity or leaching behaviour of cement encapsulated radioactive waste is crucial to ensure the overall safety of a storage/disposal system.

The research presented in this thesis evaluates the diffusivity of strontium, caesium and cobalt when added as inactive forms to BFS:OPC and PFA:OPC formulation as their chlorides and for strontium when added as chloride and carbonate. The cylindrical cement paste samples (CPS) having diameter of 3.2 cm and height 5.3 cm were immersed in re-circulating test solutions consisting of de-ionised water, concentrated Sellafield pore water (CSPW), diluted Sellafield pore water (DSPW) and bacterial inoculated water, John Innes Soil Solution (JISS). Strontium carbonate was selected to determine the influence of a water

insoluble compound on diffusivity of the cation. Freshly cured and aged BFS:OPC samples were also studied to evaluate the impact of carbonation on cation diffusivity. Chloride salts were used, as these would be benign to microorganisms, i.e. would not stimulate or support growth unlike nitrate or sulphate anions. The outcome of this study indicate that the make-up water composition affected the segregation of inherent and added cations in the cement paste samples and also both the bleed water volume and physical characteristics of the cement paste samples. Strontium when added as a soluble salt to the make-up water influenced the rate of diffusivity. Depending on the type of formulation (BFS:OPC, PFA:OPC), a direct correlation was observed between diffusivity of Sr^{2+} and total amount of Ca^{2+} present in the CPS. The rate of diffusivity and the depth of cation diffusion was significantly higher in 3% $SrCl_2$ PFA:OPC having lower concentration of Ca^{2+} compared to its BFS counterpart. The concentration of the added salt to the make-up water also affected the diffusivity. The difference in the diffusivity was observed between closed and open diffusivity system. The solubility limits were not a factor in open circuit which was comparable with the pH values; contrary to the closed circuits. The concentration of cations and anions in the test solution influenced strontium and caesium diffusivity. The diffusivity of sulphate was influenced by the nature of the cation added to the make-up water. Strontium had the greatest effect on lowering the diffusion primarily due to the formation of sparingly soluble strontium sulphate. The pH values of the circulating JISS test solutions from all the contaminated cement samples were lower in comparison with control, which was comparable with viable population in the circulating system. There was no significant viable

population measured in the JISS from control CPS. The JISS test solution composition retard strontium diffusivity but accelerated caesium diffusion in comparison with distilled water values, this retardation could be due to the inherent sulphate content (≈8600 ppb) of the JISS test solution.

This work provides fundamental understanding of the physic-chemical factors influencing the diffusivity of cations from BFS:OPC and PFA:OPC formulations. The scheme i.e. closed circuit recirculation adopted in this research would be more fitting of the real situation i.e. stagnation followed by percolation and therefore diffusivity of ions will be greatly influenced by the test solution chemistry and composition.

Table of contents

Chapter 1: Introduction

Chapter 2: Materials and methods

Chapter 3: Cement chemistry discussion

Chapter 4: Diffusivity from BFS:OPC CPSs with distilled water as a test solution

Chapter 8: Diffusivity from BFS:OPC CPSs with John Innes soil solution as a test solution

Chapter 9: Diffusivity from PFA:OPC CPSs with John Innes soil solution as a test solution

Chapter 10: Conclusions

List of Tables

List of figures

List of abbreviations

BFS   Blast furnace slag

cfu   colony-forming unit

CPS   Cement paste sample

C-S-H   Calcium silicate hydrate phase

CSPW   concentrated Sellafield pore water

D_e effective diffusion coefficient

DSPW   diluted Sellafield pore water

d-v   diffusivity vessel

DW   distilled water

GDF   Geological disposal facility

HLW   High Level Waste

ICP-MS   Inductively coupled plasma mass spectroscopy

ILW   Intermediate Level Waste

JISS   John Innes No. 3 soil solution

K   Equilibrium constant

K_{SP} solubility product

LLW   Low Level Waste

MIC   Microbial induced corrosion

NFC   Nuclear Fuel Cycle

OPC   Ordinary Portland cement

p   Pearson coefficient

PFA   Pulverised fly ash

PGRC	Phased Geological Repository concept
Q	Reaction quotient
r-v	reservoir vessel
SEM-EDAX	Scanning electron microscopy - energy dispersive X-ray
SOB	sulphide oxidising bacteria
SRB	sulphate reducing bacteria
w/c	Water cement ratio

Chapter 1: Introduction

1.1 Radioactive waste

At each and every stage of the Nuclear Fuel Cycle (NFC) wastes/effluents are produced either in liquid, or solid or gaseous form from normal daily operations (Figure 1.1) [1].
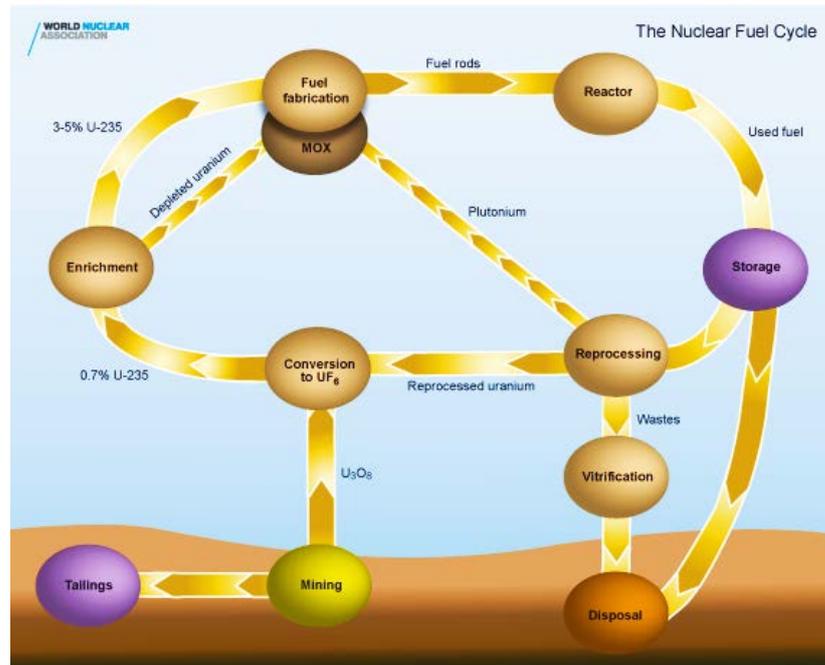
Figure 1.1 Illustration of the Uranium Nuclear Fuel Cycle (NFC) [2]

In the future, decommissioning wastes will become the major contributor, as most of the currently operating reactors will be retired by 2023 [3]. Radioactive waste is also produced from other sources such as medicine, universities, military operations and industries. Radioactive waste can be defined as "material that contains or contaminated with radionuclide at concentrations or activities greater than clearance level as established by individual countries and regulatory authorities" [4]. The difference between any other non-radioactive

waste/chemical waste and radioactive waste is that the latter can be accompanied with significant levels of ionising radiation and may require immobilisation to prevent spreading around the biosphere. During the normal operation of a typical reactor over 200 radionuclides are produced; most of the radionuclides are relatively short-lived and decay to low levels within a few decades [5]. Some radioactive waste has the potential to specifically target aquatic and terrestrial ecosystems, due to their long half-lives and damaging effects on cells as compared to other chemical pollutants [6]. The radioactive wastes consist of various irradiated materials, which is a subject of concern. The main objective of radioactive waste management is to deal with it in a manner that protects human health and the environment. It is sensible to understand various classifications of wastes to execute the appropriate management system.

1.1.1 Composition and classification of waste radioactive waste

The options for disposal of nuclear waste will be dependent on the radionuclide content of the waste (Table 1.1). These wastes/effluents can be classified as Low Level Waste (LLW), Intermediate Level Waste (ILW) and High Level Waste (HLW) depending on their radioactive content [7].

Table 1.1 Classification of radioactive waste in the UK [8]

LLW	The largest volume of wastes produced is LLW, from cooling waters, plant operations, and across the nuclear fuel cycle including some parts of fuel reprocessing cycle (>4 MBq/m^2 alpha, to 12 MBq/m^2 beta/gamma), which contain only small levels of radionuclides and certain nuclide which decay in relatively short period of time.
ILW	ILW wastes, from laboratory operations and fuel reprocessing, contain higher amounts of radioactivity than LLW and may require special shielding. It mainly comprises resins, chemical sledges and reactor components, graphite from reactor cores, as well as contaminated materials from reactor decommissioning.
HLW	HLW consists of highly radioactive fission products, used fuel itself and some transuranic elements generated in the reactor core and are the type of nuclear waste with the highest activity (> 3.7×10^6 kBq/m^2 alpha, to > 37×10^6 kBq/m^2 beta/gamma). Due to the high level of radioactivity, the heat produced by the radioactive decay of the material requires cooling, as well as special shielding during handling and transport

Most of the wastes/effluents arising at the front end of the cycle contain natural occurring radioisotopes and are likely to be categorised as low level wastes but the quantities involved will be significant. After the fuel has undergone irradiation, wastes/effluents are produced that fall into the Intermediate and High Level Waste categories. These wastes are substantially smaller in quantity but as they

contain fission products and other actinides require more engineered treatment and disposal systems.

LLW has a comparative short half-life with 90% of the elements becoming harmless after 100 years and is currently disposed of at the Drigg landfill site in Cumbria. Most ILW that has been produced since 1990 is currently being held in temporary surface storage facilities at various locations within the UK. The period of risk to public spans from hundred years to over one thousand years. The spent fuel is reprocessed; the separated waste is vitrified by incorporating it into borosilicate (Pyrex) glass which is sealed inside stainless steel canisters for eventual disposal [8].

1.1.2 UK radioactive waste inventory

The Radioactive Waste & Materials Inventory, updated every three years, provides the latest national record on radioactive wastes and materials in the UK. An overview of these data is given in Table 1.2. The negative number for HLW future arising indicates that the volumes will fall in the future due to two reasons, one being vitrification of waste which is one third of the volume of the original waste. Secondly, the UK is returning processed HLW to overseas customers in vitrified forms [9].

Table 1.2 UK Radioactive Waste inventory at 1 April 2013 [9]

Waste category	Volume (m^3)		
	Reported at 1 April 2013	Estimated future arisings	Lifetime Total
HLW	1,770	-700	1,080
ILW	95,600	190,000	286,000
LLW	66,700	1,300,000	1,370,000
Total	164,070	1,489,300	1,657,080

1.2 Radioactive waste disposal

Nuclear waste disposal is highly regulated with in many instances decades of proven experience, but for ILW and HLW research is still underway to ensure the selected routes i.e. deep geological disposal can meet stringent requirements [10]. There have been emphases on the disposal of irradiated graphite (i-graphite) that will arise from the decommissioning of UK graphite moderated reactors; Magnox and AGRs. All ILW waste such as Magnox swarf, i-graphite etc. will be encapsulated in cement within a suitable metal container, stored prior to being deposited in a Geological Disposal Facility (GDF) [11]. I-graphite is categorised as ILW largely due to its ^{14}C content (10 to 100ppm) as the Drigg's (LLW repository for the UK) ^{14}C authorisation is so restrictive that only a fraction of the UK's i-graphite (~ 95,000 tones Magnox and AGR) could be disposed of [12].

ILW contain enough radioactivity that it requires special treatment to minimise any potential release into environment. Nuclear Decommissioning Authority (NDA) has developed Phased Geological Repository concept (PGRC) (Figure 1.2) for safe and long-term management of radioactive waste, which is a multi-barrier, multi-phased approach based on placing the waste deep underground, beyond any disruption from any man – made events.

The phased nature of the PGRC involves number of processes/stages in the management and eventual disposal of radioactive waste. Figure 1.3 shows the summary of key stages involved in the radioactive waste management in PGRC.

Physical Containment	Geological Isolation	Chemical Conditioning	Geological Containment
Interim surface storage: ILW and LLW in steel or concrete boxes, ILW and LLW immobilised in cement grout in steel drum	No backfill	Alkaline Sorbing Cement-based backfill Material	Low water flow Physical stability
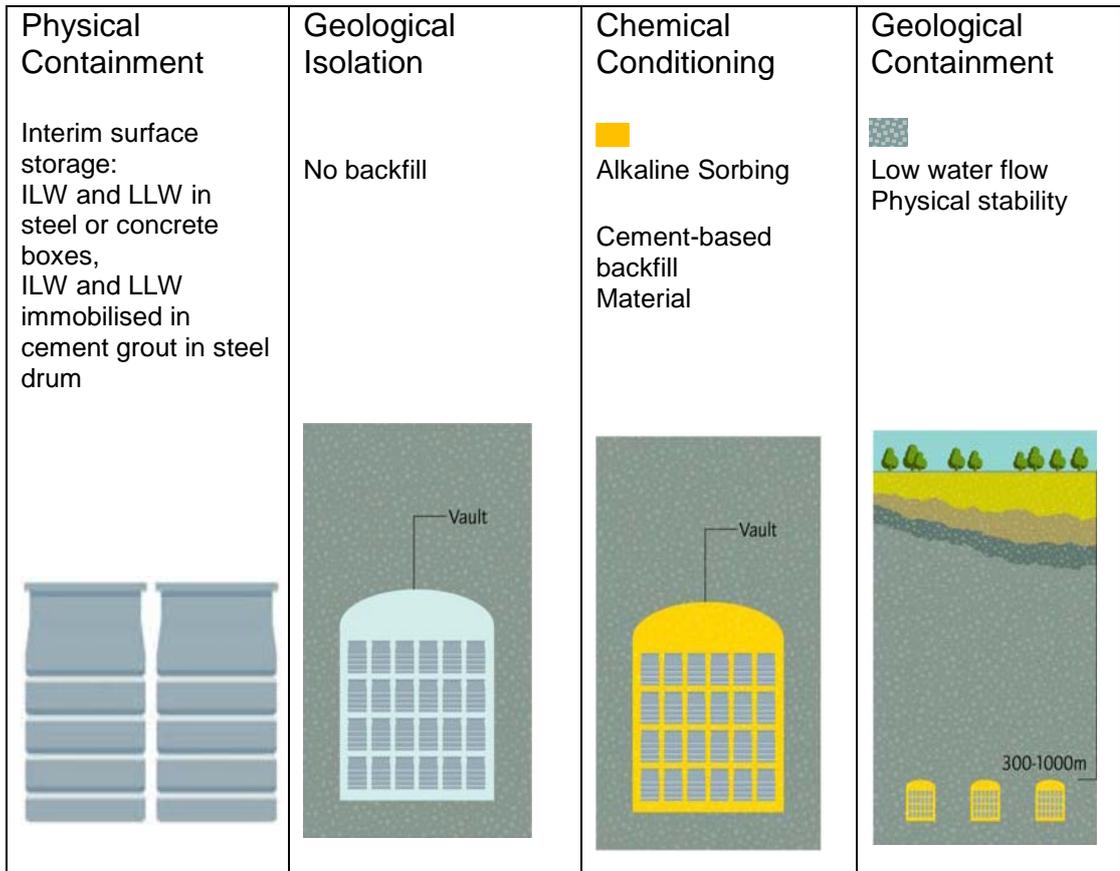
Figure 1.2 Phased geological repository concept [13]

Phase I
Immobilisation and packaging of waste
Encapsulated within cement-based grouting material within a standardised highly engineered stainless steel drum

⬇

Phase II
Interim surface storage
Packaged wastes would then be held at the site of origin in surface stores that have 50 years design life.

⬇

Phase III
Transport to a repository
The waste packages would then be transported to a repository

⬇

Phase IV
Waste emplacement
The waste packages would be emplaced in large built vaults that have been excavated in a stable geological environment deep underground.

⬇

Phase V
Monitoring and operational phase
Extended period, ten to hundreds of years. The repository and its contents would be monitored and the waste would be retrievable.

⬇

Phase VI
Backfilling of the repository
The repository vaults could be backfilled with a specially developed cement-based material which would provide one more barrier to the waste.

⬇

Phase VII
Sealing and Post-closure phase
When backfilling has been completed, the repository can be closed and sealed. No further human management would be involved.

Figure 1.3 The PGRC for long term management of HLW/ILW

1.3 Immobilisation of waste

Immobilisation of waste is essential part of waste management in order to convert the waste into to a form suitable for further handling, transport storage and

7

disposal. Technically, the purpose of stabilisation is to convert the waste to a physically and chemically more stable form, by binding the waste into the cement. Cementation is considered as a most widely robust and cost-effective technology for conditioning of ILW [14]. For most ILW, the waste will be immobilised in cement-based materials within stainless steel drums.

Encapsulation of wastes using Ordinary Portland Cement (OPC) has several benefits, which include:

(a)   inexpensive and mechanically, physically and chemically stable for handling, transport and disposal.

(b)   provide radiation shielding

(c)   maintain a high pH which in turn decreases radionuclide solubility

(d)   can incorporate many ions into solid solution and are tolerant to a wide variety of wasteforms.

Although cementation is widely used within the civil nuclear industry worldwide for encapsulation of higher activity wastes (such as ILW), some of the waste streams generated by the industry are difficult to encapsulate using this method and other techniques have been evaluated [15]. Most fall into the category of polymeric encapsulation and studies have shown that they provide a number of advantages for treatment of contentious waste streams. Their superior mechanical properties allow for good waste loadings (up to 75 % by weight for graphite, for example), allowing the number of packages to be reduced, while maintaining the integrity of the waste forms. The potential for polymers to degrade radiolytically whilst stored or even worse during disposal liberating gaseous products is a major consideration of the regulatory authorities.

1.4 Cement

Cement or Ordinary Portland Cement (OPC) in particular, can be defined as a bonding material having adhesive and cohesive properties used in conjugation with additives such as stones, sand and other additives/aggregates [16]. The term hydraulic cement derives from the fact that the cement have properties of setting and hardening in presence of water. The name "Portlanland" originates from a trade name used by Joseph Aspdin (1779-1835) in 1824 who patented the clay and limestone cement, because it looked like the stone quarried on the isle of Portland. Portland cement was first used in the civil engineering project by Isambard Kingdom Brunel (1806 -1856), as the lining for Thames Tunnel [16].

OPC is produced by burning limestone and clay or shale (source of aluminosilicates) at high temperature (1500°C) to produce cement clinker. The final product consist of ground 95% cement clinker with 5% gypsum to produce the final product cement. The process can be carried out dry or mixed with water; depending on the technique employed, it's classified as dry or wet. About 78% of cement produced in Europe is generated using the dry process. Calcium sulphate which is commonly referred to as gypsum controls the rate of settling and influences the rate and strength development. A typical clinker has a composition of 67% CaO, 22% SiO_2, 5% Al_2O_3, 3% Fe_2O_3 and 3% other materials [16]. The composition of OPC depends on the origin of the limestone and clay used in the manufacturing process. Cement is categorised into five different types under European standard EN 197-1 [17] (Table 1.3).

Table 1.3 Categorisation of cement under European standard EN-197-1[17]

Category	Description	Proportion of cement clinker	Proportion of other constituents
CEM I	Portland cement	95-100%	0-5%
CEM II	Blended cement (sub-divided depending on the material used, e.g. 'Portland fly ash cement', 'Portland slag cement', 'Portland limestone cement', etc.)	65-94%	6-35%
CEM III	Blastfurnance cement (incorporating ground granulated blastfurnance slag or G.G.B.S.)	5-64%	35-95%
CEM IV	Pozzolanic cement (incorporating natural or synthetic pozzolanic material, e.g. volcanic ash)	45-89%	11-55%
CEM V	Composite cement (incorporating both G.G.B.S. and pozzolanic material)	20-64%	18-50% G.G.B.S 18-50% Pozzolanic material.

1.4.1 Cement Composites

The term blended cement refers to composites of cements that are hydraulic cements composed of OPC and one or more inorganic materials that play an important role in cement hydration reaction and hydration/final products. Admixtures such as $CaCl_2$, also influences the cement hydration process but do not contribute to the final product. The most important additives are Blast Furnace slag (BFS) and Pulverised Fly Ash (PFA) (Table 1.4). Blended cement with up to 90% BFS and 75% PFA, are currently being employed in nuclear industry for encapsulation [18, 19].

1.4.1.1 Blast Furnace Slag (BFS)

BFS is a by-product generated during iron making process. The limestone that has been used to remove the acidic impurities from iron ore are broken down to form carbon dioxide and calcium oxide in the high temperature of blast furnace. The calcium oxide reacts with the acidic impurities in molten steel to transfer them into blast furnace slag. The composition of slag varies depending on the nature of ore, the composition of limestone flux and the kind of iron being made. The major constituents of BFS include lime, silica, alumina and magnesia. The chemical composition of BFS is CaO (30%-50%), SiO_2 (28%-38%) and Al_2O_3 (8%-24%). In the UK, BFS is produced in three steel making facilities at Teesside, Scunthorpe and Port Talbot [16].

1.4.1.2 Pulverised Fly Ash (PFA)

PFA is obtained by electrostatic or mechanical precipitation of dust from flue gas that are generated after combustion of coal in coal fired power station. PFA falls into subdivision of artificial pozzolanas and consist of silica and alumina. The chemical composition depends on the inorganic mineral composition of the coal gangue. Based on calcium content, PFA is categorised into two types: low – calcium flyash (Class F), containing less than 10% of analytical CaO and high-calcium flyash (class C), containing 15-40% analytical CaO [20]. Low-calcium flyash is predominantly being used due to technical benefits and economic factors [21, 22].

Table 1.4 Composition of OPC, BFS and PFA (%) (literature values) [23-25]

Material	CaO	SiO$_2$	Al$_2$O$_3$	Fe$_2$O$_3$	MgO	SO$_3$	Na$_2$O	K$_2$O
OPC	61.3	20.1	4.2	2.5	3.1	4.0	0.2	0.4
BFS	45.3	33.9	13.1	1.7	2.0	trace	n.d.	n.d
PFA	3.1	46.2	27.0	10.4	2.0	1.6	0.9	3.3

From the Table 1.5, the main constituents of cement can be seen to be di and tri calcium silicate/aluminosilicates. Thus addition of water forms major component which include calcium silicate hydrates (C-S-H) and portlandite Ca(OH)$_2$. The chemistries of these components must be considered when determining the stability of cement and concrete.

Table 1.5 Composition of Portland cement [16]

Cement Compound	Chemical Formula
Tricalcium silicate (C$_3$S)	Ca$_3$SiO$_5$ or 3CaO·SiO$_2$
Dicalcium silicate (C$_2$S)	Ca$_2$SiO$_4$ or 2CaO·SiO$_2$
Tricalcium aluminate (C$_3$A)	Ca$_3$Al$_2$O$_6$ or 3CaO·Al$_2$O$_3$
Tetracalcium aluminoferrite (C$_4$AF)	Ca$_4$Al$_2$Fe$_2$O$_{10}$ or 4CaO·Al$_2$O$_3$·Fe$_2$O$_3$
Gypsum	CaSO$_4$·2H$_2$O

1.5 Degradation of concrete

The ultimate destination of some of these encapsulated wastes is in a deep geological facility (GDF), where for many years the wastes will remain inert to their environment. The integrity of the waste form will have to meet stringent conditions, not least timeframe; for a deep geological repository the integrity will be considered over a 100,000 years, due to the GDF conditions as they present significant challenges with the varying environment conditions from operation to

post closure. These varying conditions will also influence the presence, growth pattern and impact of microorganisms on encapsulated waste. The ability of cement-based materials to resist the deterioration depends on the environmental conditions as well as material properties. Most cement hydration phases are unstable below pH 10. This raises a concern in regard to interaction of hardened cement paste in natural water which is near neutral pH and may have low mineral content, it is one of the worst case scenario which can be envisaged [14, 26], this poses a risk to thermodynamic equilibrium of cement paste solids with its pore solution may lead to dissolution. In GDF of seeping water, concrete durability will be potentially affected by pH, redox condition and the salinity of incoming ground water. This produces a progressive neutralisation of the alkaline nature of the cement paste, removing alkalis and dissolving portlandite, i.e. calcium hydroxide and calcium silicate hydrate (C-S-H) gel [27]. Not surprisingly, the interactions between the nuclear waste, cement, steel container, ingress of pore water and leaching of radionuclides, have received extensive studies [28-32] . However, most of these studies are of short duration and have used distilled/deionised (d/d) water which characterises the concentration gradient, diffusion leaching type of studies. The influence of salinity and presence of ions in leachate is not well known despite the fact that several countries (Canada, Finland, Sweden, possibly UK) are planning to emplace the waste in GDF which may likely have ingress of saline water and/ or brine.   Few of these studies have been carried out using accelerated leaching [33-37] . Although such studies have generated data on long –term leaching scenario, they do not replicate the actual leaching process that might take place in GDF facilities. There have been few studies carried out on leaching concrete material in the presence of aqueous medium with high salinity

and ionic concentration, which may represent the ground water leaching scenario in GDF. However, such studies have been carried out cementitious materials which have been subjected to harsh marine environment [30]. There are few studies that have addressed the implications of microbial activity on pore water chemistry and hence on the mobility of radionuclides under investigation. Those studies that have included microbial activity have tended to concentrate on the implications to encapsulated spent fuel in a thick-walled copper cylinder (direct disposal) [38].

The use of cement and potential effect of groundwater and minerals has raised many concerns and assurance is needed in terms of their integrity and subsequent release of radionuclide from the encapsulated waste form. Although cement (in the form of concrete) has been used for underground constructions for many years, scant information is known about its long-term integrity as an encapsulated wasteform, the nature of chemical interactions between hardened cement paste and groundwater in particular, saline water and brine. Although the durability of the cementitious material has been confirmed over periods in excess of 100 years; has primarily been designed for civil engineering purposes. The use of OPC was not designed for the purpose of waste encapsulation for disposal.

The vulnerability depends on both internal properties of the material and the external environmental factors that contribute to the degradation process. Degradation of concrete can take place by various mechanisms such as alkali - silica reaction, carbonation, chloride or sulphate attack, leaching, abrasion, corrosion etc. [16].

1.5.1 Dissolution in ground water

Cement paste degradation takes place due to combined effect of diffusion-transport effects and chemical reactions. One of the major factor contributing towards the dissolution of hardened cement paste is its porous nature, in which case a large amount of water flow may be able to dissolve the sparingly soluble components present in the cement paste. This transportation is diffusion controlled when the pore size distribution of cement paste is small. As the volume of the flow paths increases it becomes convection controlled [39, 40].

The difference in the concentration causes the net transfer of ions from higher concentration (concrete) to lower concentration (aqueous solution) in the case of diffusion. This relevant property of concrete is referred to as diffusivity [16].

Steady-state diffusion is normally assumed to be the controlling step when determining the leachability of nuclear wastes, when encapsulated into cements/binders, hence Fick's law is assumed to be the rate controlling mechanism for release [41].

This diffusion is best described by Fick's Law; where no pressure head exists and the magnitude of mass transfer by diffusion is dependent on the concentration gradient across the medium concerned:

$$F = -D\frac{dC}{dx}$$

 Where

F = mass flux (mass of solute per unit area per unit time)

D is diffusion coefficient (area per unit time) and

dD/dx is the concentration gradient.

15

The dissolution and effective migration of encapsulated cations/radionuclides from cement matrix to surrounding aqueous media will take place once the dissolution of C-S-H gel and change in pH takes place.
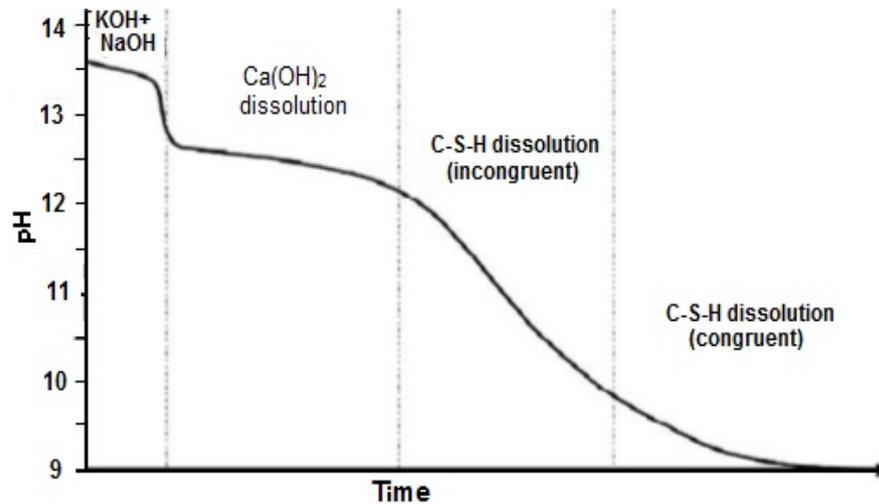
Figure 1.4 Predicted evolution of pore solution pH during leaching by pure water [42].

The chemical changes taking place due to the movement of water into the porous structure can be explained by using Figure 1.4. The contents of pore water is highly charged with Na^+ and K^+ and Ca^{2+} and OH^-, this creates a concentration gradient between a aqueous solution with low mineral content and interstitial solution. The movement of water into the hardened cement paste will bring down the pH by initially dissolving the most soluble species i.e. Na^+ and K^+ which controls the pH of the pore solution above 13 at initial stages of dissolution. This stage will produce high plume of pH in the surrounding ground water (if stagnant conditions exist). The stability and the thermodynamic equilibrium of pore solution with its solid is disturbed once the pH of the pore water is changed [26].The

presence of strong alkali (NaOH and KOH) are dominant in pore water solution which gives the pH values of 13.5; at high pH, the solubility of Ca^{2+} is controlled by Na^+ and K^+ in the pore fluid. Once the alkali have been leached out, the pH of pore fluid which comes down to 12.5 is controlled by $Ca(OH)_2$ [37]. The relatively high content of unreacted $Ca(OH)_2$ in the hardened cement paste maintains this pH for a longer time. The presence of Mg^{2+} and CO_3^{2-} ions in the ground water may precipitate to give brucite ($Mg(OH)_2$). Once all the unreacted $Ca(OH)_2$ has been removed, the Ca/Si ratio falls down to about 1.8 from its initial value of 4.5. At this point depending on the Ca^{2+} and SiO_4^{4-} content of the leachate, two possible processes may take place:

(a)   In low salinity ground water or distilled water, slow congruent dissolution of CSH takes place which drops the pH continuously to around 10.8, until all the CSH is removed. This process takes considerable time.

(b)   The ground water containing significant amount of Ca^{2+} and SiO_4^{4-}; incongruent dissolution of CSH takes until Ca^{2+} and SiO_4^{4-} are completely removed. The presence of Ca^{2+} and SiO_4^{4-} may form minerals such as ettrigent and brucite, until the buffering capacity of the cement is consumed. Brucite can form protective layers on cement paste, hence may slow down the dissolution process in saline ground water. The high plume of pH will persist in stagnant water and will influence the absorption of cations/radionuclides except some of the alkaline metals such as Cs^+ and Sr^{2+} which are poorly absorbed into the cement [43].

1.5.2 Carbonation

Deterioration of cement paste takes place due to its reaction with carbon dioxide. Dissolved species of carbonate and bicarbonate react with main cement hydrates, i.e. calcium silicate hydrate, calcium hydroxide and various calcium aluminate or ferro-aluminate hydrates, in three ways, depending on its mode of delivery and surrounding environment [14]:

(a)   Added as an aggregate, calcium carbonate, a supplementary cementing material or with waste [44]

(b)   In gaseous form, as carbon dioxide from local environment [27].

(c)   Dissolved in ground water [27]

Carbonation of cement paste takes place in following sequential manner

$$Ca(OH)_2 \text{ (s)} + CO_2(g) \rightarrow CaCO_3 \text{ (s)} + H_2O \qquad (1.1)$$
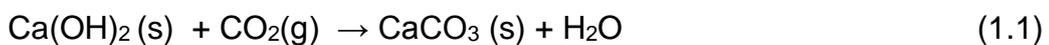
Calcium hydroxide plays a predominant role in the carbonation process, however, other hydration products of cement such as C-S-H and unhydrated cement compounds can react with CO_2 in following manner.

$$C_xS_yH_z + (x-x')CO_2 \rightarrow C_{x'}S_yH_{z'} + (x-x')CaCO_3 + (z-z')H_2O \qquad (1.2)$$
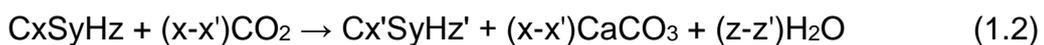
As shown in the reaction 1.2, the composition of C-S-H changes upon its depletion of calcium content. As the carbonation process continues, Ca:Si ratio

decreases until C-S-H is completely decalcified and finally transformed into calcium carbonate and highly polymerised silica gel. (1.3)

$$CxSyHz + xCO_2 \rightarrow xCaCO_3 + ySiO_2 + zH_2O \qquad (1.3)$$
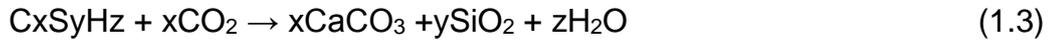
The carbonation doesn't proceed to other hydrates until the pH has dropped below 12.4 [45].

1.5.2.1 Carbonation of unhydrated cement

Carbonation can also accelerate the hydration process of cement paste by converting C_3S and C_2S into calcium carbonate and C-S-H, thus

$$C_3S + yH_2O + (3- x)CO_2 \rightarrow xCSy\ H + (3- x)CaCO_3 \qquad (1.4)$$

$$C_2S + yH_2O + (2- x)CO_3 \rightarrow xCSy\ H + (3- x)CaCO_3 \qquad (1.5)$$
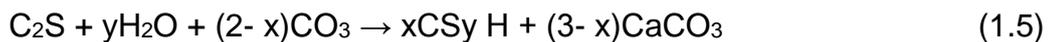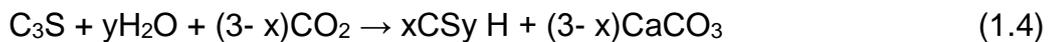
Carbonation affects the physical properties of the hardened cement paste. The conversion of soluble cement hydrates to relatively insoluble phases, leads to alteration of microstructure of hydrated paste [46, 47], thus reduces the permeability and hence leaching of some of the waste form [48]. However, the dissolution of $Ca(OH)_2$ and C-S-H buffer brings down the pH of pore solution. This may increase the solubility of some of the cations/radionuclides from encapsulated waste form [49]. Reference studies have shown that the totally carbonated layer will have a pH of about 8.3 [50]. Carbonation may also lead to

shrinkage due to the evaporation of waste generated from the carbonation reaction [45], hence cracking of the cement paste. This would influence the leaching and mobilisation of encapsulated waste form.

1.5.3 Chloride interaction

The interaction of chloride and cement has received significant attention [51, 52] in relation with corrosion of steel reinforced concrete materials. Possibilities of chloride in concrete arises if it is made up with seawater or saline groundwater or use of sea-dredged aggregates. Chloride present in the mixture generally enters the AFm (ferroaluminate) phase with 60% of the Cl^- bound to the cement paste as monochloroaluminate and the remainder dissolved in the pore water [53, 54]. When Cl^- in combination with the AFm phase, results in the formation of Friedel's salt ($4CaO.Al_2O_3.(Cl,OH)_{10}$), above 40°C, below 20°C, the trichloride complex (AFt) is formed. The degradation by chloride ingress mostly affects the corrosion of reinforcement steel bars in the concrete [16]. The high pH of the pore water maintains the passivation of steel. However, chloride ion in the presence of water and oxygen destroys the protective oxide film; causing chloride induced corrosion of steel [27, 54].

1.5.4 Reaction with sulphate ion

Interaction with sulphate ion with cement paste takes place as internal sulphate (derived with in the cement matrix), as well as external sulphate attack. Sulphate is commonly found in ground water with calcium, magnesium and to lesser extent sodium [27, 30]. There have been several studies on sulphate attack on cement paste leading to physical expansion, leading to cracking and spalling. Both the mechanisms, internal and external sulphate attack will produce gypsum from the

reaction with free $Ca(OH)_2$. The gypsum produced may further react with C-S-H to produce ettringite and may degrade the cement paste [54].

1.5.5 Organic interaction

The other possibility of affecting the pH of cement paste is interaction of encapsulated organic material and subsequent production of HCO_3^-, from the degradation of cellulose and gloves and HCl, due to radiolysis of chlorinated polymers such as PVC, will react with OH groups and lower the pH [54, 55], hence affecting the stability of encapsulated waste.

1.5.6 Microbial degradation

The use of cementitious material in the building industry goes back for centuries. Thus, there is a relatively large body of data available on the susceptibility of concrete to microbial attack [56]. One of the concerns raised is the survival/existence of a viable population of microorganisms at a pH value equivalent to that of repository concrete that can possibly influence by its performance by degrading activities such as acid production [57]? Research evidence has shown that extremophiles can survive at a pH as great as 12 in laboratory conditions [58]. A number of studies on underground sewers , roads and bridges, have shown that that the integrity of concrete over extended timescales can be influenced by microorganisms [59, 60]. These studies have shown the presence of sulphur-oxidizing bacteria such as *Acidithiobacillus thiooxidans*, which produces sulphuric acid under aerobic conditions through the oxidation of reduced sulphur, sulphide, and thiosulfate compounds [60]. The sulphuric acid produced dissolves the C-S-H and portlandite cement constituents [61]. Another example of acid-mediated degradation, is that mediated by acid

nitrifying bacteria that use inorganic nitrogen compounds (i.e., ammonium, nitrite). However, there will be a limited supply of oxygen in GDF in contrary to sewers and roads and bridges. It is envisaged that , oxygen would no longer be available once utilised for corrosion, mineral dissolution and microbial redox reaction [56]. Microbial growth in any habitat will depend on the availability of nutrients and is usually controlled by growth-limiting factors such as the presence of the macronutrients, carbon, nitrogen and phosphorus [62].

1.5.6.1 Micro-organisms involved in the biodegradation of concrete

The deterioration of cementitious material is caused by biotic and abiotic factors and can be categorised by their mechanism of attack. A summary of microbial degradation of concrete is shown in Figure 1.5. The first report of concrete degradation dates back to 1900 [63] by Olmstead and Hamlin who reported the corrosion of concrete sewage pipes due to their exposure to the hydrogen sulphide gas. Early workers reported that this corrosion resulted from a chemical reaction between the sewage and the walls of sewage pipes. A range of chemical by-products/species produced as a result of microbial metabolism have a detrimental impact on cementitious material.
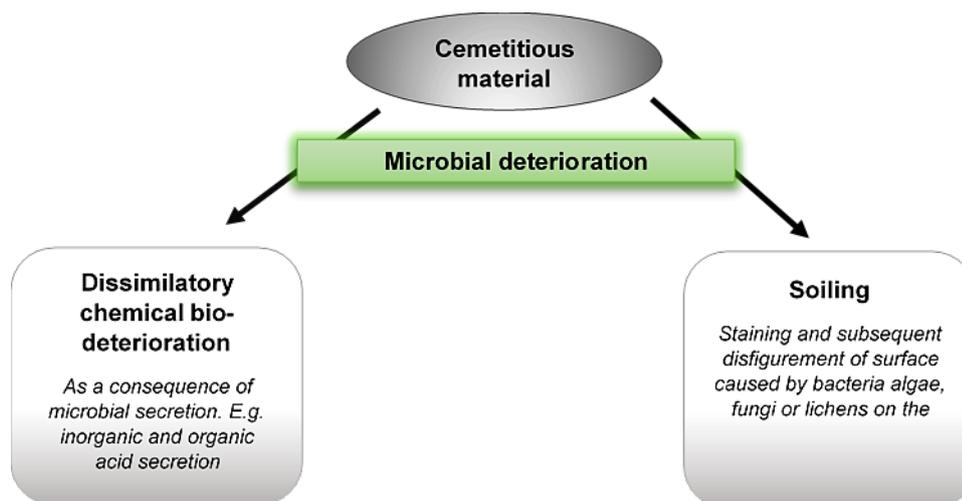
Figure 1.5 Microbial deterioration of cementitious material

1.5.6.1.1 *Sulphur Species*

Microbial metabolism plays an important role in mineral transformation, and global cycling of the elements throughout nature by Sulphur bacteria, have a significant role in metabolising sulphur (Figure 1.6). Depending on their metabolic activities, sulphur bacteria are classified as sulphide oxidising bacteria (SOB) and sulphate reducing bacteria (SRB). Sulphur is a major microbial metabolite of Sulphur bacteria.

(a)   sulphide oxidising bacteria (SOB)

Sulphur oxidation involves the oxidation of reduced sulphur compounds, such as sulphide, inorganic sulphur, and thiosulfate to form sulphuric acid. SOBs, chemolithotrophs , are able to carry out a reaction, coupling the reduction of carbon dioxide to sulphide oxidation; reduced sulphur compounds are converted to sulphite and subsequently converted to sulphate by the enzyme sulphite oxidase [64]. These organisms are blue-green or purple as a result of presence

23

of photosynthetic pigments. *Beggiatoa, Chromatiium and Chlorobium* are some of the examples of sulphur oxidising bacteria.

(b)   The sulphate reducing bacteria (SRB)

SRBs are a group of anaerobic bacteria commonly involved in degradation of materials such as concrete structure and metals. As a result of their unique form of respiration, these group of organisms use sulphur as biological pathway and expel the resulting hydrogen sulphide as waste. The resulting hydrogen sulphide may combine with oxygen to form a product which may be utilised by aerobic *Thiobacilli,* this may eventually lead to the formation of sulphuric acid which can be detrimental to concrete [59].
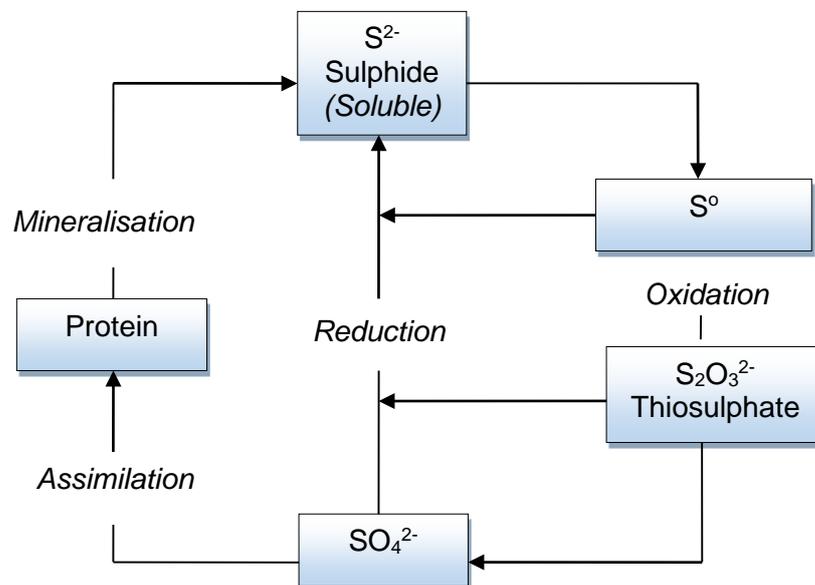
Figure 1.6 The microbial sulphur cycle [65]

1.5.6.1.2 *Nitrogen bacteria*

Nitrogen is a major microbial metabolite and microbial nitrogen transformations have the potential to significantly influence the degradation of concrete [59, 65]. These bacteria form nitric acid, and obtain energy needed for carbon dioxide reduction by a two-step (Figure 1.7). Some of the examples of nitrifying bacteria are *Nitrosomonas, Nitrosovibrio and Nitrobacter* [59].
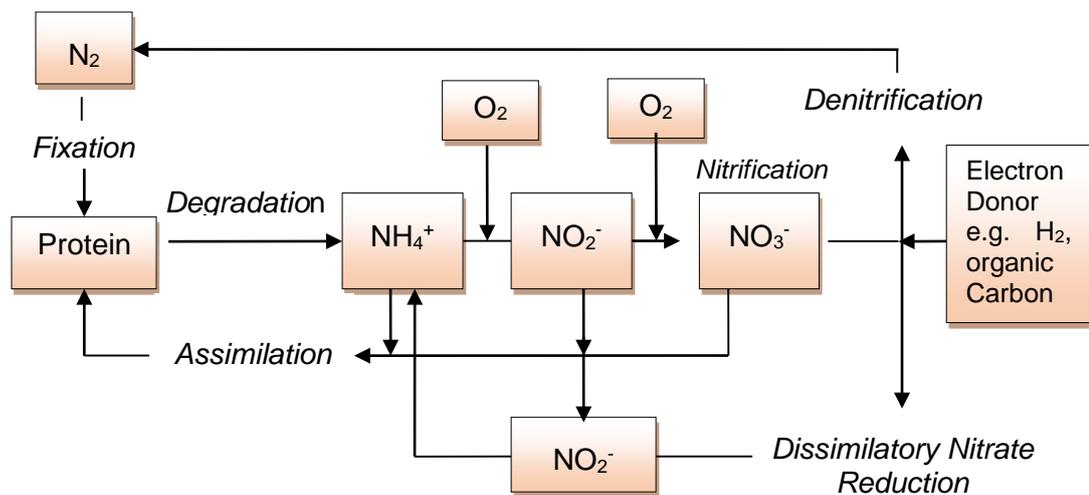
Figure 1.7 The microbial nitrogen cycle [65]

1.5.6.1.3 *Heterotrophic Fungi*

A wealth of information exists on the weathering and deterioration of concrete by hyphal penetration and bio- corrosive activity of heterotrophic fungi [60, 66-69]. The production of organic acids by fungi play an important role in degradation of cementitious material. Some of the examples of fungal genera known to degrade concrete structures are *Exophilia, Penicillium, Aspergillus, Cladosporium, Alternaria, Aureobasidium, Ulocladium and phoma* [68, 69].

1.6 Potential for microbial activity under conditions within GDF

Any GDF will have a period before closure and post-closure. The pre-closure phase involves storage and packaging at a nuclear facility, which will then be transported to an ILW surface handling facility and subsequently placed in the underground repository in the GDF awaiting closure/backfilling. The period prior to closure may last from ten years to few hundred years. Post-closure period will involve backfilling and sealing, during which no further human management will be involved.

A recent review on Microbiologically Influenced Corrosion (MIC) induced in waste packages by Humphreys et al. [70], indicated that the UK's geological environment that could plausibly hold a GDF will have an indigenous population of microorganism. Although microbes will be present in both pre- and post-closure phases, depending upon the particular conditions they may not be metabolically active [65]; microorganisms will vary spatially and temporarily. The report also talks about presence of SRBs in severely hyper-alkaline conditions within "supercontainers". The report further says that that micro-organisms will occur within at least some parts of most waste forms, on the surfaces of metal waste canisters and within the natural environment of a GDF, possibly as a dormant form of bacteria. These micro-organisms may be active to greater or lesser degrees, depending upon the particular physic-chemical conditions within the waste, engineered barrier or rock-water system within which they occur [65].

1.6.1 The potential microbial activity during pre-closure period

It is likely that the potential microbial activity will be present during the pre-closure phase of GDF, in particular within ILW areas, rather than the HLW. areas

Absence of free water, organic matter and heat producing high radiation from a HLW, may restrict the growth of some microorganism, however, evidence has shown the presence of viable population of micro-organism in the nuclear ponds which confirms that some of the micro-organism have high resistance to radiation [71-73]. Most aerobic microbial activity will occur during pre-closure phase and may subsequently affect the handling and transport of waste packages. During pre-closure period, aerobic degradation will be encouraged involving fungi and acidophilic bacteria, producing organic acid, from cellulose degradation, very unlikely that the GDF will become anaerobic during this phase [65]. The presence of artificial light may influence the phototrophic microbial growth (algae and photosynthetic bacteria) in the presence of moisture, eventually resulting in biofilm formation and this may influence the anaerobic microbial activities. The potential source of sulphate would likely be ground water, which will influence the SRB and SOB growth. Summary of initial screening of the ILW pre-closure environments (Table 1.6) [65] indicates, in all the three phases of pre-closure (interim storage, pre-backfilling and post-backfilling pre final) microbes, a source of sulphate and energy will be present.

Table 1.6 Initial screening of the ILW pre-closure environments [65]

	Microbes Present	Sulphate Present	Energy Sources
Interim Storage	Yes - wide range of organisms dominated by environmental isolates transported by air, human contact activity and associated with the waste.	Low levels of sulphate present external to the waste form. Potential sources include vehicle emissions. Potential sulphate sources present in waste.	The energy sources available to drive microbial activity include: light, organic waste components; organic additive in the encapsulants; reduced N and S compounds in the waste; corrosion; organic contamination e.g. diesel fumes.
Pre-backfilling GDF Storage	As above plus some potential contamination by microbes present in the rocks and groundwater.	As above.	
Post-backfilling, pre- final GDF closure	As above plus greater potential contamination by microbes present in the rocks and groundwater.	As above plus sulphate available in the groundwater and associated with the rocks (which may be mobilised by groundwater).	As above, but no light or further organic contamination from operations (e.g. from diesel fumes).

1.6.1.1 Microbiologically Induced Corrosion (MIC) and biofilm

Localised corrosion/degradation is initiated by aerobic microorganisms when they form biofilms. Biofilms are a heterogeneous structures that, trapping dirt and other particulate materials, increasing the disfiguring effects of the biofilm and making the structures more difficult to clean [68]. Biofilm consist of consortia of micro-organisms embedded in extracellular polymeric matrix (EPM). The polymers are generally of polysaccharides which act as a glue for trapping dirt and other particulate matter [60, 68], thus creating a wide variety of electrochemical environments. In addition the sedentary or sessile (attached)

organism can utilise different carbon sources than free floating (planktonic) organism and produce different degrading enzymes and may become more resistance to anti-microbial agents. Studies have shown that biofilms can be formed under a variety of conditions including those with low nutrition levels [74] including spent nuclear fuel ponds [75]. Numerous features and biofilm formation are described by Busscher and Van der Mei [76].

A relatively large variety of micro-organisms may affect overall performance of deep GDF [65] that may facilitate:

(a) potential for direct damage to storage container by creating corrosion-aggressive environment, hence

(b) deterioration of concrete and engineered barrier system (EBS) components and this may

(c) influence the mobility and transfer of leached cations/radionuclides from near to far-field environment.

1.6.2 The potential microbial activity during post-closure period

The post-closure period will initially have a period of oxidation, this will occur immediately after GDF closure and the availability of reduced sulphur and nitrogen compounds. The late post-closure period will be anaerobic, where sulphate reduction to sulphide may lead to increased degradation of concrete. The presence of ground water may contribute significantly as a source of sulphate [56]. The potential source of sulphate would be from buffer and backfill material which will influence the activity of SRBs and biofilm formation. In an anaerobic environment, microbes can generate both inorganic (sulphuric and nitric acids) and organic acids e.g. (acetic acid) [61]. The summary of potential organic and

inorganic acid generated by microorganisms is listed in Table 1.7. These acids produced by micro-organisms are detrimental to integrity of cement paste in particular CSH phase. Studies by BNFL scientists demonstrated that sulphur-oxidising bacteria (SOB) could degrade concrete structures by up to 8mm/year. Two of the supervisors (Eccles and Morton) involved with this project patented this work [77] .

Table 1.7 Potential organic and inorganic acids produced by microorganism [65].

Inorganic Acids		Organic Acids	
Substrates	Products	Substrates	Products
Reduced nitrogen and sulphur compounds e.g. NH_4, mineral sulphides, and elemental sulphur. Nitrogen and sulphur containing wastes e.g. ion exchange	Nitric and sulphuric acids.	Dissolved organic carbon, alkaline cellulose degradation products e.g. Iso- saccharinic acid (ISA), organic waste components e.g. cellulose, cement additives e.g. plasticisers, H_2 and CO_2.	Volatile fatty acids e.g. acetic, propionic, butyric.

1.7 Cations/radionuclides of interest

The selection of the three cations/radionuclides in the present research was based on their chemistries, importance in nuclear waste management and interactions with cement paste [78, 79].

1.7.1 Strontium

Strontium is an alkaline earth metal, a mirror of calcium [80]. ^{90}Sr is a by-product of the fission of uranium and plutonium in nuclear reactors. It is classified as one of the long lived component of nuclear waste, with a half-life of 30 years. Due to its similarities with Ca^{2+}, it is easily taken up as a calcium into the human body.

This raises a concern if radioactive ^{90}Sr is absorbed. In this case, it concentrates in teeth and bones and continues to emit radiation causing severe damage. In cement paste, Sr^{2+} forms sparingly soluble strontium or calcium/strontium carbonate or sulphate, which is well retained in the cement matrix. Reference studies have shown that the hydration products of C_4AF and C_3A can completely accommodate low Sr^{2+} levels [80].

1.7.2 Caesium

Caesium, alkali earth metal is very similar to potassium and sodium. It is accumulated in biological system by potassium pathways. ^{137}Cs is a major constituent of nuclear spent fuel and has a relatively long half-life of 30 years. Chernobyl accident released large amount of ^{137}Cs into the environment and subsequent research has highlighted the fate of caesium in the natural environment [67]. Caesium ion is highly soluble in the pore water of hardened cement paste [79] and thus is a matter of concern in regard to encapsulation of wasteform containing caesium.

1.7.3 Cobalt

Cobalt is an essential transition metal having biological function for growth of all organism, in particular cyanocobalamin, vitamin B12. ^{60}Co is generated in nuclear facilities by neutron bombardment of steel, concrete and graphite. It is a short-lived radionuclide with a half-life of 5.27 years. Studies have reported that ettringite accommodating Co^{2+} at the M^{2+} site in the crystal structure [81], while other studies have indicated that it was strongly sorbed onto CSH gel [82].

1.8 Aims and objective of project

Predicting the diffusivity of radio-nuclides from encapsulated waste during disposal is a crucial consideration in selecting an immobilisation technique. Low matrix solubility confers minimal release of radio-nuclides. The diffusivity or leaching behaviour of cement encapsulated radioactive waste is crucial to ensure the overall safety of a storage/disposal system. Experiments to identify leaching behaviour of cementitious waste forms and to demonstrate their acceptance for storage and disposal have been undertaken. These have included both laboratory-scale [36, 83] and larger-scale studies that try to replicate conditions similar to those expected in a disposal environment [84]. For these latter studies the long term performance of the waste form and implications to the near-field environment is needed.

The earlier cement waste form experiments were in sixties [84] that used water as the infiltration medium; since then the experiments have become more representative of conditions both waste form and geological. Nonetheless very few studies have addressed the implications of microorganism activity on the diffusivity of radio-nuclides from encapsulated waste.

This project evaluates the diffusivity of strontium, caesium and cobalt when added as inactive forms to OPC:BFS and PFA:OPC formulation as their chlorides and for strontium when added as chloride and carbonate.

The objectives/aims of this project were to measure the rate of diffusivity of three cations simulating their fission products. These measurement would require studying the influence of:

(a)   Cement paste composition (BFS:OPC and PFA:OPC)

(b)   Hydration of cement

(c)   Added chloride salt to the makeup water

(d)   These salts on pore water composition

(e)   The design of the diffusivity experiments e.g. open and closed systems

(f)   The test solution composition e.g. distilled water (DW), concentrated Sellafield pore water (CSPW), diluted Sellafield pore water (DSPW) and John Innes soil solution (JISS).

Chapter 2: Materials and methods

2.1 Materials and chemicals

The chemicals utilised in the experiments (listed below) were analytical grade and purchased from Sigma-Aldrich (UK). The Ordinary Portland cement (OPC), Blast Furnace Slag (BFS) and Pulverised Fly Ash (PFA) were kindly supplied by National Nuclear Laboratory, Preston Laboratory. These materials were received without detailed specification sheets and therefore production batch numbers, date of manufacture etc. cannot be reported. However, the analysis of as received OPC, BFS and PFA are given in Table 4.2 and Table 5.2

2.2 Preparation of cement paste samples

Cement paste samples were prepared using two different types of additives. These included, Blast Furnace Slag (BFS) and Pulverised Fly Ash (PFA) in order to study the comparative leaching pattern and capability of retention of encapsulated inactive cations representing strontium, caesium and cobalt radionuclides. A cement paste with consistency $w/c = 0.37$ was prepared by using a similar methodology to that employed by the National Nuclear Laboratory in Preston [85]. This was achieved by mixing required quantity of Ordinary Portland Cement (OPC), additives (BFS or PFA) and water or solutions of inactive cations (Sr^{2+}, Cs^+ and Co^{2+}) as chloride or carbonate, in a mixer as shown in Table 2.1. The required percentage of cobalt chloride solution i.e. 3% could not be achieved because of the solubility of cobalt chloride in the water. The metals were selected based on the content of the major radionuclides present in the nuclear waste and also for their different chemical properties. A required quantity of distilled water or cation chloride/carbonate solution was poured into the mixer (Rachel Allen stand mixer™, 650 watts) container. OPC was added to the mixer container in increments of one-fifth of total quantity taking 1 minute for each addition followed

by BFS to the OPC slurry in a similar manner to OPC addition. The final, paste after stirring for a further 2 minutes, was then spooned into small plastic bottles of 60 ml capacity (CPS dimensions 32 mm dia by 50 to 57 mm height), tapped several times to remove entrapped air bubbles and finally capped and agitated for a further for 4 minutes to ensure uniform mixing and minimal air entrapment. A total of 9 sets of each BFS:OPC and PFA:OPC cement paste samples were prepared, i.e. (i) control; (ii) ≈3% strontium chloride; (iii) ≈0.3% strontium chloride; (iv) ≈3% caesium chloride; (v) ≈0.3% caesium chloride; (vi) ≈3% strontium carbonate; (vii) ≈0.3% strontium carbonate; (viii) ≈1.3% cobalt and (ix) combined metal chloride (≈3% $SrCl_2$, ≈3% CsCl and ≈1.3% $CoCl_2$). After 7 days the caps were removed to allow the bleed water either to evaporate or re-adsorb. After 45 days, the cement paste samples were removed by gently tapping the base of the plastic bottle and left standing in the laboratory (Figure 2.1, Table 2.2) until employed in the diffusivity experiments. Detailed summary of sample dimensions, cation concentration, and specific gravity of cation solution of each CPS is mentioned in appendix 2.1 and 2.2.

Table 2.1 Cement paste mixture proportions

CPS	BFS	OPC	PFA	Water	Total mass
			(Kg)		
BFS:OPC	1.2	0.4	0	0.59	2.19
PFA:OPC	0	0.4	1.2	0.59	2.19
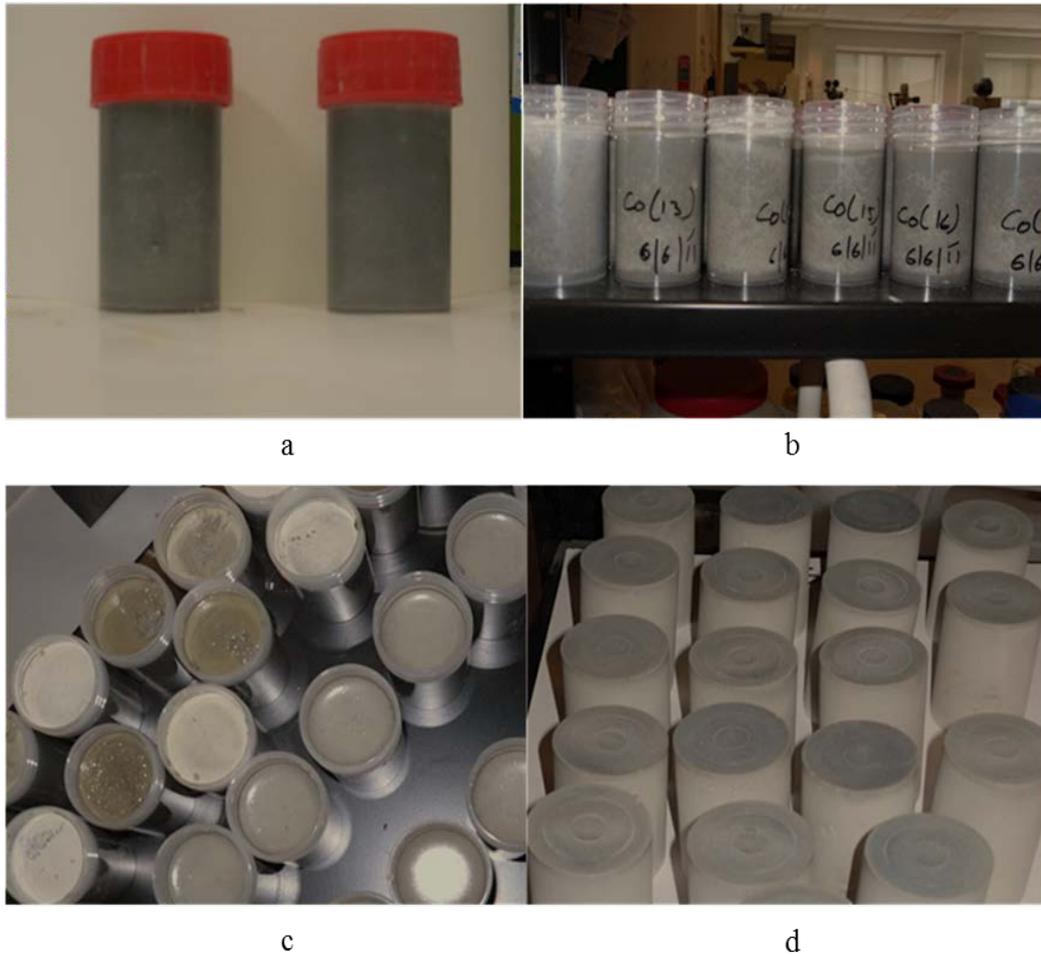
Figure 2.1 (a) freshly prepared CPS, (b, c) caps were removed after seven days

(d) samples left open for further curing

Table 2.2 Dimensions of cement paste samples (CPS)

	Height (cm)	Diameter (cm)	weight (g)
CPS	5.0 - 5.7	3.2	77.7 - 100.6

2.3 Analysis of cement materials and hardened cement paste

Analysis of the whole CPS (cylinder) was not undertaken, but the composition of cation/anion was estimated from EDAX analysis of OPC, BFS and PFA. However, to measure the uniformity of the samples, they were dissected into three equal sections, i.e. top, middle and bottom (Figure 2.2), using a tile cutter (Erbauer ™ 750W Tile Saw 230V, UK). The sectioning was carried out on three different occasions during the course of this research, prior to the start of new diffusivity experiments, to understand the pore size distribution along the vertical column of cement cylinder and also to examine the distribution of metal ions.
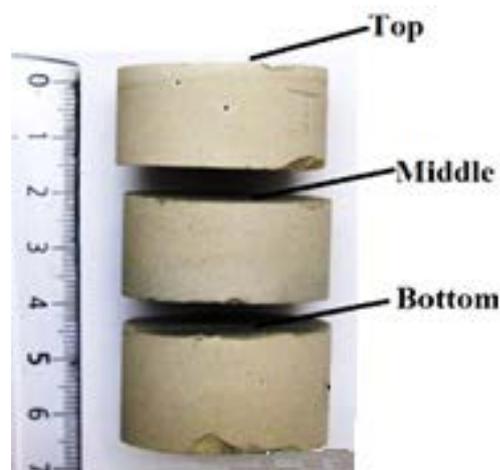
Figure 2.2 Dissected CPS named as top; middle bottom; side and base layer for elemental analysis.

2.3.1 Analysis of OPC, BFS and PFA

Elemental analyses of cement materials (OPC, BFS and PFA) were carried out using a Scanning Electron microscope/Energy dispersive X-ray spectroscopy (SEM/EDX). A Quanta 200™ SEM with EDAX™ EDX system was used for SEM/EDX analysis at the accelerating voltage of 20 kV. Each material was fixed

to an adhesive carbon pad attached to an aluminium stub. These stubs were placed upon the stage in line with the electron beam into the vacuum chamber of the SEM and the analysis was carried employing a magnification of 140x. EDX analysis was carried out by using a semi quantitative programme Genesis EDAX SEM Quant ZAF version 3.51.

2.3.2 Chemical analysis of CPS

Crushed CPS of ≈100 mg from each layer was boiled in 25 ml of concentrated HNO_3 at 130°C for 30 minutes. The resulting solution was diluted with de-ionised water to 500 ml in standard volumetric flask. The solution was analysed by Inductively Coupled Plasma Mass Spectrometry (ICP-MS, Thermo X series™, UK) for Na^+, K^+, Ca^{2+}, Sr^{2+} and Cs^+.

2.3.3 Water content of CPS

The water content of the CPS was measured as follows: Approximately 1 gram of crushed CPS from each section was weighed using a calibrated balance and placed in a crucible in a conventional oven for (≈ 14-16 hours) at 105°C. The dried sample was then transferred to desiccator before measuring the weight loss. The difference in weight (before and after) was calculated and expressed as the water content of CPS.

2.3.4 Surface and pore-size area

The nitrogen adsorption method (BET) [86] which is based on the physical adsorption of gas molecules on a solid surface, was employed to measure the surface area and porosity of cement paste samples. There are numerous methods used for the surface area and porosity measurements [87]. The most common method is BET method based on the work of Brunauer, Emmett, and

Teller [86]. The basic concept behind the gas sorption technique is physical adsorption of gases or vapours on surfaces of solids and to the walls of the pores within the studied solid. The surface area is determined by the amount of gas absorbed at the given pressure. The standard BET equation is written as:

$$\frac{P_{rel}}{V(1-P_{rel})} = \frac{1}{V_m C_{BET}} + \frac{P_{rel}(C_{BET}-1)}{V_m C_{BET}}$$

Where

P_{rel} is the pressure of the gas in equilibrium with the specimen P, relative to the saturation vapour pressure $P0$. V is the amount of gas adsorbed at pressure P. C_{BET} is a constant and V_m is the amount of gas required for a monolayer of coverage. The specific surface area, S (m^2/g), may then be calculated using following equation

$$S = \frac{N_m \sigma}{m}$$

Where Nm is the number of gas molecules in one monolayer and may be substituted for (Vm/v) where v is one molecular volume. σ is the cross sectional area of a gas molecule and m is the mass of the specimen.

To determine the surface area and porosity, $\approx$ 1.5 grams of crushed cement paste sample from each section was weighed using a calibrated weighing balance and placed in a sample tube and degassed overnight at 105°C [88], until the vacuum reached 5 mm Hg. After degassing, samples were weighed and placed in the analysis chamber (Micrometric ASAP 2010™). The nitrogen BET surface area and pore size area values were calculated automatically by the system software and reported as m^2/g.

2.4 Experimental setup and procedure

2.4.1 Closed circuit diffusivity system

Dynamic diffusivity measurements of cations and two anions from the prepared cement paste samples were achieved using the following experimental arrangement. A polypropylene diffusivity vessel (d-v) and polypropylene reservoir vessel (r-v) each of 120 ml volume, were connected via plastic tubing to a peristaltic pump (Watson Marlow™ 323 series). Each specimen (3.2 X 5. ± 0.4 cm) was placed inside the d-v containing a plastic platform to prevent the cement paste sample blocking the bottom liquor inlet. A polypropylene air-tight lid with a top outlet connected the d-v to the r-v as illustrated in Figure 2.3. A constant flow rate of 5ml per minute of test solution over the cement paste sample was maintained using the peristaltic pump. The pump was capable to supplying test solution to 5 d-vs. The vessels were placed on wooden racks i.e. without stirring, shaking or agitation. Sampling of the test solution was achieved via the r-v at planned time intervals, at seven day intervals 20 ml of test solution was pipetted from all the r-vs and an equivalent volume of test solution was added to maintain constant volume in the circuit (200 ml). This volume was sufficient to ensure the cement paste sample was completely submerged at all times.
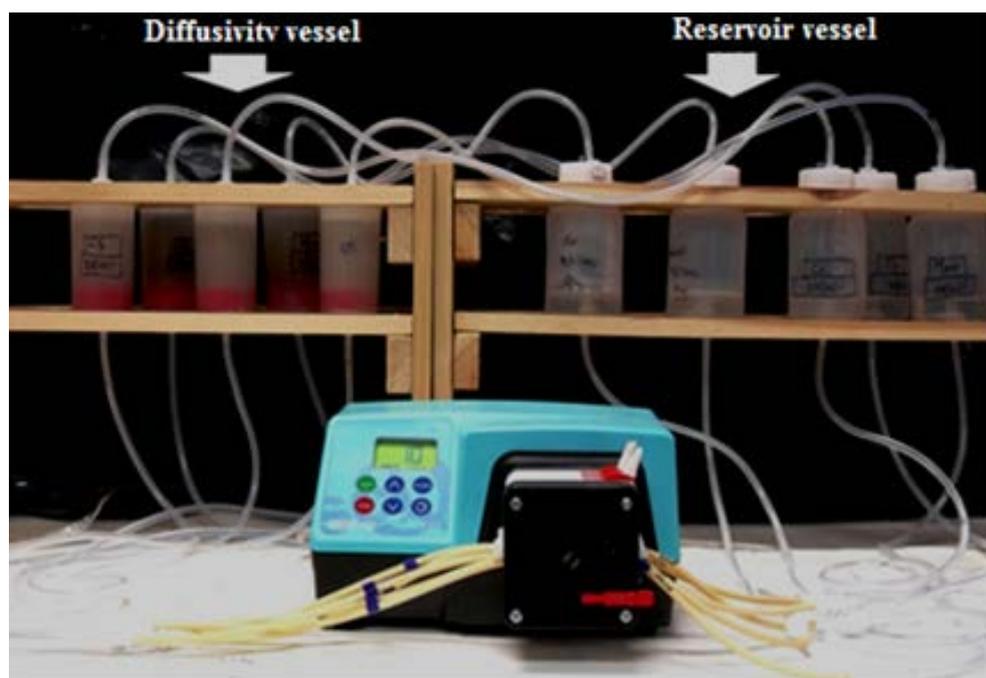
Figure 2.3 Experimental setup of closed circulating leaching system showing diffusivity vessel containing CPS and reservoir vessel.

2.4.2 Open circuit diffusivity system

Open circuit diffusivity studies were carried out using tap water; which was continuously supplied to the diffusivity vessel. A constant pump flow rate of 10 rpm (equivalent to 5ml per minute), was maintained using a peristaltic pump. Test solutions were collected in 40L plastic reservoir vessel. Sampling of test solutions was carried out after every 3rd and 4th day; the remaining test solution was discarded due to the limited capacity of the reservoir (Figure 2.4). Analysis of tap water was carried out using ICP-MS and Ion chromatography for cations and anions respectively, which was cross checked with water analysis data published by United Utilities for Preston area code PR1.
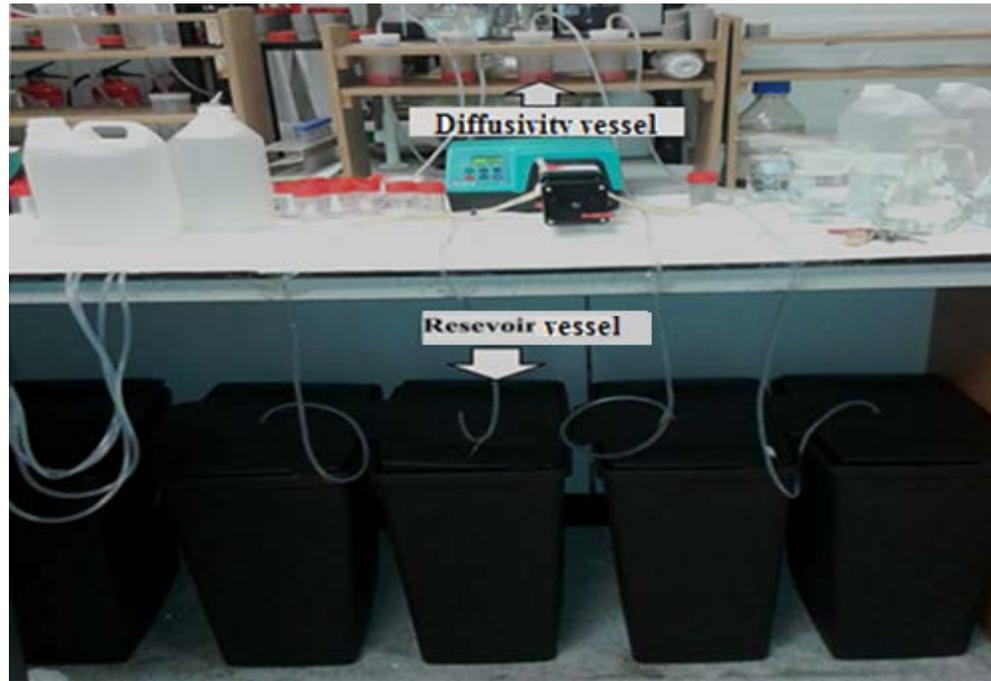
Figure 2.4 Experimental setup of open leaching system showing diffusivity vessel containing CPS and reservoir vessel.

2.4.3 Nature of test solution

Diffusivity studies were carried using five different types of test solutions: distilled water (DW); diluted Sellafield pore water (DSPW); concentrated Sellafield pore water (CSPW), tap water and John Innes No 3 soil solution (JISS).

2.4.3.1 Preparation of simulated Sellafield pore water

The simulated pore waters, diluted Sellafield water (DSPW) and concentrated Sellafield pore water (CSPW) were prepared in accordance with compositions reported by King et al. given in Table 2.3 [65]. The CSPW was prepared by dissolving the salts in de-ionised water using the following recipe: $MgCl_2$ (29 mmol/L), $CaCl_2$ (7.5 mmol/L), Na_2SO_4 (51.15 mmol/L), Na_2CO_3 (0.35 mmol/L), NaCl (3060 mmol/L) and KCl (8.40 mmol/L). To prepare DSPW, 1 ml of stock

CSPW solution was diluted with de-ionised water to 1L in standard volumetric flask.

Table 2.3 Nominal composition of the test solution used.

Parameter	Units	1 Concentrated Sellafield pore water (CSPW) *Sellafield BH3, DET1*	2 Diluted Sellafield pore water (DSPW) *Sellafield BH9B, SPFT3*
pH	pH	6.8	6.8
Na^+	mg/L	71600	19.3
K^+	mg/L	327	1.47
Mg^{2+}	mg/L	696	13
Ca^{2+}	mg/L	300	40.7
SiO_4^{4-}	mg/L	2.67	5.24
Cl^-	mg/L	108000	14.5
SO_4^{2-}	mg/L	4910	4.01

2.4.3.2 Preparation of John Innes Soil Solution (JISS)

The John Innes soil solution was prepared by following protocol. Approximately 5 grams of John Innes no 3 soil compost was suspended in 1L of deionised sterile water. This soil suspension was agitated for 2 minutes and allowed to settle overnight, which was then filtered through glass wool. The viable count of bacteria present in this solution was determined by using serial dilution techniques and as colony forming units (cfu), per ml of solution [89].

2.5 Chemical analysis of test solutions

2.5.1 pH measurement

The pH values of the test solutions were measured for all sampling points using a HANNA™ HI 2215 pH/ORP Meter. The pH electrode was calibrated prior to every measurement using buffer solutions of pH 4, 7 and 10.

2.5.2 ICP-MS

Inductively Coupled Plasma Mass Spectrometry (ICP-MS, Thermo X series™, UK) was used to measure the concentration of Na^+, Ca^{2+}, Co^{2+}, Sr^{2+} and Cs^+ present in test solution, using 0.1 mg/L of rhodium as an internal standard. All the samples were diluted with 2% (v/v) nitric acid. The instrument was calibrated using multielement standard solution for ICP-MS (Sigma-Aldrich, UK) (0.01 to 2 ppm), with calibration checks and blanks run after every 10 samples to check the instrument drift was within 10%, if the drift was over 10% samples were rerun. All calibrations gave R^2 values > 0.99.

ICP-MS was tuned on weekly basis with 10 ppb standard multielement tune A solution (Thermo Scientific, UK).

2.5.3 Ion Chromatography

Ion chromatography (Dionex ICS-2000 series™, UK) was used for the determination of Cl^- and SO_4^{2-}. All the samples were diluted 20 fold in de-ionised water before analysis. The instrument was calibrated using Cl^- and SO_4^{2-} standard solutions (2 - 250 ppm) diluted from a stock solution (500 ppm), prepared from salts (KCl and K_2SO_4). Standards were regularly re-run (after every 10 samples) and if instrumental drift was > 10%, samples were rerun. Instrument parameters are shown in Table 2.4.

Table 2.4 Instrument parameters for Dionex ICS-2000 for the determination of Cl$^-$ and SO$_4^{2-}$ in test solution

Instrument	Dionex ICS-2000
Eluent	5 mM KOH
Column	Dionex IonPac ASII
Flow rate	1 ml min^{-1}
Detection	50 mA current
Temeperature	25°C
Injection volume	25 µL
Software	Chromeleon 6.80

2.6 General growth media for the isolation and propagation of microorganisms

Media used for the general isolation of bacteria and fungi were: Nutrient Agar (NA), Nutrient broth (NB), Malt extract Agar (MA). Each medium was autoclaved at 121ºC for 20 minutes. Agar plates and slopes were prepared as required and stored at 4ºC until further use.

2.7 Characterisation of heterotrophic bacterial isolates

The bacterial isolates were tentatively identified in to broad microbial categories using primary diagnostic tests including their Gram reaction (positive or negative); morphology (rods or cocci), endospore formation (present or absent), and motility (by hanging-drop preparation) [90]. Where possible all isolates were sub-cultured and stored on slopes for future work.

2.8 Characterisation of fungal isolates

The characterisation of fungal isolates was achieved by examining the colony morphology, hyphal nature and the sporing structure using lactophenol cotton blue (LPCB) wet mount technique [91]. The identification of fungi was carried out by Professor L.H.G Morton, University of Central Lancashire, Preston.

2.9 Viable counts of bacteria

The presence of viable communities in the JISS test solution was carried out by using serial dilution technique and was expressed as colony forming units (cfu), per mL of solution [89].

2.10 Statistical analyses

As the data sizes were small (n< 30), the nonparametric Mann-Whitney U-test [92] was employed for the comparisons between two data sets of CPS and test solutions. Any correlations between variables were determined using the Pearson correlation coefficient. The statistics had an acceptance criteria of being statistically significant when $P < 0.05$.

2.11 Diffusion coefficient

The diffusion coefficient values for various ions at various stages of our experiments were calculated using semi-infinite media diffusion model. This model assumes that the contaminant concentration in the solid remains uniform, where leaching is diffusion controlled, and that the concentration at the solid-liquid interface is zero. In addition, this model applies to a situations where the cumulative fractional release is less than 20% [93], which was typical of our datasets.

Using this model, the diffusivity co-efficient of cations were calculated using following expression

$$\frac{\sum a_n}{A_o} \bullet \frac{V}{S} = \sqrt{2 \cdot \frac{D_e t}{\pi}}$$

where

a_n = amount of cations released during time interval n;

A_o = initial amount of cations in CPS;

V = volume of CPS;

S = surface area of the CPS;

D_e = effective diffusion coefficient; and

t = time period of diffusivity/leaching (days)

2.12 Rate of diffusivity

The rate diffusivity was calculated using the following expression

$$\text{Rate of diffusivity } (\mu g/cm^2/day) = \frac{\text{cumulative concentration of ion (ppb)}}{5 \times \text{surface area } (cm^2) \times \text{time period (days)}}$$

The rate of diffusivity values ($\mu g/cm^2/day$) quoted in the numerous graphs in the chapters 4 to 9 are a reflection of parametric changes on the release of cations and anions from the cement paste samples. These values are not diffusion coefficients as discussed in chapter 3 page 92 as they have not taken in to

consideration the initial content of the cement paste sample of the particular cation/anion.

All the steps were taken to ensure quality of data, weighing balanced was checked with standard weights before weighing the sample; all the glassware were thoroughly washed and triple rinsed with de-ionised water and dried at 80°C. Standardised aseptic techniques were followed while carrying out microbiological procedures and analysis.

Chapter 3: Cement chemistry discussion

3.1 Introduction

This chapter encompasses both:

a. a description of the fundamentals of cement chemistry to allow the reader to understand and appreciate some of the subtleties that influence this chemistry prior to engagement with the results.

b. some results/data that have been generated in this PhD project are included to emphasise and underpin this understanding.

The chapter has been formatted in this manner also for the ease of reading and for ergonomic reasons, i.e. to minimise the reader flicking from one chapter to another and to minimise duplication of data/results in more than one chapter. The bulk of the diffusion data is reported in subsequent chapters that are devoted to a specific parametric topic.

3.2 Physical properties of cement paste composition

3.2.1 Preparation/ composition confirmation

The measured compositions of the as received OPC, BFS and PFA from the NNL were similar with other cements, slags and fuel ash used in waste encapsulation [94]. The cation (Sr^{2+}, Cs^+ and Co^{2+}) concentrations selected were based on likely compositions of encapsulated nuclear waste [4]. Cation chloride and carbonate compounds were selected taking into consideration experiments involving influence of microorganisms on the diffusivity of cations from the CPS. Use of other cation compounds such as their nitrates or sulphates would influence the

genera and metabolic activity of microorganisms present in the test solution, not necessarily reflecting a realistic situation.

The hydration of OPC and additives such as BFS and PFA has received significant attention for a variety of reasons. Some of these studies have addressed the ratio of water to cement (*w/c*) and its impact on the formation of the various phases produced during hydration, strength, porosity, tortuosity, pore size etc. of the cement pastes [95, 96]. Other studies have concentrated on the chemistry of make-up water and how for example the inclusion of salts in this water influences the pore water chemistry [97]. Although our studies are restricted to only one *w/c* namely 0.37 and two formulations with BFS:OPC and PFA:OPC (3:1 ratio for each), the composition of the make-up water has been varied due to the inclusion of cation chlorides (Sr^{2+}, Cs^+, Co^{2+} and mixture of all three) and largely at two concentrations ($\approx$120 g/L and $\approx$12 g/L). These different water compositions (pore and free), their chemistries and subsequent impact on the diffusivity/leachability of added and inherent ions (such as Na^+, K^+, Mg^{2+}, Ca^{2+} and SO_4^{2-}) in BFS/PFA:OPC have been studied. It is sensible at this stage of the thesis to consider cement hydration, pore water chemistry and their impacts on cation/anion diffusivities.

3.2.2 Hydration

The hydration of cement is a series of irreversible exothermic chemical reactions between cement and water. The reaction of water with the cement in concrete is extremely important to its properties and may continue for many years. Portland cement consists primarily of calcium aluminates and calcium silicates as illustrated in Table 3.1and Figure 3.1 below:

Table 3.1 Typical composition of Portland cement with chemical composition and weight percentage [16].

Cement Compound	Weight Percentage	Chemical Formula
Tricalcium silicate (C_3S)	50%	Ca_3SiO_5 or $3CaO \cdot SiO_2$
Dicalcium silicate (C_2S)	25%	Ca_2SiO_4 or $2CaO \cdot SiO_2$
Tricalcium aluminate (C_3A)	10%	$Ca_3Al_2O_6$ or $3CaO \cdot Al_2O_3$
Tetracalcium aluminoferrite (C_4AF)	10%	$Ca_4Al_2Fe_2O_{10}$ or $4CaO \cdot Al_2O_3 \cdot Fe_2O_3$
Gypsum	5%	$CaSO_4 \cdot 2H_2O$

Gypsum controls the rate of setting and influences the rate of strength development.

Figure 3.1 composition of cement clinker [98]

Addition of water allows each of the compounds to undergo hydration process contributing to the final concrete product. During this process, tri-calcium silicate (C_3S) reacts quickly and is responsible for most of the early strength (first 7 days). The reaction products calcium hydroxide ($Ca(OH)_2$) and calcium silicate hydrate (C-S-H) phase are formed [95]. Di-calcium silicate (C_2S), rather reacts slowly and contributes only to the strength at later times. Similar reaction products with significantly lower amount of $Ca(OH)_2$ are formed in comparison with C_3S

hydration. C_3A reacts much faster than C_3S and C_2S liberating a large amount of heat during first few days. However, calcium sulphate present in the cement retards the hydration rate of C_3A [16]. Tetracalcium aluminoferrite (C_4AF) reduces the heat of hydration and also helps the setting properties of cement [99].

The hydration process takes place via two mechanisms:

(a) through solution hydration

(b) solid state hydration.

These hydration reactions are illustrated in the Figure 3.2 [100]
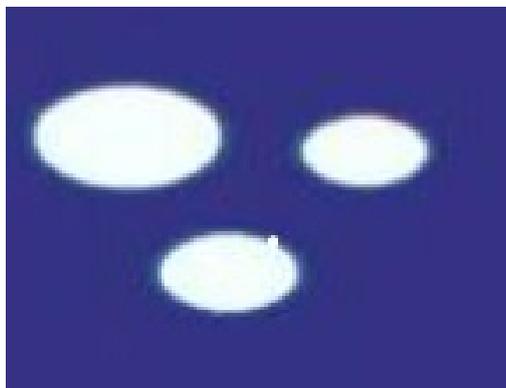
Cement grain in water
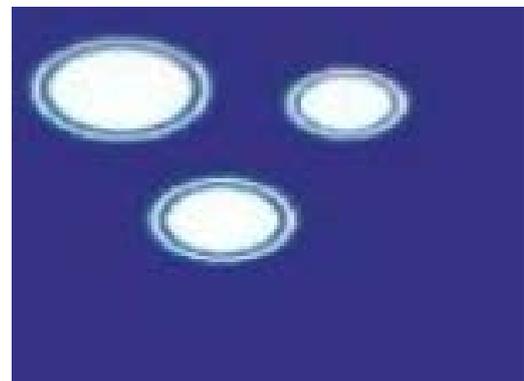
Growth of colloidal coating calcium silicate (CSH) gel
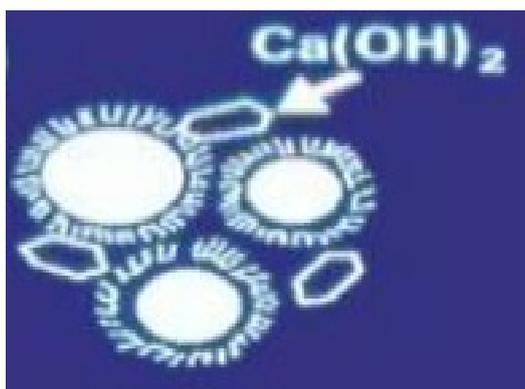
Local disruption and secondary growth of CSH gel with some crystallisation of Calcium
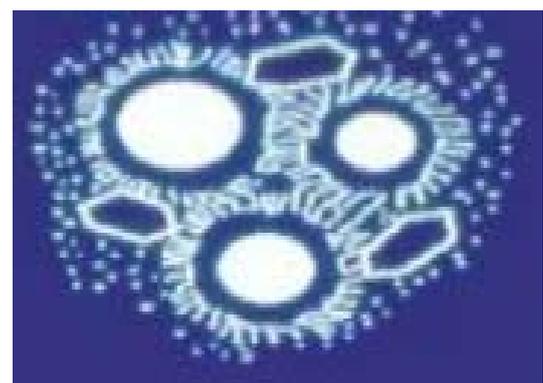
Continued growth of CSH gel with infilling by CSH gel and calcium hydroxide crystals.

Figure 3.2 Cement hydration process [100]

There are five stages of cement hydration that occur comparatively quickly (stage 1 less than 15 minutes) to stage 5 that can occur over many years. These stages are reported in

Table 3.2*: The five stages of concrete curing*

Stage no	Reaction	Kinetics of reaction	Chemical process	Time period	Illustration[100]
1	Initial hydrolysis	Chemical control; rapid	Dissolution of ions	< 15 minutes	
2	Induction period	Nucleation control; slow	Continued dissolution of ions	2 – 4 hours	
3	Acceleration	Chemical control; rapid	Initial formation of hydration products	2 – 4 hours	
4	Deceleration	Chemical and diffusion control; slow	Continued formation of hydration products	Several hours	
5	Steady state	Diffusion control	Slow formation of hydration products	years	
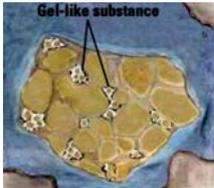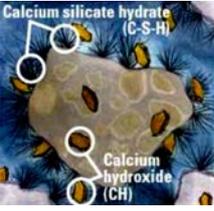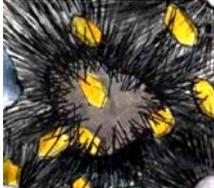
The hydration reactions of silicates, aluminates and aluminoferrites are:

a. $2Ca_3SiO_5 + 11\ H_2O \rightarrow 3\ CaO.2SiO_2.8H_2O + 3\ Ca(OH)_2$
    Calcium silicate hydrate
    (C-S-H)

b. $Ca_2SiO_4 + 9H_2O \rightarrow 3\ CaO.2SiO_2.8H_2O + 3Ca(OH)_2$
    Calcium silicate hydrate
    (C-S-H)

c. $Ca_3Al_2O_6 + 3CaSO_4.2H_2O + 26H_2O \rightarrow 6CaO.\ Al_2O_3.\ 3SO_3.\ 32H_2O$
    Ettringite

d. $Ca_3Al_2O_6 + 6\ CaO.\ Al_2O_3.\ 3SO_3.\ 32H_2O + 4H_2O \rightarrow 3\ (4CaO.Al_2O_3.\ SO_3.\ 12H_2O)$
    Calcium mono-sulphoaluminate

e. $Ca_3Al_2O_6 + Ca(OH)_2 + 12H_2O \rightarrow 4CaO.Al_2O_3.\ 12H_2O$
    Tetra-calcium aluminate hydrate

f. $4CaO.Al_2O_3.Fe_2O_3 + 10H_2O + Ca(OH)_2 \rightarrow 6CaO.\ Al_2O_3.\ Fe_2O_3.\ 12H_2O$
    Calcium aluminoferrite hydrate

Several factors influence the process of hydration:

- chemical composition of cement

- cement type

- sulphate content

- fineness of aggregates/additives

- water: cement ratio

- curing temperature

- effects of additives (BFS, PFA etc.)

All of the above factors except nature of additives remained unchanged in our studies, however the nature and concentration of the salt added to the makeup water was changed as previously described. It was anticipated that using different salts in makeup water would affect chemical reactions with the various phases during curing and the formation of calcium hydroxide and hydrates. Cement

hydration in the presence of chloride, as is the case for the majority of our diffusivity experiments, Friedel's salt ($3CaO.Al_2O_3.CaCl_2.10H_2O$) and Kuzel's salt ($3CaO.Al_2O_3.0.5CaSO_4.0.5CaCl_2.10H_2O$) can be formed in concrete [101]. Formation of these salts could be accentuated by the Cl^- in the makeup water in our studies. Inherent Cl^- present in OPC (0.11 wt%), BFS (0.26 wt%) and PFA (0.05 wt%) also contributes to formation of these salts (Table 4.2 and Table 5.2). It has been demonstrated that there is a chemical equilibrium between the chloride concentration in hydration products and the chloride concentration in the pore water solution [102]. The distribution of chloride in concrete depends on the total chloride content. The amount of bound chloride decreases with decreasing content of dissolved chloride in the pore solution [103]. It has also been shown that the amount of chloride in the pore solution increases significantly on carbonation [104].

The CPSs that had been aged in the laboratory environment for 240 days would undergo some carbonation, but as this conversion is a relatively slow process and the depth of penetration, would be insignificant for this time period i.e. only a few mm.

It is unlikely that the solid $SrCO_3$ added at the cement paste make-up stage interacted during curing/post-curing with other materials/hydrates as on dissection of the appropriate cement paste samples, the $SrCO_3$ particles were clearly visible and relatively uniformly distributed throughout the cylinder. This is not surprising as the $SrCO_3$ is only partially soluble in water ($K_{sp} = 10^{-10}$).

3.2.3 BFS v/s PFA

The influence of cement paste composition on the leaching of radionuclides has received some attention, but with the greater number of publications targeting the influence of the water to cement ratio [105-108]. Various compositions excluding the water ratio have included incorporating other minerals such as Blast Furnace Slag (BFS), Pulverised Fly Ash (PFA) and others to variety of superplasticisers [109-112]. As reported in this thesis only the impact of incorporating BFS and PFA with a water to cement ratio of 0.37 in cement paste samples on the diffusivity of simulated radionuclides (Cs^+, Sr^{2+} and Co^{2+}) have been addressed. Although the chemical composition of BFS or PFA in the cement paste ought to have marginal impact on the diffusivity of cations and anions from the cement paste samples; the data reported later indicates this is quite contrary.

Addition of siliceous materials, such as BFS and PFA to cement has number of benefits such as to increase strength of the wet mix, to reduce heat evolution during set and to improve the durability and resistance to chemical attack [25]. PFA, artificial pozzolanas, contain un-melted residual minerals such as quartz as well as mullite, graphite, spinel which are thermally generated, contained within a glassy matrix [113]. These additives have a profound impact on the mineralogy of the cement paste composition during and post-curing. The engineering benefits include enhanced resistance to thermal cracking due to lower heat of hydration, improvement of ultimate strength, reduced permeability due to pore refinement, and a better durability to chemical attacks such as chloride, sulphate water, soil and alkali- aggregate expansion. Replacement of cement by BFS reduces the C_3A content of the material and decreases the CH content and the permeability of the mortar/concrete [114]. The

reaction of pozzolanic material with calcium hydroxide liberated by the hydrating Portland cement which forms cementitious compounds generally known as C-S-H gel can be represented as:

$$C_3S + 6H \rightarrow C_3S_2H_3 + 3Ca(OH)_2$$

$$3C_3S + 4H \rightarrow C_3S_2H_3 + 3Ca(OH)_2$$

$$Ca(OH)_2 + (SiO_2 + Al_2O_3) \rightarrow C_3S_2H_3 + \text{other components}$$
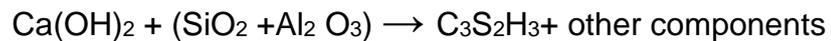
Thus increases the properties of hardened cement paste. In our studies, the cement paste mixture preparation of PFA:OPC showed high fluidity in comparison to the BFS: OPC mixture. During the curing stage, loss of liquid (bleed) was more prominent in BFS:OPC cement paste samples in contrary to the PFA:OPC cement paste samples, lost considerably smaller quantity.

3.2.4 Distribution of water

Make-up water distributes via three different interactions: water that was chemically bound into the cement paste, the physically bound or "glassy water" that interacted with the surface of the gel pores in the paste (free water), and unbound water molecules that are restrained within the larger capillary pores of cement paste (pore water) [115]. Free water and pore water of all the cement paste samples were measured by weight loss at 105^0C (section 2.3.3) [16]. Some workers have suggested that gel water may also be lost at this temperature [116]. Although the volume of make-up water gave a *w/c* of 0.37 this ratio excluded the moisture associated with the OPC, BFS and PFA which was measured 26.2%, 0.2% and 0.1% respectively (Table 4.2 and Table 5.2). This moisture content represents in the cement paste cylinders about 4% w/w average which is

equivalent to 3.4 g and 3.0 g for BFS:OPC and PFA:OPC CPSs respectively. The actual influence of this moisture content will remain consistent throughout. This is due to the fact that higher percentage of moisture comes from OPC, which was constant along with the amount of water used in all the CPS preparations. It is generally accepted that a *w/c* of about 0.25 is required to fully hydrate the calcium silicates but complete hydration rarely occurs below a *w/c* of 0.38 [117] cf our ratio of 0.37 but excludes moisture levels of the original materials. At this point hydration will proceed leaving a small amount of water in fine gel pores. The hydrated cement is a porous mass of C-S-H gel comprising of both hydrated and unhydrated cement particles along with several different types of water. A chemically combined "bound water" is non evaporable and forms a definite part of hydrated compounds, whereas unbound water is free and evaporable present in the different types of pores [117]; the moisture content of the original materials must fall into unbound water. The hydration process will stop if there is insufficient water to fill the gel pores. Water also fills the capillary pores between the hydrated cement particles. As hydration proceeds, the formation of more hydration products decreases the amount of water in capillary pores and grow into the space while the gel water increases, reducing overall porosity. Studies have shown that at complete hydration, 1 g cement binds 0.23 g water and 0.19 g of strongly physically bound water, so complete and uninhibited hydration requires a *w/c* of ≈0.42 [117]. If the moisture levels in the original feed materials are included with make-up water volumes then *w/c* is very close to this number.

In addition to the *w/c* other factors can influence porosity, in our study the composition of make-up water and subsequent reactions of dissolved salts with C-S-H gels and other hydrates were considered. Although the hydration process

of cement continues over many months if not years with implications to chemistry and diffusivity of ions, the distribution of make-up water within the cement paste samples will reach a steady state within the first few weeks of curing. It is the distribution of this water and its corresponding composition that can influence the kinetics and thermodynamics of ion diffusivity [118].

The first partitioning of make-up water occurs due to bleed loss, which is dependent on both the *w/c* value and cement paste composition i.e. ratio of OPC to additives [119]. From previous concrete bleed water studies the information suggests that our *w/c* of 0.37 (but corrected to near 0.42 due to the moisture content of original feed materials) would be about 0.9 g [120] i.e. 0.9 cm^3 which represents a height of about 1mm in the moulds used to prepare our cement paste samples. Observations after 7-day curing recorded a height of 2 to 3mm of bleed water on the surface of the cement paste cylinder, this difference could be due to the presence of cations in the make-up water as previously reported in this thesis. The addition of cations not only influenced bleed water volume but the surface of the cement paste cylinder. The loss of bleed water took shorter duration of time from ≈3% $SrCl_2$ CPS in comparison with control CPS which was substantially slower than all other CPSs. However, there was no bleeding noticed from 3%$SrCO_3$ CPS.

Although the same ratio of water to cement/additive was used for all the studies, the influence of added chloride salt affected both free water value and the pore volume and consequently would affect the pore water value. The bound water, free water and pore water values calculated from the moisture content (section 2.3.3) of their respective ≈86 g BFS:OPC CPS used in our diffusivity experiments are reported in Table 3.3. The corresponding values in Table 3.4 are for

PFA:OPC, but in this case the weight of cement paste samples was on average ≈74g.

Table 3.2 Water distribution in some BFS:OPC CPSs

CPS	Makeup water + moisture (g)	Free water and pore water (g)	(%)	Bound water (g)	(%)
control	26.2	11.9	45.4	14.3	54.6
≈3% SrCl$_2$	25.5	19.3	75.7	6.2	24.3
≈3% CsCl	25.8	16.7	64.7	9.1	35.3
≈1.3% Co Cl$_2$	26.2	17.9	68.3	8.3	31.7
combined cation chlorides	24.6	17.6	71.5	7	28.5

Table 3.3 Water distribution in some PFA:OPC CPSs

CPS	Makeup water + moisture (g)	Free water and pore water (g)	(%)	Bound water (g)	(%)
control	23.2	3.2	13.8	20	86.2
≈3% SrCl$_2$	23.2	5.6	24.1	17.6	75.9
≈3% CsCl	22.6	3.8	16.8	18.8	83.2
≈3% SrCO$_3$	21	3.9	18.6	17.1	81.4

3.2.5 Segregation and bleeding

The differences in the size of particles and specific gravity may cause the segregation of aggregates during the settling and curing stage of cement mixture [16]. Segregation is generally overcome by adequate vibration, but not over-vibration of the cement mix, to prevent the lighter and denser materials partitioning [121]. As hydration processes also occur during the first phases of curing, the segregation of aggregates will also lead to differences in the water

profile. Although our cement paste samples were agitated only for 4 minutes after mixing the OPC, BFS or PFA and make-up water; segregation was evident on dissection of the cured CPS cylinders. Segregation affected cation distribution of both added cations in the make-up water such as Cs^+ and Sr^{2+} but also inherent cations present in both OPC and BFS or PFA such as calcium (Figure 3.3). This segregation was also instrumental in affecting water (Table 3.3 to 3.4) and pore size distribution (Figure 3.4 to 3.5). As few, if any, previous studies have monitored segregation with make-up water composition, we postulate that the following sequence is likely to occur:

(a) hydration of OPC, BFS or PFA particles, not necessarily complete hydration, which allows

(b) the cations present in make-up water to be absorbed on to the surface of OPC, BFS or PFA particles and/or to react with these particles resulting in; the chemistry of hydrates being influenced, producing either increased gel formation and/or further insoluble matter that impacts on pore size and pore volume.

From the distribution of cations i.e. enrichment in the upper regions would suggest that adsorption on to less dense additives occurred and/or a chemical reaction occurred between the added cations and hydrates to produce lighter, slightly more voluminous solids and smaller, denser particulate material settled to the lower regions affecting pore size and water distribution. This segregation could have been exacerbated by the density of the make-up water which ranged from 1.0 g/cm^3 for distilled water to 1.3 g/cm^3 for mixed cations (Cs^+ plus Sr^{2+} and Co^{2+}), with densities of 1.14 and 1.08 for strontium chloride and caesium chloride make-up water respectively. The more dense liquors will uphold the less dense

particles with more dense and possibly smaller particles settling to achieve a better packing fraction with a reduction in pore volume.

	Sr contaminated CPS		Cs contaminated CPS	
	% Sr	% Ca	% Cs	% Ca
Top	2.96	31.6	3.11	26.6
Middle	3.13	26.1	2.93	23.1
Bottom	1.75	16.2	2.2	21.1
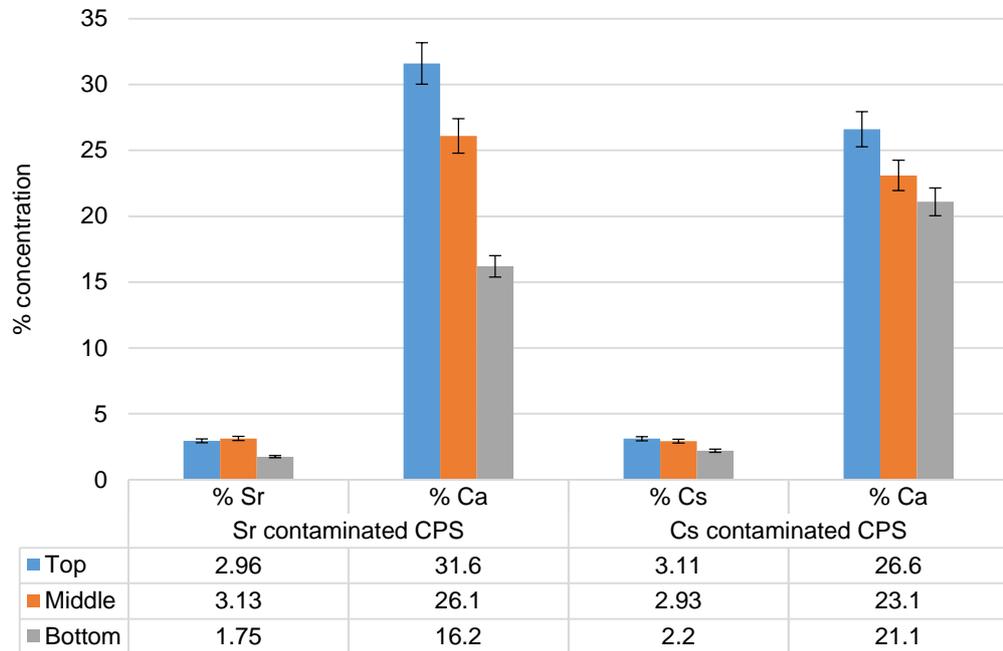
Figure 3.3 Segregation of Ca^{2+} and added cations

	Control	3% SrCl2	3% CsCl	3% SrCO3
Top	7.1	12.8	1.2	5.8
Middle	4.8	8.2	3.6	4.6
Bottom	3.7	6.3	2.2	4.1
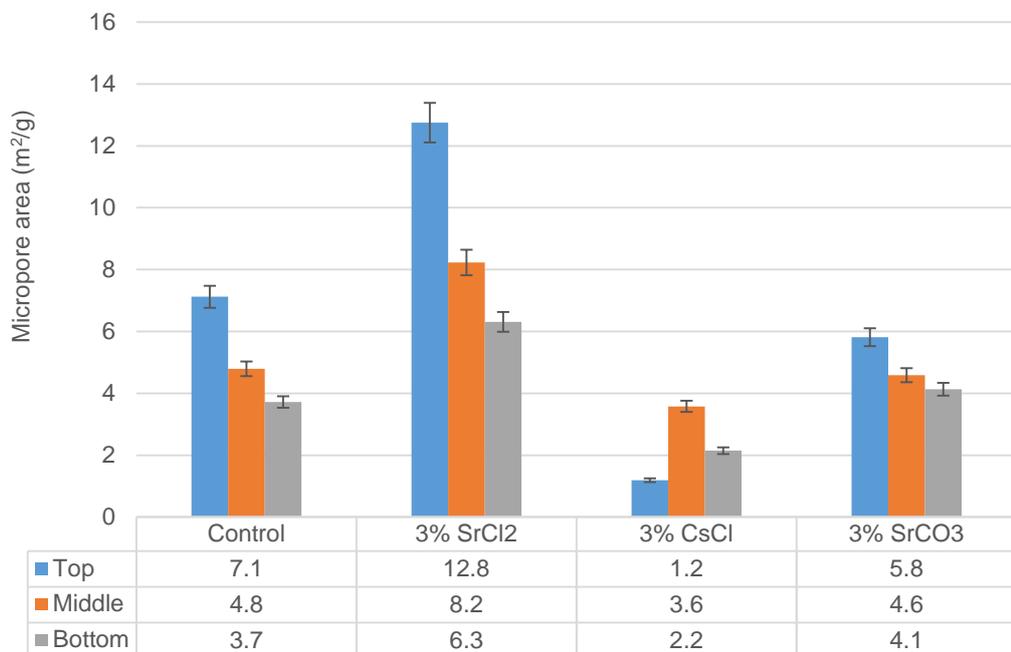
Figure 3.4 Micropore area of BFS:OPC CPSs

	Control	3% SrCl2	3% CsCl	3% SrCO3
■ Top	4.0	3.4	3.0	3.8
■ Middle	3.1	2.2	4.2	3.5
■ Bottom	4.5	3.5	3.5	4.0
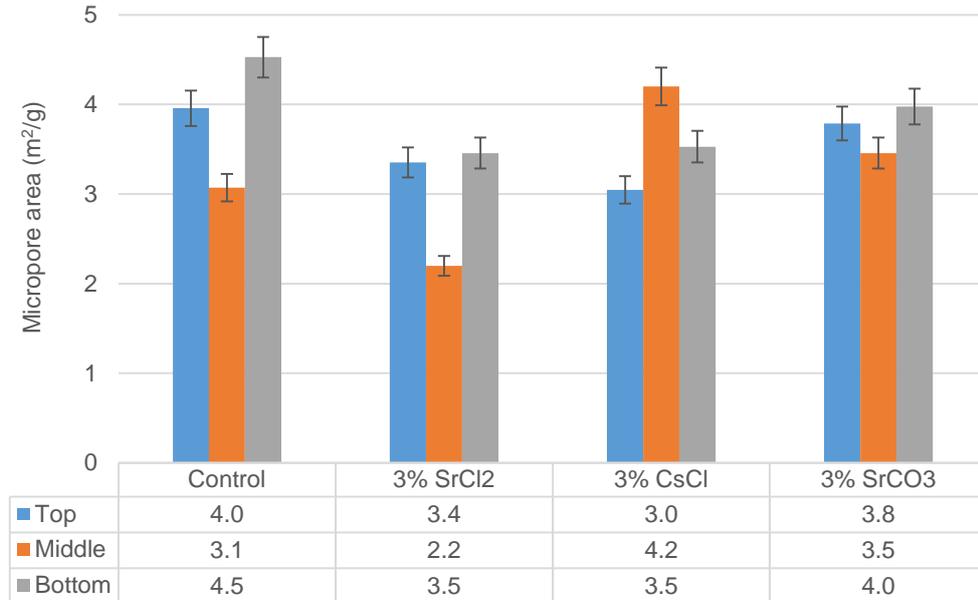
Figure 3.5 Micropore area of PFA:OPC CPSs

3.2.6 Pore water composition

The composition of pore water is influenced by:

(a)   composition of make-up water,

(b)   formulation of cement paste,

(c)   curing time.

At initial stages, the pore water contains largely alkali hydroxides which will become depleted at the surface due to the recirculation of test solution in our experiments as the diffusivity of sodium and potassium first, but then replaced by calcium hydroxide liberated from the solid cement phases. This transformation reduces the pH of pore water from a peak of about 14.0 to around 12.0. Hydroxyl concentration of pore water also decreases with increasing level of cement substitution by PFA; this hydroxyl reduction also occurs when BFS substitutes for cement but the effect is less marked than for PFA because of calcium content.

63

When chloride as sodium chloride is incorporated into the make-up water the dissolved chloride concentration of pore water decreases with hydration over a short timescale i.e. 4 days and is also reduced by a higher *w/c* [121]. This is attributed to the incorporation of Cl^- in to Friedel's salt, the formation of this salt increases over the period of time.

In the early stages of hydration the concentration of sodium and potassium cations are typically 0.05 to 0.2M and 0.1 to 0.6M respectively depending on the OPC formulations but for calcium ions a fraction of these concentrations (<0.05M) [16, 54]. Sulphur possibly as sulphate in pore water is generally a few thousand micro-molar concentration, with the hydroxyl concentration significant around 0.2M. The presence of these ions affects the ionic strength of pore solution and hence the solubility of cement hydrates, but total dissolution of these hydrates is highly unlikely and presents challenges in determining which are physically or chemically bound.

Understanding the pore water chemistry will assist in the interpretation of cation diffusivity from the cement paste samples.

3.3 Chemistry of solid and liquid system

In the present research, the experiments were designed to simulate two leaching conditions:

(a)   diffusivity occurring in stagnant water where the reaction can reach equilibrium and

(b)   diffusivity in mobile or stirred water where the reaction may not reach equilibrium.

Cementitious material in an aqueous solution is an excellent example of salt in a solvent. De-ionised water is the most aggressive aqueous surrounding for concrete because of its lower ionic strength. Dissolution of concrete occurring in stagnant water can reach equilibrium resulting in a saturated solution. The reaction quotient (Q) is equal to the solubility product (K_{SP}) of respective reactants. The reactant with lower K_{SP} will most likely to dissolve first in comparison with the reactants with higher K_{SP} values.

If "Q" is greater than K_{SP}, the solution reaches to over-saturation state and the dissolved salt will precipitate until the reaction equilibrium (K) is reached. If the "Q" is smaller than K_{SP}, there is under-saturation and the salts will dissolve until the K_{SP} is reached [39].

In the case of mobile phase, the mobile water, rate of reaction and diffusion velocities play an important role.

The steps involved in the mobile phase can be represented as follows:

(a)   The time taken for water to reach the reaction place

(b)   The chemical reaction taking place (e.g. $Ca(OH)_2 \rightarrow Ca^{2+} + 2OH^-$)

(c)   The time taken for products (Ca^{2+}, $2OH^-$) to leave the reaction place.

Step 1 and 3 are the rate determining steps and depend on the dissolution velocities of the reaction and products [39]. However, ion strength and common ion effect also influences the reaction.

All the solid substance in hardened cement paste and in the pore solution are in thermodynamic balance with each other and surroundings. This balance is disturbed in a leaching process and the dissolution of these substance depend on their solubility products.

The soluble compounds that could have been present in the test solution and their respective K_{sp} and K values are provided in Table 3.5. The solubility product values are designated to the compounds which are sparingly soluble.

Table 3.4 The Ksp and K values of possible soluble compounds present in the test solution

Cation	Compound	Solubility product	solubility at room temperature in water		Equilibrium constant
		K_{sp}	g/L	mmol/L	(K)
Ca^{2+}	$CaSO_4.2H_2O \rightarrow Ca^{2+} + SO_4^{2-} +2H_2O$	$10^{-4.58}$	2.49	14.0	$10^{2.3}$
	$Ca(OH)_2 \rightarrow Ca^{2+} + 2OH^-$	$10^{-5.2}$	1.85	24.9	$10^{1.22}$
	$CaCO_3 \rightarrow Ca^{2+} + CO_3^{2-}$	$10^{-8.48}$	0.01	0.35	$10^{3.22}$
	$CaCl_2 \rightarrow Ca^{2+} + 2Cl^-$		595	5,360	
Sr^{2+}	$SrSO_4 \rightarrow Sr^{2+} + SO_4^{2-} +2H_2O$	10^{-7}	0.11	0.6	
	$Sr(OH)_2 \rightarrow Sr^{2+} + 2OH^-$	10^{-3}	4.1	33.7	
	$SrCO_3 \rightarrow Sr^{2+} + CO_3^{2-}$	10^{-10}	0.01	31.3	
	$SrCl_2 + Sr^{2+} + 2Cl^-$		435	2,744	
Mg^{2+}	$MgSO_4 \rightarrow Mg^{2+} + SO_4^{2-} +2H_2O$		260	2,159	
	$Mg(OH)_2 \rightarrow Mg^{2+} + 2OH^-$		0.01	0.2	
	$MgCO_3 \rightarrow Mg^{2+} + CO_3^{2-}$		0.11	1.3	
	$MgCl_2 + Mg^{2+} + 2Cl^-$		542.5	5,698	
Na^+	$NaOH \rightarrow Na^+ + OH^-$		420	10,652	
	$NaCl \rightarrow Na^+ + Cl^-$		357	6,102	
	$Na_2SO_4 \rightarrow 2Na^+ + SO_4^{2-}$		47.6	335	
	$Na_2CO_3 \rightarrow 2Na^+ + CO_3^{2-}$		71	700	
K^+	$KOH \rightarrow K^+ + OH^-$		970	17,290	
	$KCl \rightarrow K^+ + Cl^-$		347	4,657	
	$K_2SO_4 \rightarrow 2K^+ + SO_4^{2-}$		68.5	393	
	$K_2CO_3 \rightarrow 2K^+ + CO_3^{2-}$		1120	8,104	
Cs^+	$CsOH \rightarrow Cs^+ + OH^-$		3995	26,367	
	$CsCl \rightarrow Cs^+ + Cl^-$		1617	9,650	
	$Cs_2SO_4 \rightarrow 2Cs^+ + SO_4^{2-}$		1670	4,615	
	$Cs_2CO_3 \rightarrow 2Cs^+ + CO_3^{2-}$		2605	7,996	

Table 3.5 Chemical equilibrium expression for each solid phase [122, 123]

Phase	Chemical composition	Chemical equilibrium expression	log Ksp
CH	$Ca(OH)_2$	$Ksp = [Ca][OH]_2$	-5.2
C-S-H	$(1.65)CaO.SiO_2.(2.45)H_2O$	$Ksp = [Ca][OH]_2$ *	-5.6
Ettringite	$3CaO.3CaSO_4.Al_2O_3.32H_2O$	$Ksp = [Ca]_6[OH]_4[SO4]_3[Al(OH)_4]_2$	-44
Hydrogarnet	$3CaO.Al_2O_3.6H_2O$	$Ksp = [Ca]_3[OH]_4[Al(OH)4]_2$	-23.1
Gypsum	$CaSO_4.2H_2O$	$Ksp = [Ca][SO_4]$	-4.6
Friedel's salt	$3CaO.CaCl_2.Al_2O_3.10H_2O$	$Ksp = [Ca]_4[OH]_4[Cl]_2[Al(OH)_4]_2$	-29.1
Brucite	$Mg(OH)_2$	$Ksp = [Mg][OH]_2$	-10.9
Mirabilite	$Na_2SO_4.10H_2O$	$Ksp =[Na]_2[SO_4]$	-1.2
Halite	$NaCl$	$Ksp = [Na][Cl]$	1.6

*C-S-H is assumed to decalcify like CH with a lower solubility constant

The major constituents of cement paste are calcium silicate hydrate (C-S-H), calcium hydroxide (CH) and aggregates as previously described and illustrated. In a leaching process, it is mainly CH that is dissolved and transported away with a diminishing CH, C-S-H will also start to dissolve (Table 3.6).

3.3.1 Influence of test solution composition

The diffusivity test solutions varied from deionised water to deionised water having been contacted with John Innes No 3 soil. The former has been the most frequently used to measure the diffusivity and leaching of radionuclides from cement paste samples. It does not however represent the most realistic liquid that is likely to come into contact with nuclear waste in a GDF or even shallow burial repository. The Sellafield pore water solutions (CSPW and DSPW) may be more representative, providing of course the GDF was sited within the vicinity of that site, but could be a good representation of the water that comes into contact

with nuclear waste buried at the low level site at Drigg. Nonetheless none of these solutions contained a key ingredient, namely microorganisms. This was certainly not true for the JISS. The chemical compositions of the various test solutions is provided in Table 3.7 for comparative purposes.

It is interesting that Preston tap water is far richer in chloride and sulphate than the JISS extract, but even these concentrations (0.32 and 0.30 mmoles/L) respectively are unlikely to have influenced the chemistry of ions in solution and diffusivity of ions from the cement paste, as the solubility of say strontium sulphate (most insoluble sulphate of the cations under investigation) in water at room temperature would be 1.75 mmoles/L (K_{sp} 3.5 x 10^{-7}).

Table 3.6 Concentration of some ions in the various test solutions (ppb)

Parameter	Test solution				
	DW	Tap water	CSPW	DSPW	JISS
pH	7	7.3	6.8	6.8	7.21
Cl^-	-	11425	108000000	14500	62
SO_4^{2-}	-	28862	4910000	4010	8588
Na^+	-	5098	71600000	19300	1541
K^+	-	313	327000	1470	3576
Cs^+	-	-	-	-	5
Mg^{2+}	-	1058	696000	13000	1009
Ca^{2+}	-	7037	300000	40700	29
Sr^{2+}	-	13	-	-	11

From the published 'recipe' of John Innes No 3 soil [124], it is more than likely that the water extract contained in addition to the ions reported in Table 8.3, nitrate and phosphate. The former would have little or no effect on the chemistry of all the cations in solution, as all nitrates are soluble, but phosphate could be

more influential than all other anions as the K_{sp} for strontium phosphate for example is 4 x 10^{-28} which is a far smaller than for strontium carbonate (5.6 x10^{-10}). This very low solubility of strontium phosphate did not hinder the release of strontium from the ≈3% strontium chloride cement paste into solution (maximum Sr^{2+} concentration in the JISS test solution for the closed system 0.34 mmoles, i.e. about 0.6% of Sr^{2+} leached from the cement paste).

3.3.2 pH effect

The pH values of the test solution during the diffusivity experiments varied from ≈7 to over 12. The initial pH value for most of these experiments was 7 (deionised water) and 7.03 (tap water), but others for example the simulated CSPW and JISS affected by the make-up salts or the ions leached from the soil, had a pH value of 6.8 and 7.21 respectively. Although pH values were regularly and routinely measured during the course of the experiments the concentration of hydroxide and carbonate were not.

The alkalinity (hydroxide concentration) can be calculated from the formula:

$$[OH^-] = K_w/[H^+] = 10^{-14}/[H^+]$$

Assuming an ideal situation i.e. vey dilute solution, then for the following pH values the concentration of hydroxide ions (Table 3.8) will be

Table 3.7 Predicted hydroxide concentration based on pH value

pH value	OH$^-$ (moles/L)
7	10^{-7}
8	10^{-6}
9	10^{-5}
10	10^{-4}
11	10^{-3}
12	10^{-2}

One of the highest variation in pH value was for the 0.3% strontium chloride contaminated BFS:OPC; the initial pH value after 7 days was 7.50 increasing to 11.85 after 105 days (Figure 4.9). This would require about 10 mmoles of hydroxide i.e. about 5 mmoles of Ca(OH)$_2$. The maximum calcium concentration measured for this experiment was 2.24 mmoles/L which suggest some of the other alkali/alkaline earth metals (Na$^+$, K$^+$, and Mg^{2+}) contributed to the pH increase.

At pH values above 12, the concentration of hydroxide ions will be equivalent to if not greater than the chloride and/or sulphate concentrations due to the anions diffused from the cement paste (for both these cations for the majority of the experiments the maximum concentration was significantly less than 10 mmoles). As will be discussed latter this concentration of hydroxide would influence the solubility of the cations; Ca^{2+}, Sr^{2+}, Co^{2+} etc.

From the Bjerrum plot (Figure 3.6) below (which is for a water with a total carbon value of 1mmole/L) the concentration of both carbonate and bicarbonate can be predicted. At pH values of about 10 and above, the concentration of HCO$_3^-$ rapidly decreases with a corresponding increase of CO$_3^{2-}$ concentration. If anything a 1mmole total carbon value for this work is an over estimation as the diffusivity

circuit was a closed system with air ingress unlikely. Even if carbon dioxide ingress into the diffusivity experimental circuit had occurred with subsequent adsorption then conversion to carbonate would have been low at pH values under 8 (less than 1mmole/L) but at higher pH values would increase to about 10 mmole at pH 9.5. Making an allowance for this adsorption/conversion at the higher pH values monitored in these experiments then the impact of carbonate on the speciation of calcium would predominate but significantly less so for Sr^{2+} and Co^{2+} when compared with hydroxide and sulphate anions K_{sp} data (Table 3.9).

Table 3.8 K_{sp} values for selected salts

anion	cation		
	Ca^{2+}	Sr^{2+}	Co^{2+}
OH^-	$5.02. \times 10^{-6}$	$6.4. \times 10^{-3}$	$1.1. \times 10^{-15}$
CO_3^{2-}	$3.36. \times 10^{-9}$	$5.6. \times 10^{-6}$	$1. \times 10^{-10}$
SO_4^{2-}	4.93×10^{-5}	$3.44. \times 10^{-7}$	
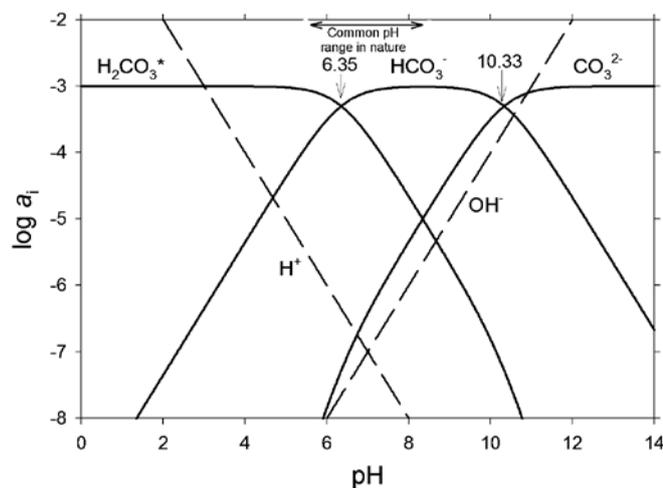
Figure 3.6 Bjerrum plot showing the activities of inorganic carbon species as a function of pH for a value of total inorganic carbon of 10^{-3} moles L^{-1} [125].

Attempts to demonstrate the influence of pH alone on the diffusivity of cations/anions were hindered and complicated by other contributors. The changes with time of cement hydrates composition in equilibrium with pore water coupled with the impact of added salts to the make-up water on the release of alkali metals and subsequently Ca^{2+} are not easily isolated. It is reasonable to assume that at lower pH values of the test solution i.e. 7 to 8 could interact with the surface of the CPS leading to leaching of alkali metals (Na^+, K^+, Cs^+) that produce soluble salts. At higher pH values (>11.0) diffusivity via pore water would predominate.

3.3.3 Diffusion/leaching

The leaching process begins when solid compounds in concrete are dissolved by surrounding aqueous phase and then transported away, either due to concentration gradients (diffusion), by the flow of water (convection) or electromigration [39]. This process occurs in a sequence of stages, which are dependent on the solubility product values of the compounds. The most soluble elements such as alkali hydroxides are removed first from the solid sample. In the second stage, the calcium hydroxide (i.e. portlandite) is dissolved, followed by the dissolution of the calcium-silicate-hydrate (C-S-H) gel phases. In a final stage other cement phases, such as ettringite are dissolved [40]. Solid materials are dissolved depends on theirs solubility (K_{sp}) and where they are located in the pore system in relation to pure water and each other. When dissolved, the ions will diffuse towards water with less content of the ions. Leaching of lime originates from the calcium hydroxide $Ca(OH)_2$, due to its large amount in cement paste and comparative easy solubility. At the same time, but to a much less amount, as long there is $Ca(OH)_2$ left, lime will also be dissolved from the other hydration products

calcium silicate hydrate (C-S-H), calcium aluminium hydrates (C$_3$A) and calcium aluminium iron hydrate (C$_4$AF), viz:

$$H_2O + [Ca(OH)_2; C\text{-}S\text{-}H; AFT; AFM] = Ca^{2+}aq$$
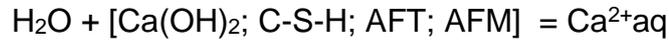
Convection flow of ions is totally governed by the water flow; generally the quickest leaching degradation of a concrete structure occurs when ions are leached by convection. Diffusion flow of ions is probably influenced by concentration gradients, inter-molecular forces between dissolved ions and intermolecular forces between dissolved ions and solid walls.

The design of the diffusivity experiments in the present research was based on the cement paste sample surface area ($\approx$ 71 cm^2), the volume of test solution (200 cm^3) in the circuit and the test solution flow rate (300 cm^3/hour). This flow rate was sufficient for good mixing but not excessive to create erosion of the cement paste samples. The data generated from the diffusivity experiments carried out on BFS:OPC and PFA:OPC CPSs with different test solutions revealed that there are number of factors which contribute towards the rate of diffusivity of cations:

(a)   The nature and the concentration of added cation

(b)   The composition of cement paste sample (BFS:OPC and PFA:OPC).

(c)   Nature of test solution used in diffusivity experiments

3.3.3.1 Nature of added cation

The rate of diffusivity of Cs^+ was higher than Sr^{2+} and Co^{2+} (Figure 3.9 to Figure 3.12). Caesium ion as Na^+, will be highly soluble in the pore water of OPC grout, which has been measure in pore water [118] and thus, leaching is diffusion controlled, whereas Sr^{2+} forms sparingly soluble strontium or calcium/strontium carbonate or sulphate, which is well retained in grout. Strontium ion is likely to substitute for Ca^{2+} in some of the compounds highlighted in Table 3.1. However, the number of Ca^{2+} present in OPC:BFS CPS (602 mmoles) were more in comparison with PFA:BFS CPS (147 mmoles) (Table 3.14). The higher content of Ca^{2+} in BFS:OPC comes from Ca^{2+} content of BFS (38.22 wt%). As mentioned earlier, the dissolution and solubility of species will depend on K_{sp} values of salts formed by Sr [$SrSO_4$ ($K_{sp}=10^{-7}$); $Sr(OH)_2$ ($K_{sp}=10^{-3}$), $SrCO_3$ ($K_{sp}=10^{-10}$)]. Caesium is readily soluble and therefore K_{sp} values do not apply. The similar behaviour of Sr^{2+} and Ca^{2+} can be explained in terms of their electronic configuration. From concrete degradation experiments, it has been shown that Sr^{2+} is strongly linked to $Ca(OH)_2$ [126]. Strontium becomes chemically bonded to concrete by the exchange of Sr^{2+} for Ca^{2+} in hydrated silicate or ettringite [127, 128]. This makes Sr^{2+} relatively less soluble in the pore water of concrete [129]. Leaching studies carried out on ^{137}Cs and ^{60}Co radionuclides from both ordinary Portland cement and cement mixed with two ratios of silica fume and ilmenite produced a decreasing pattern of diffusivity as $^{137}Cs > {}^{60}Co$, indicating the larger diffusion coefficient for caesium in waste matrices [83].

The diffusivity of cations is dependent on the age of the cement paste sample. The rate of diffusivity of Sr^{2+} from non-aged CPS (Figure 4.2) was higher than the aged 3% $SrCl_2$ (Figure 4.7) and 3% $SrCO_3$ (Figure 4.16). Similar results were

found in case of Cs^+ diffusivity (Figure 4.3 and Figure 4.8). This could be due to the effect of aging and carbonation process that may have decreased the porosity and hence lowered the diffusion of cations. The carbonation reaction leads to the reduction in the porosity of cement paste and contributes to formation of protective layer at the surface of cement paste [27, 130]. Studies have shown that the formation of calcite as a result of carbonation, reduces the porosity due to higher molar volume (36.9 cm^3/mol compared to 33.1cm^3/mol for CH) [27].

The micro-pore areas of aged and $SrCO_3$ CPSs were lower than the non-aged CPSs (Table 4.5). As mentioned earlier, carbonation leads to the formation of calcium carbonate, silica gel and metallic oxides which over the period of time begin to accumulate in the pores of concrete grout resulting in the physical and chemical changes to cementitious waste forms. Much of the research on carbonation of cementitious materials, however, has focused upon structural aspects i.e., compressive strength, permeability and creep in reinforced concrete [131-134]. Nevertheless, scant information exists regarding the influence of carbonation on the chemical properties of cement-based materials with respect to the diffusivity of encapsulated waste. Few of such studies have been carried out on accelerated carbonation process [135-139] that produced lowered diffusional release of strontium but increased the release of other metal ions [139]. Lower diffusivity of Sr^{2+} from aged CPS could be attributed to formation of $SrCO_3$ ($K_{sp}= 10^{-10}$).

There is a strong correlation between the diffusivity of metal ions through a cement paste and *w/c*. As mentioned earlier, the *w/c* determines the porosity of the cement paste sample. Studies have shown that the change in the *w/c*

between 0.2 and 0.7 could increase the diffusivity of Cs^+ by up to 3 order magnitude [140].

Incorporation of Sr^{2+} as an insoluble salt such as carbonate has affected the physio chemical features of the CPS. Calcium carbonate, similar to $SrCO_3$ enhances the hydration of cement paste. Portland–limestone cements are the most widely used cements according to the European cement standard ENV 197-1 [141]. Since early 1980, the Canadian cement standard (CSA 1998 - CAN/CSA-A5) permits the use of 5% ground limestone in Portland cement [142] and in more than 25 countries. The considerable lower rates of diffusivity of Sr^{2+} from CPS incorporated with $SrCO_3$ (Figure 4.12) compared to the $SrCl_2$ (Figure 4.2) is attributed to the difference in their solubility which is significantly higher for $SrCl_2$. The outcome from the diffusivity experiments with CPS incorporated with $SrCO_3$ suggests that further research is required with CPS incorporating carbonate in cement paste samples to ascertain the rates of diffusivity of Cs^+ and Sr^{2+}, when fillers are used in the formulation. It is envisaged that addition of $CaCO_3$/ limestone as a filler will reduced the rates of diffusivity of encapsulated cations to an insignificant level. Caesium carbonate is quite soluble and therefore any effect will have to be due to pore blocking.

Incorporation of Sr^{2+} as a carbonate has also affected the pH of the test solution. The pH of the test solution starts to fall after 100 days of diffusivity in both the 0.3% and 3% incorporated $SrCO_3$ CPS (Figure 4.11 and 4.12). The surface wash-out rather than the diffusion could be attributed towards the lower rates of diffusivity of cations and anions after 100 days. The use of filler/$CaCO_3$ may be beneficial for waste disposal/cement encapsulation of waste, our experiments have shown the lower rate of diffusivity of cations.

It is suggested that the effect of $CaCO_3$ is only physical [16]. Presence of carbonate salt in the CPS has also lowered the rate of diffusivity of Ca^{2+}, Na^+, SO_4^{2-} in both the formulations. The presence of carbonate salt reduced the diffusivity of Ca^{2+} by a factor of $\approx$ 27 in comparison with CPS chloride salt of Sr^{2+}. The effect is more pronounced in PFA:OPC; the rate of diffusivity was reduced significantly in comparison with BFS:OPC 3% $SrCl_2$. This is due to the effect of mass action; the amount of Ca^{2+} present in PFA:OPC CPS (147 mmoles) which was significantly smaller than BFS:OPC CPS (602 mmoles) (Table 3.14).

Another interesting feature observed; incorporation of Cs^+ in the CPS has lowered the rate of diffusivity of Ca^{2+} by a factor of $\approx$ 12 in comparison with control CPS and 54 times slower in comparison with 3% $SrCl_2$ (Figure 4.1 to Figure 4.3). The diffusivity of Cs^+ is comparable with measured pH values of the test solution (DW). Cs^+ is highly soluble in the pore water, it is more than likely that Cs^+ will behave like Na^+ and K^+ in the pore water because of their similarities in solubility properties and position in the periodic table. Caesium diffused out much before other alkali metal ions. This attributed to the concentration of Cs^+ (21.31 mmoles) present in the CPS which was far greater than the Na^+ (12.6 mmoles) and K^+ (11.3 mmoles). The sequence of diffusivity of metal ions shown in 3% CsCl CPS in both the formulation is similar i.e. $Cs^+ > Cl^- > K^+ > SO_4^{2-} > Na^+ > Ca^{2+}$. However the sequence of diffusivity shown in the 3%$SrCl_2$ CPS is $Cl^- > Ca^{2+} > Sr^{2+} > K^+ > SO_4^{2-} > Na^+$, this demonstrates the binding nature of both Sr^{2+} and Cs^+ is one of the major factor contributing their rate of diffusivity. When both the Cs^+ and Sr^+ incorporated together in cement paste sample the sequence of diffusivity of metal ions was $Cl^- > Cs^+ > Ca^{2+} > K^+ > Sr^{2+} > SO_4^{2-} > Na^+$ (Figure 4.5) indicating that Cs^+

diffuses faster than Ca^{2+} which is significant and needs special attention to lower its diffusivity.

An interesting feature is, the rate of diffusivity of Cs^+ remains the same when added as a single cation or as a cation combined with battery of cations (Sr^{2+}, Co^{2+}). There was no significant difference ($p > 0.05$) observed in the rate of Cs^+ from 3% CsCl and combined metal CPS. However such pattern is not observed with Sr^{2+} and Co^{2+}. When strontium encapsulated/added in combination with other cations of interest; the diffusivity reduced by a factor of 1.5. This suggests that the diffusivity of Sr^{2+} changes based on its status how it's been added, single cation or a as a mixture with other cations/ radionuclide. The same is not applicable to Cs^{2+}. This attributes to the nature of binding of Cs^{2+}. Caesium ion is highly soluble in pore water like other alkali cations Na^+, K^+ [31, 143]. The degree of chloride binding is influenced by the nature of cation chloride added to the make-up water. Due to their similar chemistry (dictated by their electronic configuration and hence position in periodic table, group II), Sr^{2+} would be expected to behave similarly to Ca^{2+} and hence the cement paste would bind more chloride, unlike Cs^+ if comparable with Na^+ that would have less bound chloride, as explained earlier. The addition of caesium chloride, if behaviour is similar to sodium chloride, would also result in higher pore solution pH in comparison with strontium chloride addition. This pH increase for CsCl addition may be explained by the following:

$$2NaCl_{(aq)} + Ca_3Al_2O_6.6H_2O_{(s)} + Ca(OH)_{2\ (aq)} + 4H_2O \rightarrow Ca_3Al_2O_6.CaCl_2.10H_2O_{(s)} + 2NaOH_{(aq)}$$
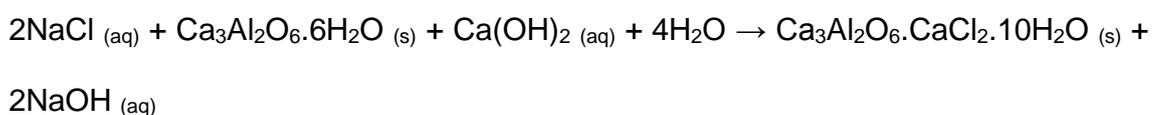
Increasing pH will also disfavour the formation of the sparingly soluble calcium hydroxide (1.859/L at room temp). This will explain why chloride binding is higher for alkaline earth metals (Ca^{2+}, Sr^{2+}) when used as the chloride source:

$$CaCl_2 \text{ (aq)} + Ca_3Al_2O_6.6H_2O \text{ (s)} + 4H_2O \rightarrow Ca_3Al_2O_6.CaCl_2.10H_2O \text{ (s)}$$
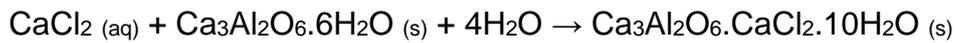
Both C_3A and C_4AF bind chloride. The ability of calcium hydroxide to bind chloride when exposed to a calcium chloride solution has been demonstrated simply by adding $Ca(OH)_2$ to the calcium chloride solution and analysing the solid and liquid phases. A similar experiment but using sodium chloride solution indicated that NaCl did not form compounds with calcium hydroxide to any significant extent. The workers postulated the following reactions:

$$2NaCl \text{ (aq)} + 4Ca(OH)_2 \text{ (s)} + 12H_2O \rightarrow CaCl_2.3Ca(OH)_2.12H_2O \text{ (s)} + 2NaOH \text{ (aq)}$$

The above reaction is negligible, but the following reaction is thermodynamically favourable:

$$CaCl_2 \text{ (aq)} + 3Ca(OH)_2 \text{ (s)} + 12H_2O \rightarrow CaCl_2.3Ca(OH)_2.12H_2O \text{ (s)}$$
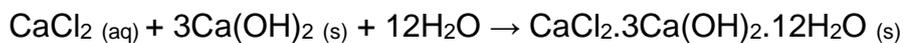
Other reactions, in addition to chloride ion substitution reactions identified above, occur in cement hydrate and between the various hydrates. The inherent sulphur particularly in BFS influences the sulphate content and alkalinity of pore solution.

Preliminary analysis of the test solution (DW) in contact with the ≈1.3% $CoCl_2$ CPS revealed that the concentration of Co^{2+} in the recirculating solution was just slightly higher than the detection limits of ICP-MS (Figure 4.4). This very dilute solution of cobalt i.e. low diffusivity supported previous leaching studies involving cobalt sludges encapsulated in cement [144]. The low diffusivity will be influenced by the K_{sp} values of sparingly soluble salts such as hydroxide and carbonate (1.1 x 10^{-15}, 1.0 x 10^{-10} respectively). It was decided therefore at an early stage of the project that further analysis of test solution samples would only produce qualitative data for cobalt; consequently cobalt sampling/analysis was discontinued.

3.3.3.2 Nature of test solution and influence on diffusivity of added cations

The diffusivity data of first 50 days were taken in consideration for comparative purpose. The mechanism of diffusivity of cement paste is dependent on nature of aqueous medium. When cementitious material is in contact with surrounding deionised aqueous medium, concentration gradient is established. This causes transport of ions from the core of the material into the surrounding aggressive solution through its porous network system. This reduces the amount of Ca^{2+} in pores, leading to disruption of portlandite and Afm, ettringite and calcite [27, 145]. The cement hydrate diffuses out depending on their solubility properties. The dissolution of $Ca(OH)_2$ is dependent on the period of exposure to aggressive solution [27, 32, 36, 146-148].

In the case of Sellafield pore water solutions, the mechanism is different. Due to its higher ionic concentration than deionised water; CSPW dissolve/s $Ca(OH)_2$ in the form of exchange reaction [27, 149]. The calculated ionic strength of this solution (3.3), which is 60 times stronger that the test solutions produced from

leaching of ions from cement paste samples, 90% of the strength comes from the sodium chloride. The ingress of sulphate from Na_2SO_4 or K_2SO_4 present in the CSPW and DSPW water into the cement paste takes place due to the pH which is around neutral. This may lead to the formation of gypsum on the layer close to which gives rise to the dissolution of $Ca(OH)_2$ [149]. The dissolution of $Ca(OH)_2$ and sulphate ingress leads to expansion of C_3S hydrate paste However, this effect is solubilised by presence of Cl^- [30]. The diffusivity of Ca^{2+} from BFS:OPC and PFA:OPC 3%CsCl increased in the presence of CSPW from by a factor of 171 and 14 respectively in comparison with DW (Figure 3.7and 3.8), this is attributed to the difference in the Ca^{2+} BFS:OPC and PFA:OPC as mentioned earlier. Lower pH values of CSPW and DSPW in comparison with DW, could also be a contributing factor towards leaching. There was no significant difference ($p>0.05$) in the diffusivity of Sr^{2+} from BFS:OPC in CSPW in comparison with DW (Figure 3.9); contrary to the effect of DSPW, which lowered the diffusivity of Sr^{2+} by a factor of 5.

In the case of 3%$SrCl_2$ PFA:OPC CPSs, the effect of CSPW is reversed in comparison with its BFS:OPC counterpart. The rate of diffusivity of Sr^{2+} from 3%$SrCl_2$ PFA:OPC decreased by factor of 5 in the presence of CSPW (Figure 3.10). The effect of CSPW is seen more prominent on 3% $SrCO_3$; in both the formulation BFS:OPC and PFA:OPC, the diffusivity of Sr^{2+} from 3%$SrCO_3$ increased significantly. This could be due to the presence of carbonate. However, the rates were in much smaller magnitude in comparison with other CPSs.

The lower diffusivity of Ca^{2+} and Sr^{2+} from BFS:OPC in DSPW may be due to the formation of brucite ($Mg(OH)_2$. The magnesium ion present in the saline water substitute for the Ca^{2+} present in cement paste resulting in the formation of

magnesium hydroxide, known as brucite which precipitates in the pores of the cement paste.

$$MgSO_4 \text{ (aq)} + Ca(OH)_2 \rightarrow CaSO_4 . 2H_2O + Mg(OH)_2$$
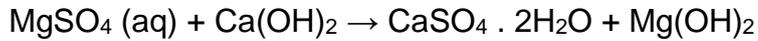
This brucite forms the protective surface layer which obstructs the further action of ions present in the aqueous medium. The pH values (9 -10) in the DSPW from 3% $SrCl_2$ were favourable for the formation of brucite. These results are comparable with Heikola's work [40]. Similar effect is noticed in other research where the diffusivity of the added cations was lowered in synthetic sea water [28]. In the case of Cs^+, the increase in the ionic concentration of the test solution has shown a positive correlation with the rate of diffusivity of Cs^+ (Figure 3.11). The diffusivity of Cs^+ increased by a factor of 1.7 and 2.5 in the presence of DSPW and CSPW respectively in comparison with DW. However, no such diffusivity patterns were observed in the case of PFA:OPC 3% CsCl experiment (Figure 3.12). There was no significant difference ($p > 0.05$) in the diffusivity of Cs^+ from DW and CSPW.

The diffusivity of weaker concentration of cation CPSs i.e. 0.3% Sr^{2+} and Cs^+ showed lower rates of diffusivity in comparison with their 3% counterpart. However, the rates of diffusivity of the added cations were similar to the diffusivity of cations from control CPS. This suggests that the mineralogical transformations in conjunction with physical (porosity, pore size etc.), concentration of cations, test solutions (aqueous environment) and chemical factors (release of $Ca(OH)_2$, pH etc.) have influenced the diffusivity of ions from the cement paste samples.

	DW	DSPW	CSPW	JISS
Control	5.66	0.32	194	8
≈3% SrCl2	45	11	233	60
≈3% CsCl	0.99	6.7	170	32
≈3% SrCO3	1.26	7.88	50	18
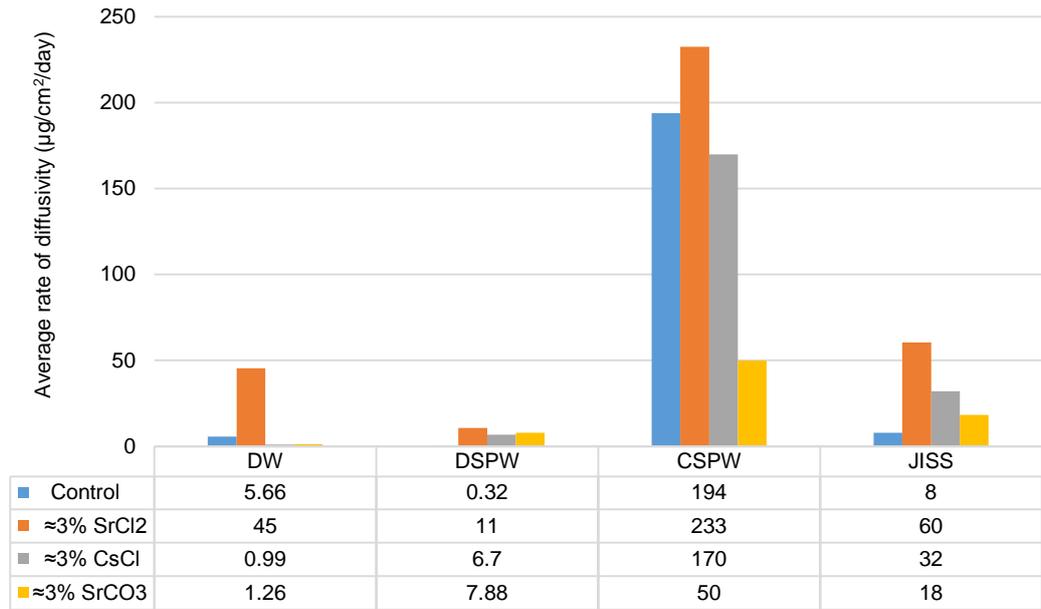
Figure 3.7 Comparative average rate of diffusivity of calcium from BFS: OPC CPSs in DW, DSPW, CSPW and JISS.

	DW	CSPW	JISS
Control	1.45	14	2.51
≈3% SrCl2	242	116	200
≈3% CsCl	1.92	25.98	4.42
≈3% SrCO3	0.93	15.97	1.12
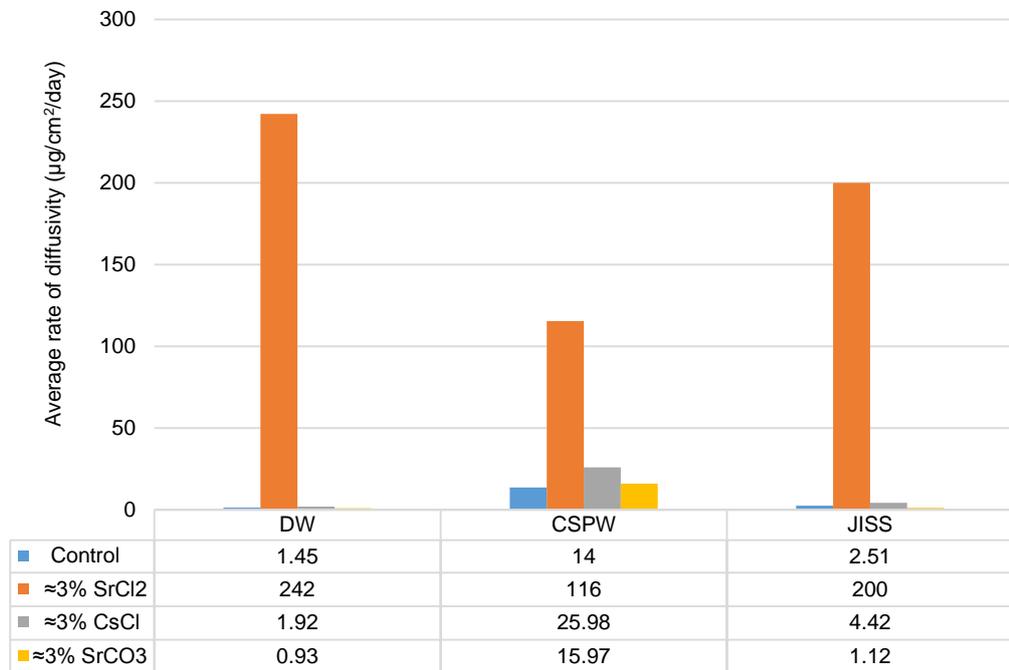
Figure 3.8 Comparative average rate of diffusivity of calcium from PFA: OPC CPSs in DW, CSPW and JISS.

	DW	DSPW	CSPW	JISS
≈3% SrCl2	35	7	43	19
≈3% SrCO3	0.05	0.05	2.58	0.82
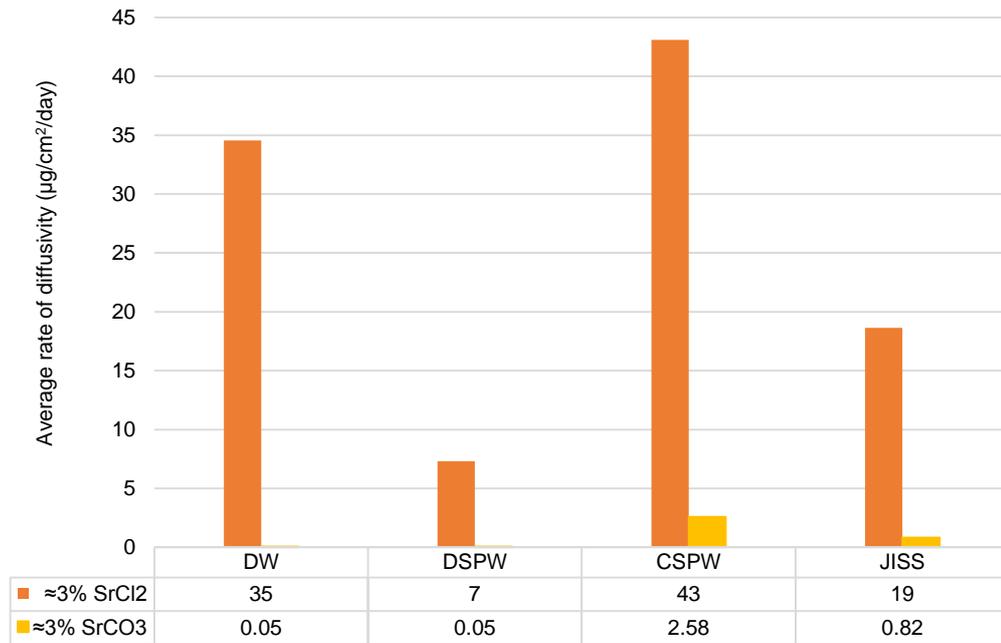
Figure 3.9 Comparative average rate of diffusivity of strontium from 3% SrCl$_2$ and 3% SrCO$_3$ BFS:OPC CPSs in DW, DSPW, CSPW and JISS.

	DW	CSPW	JISS
≈3% SrCl2	171	35	128
≈3% SrCO3	0.04	1.45	0.04
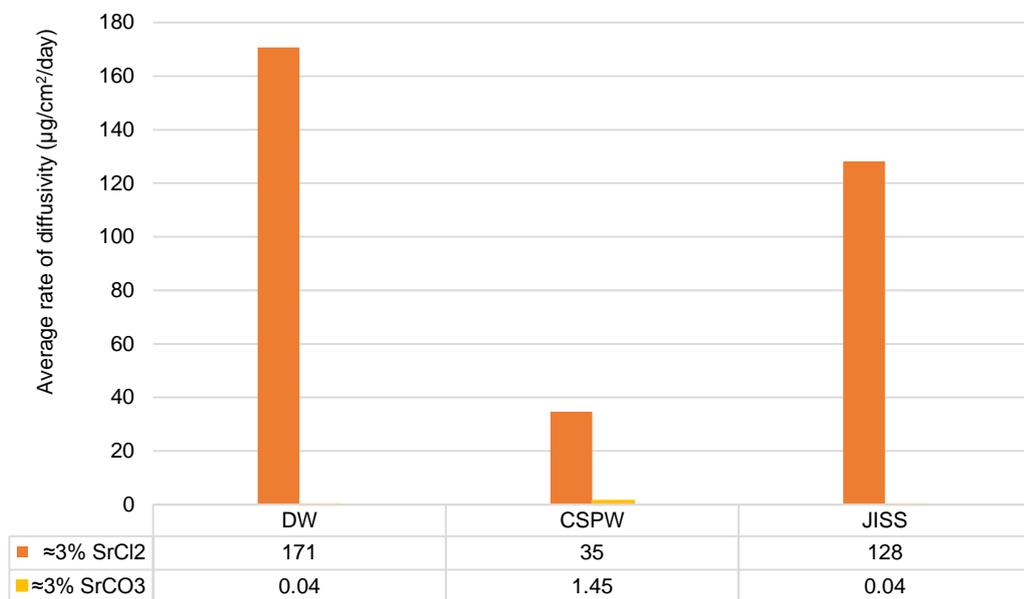
Figure 3.10 Comparative average rate of diffusivity of strontium from 3% SrCl$_2$ and 3% SrCO$_3$ PFA:OPC CPSs in DW, CSPW and JISS.

	DW	DSPW	CSPW	JISS
≈3% CsCl	40	67	102	191
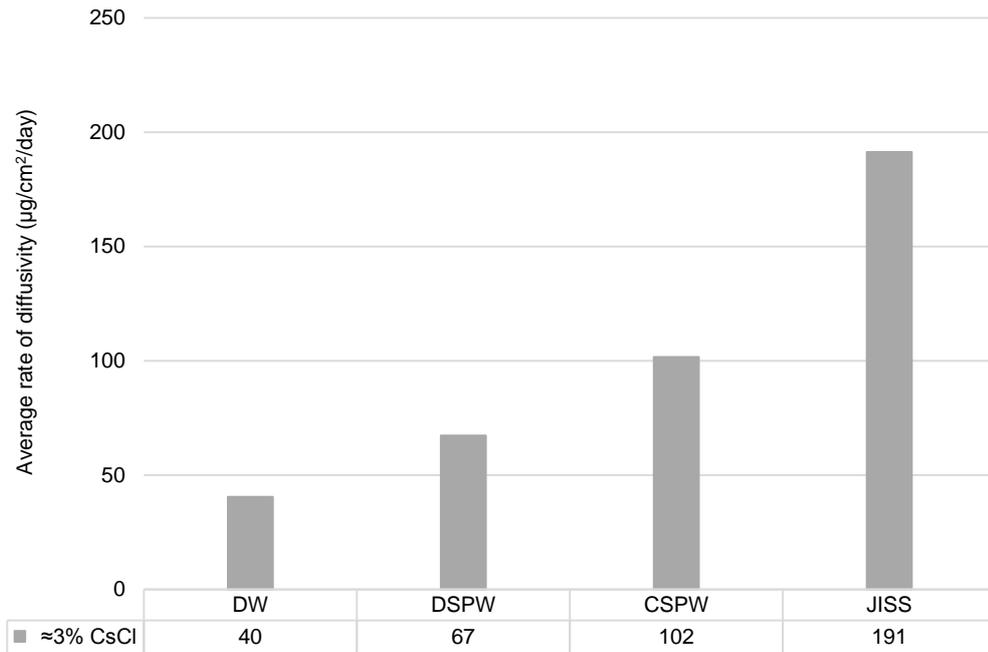
Figure 3.11 Comparative average rate of diffusivity of caesium from 3% CsCl BFS:OPC CPSs in DW, DSPW, CSPW and JISS.

	DW	CSPW	JISS
≈3% CsCl	460	516	408
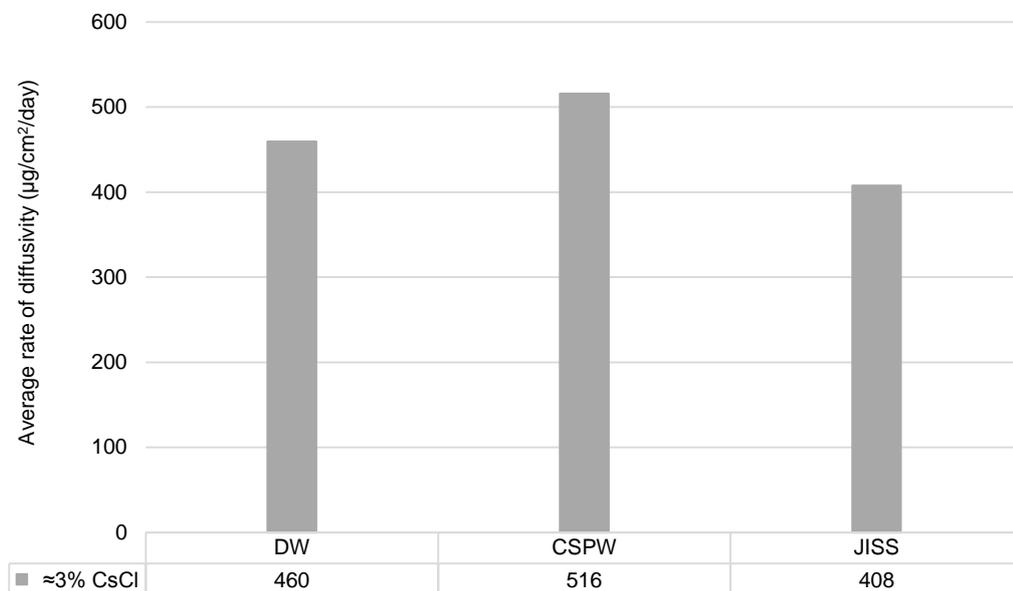
Figure 3.12 Comparative average rate of diffusivity of caesium from 3% CsCl PFA:OPC CPSs in DW, CSPW and JISS.

85

3.3.4 Open vs closed system

At the outset the closed circuit arrangement was selected as the initial work programme involved a significant number of parameters to be undertaken and it was considered at the time the experiments could continue for a significant time period (>100 days). In addition even at this early stage the implications of introducing microorganisms in to the circuit and subsequent mode of operation were considered, knowing that removal of samples from the circuit with addition of an equivalent amount of test liquor would disturb the equilibrium and likely to create challenges in analysing the data. The size of the cement paste samples and vessels (diffusivity vessel and reservoir vessel) and circuit design were also addressed to ensure:

(a)   a realistic cement paste sample size (surface area) was used

(b)   an appropriate volume of test solution that could accommodate the removal of a representative sample for analysis

(c)   the volume of microbial extract (JISS) to be added to the circuit was sufficient to produce an effect

(d)   the ratio of surface area of the cement paste samples to the volume of the test solution was acceptable

(e)   the circulation of the test solution through the diffusivity vessel was sufficient for good mixing (0.002cm/sec) but without creating erosion of the cement paste sample walls.

(f)   The test solution in the diffusivity vessel was replenished at least once per hour.

These flow conditions were replicated for the open circuit arrangement.

The design of open circuit arrangement was such that the data produced could be as comparable as possible with the closed circuit experiments. This required:

(a)   the same size of cement paste samples

(b)   a similar flowrate of test solution

but this open arrangement would have a significantly different surface area to volume ratio for final test solution volume.

The logistics of accommodating nearly 50 litres/week of test solution for each open circuit experiment in the laboratory for about 30 to 40 days was a significant factor. This volume of solution influenced the decision to use tap water, but the data would be comparable with the closed circuit experiment using tap water results.

The concentrations of ions in the test solutions from the closed and open circuit experiments were significantly different; the closed circuit as seen from the results section had on three or four perturbations due to some of the cations/anions reaching their solubility limits, but with a new equilibrium when fresh test solution was added to the circuit. Solubility limits were not a factor in the open circuit, as the concentration of ions were significantly lower but the total quantity of ions leached were significantly higher and consequently the total quantities of ions leached were far greater (Table 3.10 and 3.11).

Table 3.9 Comparison of total cations removed from the BFS:OPC cement paste samples with tap water

BFS:OPC CPS	arrangement	pH	mmoles*						
			Na^+	K^+	Cs^+	Ca^{2+}	Sr^{2+}	Cl^-	SO_4^{2-}
control	Closed circuit	10.7-12.1	4.2	13	-	13.9	-	4.2	2.7
≈3%SrCl$_2$		11.2- 2.03	5.2	6.2	-	13.2	3.8	43.	2.2
≈3%CsCl		9.01-11.59	1.7	2.6	7.8	0.6	-	3.2	0.5
≈3%SrCO$_3$		7.78-12.27	3.15	1.1	-	2.5	<0.05	2.6	0.5
control	Open circuit	7.28-7.5	0.18	<0.05	-	0.2	-	0.08	0.45
≈3%SrCl$_2$		7.26-7.54	0.02	<0.05	-	0.27	<0.05	0.01	0.48
≈3%CsCl		7.1-7.67	0.17	0.01	0.05	0.26	-	0.21	0.5
≈3%SrCO$_3$		7.22-7.79	0.19	<0.05	-	0.17	<0.01	0.07	0.49

*at maximum concentration of ion measured during the experiment

Table 3.10 Comparison of total cations removed from the PFA:OPC samples with tap water

PFA:OPC CPS	arrangement	pH	mmoles*						
			Na^+	K^+	Cs^+	Ca^{2+}	Sr^{2+}	Cl^-	SO_4^{2-}
control	Closed circuit	11.98- 2.13	8.3	6.8	-	0.3	-	1.2	2.8
≈3%SrCl$_2$		7.47-8.69	20.4	14		34.6	11.6	263.5	1.0
≈3%CsCl		1.95-12.02	7.2	7.1	21.1	0.4	-	52.8	2.6
≈3%SrCO$_3$		1.99-12.02	7	5.7	-	0.3	<0.05	3.7	2.7
control	Open circuit	7.63-8.08	0.28	0.04	-	0.21	<0.01	0.24	0.28
≈3%SrCl$_2$		7.56-7.87	0.28	0.08	-	0.38	0.03	1.26	0.29
≈3%CsCl		7.62-7.87	0.28	0.05	0.12	0.20	-	0.42	0.28
≈3%SrCO$_3$		7.22-7.81	0.19	<0.01	-	0.17	<0.01	0.07	0.49

*at maximum concentration of ion measured during the experiment

As solubility factors were not controlling parameters and diffusion gradients would be common for all open comparable systems, analysis of the data was relatively straightforward. The development of diffusion gradients within the diffusivity

vessel for the closed circuit between the CPS surface and test solution at the interface were worthy of consideration as this could give rise to the re-sorption of cations, particularly the alkali metals (Na^+, K^+ and Cs^+) onto mineral sites in the cement paste sample. This is discussed in more detail in a following section.

The ultimate consideration in the design of the experiments was to simulate the likely interaction of ground water with a wastes in a GDF. It was considered that a more ebb and flow arrangement would occur in preference to a continuous flow through. The closed circuit arrangement with removal of saturated solution and addition of fresh test solution would best resemble the former and more than likely produce more realistic data of value to the nuclear industry.

The experimental conditions/arrangements used in this work provide worst case and best (real) case scenarios when considering mobility of radionuclides from a GDF. The worst case scenario is for the open circuit when solution equilibria are unlike to be achieved thus allowing for near continuous diffusion of ions from the cement paste into the flowing water. With a closed circuit arrangement (real case scenario) various equilibria (Ksp) will be established which will impinge on the solubility of sparingly soluble compounds such as calcium hydroxide, carbonate, sulphate as well as some of these salts of strontium and magnesium. At this time of reporting this diffusion data it is not possible to give a more precise prediction as the flow of water into/through a GDF will be governed by numerous factors not least time.

3.4 Chemistry and interaction of anions

3.4.1 Chloride interaction

If the concrete is made up with seawater or other saline waters or as used in our case incorporated chloride salt in the makeup water, the resulting concrete will have a comparatively low chloride content. Any chloride in the mixture generally enters the AFm (ferro-aluminate) phase with 60% of the chloride bound to the cement paste as mono-chloro-aluminate and the remainder dissolved in the pore water [53, 54]. At comparatively high chloride concentrations, other salts such as $3CaO.CaCl_2.15H_2O$, can form [129] . When chloride is combined with the AFm phase, the resulting compound is known as Friedel's salt ($4CaO.Al_2O_3.(Cl, OH)_{10}$) which is stable at higher pH and above 40 °C. Below 20°C, the tri-chloride complex (AFt) is formed [150].

3.4.2 Internal sulphate attack

The diffusion of internal sulphate has received less attention. Internal sulphate arises from oxidation of sulphide to sulphate present in the additives [54, 151-153]. Most of the research has concentrated on the degradation of cementitious material by external sulphate attack [154, 155]. This internal sulphate may react with free portlandite to give gypsum

$$Ca(OH)_2 + MSO_4 = CaSO_4 + M(OH)_2$$
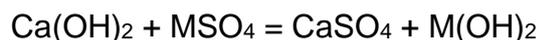
where M may be a monovalent or bivalent cation

Alternatively, sulphate may react with the hydrated calcium aluminates to form calcium sulpho-aluminate followed by sparingly soluble ettringite. The gypsum

produced in the above equation may further degrade the concrete by reaction with CSH to produce ettringite.

From the diffusivity experiment; the cumulative concentration of diffused sulphate in the presence of various test solution is significant; taking into consideration aerobic and facultative anaerobic microbial species having abilities to tolerate a wide range of environmental conditions; temperature, pH, salinity [60-62]. Biogenic sulphuric acid producing bacteria of *Thiobacillus sp.* have properties of oxidizing sulphur, sulphides and thiosulphates to sulphuric acid under aerobic conditions [156]. Impact of microorganism on cementitious material is discussed in next section. Irrespective of formulation (PFA:OPC, BFS:OPC); the rates of diffusivity of SO_4^{2-} in DW is fairly similar in both the formulations (Figure 3.13 and 3.14)

	DW	DSPW	CSPW	JISS
Control	31	27	108	36
≈3% SrCl2	15	16	84	19
≈3% CsCl	6	35	102	75
≈3% SrCO3	6	22	14	112
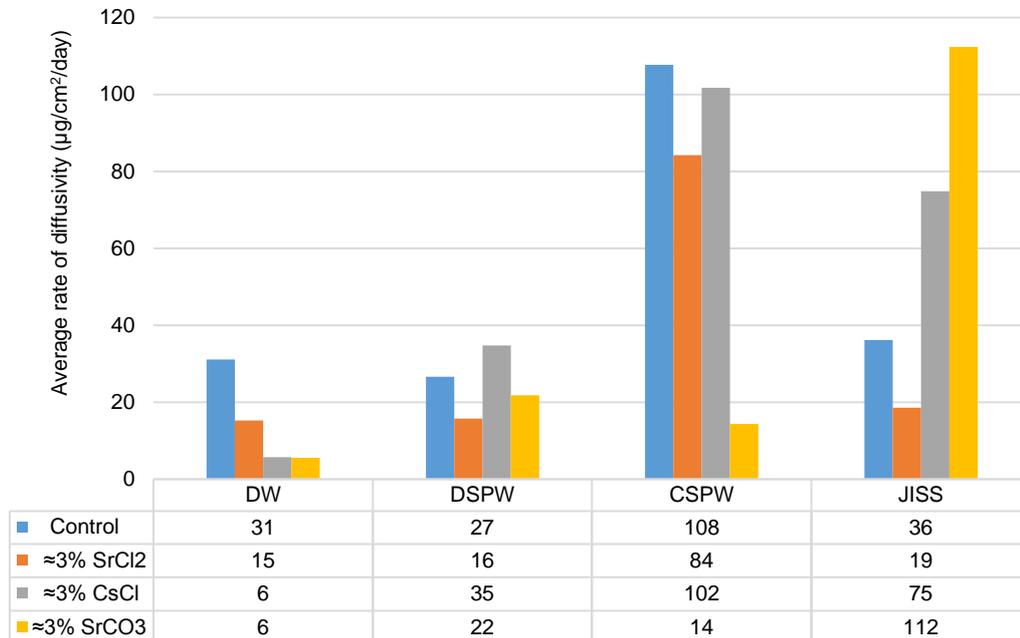
Figure 3.13 Comparative average rate of diffusivity of sulphate from BFS:OPC CPSs in DW, DSPW, CSPW, JISS.

	DW	CSPW	JISS
■ Control	45	56	57
■ ≈3% SrCl2	17	21	19
■ ≈3% CsCl	43	140	71
■ ≈3% SrCO3	39	121	69
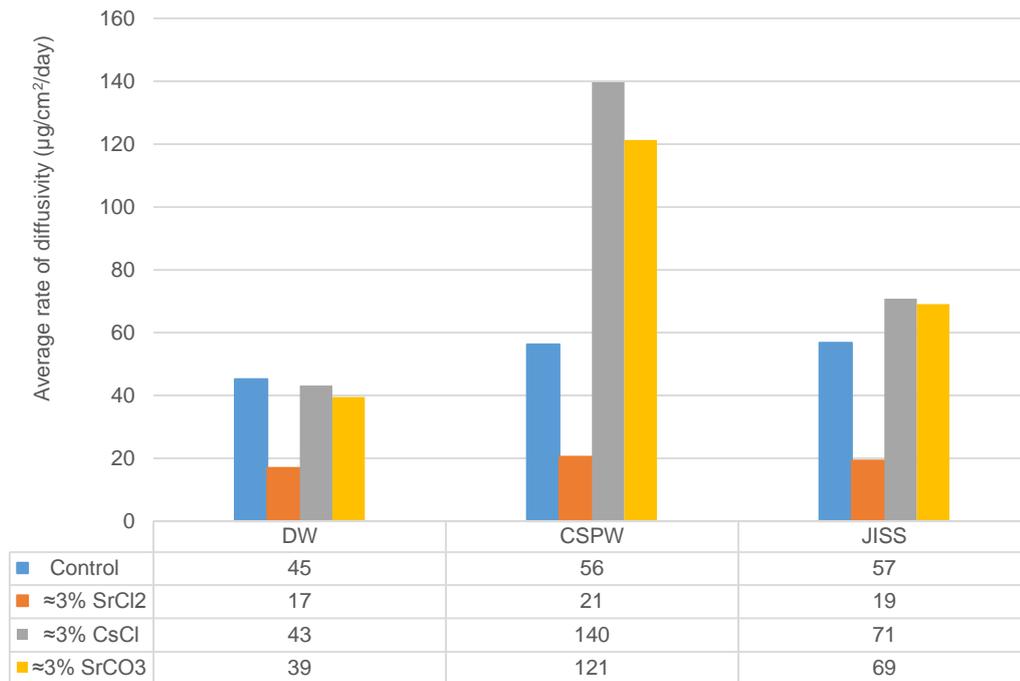
Figure 3.14 Comparative average rate of diffusivity of sulphate from PFA:OPC CPSs in in DW, CSPW, JISS

3.5 Diffusion coefficient values of cement paste samples

The mobility of encapsulated nuclear waste depends on the nature of binding of the radionuclide in the cement matrix, physic-chemical properties of cement paste/formulation and the relationship of cementitious material to its environment. Two possible conditions may occur in GDF:

(a) Where one side of the cement paste is in contact with a solution (ground water) but the reverse side is exposed to the atmosphere then the solution (ground water) can pass through the concrete sample, and the concrete pore water will be continuously renewed and the leaching will be fast. Moreover, the passing ground water will dissolve components, which in turn will increase the porosity and the degree of penetration. This passage of ground water, however, requires a water pressure or some other force to drive the water through the

concrete [39]. The flow of water may reduce due to autogenous healing [157]. However, it is not clear whether the condition in a repository will be suitable for crack healing; especially if the cement is extensively modified with slag or fuel ash [158]. As concrete is porous there is a relationship between porosity, thickness, pressure and transmissivity of concrete. Flow in capillary pores in saturated concrete follows Darcy´s law for laminar flow through a porous medium [159] .

On the other hand, (b) when cement paste is completely submerged then the pressure will be equalised and no water will penetrate the cement paste. Dissolution will then be controlled by diffusion through the surface of the concrete. The driving force for diffusion controlled leaching will be the concentrations difference between the pore solution and the external water

The calculated diffusion coefficient values from the expression mentioned in section 2.11 are shown in Table 3.12 (BFS:OPC) and Table 3.13 (PFA:OPC).

Table 3.11 Diffusion coefficient values (D_e) from BFS:OPC CPS

CPS	Test solution	Time period (days)	pH value	Calculated D_e values (cm^2/day)						
				Na$^+$	K$^+$	Cs$^+$	Ca^{2+}	Sr^{2+}	Cl$^-$	SO$_4^{2-}$
BFS:OPC Control	DW	7	10.7 – 12.1	1.22×10^{-4}	$4.34 \times 10\text{-}5$		5.37×10^{-9}			2.29×10^{-5}
		201		6.74×10^{-7}	1.8×10^{-5}		6.82×10^{-10}			1.57×10^{-7}
		At max conc.		9×10^{-5}	2.02×10^{-4}		7.29×10^{-8}		8.83×10^{-4}	1.63×10^{-5}
				[21]	[112]		[126]		[21]	[21]
≈3% SrCl$_2$		7	11.2 – 12.03	1.59×10^{-4}	1.55×10^{-4}		2.15×10^{-7}	2.38×10^{-6}	2.53×10^{-4}	4.44×10^{-6}
		201		5.49×10^{-7}	7.71×10^{-7}		5.25×10^{-9}	3.5×10^{-8}	1.38×10^{-6}	5.76×10^{-8}
		At max conc.						2.78×10^{-6}	1.19×10^{-4}	
								[21]	[70]	
≈3% CsCl		7	9.01 – 11.59	5.25×10^{-6}	1.24×10^{-5}	$1.95 \times 10\text{-}5$	5.39×10^{-10}		1.96×10^{-5}	1.25×10^{-6}
		207		1.26×10^{-6}	2.56×10^{-6}	$6.58 \times 10\text{-}5$	6.02×10^{-9}		6.92×10^{-5}	9.94×10^{-10}
		At max conc.				$1.06 \times 10\text{-}5$			7.33×10^{-6}	
						[192]			[35]	
combine		At max conc.	10.64 – 12.59			$1.49 \times 10\text{-}5$		9.33×10^{-7}	1.17×10^{-3}	
						[35]		[35]	[35]	
Control	JISS	At max conc.	10.73 – 11.2	1.99×10^{-5}	4.25×10^{-6}		3.92×10^{-9}		1.81×10^{-5}	1.66×10^{-5}
				[35]	[35]		[35]		[42]	[28]
≈3% SrCl$_2$	Tap water (closed system)	At max conc.	7.86 – 8.05	1.67×10^{-4}	3.09×10^{-5}		8.61×10^{-7}	4.29×10^{-5}	4.81×10^{-5}	5.07×10^{-6}
				[7]	[14]		[7]	[7]	[7]	[14]
Control	Tap water open	4	7.28	6.51×10^{-3}	3.44×10^{-5}		3.0×10^{-6}	5.08×10^{-9}	$3.75 \times 10\text{-}1$	4.28×10^{-2}
≈3% SrCl$_2$		4	7.26	7.55×10^{-3}	3.63×10^{-5}		5.22×10^{-6}	5.93×10^{-7}	$3.88 \times 10\text{-}5$	2.00×10^{-2}
≈3% CsCl		4	7.1	5.48×10^{-3}	1.15×10^{-4}	4.52×10^{-4}	3.11×10^{-6}		$5.83 \times 10\text{-}3$	2.3×10^{-2}

The values in "[ ]" are the time in days for the ion to reach its maximum concentration.

Table 3.12 Diffusion coefficient values (D_e) from PFA:OPC CPS

CPS	Test solution	Time period days	pH value	Calculated D_e values (cm^2/day)						
				Na$^+$	K$^+$	Cs$^+$	Ca^{2+}	Sr^{2+}	Cl$^-$	SO$_4^{2-}$
PFA/OPC	DW	7	11.98 – 12.13	1.35×10^{-4}	1.01×10^{-4}	8.01×10^{-7}	4.10×10^{-9}			1.5×10^{-4}
Control		49		1.73×10^{-5}	1.00×10^{-5}	1.14×10^{-7}	5.25×10^{-10}			2.37×10^{-5}
≈3% SrCl$_2$		7	7.47 – 8.69	1.00×10^{-3}	5.26×10^{-4}		1.05×10^{-4}	5.58×10^{-5}	7.98×10^{-4}	2.4×10^{-5}
		49		7.04×10^{-5}	3.16×10^{-5}		6.45×10^{-6}	3.64×10^{-6}	5.64×10^{-3}	2.15×10^{-6}
≈3% CsCl		7	11.95 – 12.02	7.62×10^{-5}	5.02×10^{-5}	1.56×10^{-3}	1.26×10^{-8}		9.22×10^{-3}	1.43×10^{-4}
		49		1.43×10^{-5}	6.8×10^{-6}	1.35×10^{-4}	1.33×10^{-9}		1.18×10^{-3}	7.86×10^{-6}
Control	JISS	At max conc.	12.11 – 12.27	5.30×10^{-5} [21]	2.65×10^{-5} [21]		3.64×10^{-9} [35]		5.35×10^{-4} [35]	6.05×10^{-5} [35]
Control	Tap water (open)	4	8.08	6.70×10^{-3}	1.94×10^{-4}		1.8×10^{-4}	9.7×10^{-7}	Not quoted	1.44×10^{-2}
≈3% SrCl$_2$		4	7.87	8.09×10^{-3}	7.45×10^{-4}		5.32×10^{-4}	2.38×10^{-5}	2.85×10^{-2}	2.0×10^{-2}
≈3% CsCl		4	7.1	1.33×10^{-4}	2.99×10^{-4}	2.65×10^{-3}	1.5×10^{-4}		3.35×10^{-2}	1.75×10^{-2}

The values in "[ ]" are the time in days for the ion to reach its maximum concentration

As can be seen from the generated data (Table 3.12 and 3.13), the calculated diffusion coefficient values (D_e) changes depending on the experiment. The diffusion of Sr^{2+} in closed circuit was 2.38 x10^{-6} cm^2/day (3% $SrCl_2$ BFS:OPC) compared to open circuit (tap water) 5.93 x10^{-7} cm^2/day. However, there was no significant difference observed in the diffusion of Sr^{2+} from PFA:OPC. The diffusion of Sr^{2+} from 3% $SrCl_2$ PFA:OPC in DW experiment were measured as 5.58 x10^{-5} cm^2/day in comparison with open circuit tap water 2.38 x10^{-5} cm^2/day.

Similar comparison was observed for Cs^+; 1.06 x10^{-5} cm^2/day (3% CsCl BFS:OPC DW) compared to 4.52 x10^{-4} cm^2/day in open circuit (tap water). The diffusion values of Cs^+ were found to remain fairly constant with time period 1.95 x10^{-6} cm^2/day (7 days) and 6.8 x10^{-5} cm^2/day (207 days), contrary to 3% $SrCl_2$ 2.38 x10^{-6} cm^2/day (7 days) and 3.5 x10^{-8} cm^2/day (201 days). Similar changes were observed in PFA:OPC.

This could be attributed to various factors as mentioned earlier. The dissolution of cement paste samples occurring in stagnant water (closed circuit) can reach equilibrium resulting in a saturated solution; the leaching process and the dissolution of these substance depend on their solubility products. Secondly, the concentrations of ions in the test solutions from the closed and open circuit experiments was significantly different. The difference in the diffusion coefficient value is due to some of the cations/anions reaching their solubility limits, but with a new equilibrium when fresh test solution was added to the closed circuit, which is also reflected on the diffusivities of soluble cations (Na^+ and K^+) and comparable with pH values. Solubility limits were not a factor in the open circuit and hence the difference in is noticed. Thus it can be deduced that the diffusion of the cations from encapsulated waste will depend on its properties,

environmental aqueous conditions (stagnant or mobile) and the type of formulation (BFS:OPC/PFA:OPC). The diffusion coefficients values calculated from the experimental data, produced from both the open and closed experiments are in good agreement with previously published data [160-162]. The conversion of cm^2/day to cm^2/sec corresponds to the literature diffusion coefficient value of respective ions. These values also support the experimental conditions used to measure the basic data can affect to some degree the final calculated diffusivity value. In our case this is not surprising as for the closed system experiments solubility equilibrium would be achieved relatively early in the experiment (around 50 days) and therefore would be expected to affect the diffusion of appropriate cations such as Cs^+ and Sr^{2+} from the pore water into the test solution. As with previously published work our diffusivity values also demonstrate that chloride and group I cations diffuse faster than other anions such as sulphate and cations e.g. calcium and strontium.

3.6 Depth of dissolution/leaching

There have been number of models developed to simulate the leaching and migration of encapsulated cations/radionuclides. Few of such models have used Fick's law of diffusion which is based on diffusion co-efficient, rate of diffusion and concentration of ions [139, 163, 164]. However, most models have failed to give a true picture of a possible depth to which diffusion of each cation occurred with respect to the amount present originally in the cement paste sample.

In our studies, this was determined using shrinking core model. According to shrinking core model, in a leaching process, the removal/dissolution of cations/solid materials leads to a diameter of unleached core that shrinks with time as leaching/dissolution proceeds with time.

Adopting an integrated approach by taking into consideration CPS of dimensions (3.2 x 5.3 cm) and the dry weights (BFS:OPC ≈ 86 and PFA:OPC ≈ 74) following assumptions have been made:

(a)   all the ions (inherent and encapsulated) leached to a certain depth

(b)   uniform leaching/dissolution of CPS in layers along the radius has occurred (Figure 3.15) , assuming that

(c)   all the CPSs were homogeneous mixture.

Table 3.13 Concentration of ions present in the CPS

CPS	mmoles							
	Na^+	K^+	Cs^+	Ca^{2+}	Sr^{2+}	Co^{2+}	Cl^-	SO_4^{2-}
BFS:OPC								
Control	11.9	10.6	0.77	565	35.4	9.6	3.8	18
≈3% $SrCl_2$	12.6	14.2	0.82	602	60.4	10.3	116	19
≈3% CsCl	12.6	11.3	21.31	601	34	10.3	24.6	19
≈1.3% $CoCl_2$	12.6	11.3	0.77	601	34	28.5	21.2	19
Combined metal	12.7	11.4	20.5	601	63.6	28.9	101	19.4
≈3% $SrCO_3$	12.1	10.6	0.7	573	47.5		3.6	17.1
PFA:OPC								
Control	25.1	25.6	0.26	138	29.7		0.36	9.1
≈3% $SrCl_2$	26.8	27.3	0.28	147	62.5		25.8	9.7
≈3% CsCl	26.7	27.2	20.8	147	31.6		20.5	9.7
≈3% $SrCO_3$	27	27.5	20.3	148	61.5		0.36	9.1

Based on our calculations, knowing the concentrations of ions present in the CPS (Table 3.14); then, in the outer 1mm shell of the cylindrical CPS there are on average 10.2 g of cement paste containing the mmoles of ions reported in Table 3.15.

Table 3.14 Predicted concentration of ions in the first 1mm of CPS

CPS	mmoles							
	Na^+	K^+	Cs^+	Ca^{2+}	Sr^{2+}	Co^{2+}	Cl^-	SO_4^{2-}
BFS:OPC								
Control	1.43	1.27	0.09	67.8	4.25		0.46	2.16
≈3% $SrCl_2$	1.39	1.56	0.09	66.2	6.64		6.42	2.09
≈3% CsCl	1.39	1.24	2.35	66.1	3.74		2.71	2.09
≈1.3% $CoCl_2$	1.51	1.36	0.09	72.1	4.08	3.42	2.54	2.28
Combined metal	1.28	1.15	2.09	60.5	6.42	2.95	10.3	1.99
≈3% $SrCO_3$	1.32	1.16	0.08	63	5.23		0.4	1.88
PFA:OPC								
Control	3.02	3.08	0.03	16.6	3.55		0.05	1.09
≈3% $SrCl_2$	2.95	3	0.03	16.2	6.88		4.58	1.07
≈3% CsCl	2.94	2.99	2.29	16.2	3.48		2.26	1.07
≈3% $SrCO_3$	2.7	2.75	2.03	1.48	6.15		0.05	1.09

The % removal of ions from the first 1mm shell was calculated using the maximum concentration of ion in the 200ml test solution (DW) for the closed circuit experiments. These values are reported in Table 3.16.

Table 3.15 % ions removed from first 1mm shell of CPS

CPS	% removed							
	Na^+	K^+	Cs^+	Ca^{2+}	Sr^{2+}	Co^{2+}	Cl^-	SO_4^{2-}
BFS:OPC								
Control	59	204	-	4	-	-	183	25
≈3% $SrCl_2$	74	100	-	4	11	-	134	21
≈3% CsCl	24	42	66	<0.1	-	-	21	4
≈1.3% $CoCl_2$	66	64	-	4	-	<0.01	304	26
Combined metal	54	383	36	7	9	-	373	14
≈3% $SrCO_3$	48	19	-	0.7	<0.01	-	130	5
PFA:OPC								
Control	55	44	-	0.03	-	-	480	51
≈3% $SrCl_2$	138	93	-	43	34	-	435	19
≈3% CsCl	49	47	184	0.4	-	-	467	48
≈3% $SrCO_3$								

The values in Table 3.16 shows that some of the ions have diffused out over 2 mm of depth for example Na^+ and K^+, which is most soluble ion in the pore solution; K^+ has diffused out over 4 mm from combined metal CPS, which could be attributed to chloride. Calcium being the most abundant cation in the CPS has shown the % release comparatively lesser than the rest of the cations. The % release of encapsulated cations (as chloride salt), Sr^{2+} and Cs^+ from PFA:OPC is significantly higher than the BFS:OPC, with Cs^+ diffusing out over 2 mm from $\approx 3\%$ CsCl PFA:OPC, which is comparable with Cl^- % removal values indicating that BFS:OPC formulation may slow down the diffusivity of these cation in comparison with PFA:OPC formulation. However, the diffusivity of Sr^{2+} when added as insoluble carbonate salt, is confined to the surface of few micron thickness. Cl^- is the most diffusible anion which has diffused out over 5 mm from control and 3% CsCl PFA:OPC CPS. This is attributed to the fact that Cl^- complexes that may have formed with Ca^{2+}, Sr^{2+} and Cs^+, are soluble in comparison with sulphate complexes, hence higher percentage of removal/depth of dissolution. An interesting feature is, the largest difference between BFS:OPC and PFA:OPC is the Ca^{2+} content; the fact that Sr^{2+} replaces Ca^{2+} in the cement paste mixture, above data shows a direct correlation between depth of Sr^{2+} diffusivity and total amount of Ca^{2+} present in the CPS. Depending on the type of formulation (BFS:OPC, PFA:OPC); the depth of Sr^{2+} diffusion was significantly higher in 3% $SrCl_2$ PFA:OPC having 147 mmoles of Ca^{2+} compared to its BFS counterpart having 602 mmoles of Ca^{2+}. The effect of mass action can be noticed in control CPS; the depth of diffusion of Ca^{2+} is smaller in PFA:OPC compared to BFS:OPC control CPS.
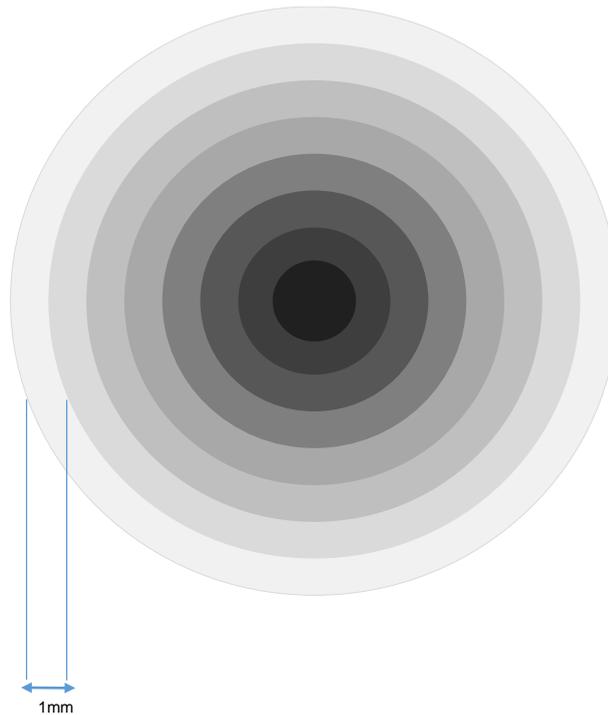
Figure 3.15 Illustration of ion disposition in CPS.

3.7   Microbial impact on migration of ions from CPS

Cementitious materials are susceptible to microbiological degradation [68, 165]. The interactions of microorganisms in the degradation of concrete and on the mobility of metals and/or radionuclides in soil and other solid matrices have received significant attention [70, 165-167]. The most fascinating feature of microorganisms is that they are composed of diverse taxa with varying nutritional demands within small microenvironments. The bioavailability of the contaminants/radionuclides depends on their chemical nature; their role in the biological system and also the physic-chemical parameters of the site which may favour their growth [168]. Studies on the impact of microbial degradation on cementitious material has revealed that the most frequent colonisers of concrete include bacteria, cyanobacteria, algae, fungi and lichens (Table 3.17). Studies by

101

BNFL scientists demonstrated that sulphur-oxidising bacteria (SOB) could degrade concrete structures by up to 8mm/year. Two of the supervisors (Eccles and Morton) involved with this project patented this work [77]. SOB were shown to mobilise radionuclides from contaminated soil, the pore water eventually achieving a pH less than 1.0 [169]. Microorganisms have the ability to grow over a wide range of pH, under elevated hydrostatic pressures, in highly alkaline conditions, in nutrient–starved conditions and at radiation levels that would be lethal to humans [170] . Throughout nature various elemental cycles including carbon, nitrogen, sulphur and oxygen occur simultaneously. In GDF the availability of waste matrices, canisters, over packs, buffers and backfills, etc., can be potential nutrient and energy sources for microorganism [171]. Microorganisms can form biofilms which induce corrosion of metal surfaces to which they are attached [172]. However, direct anaerobic corrosion of concrete is not known, although anaerobic degradation of organic acids and their impact on concrete could be a significant factor [173] under aerobic conditions. Additionally, microbial gas generation [174] may lead to further microbial transformation. This could lead to an increase in radionuclide mobility and may, in time, impact on the far-field system with a pathway into the food-chain and/or other receptors.

The experiments in the present research were designed to simulate an actual GDF scenario where the microbial population will be influenced by environmental conditions such as availability of nutrients and energy for their growth and metabolism [70]. It is very likely that GDF will remain aerobic for few years in post-closure period. Our experiments were carried out using minimum growth media, and no additional growth media were added to the test solution. The viable

population of bacteria and fungi present in test solution (JISS) had only nutrients and carbon source present in the circulating system available to them. The colonisation of the cementitious material begins with those organisms that are able to cope with the highly alkaline conditions. This primary colonisation alter the micro-environment and create a new organism for colonisation [168]. Most of the cations present in cement paste samples will directly or indirectly support the growth and metabolism of the fungal species. Some of these cations are Na^+, Mg^{2+}, Ca^{2+}, Mn^{4+}, and Fe^{3+} [175]. Bacterial cells have high tolerance to these metals in biological functions compared to those without biological significance. These metals either serve as a functional metal ion in metabolic process/enzymatic reactions, or support the structural development of the cell envelope. Bacteria can cope with high concentrations of metal ions depending on the external condition [176].

Microorganisms treat contaminants in two ways; (i) immobilisation and (ii) mobilisation; the former reduces their bioavailability, whereas the latter increases their potential toxicity by increasing their bioavailability and transfer; which in turn depends on the chemical nature and biological function or biochemical significance of the metallic species. Several key microbial processes are involved in the mobilisation and immobilisation of metal compounds by one or more mechanisms which are presented in Table 3.18 . These processes depend on the environmental and physic-chemical conditions, e.g. pH, water/moisture, inorganic and organic molecules, compounds, colloids and particulates present.

Table 3.16 Microorganisms involved in the biodegradation of concrete [69].

Concrete degrading organisms

Bacteria

Thiobacillus intermedius [177, 178]
Thiobacillus neapolitanus [178, 179]
Thiobacillus novellus [178, 179]
Thiobacillus thioparus [178, 179]
Acidithiobacillus thiooxidans [178-181]
Thiomonas perometablis[181]

Fungi

Alternaria sp [182]
Cladosporium cladosporioides [182]
Epicoccum nigrum [182]
Fusarium sp [177, 182]

Mucor sp [182]
Penicillium oxalicum [182]
Pestalotiopsis maculans [182]
Trichoderma asperellum [182]
Aspergillus niger [183]
Alternaria alternate [184]
Exophiala sp.[184]
Coniosporium uncinatum [184]

Algae

Chaetomorpha antennina [185]
Ulva fasciata [185]

Lichens

Acarospora cervina [186]
Candelariella ssp [186]

Table 3.17 The major mechanisms of microbial metal interaction [175, 187]

Mobilisation	Immobilisation
1. <u>Enzymatic oxidation</u> $UO_2 + 2Fe^{3+} \rightarrow UO_2^2 + Fe^{2+}$ Autotrophic leaching, e.g.*Thiobaccillus ferroxidans*, *T. thiooxidans.* $4Fe^{2+} + O^2 + 4H^+ \rightarrow 4Fe^{3+} + 2H_2O$	1. <u>Precipitation</u> e.g.Sulphate-reducing bacteria strictly anaerobic bacteria
2. <u>Enzymatic reduction</u> facultative and obligate anaerobic microorganisms $UO_2^{2+} \rightarrow UO_2$ $Fe^{3+} \rightarrow Fe^{2+}$ $Mn^{4+} \rightarrow Mn^{2+}$	2. <u>Biosorption</u> e.g. extracellular polymeric substances (EPS), metal binding proteins.
3. <u>Complexation</u> Metal + ligand $\rightarrow$ metal complex Citric acid, tricarboxylic acid released during microbial degradation	3. <u>Bioaccumulation</u> Transport phenomena involving ion pump, ion channel, endocytosis, complex permeation, and lipid permeation

3.7.1 Mobilisation of metal ions

Mobilisation of metals from a substrate is through autotrophic and heterotrophic leaching, chelation by microbial metabolite by the action of siderophores and by methylation. The majority of biologically mediated leaching of metal ions take place as a result of autotrophic metabolism which is carried out by chemolithotrophic acidophilic bacteria such as *Thiobacillus ferrooxidans and T. Thioxidans*, which obtain energy from oxidation of ferrous iron or reduced sulphur compounds. The end products of autotrophic leaching releases Fe (III) or H_2SO_4. The organisms involved in enzymatic reduction are heterotrophic anaerobes, few of them are facultative and oxygen may also be respired. The reduction of Fe (III) and Mn (III) to Fe (II) and Mn (II) respectively, may also release the metals

attached to their respective oxides [188-190]. This process may also be enhanced by presence of humic substances [175, 191]. Microbial degradation also releases various organic acids which have been found to have metal complexation ability. Several studies have shown that citric and oxalic acid are commonly released in the surrounding environment by fungal hyphae that form stable complexes with various metals [192]. The soil fungus *Aspergillus niger* has shown the ability to solubilise a wide range of insoluble metal compounds, including phosphate, sulphide and mineral ores [193]. This fungus produces organic acids and acidifies the surrounding medium irrespective of presence of metal compounds. Studies indicated that, altering the concentrations of Nitrogen, Phosphorous or pH can enhance the production of organic acids [193]. In manganese deficient growth media; 600 mM of citric acid is produced by *A niger,* another example of fungal leaching is that mediated by *Penicillium simplicissimum* [66]. This fungus, isolated from a contaminated site was shown to leach Zn^{2+} from insoluble ZnO contained in industrial filter dust, by producing citric acid (7100 mM) [194]. Citric acid derived from a fungal strain of *P simplicissimum* has shown a much greater ability to leach Al^{3+} than pure citric acid [61]. In an iron deficient medium; microorganisms produce specific iron chelators known as siderophores. These compounds possess catecholate, phenolate or hydroxamate as their binding groups. Most fungi possess intracellular siderophores as iron storage compounds [195]. Over the past few years many siderophore or siderophore-like compounds have been identified from various biological systems [196]. Although siderophores are primarily selective for Fe(III); studies have shown that they can also complex other metals and radionuclides [197].

3.7.2 Immobilisation of metal ions

Immobilisation of toxic metals and radionuclides by microorganisms is achieved by biosorption to cell wall, exctracellular polysaccharides (EPS), and intracellular bioaccumulation/precipitation around cell wall [175]. Immobilisation processes have received considerable attention due to their potential in detoxification of toxic waste [198]. The accumulation of metals by bacterial cells takes place in two broad processes (i) passive adsorption which is independent of metabolism and (ii) active adsorption which is dependent on element-specific transport system and is metabolism dependant [168]. In the majority of cases, the passive adsorption plays an important role in metal accumulation due to the scarcity of nutrients. Active adsorption requires energy. However, passive adsorption is faster than active [61, 199]. Bacteria can cope with high concentration of metal ion depending on the external condition [175]. Biosorption by cell walls, involves EPS and proteins. Many such exopolymers serve as a source of polyanions which can interact with cationic metal/radionuclide species, under natural conditions [200]. In the case of fungi, chitin, phenolic polymers and melanins possess potential metal-binding sites for radionuclides [201]. Precipitation can take place as a result of release of sulfide due to sulfate reduction by sulpfate-reducing bacteria (SRB). Most metal sulfides formed are insoluble and the solubility product of these metal sulfides is in the range of 4.65 X 10^{-14} (Mn) to 6.44X 10^{-53} (Hg). Reference studies have shown that extreme reducing conditions created by SRB can also reduce uranium (VI) [202].

In the present research, genus level identification of bacteria showed the presence of *Actinomyces spp*, which readily colonises concrete structures leading to formation of a biofilm [68]. This biofilm can trap other particulate

material making the concrete surface susceptible for degradation [177]. Presence of *Cladosporium spp.*; the most frequently detected fungal species on damp or water-damaged building materials [203], were isolated from all the test solutions except the control CPS. There have been several studies on the melanin containing dark-pigmented *Cladosporium cladosporioides,* which is predominantly present in soil, showed accumulation of radionuclides, especially ^{137}Cs [204]. Fungal species isolated from within and around the Chernobyl nuclear reactor detected presence of several species of *Cladosporium* [67, 200]. The colonisation of cementitious materials by fungi is dependent on pH which normally takes place once the pH has dropped sufficiently depending on the availability of nutrients [189, 200]. In the present study the colonisation of fungi occurred in the later stages of the experiment indicating that these heterotrophs are late colonisers of cementitious materials which might be using the organic remnants of primary colonisers as a carbon source. The pH values of JISS is comparable with the presence of viable bacterial count in the circulating system (Table 3.19 and 3.20). The circulating system with viable population of bacteria were measured having lower pH values. Bacteria have ability to acidify or neutralise the cytoplasm depending on the external environmental conditions, to maintain the optimal function and their structural integrity [205].

Table 3.18 Summary table showing pH values and microbial analysis of JISS from BFS:OPC JISS experiment

Experiment	BFS:OPC CPS		pH range of JISS	Total viable count (cfu)	Gram stain	motility
BFS:OPC JISS	(a)	Control	10.73 - 11.2	3	NR*	NR*
	(b)	≈3% SrCl$_2$	7.29 - 8.09	4.7 x10^7	G+ve	-
	(c)	≈3% CsCl	6.77 - 7.87	1.9 x 10^7	G+ve	+ -
	(d)	≈3% SrCO$_3$	7.53 - 7.93	9.1 x 10^4	G+ve	+ -

*None recorded

Table 3.19 Summary table showing pH values and microbial analysis of JISS from PFA:OPC JISS experiment

Experiment	PFA:OPC CPS	pH range of JISS	Total viable count (cfu)	Gram stain	motility
PFA:OPCJISS	(a) Control	12.11 - 12.27	NR*	NR*	NR*
	(b) ≈3% $SrCl_2$	8.07 - 8.47	0.57×10^7	G+ve	-
	(c) ≈3% CsCl	11.63 - 11.99	NR*	NR	NR*
	(f) ≈3% $SrCO_3$	12.05 - 12.19	2.3×10^3	G+ve	-

*None recorded

The test solution (JISS) retard Sr^{2+} diffusivity but accelerated Cs^+ diffusion in comparison with distilled water values (Figure 3.9 to 3.12). This could be attributed to the inherent sulphate content (≈ 8600 ppb) of the JISS test solution (Table 3.7) and also the presence of both motile and non-motile bacteria in JISS from 3% CsCl circulating system (Table 3.19).

Another factor that might have contributed towards the mobility of encapsulated ions is presence of humic substance [206]. Humic substances are naturally occurring heterogeneous mixtures of organic molecules that play an important role in behaviour and fate of metal ions in the natural environment, by controlling their concentration in soil and natural waters [207]. The presence of humic acid have not been measured in the present study. There are three major fractions of humic substance: fulvic acid, Humic acid and Humin, which are polydiverse mixture of natural organic polyelectrolyte having different functional group to which metal ions/ radionuclide bind [191]. The ability of humic substance to absorb Sr^{2+}, Cs^+, Co^{2+} has been well documented [208, 209].

It is thought therefore, the cumulative effect of presence of motile bacteria, fungi and presence of humic substances might have lowered the pH and influenced the diffusivity of cation from BFS:OPC CPSs.

Chapter 4: Diffusivity from BFS:OPC CPSs with distilled water as a test solution

4.1 Aims of study

This chapter aims to evaluate the influence of concentration and nature of cation on their diffusivity when encapsulated in BFS:OPC in contact with distilled water.

4.2 Introduction

In this chapter, a series of diffusivity experiments have been carried out on non-aged CPSs to evaluate the diffusivity of caesium and cobalt when added to BFS:OPC formulation as their chlorides and for strontium when added as chloride and carbonate. Strontium carbonate was selected to determine the influence of a water insoluble compound on diffusivity of the cation. In case of aged CPS diffusivity experiment, samples were allowed to cure for 240 days in the laboratory atmosphere. Diffusivity studies on these 8 month old samples were carried out to compare the rates with that of non-aged samples' in order to have a better understanding of the encapsulated waste that has been standing in an interim store and/or in a GDF over a long period of time prior to closure period. Diffusivity studies were also carried on CPSs encapsulated with ≈0.3% Cs and Sr chloride and Sr carbonate salts to demonstrate the influence of cation and anion concentration on the diffusivity of the encapsulated cation. The experimental conditions were kept identical in all the diffusivity circulation experiments. A total of six sets of diffusivity experiments (Table 4.1) were carried out using distilled water and two sets using tap water as a test solution for comparative purposes; tap water was selected for the 'open' diffusivity experiments. The logistics of accommodating nearly 50 litres/week of test solution for each open circuit experiment in the laboratory for about 30 to 40 days was a logistic significant factor. This volume of solution influenced the decision to use tap water. Each experiment consisted of one to five sets of closed circulating

diffusivity circuits with OPC: BFS cement paste and different cation characteristics.

The data generated from these experiments will serve as a baseline for further diffusivity studies involving simulated ground water and microorganisms.

4.3   Cement paste samples

Diffusivity experiments were carried out on 17 different cement paste samples, details of which are mentioned in Table 4.1.

Table 4.1 Cement paste samples and test solution used

Experiment	BFS:OPC Cement paste samples	Test solution
1	(a) Control (b) $\approx$3% $SrCl_2$ (c) $\approx$3% CsCl (d) $\approx$1.3% $CoCl_2$ (e) Combined metal ($\approx$3% $SrCl_2$, $\approx$3% CsCl and $\approx$1.3% $CoCl_2$)	Distilled water
2	(a) Aged Control (b) Aged $\approx$ 3% $SrCl_2$ (c) Aged $\approx$ 3% CsCl	Distilled water
3	(a) $\approx$0.3% $SrCl_2$ (b) $\approx$0.3% CsCl	Distilled water
4	(a) $\approx$3% $SrCO_3$ (b) $\approx$0.3% $SrCO_3$	Distilled water
5	(a) Control (b) $\approx$3% $SrCl_2$ (c) $\approx$3% CsCl (d) $\approx$3% $SrCO_3$	Tap water (open circuit)
6	(a) $\approx$3% $SrCl_2$	Tap water (closed circuit)

4.4 Results

The compositions of the as received OPC and BFS from the NNL were comparable, possibly with the exception of moisture, with other cements and slags used in waste encapsulation (Table 4.2). The moisture content of the OPC was not taken into account when preparing CPSs. During the curing stage, the CPSs lost the pool of liquid that had collected on the upper surface during the first 7 days and on removal from the small polythene bottle gradually changed colour from distinct grey to light grey as shown in Figure 2.1. This change in colour was also accompanied a change in the cylinder surface texture from smooth to less smooth and was possibly due to the cement paste adsorption of carbon dioxide from the laboratory atmosphere. The incorporation of cation, either Cs^+, Sr^{2+}, Co^{2+} or a mixed cation regime affected both the rate of liquor loss and the surface finish of the cement paste sample. Addition of cobalt, for example, produced a more marble effect type finish whilst the others were less well polished. The loss of bleed water took shorter duration of time in ≈3% $SrCl_2$ CPSs. The loss of bleed water from control CPS was substantially slower than all other CPSs, however, there was no bleeding noticed on the top surface during the curing stage of 3%$SrCO_3$. The variable rate of loss of liquor from the upper cement paste sample surface was instrumental for sectioning three CPSs (control, 3% $SrCl_2$ and 3% CsCl) (Figure 2.2).

Table 4.2 Analysis of as received OPC and BFS (%).

Material	Na^+	K^+	Cs^+	Ca^{2+}	Mg^{2+}	Sr^{2+}	Cl^-	SO_4^{2-}	moisture
OPC	0.6	0.63	0.06	42.64	1.36	4.61	0.11	1.37	26.2
BFS	0.44	0.74	0.20	38.22	3.48	4.92	0.26	0.63	0.2

4.4.1 Chemical analysis of cement paste

Table 4.3 shows the analysis of the dissected ≈3% $SrCl_2$ and ≈3% CsCl CPSs indicating that segregation of the cation had occurred during curing, with segregation being more prominent in the ≈3% $SrCl_2$ CPS, may be indicative of the surface area and micro-pore area being significantly larger than the ≈3% CsCl CPS. The average of the measured cation concentration for both Cs^+ and Sr^{2+} is consistent with the amount of cation added during the cement paste preparation. The higher surface area and micro-pore size of the ≈3% $SrCl_2$ CPS could also account for the higher moisture content.

Table 4.3 Cation, surface and micro-pore area analysis ≈3% $SrCl_2$ and ≈3% CsCl CPS

Dissected BFS:OPC sample	≈3% $SrCl_2$ CPS			≈3% CsCl CPS		
	% Sr	Micro-pore area	Surface area	% Cs	Micro-pore area	Surface area
		m^2/g			m^2/g	
Top	3.0	12.8	48.5	3.1	1.2	26.3
Middle	3.1	8.2	38.9	2.9	3.6	26.8
Bottom	1.8	6.3	23.0	2.2	2.2	20.0

4.4.2 Moisture content of CPS

A significant difference was observed in the moisture content of top two sections measured of control and CPSs encapsulated with chloride salts of %3 Sr and Cs in comparison with CPS encapsulated with carbonate salt of 3% Sr (Table 4.4). This difference in moisture content can be compared with significant difference in bleeding observed for all other CPS except ≈3% $SrCO_3$ CPS.

Table 4.4 % moisture content of BFS:OPC CPS

	Control	≈3% SrCl$_2$	≈3% CsCl	≈1.3% CoCl$_2$	combined metal	≈3% SrCO$_3$
Top	16.6	26.6	21	20.1	27.3	5.9
Middle	13.4	22.5	22.7	23.6	17.9	5.2
Bottom	12.1	19	15.2	19.5	16.8	5.1

4.4.3 Average micropore and surface area micropore area analysis of cement paste sample measured by BET method

The average micropore and surface area results of all the CPSs are shown in Table 4.5. The values of micropore area of the CPSs prior to the diffusivity experiments were in the range of 1.0 – 9.10 m^2/g. The micropore area of the CPSs containing strontium chloride were higher compared with the other CPSs. Cement paste containing cobalt chloride had the lowest micro-pore area. Surface area of the CPSs were in the range of 11.6 – 42.9 m^2/g. The surface area of control and ≈3% SrCl$_2$ CPS were higher than Cs contaminated CPSs.

Table 4.5 Average micropore and surface area of cement paste samples measured by BET method prior to diffusivity experiments

CPS	Micropore area	Surface area
	(m^2/g)	
Control	5.2	42.9
≈ 3% SrCl$_2$	9.1	36.8
≈ 3% CsCl	2.3	24.4
≈ 1.3% CoCl$_2$	1.0	20.0
combined metal	7.3	36.6
Aged control	4.4	31.8
Aged ≈ 3% SrCl$_2$	8.5	22.3
Aged ≈ 3% CsCl	1.4	13.1
≈ 0.3% CsCl	3.1	19.2
≈ 0.3% SrCl$_2$	4.2	19.2
≈ 0.3% SrCO$_3$	5.3	22.0
≈ 3% SrCO$_3$	4.8	23.0
Control (open circuit)	2.7	24.2
≈ 3% SrCl$_2$ (open circuit)	5.42	22.8
≈ 3% CsCl (open circuit)	1.3	11.6
≈ 3% SrCO$_3$ (open circuit)	2.7	21.2
3% SrCl$_2$ (tap water)	5.44	22.6

4.4.4 Test solution analysis

4.4.4.1 pH values

The pH values of the test solutions after the first few days of the diffusivity experiments increased from about 7.0 (natural pH value of de-ionised water) to 9 - 13, except in the case of test solutions with strontium carbonate samples; this increase is not unexpected as calcium salts will gradually diffuse from the cement. After about 70 days the pH values for the Cs chloride and Sr carbonate

experiments decreased, with the decrease more pronounced for cement paste with higher concentration of carbonate (Figure 4.12). pH values of the test solutions from control and ≈ 3% $SrCl_2$ test solutions showed a similar trend in pH (Figure 4.1 to 4.2). However, ≈3% CsCl, ≈1.3% $CoCl_2$ and combined metal test solutions, showed a somewhat similar trend until day 42 (Figure 4.3 to 4.5). There was no significant difference in the pH values observed for aged and non-aged cement paste sample test solutions (Figure 4.6 to 4.8). The pH values of the tap water test solutions increased from 7.1 (natural pH of tap water) to 8.05 in both close and open diffusivity circuits.

4.4.4.2 Chemical analysis of test solution

All the diffusivity data have been normalised for dilution effect and cation/anion composition of tap water (Table 4.6). The rates of diffusivity of all the experiments are shown in Figure 4.1 to Figure 4.17 and the values are shown in appendix 4.1 to 4.17. In the following sub sections the average diffusivity data have been used for comparative purposes.

Table 4.6 Analysis of tap water

| Sample | Concentration in ppb | | | | | | pH |
	Na^+	K^+	Mg^+	Ca^{2+}	Cl^-	SO_4^{2-}	
Tap water	3984	365	1716	7160	828	13520	7.17

4.4.4.2.1 *Strontium*

The highest rate of diffusivity of Sr^{2+} was measured for the ≈3% $SrCl_2$ followed by combined metal and aged ≈3% $SrCl_2$ paste sample. The rate of diffusivity of Sr^{2+} in closed circuit tap water experiment was statistically significant ($p> 0.05$) with that of Sr^{2+}diffusion from combined metal CPS. The average rate of diffusivity

from aged ≈3% $SrCl_2$ (6.5 µg/cm^2/day) CPS was half the average rate of diffusivity of Sr from non-aged ≈3% $SrCl_2$ CPS (14 µg/cm^2/day). Strontium from ≈3% $SrCO_3$ CPS (0.026 µg/cm^2/day) diffused out at significantly slower in comparison with ≈3% $SrCl_2$ CPS (6.5 µg/cm^2/day). However, the rates of diffusivity of Sr^{2+} from ≈3% $SrCO_3$ and ≈ 0.3% $SrCO_3$ showed a similar trend in diffusivity and were similar to the rates of diffusivity of Sr^{2+} from control sample. The average rates of diffusivity of Sr^{2+} from ≈0.3% $SrCl_2$ (0.26 µg/cm^2/day) was 76 times lower than its 3% counterpart. The results obtained from open circuit diffusivity experiment confirmed the trend of Sr^{2+} diffusivity found in the closed circuit diffusivity experiments. Strontium from ≈3% $SrCl_2$ paste sample diffused out faster than the Sr^{2+} from ≈3% $SrCO_3$ CPS.

4.4.4.2.2 *Caesium*

The rate of diffusivity of Cs^+ from non-aged ≈3% CsCl CPS was faster and significantly similar ($p > 0.05$) to the Cs^+ diffusivity from combined metal CPS. The average rate of diffusivity of Cs^+ from aged ≈3% CsCl CPS (8.4 µg/cm^2/day) was measured 2.6 times lower than the average rate of diffusivity of Cs^+ from non-aged ≈3% CsCl CPS (22 µg/cm^2/day). Caesium from ≈0.3% CsCl CPS (1.5 µg/cm^2/day) diffused out ≈12 times slower than the rate of diffusivity of Cs^+ from ≈3% CsCl CPS (17.8 µg/cm^2/day). This confirms that the rate of diffusivity depends on the concentration of the cation added to the cement paste sample. The diffusivity rate of Cs^+ was found to be 2 to 6 times higher than Sr^{2+} from all the CPSs.

4.4.4.2.3 *Cobalt*

The rate of diffusivity of Co^{2+} from $\approx 1.3\%$ $CoCl_2$ was found lowest of all the cations from CPS. The sequence of diffusivities of the added cation were shown as Cs^+ > Sr^{2+}> Co^{2+} from individual CPS as well as from combined metal CPS.

4.4.4.2.4 *Calcium*

The diffusivity of Ca^{2+} from $\approx 3\%$ $SrCl_2$ and $\approx 1.3\%$ $CoCl_2$ CPS was similar ($p>0.05$) and measured as 5 times higher than the control CPS. Calcium from combined metal CPS (14 $\mu g/cm^2/day$) and aged $\approx 3\%$ $SrCl_2$ CPS (15 $\mu g/cm^2/day$) diffused out at the similar rate; was measured 3 times higher than the rate of diffusivity of Ca^{2+} from non-aged control CPS (5 $\mu g/cm^2/day$). The average rate of diffusivity of Ca^{2+} from $\approx 3\%$ CsCl CPS (0.4 $\mu g/cm^2/day$) was 12 times lower than the non-aged control CPS (5 $\mu g/cm^2/day$) and was found to be lowest of all the samples. However, the diffusion of Ca^{2+} from aged $\approx 3\%$ CsCl CPS (8 $\mu g/cm^2/day$) was found to be 20 times higher than non- aged $\approx 3\%$ CsCl CPS (0.4 $\mu g/cm^2/day$) and ≈ 6 times higher from 0.3% CsCl (3.2 $\mu g/cm^2/day$) compared to non-aged $\approx 3\%$ CsCl (17.8 $\mu g/cm^2/day$ for 105 days). The average rate of diffusivity of Ca^{2+} from $\approx 0.3\%$ $SrCl_2$ (6.1 $\mu g/cm^2/day$) was measured 4.5 times lower than the average rate of diffusivity of Ca^{2+} from its 3% counterpart (27.5 $\mu g/cm^2/day$ for 105 days). Calcium from $\approx 3\%$ $SrCO_3$ CPS diffused out at faster rate in comparison with $\approx 0.3\%$ $SrCO_3$ CPS. The diffusion of Ca^{2+} from the CPS in the open circuit experiment showed the similar pattern of diffusivity in comparison with close circuit experiment with higher rate of Ca^{2+} diffusivity from $\approx 3\%$ $SrCl_2$ (1.9 $\mu g/cm^2/day$) compared to $\approx 3\%$ CsCl CPS (0.8 $\mu g/cm^2/day$). However, the rate of diffusivity of Ca^{2+} from $\approx 3\%$ $SrCO_3$ (0.01 $\mu g/cm^2/day$) was found to be lowest in contrast with closed circuit experiment.

There was no significant difference ($p > 0.05$) observed between the Ca^{2+} diffusivity from ≈3% $SrCl_2$ in DW (65 µg/cm^2/day) and in closed circuit tap water (50.8 µg/cm^2/day).

4.4.4.2.5 *Sodium*

The rates of diffusivity of Na^+ from non-aged control, ≈1.3% $CoCl_2$ and ≈3% $SrCl_2$ CPSs were fairly in similar range (3.8 – 4.8 µg/cm^2/day). The lowest rate of diffusivity was seen in the test solution of ≈3% CsCl CPS (1.3 µg/cm^2/day) and combined metal CPS (1.1 µg/cm^2/day). Sodium diffused out at higher rate from ≈0.3% $SrCl_2$ and ≈0.3% CsCl CPSs. Sodium from ≈3% CsCl CPS (1.2 µg/cm^2/day) diffused out 7 times slower in comparison with ≈0.3% CsCl CPS (8.8 µg/cm^2/day). However, there was no significant difference ($p > 0.05$) in the rate of diffusivity of Na^+ observed between ≈3% $SrCl_2$ and ≈0.3% $SrCl_2$ CPS. In the case of aged sample, the average rate of diffusivity of Na^+ from ≈3% CsCl CPS (2.7 µg/cm^2/day) was two times higher than non-aged ≈3% CsCl CPS (1.3 µg/cm^2/day). However, sodium from aged and non-aged ≈3% $SrCl_2$ CPS diffused at relatively similar rates ($p > 0.05$). The rate of diffusivity of Na^+ from ≈3% $SrCO_3$ and ≈0.3% $SrCO_3$ CPS showed a similar trend of diffusivity ($p > 0.05$). There was no significant difference in the diffusivity of Na^+ observed in open circuit experiment from all the CPSs. The rate of diffusivity of Na^+ from ≈3% $SrCl_2$ CPS in DW and close tap water experiment was found to be similar ($p > 0.05$).

4.4.4.2.6 *Chloride*

Chloride from combined cation CPS diffused (270 µg/cm^2/day) out higher than the rest of the CPSs. This is attributed to the concentration effect, the concentration of Cl^- in combined metal CPS (101 mmoles) was higher than all

other CPS, however, significantly similar to Cl⁻ concentration from ≈3% SrCl$_2$ (58.3 mmoles) (Table 4.7). The diffusivity of Cl⁻ from strontium encapsulated CPSs was higher than caesium encapsulated CPSs. The average rate chloride diffusivity from aged ≈3% CsCl (19 µg/cm^2/day) was measured ≈4 times higher than non-aged ≈3% CsCl CPS. The rate of diffusivity of Cl⁻ from ≈3% CoCl$_2$ (60 µg/cm^2/day), non- aged ≈3% SrCl$_2$ (57 µg/cm^2/day), and aged ≈3% SrCl$_2$ (63 µg/cm^2/day), was found to be in similar range having similar trend of diffusivity. Chloride from ≈0.3% SrCl$_2$ (24 µg/cm^2/day) diffused out 3.5 times slower than the diffusivity of Cl⁻ from their ≈3% SrCl$_2$ (82.7µg/cm^2/day). The results obtained from open circuit diffusivity experiment are in agreement with the closed circuit diffusivity. The average rate of diffusivity of Cl⁻ from control (3 µg/cm^2/day) and ≈ 3% SrCO$_3$ (3 µg/cm^2/day) was found to be lowest and significantly similar, indicating that the Cl⁻ diffusion is due to added cation chloride. The average rate of diffusivity of Cl⁻ from ≈3% SrCl$_2$ in closed circuit tap water (468 µg/cm^2/day) was 3 times higher than average rate of diffusivity of Cl⁻ from ≈3% SrCl$_2$ CPS (153.5 µg/cm^2/day) in DW.

Table 4.7 Concentration of Cl⁻ calculated in BFS:OPC CPS in mmoles

BFS:OPC CPS	Cl⁻ concentration (mmoles)
Control	3.8
≈ 3% $SrCl_2$	58.3
≈ 3% CsCl	24.6
≈ 1.3% $CoCl_2$	21.2
combined metal	101
≈ 0.3% $SrCl_2$	6.5
≈ 0.3% CsCl	5
≈ 0.3% $SrCO_3$	3.6
≈ 3% $SrCO_3$	3.7

4.4.4.2.7   *Sulphate*

The highest rate of diffusivity of sulphate was observed in the test solution of aged ≈3% $SrCl_2$ followed by aged ≈3% CsCl. The average rate of diffusivity of SO_4^{2-} was ≈8 times greater from aged ≈3% $SrCl_2$ CPS (47 µg/cm^2/day) compared to non-aged ≈3% $SrCl_2$ CPS (6 µg/cm^2/day). This is comparable to the Cl⁻ diffusion, however, the diffusion of SO_4^{2-} is from inherent anion in the OPC and/or BFS and was not added to the CPS (Table 4.8). In the case of ≈3% CsCl, the diffusivity from aged CPS (27 µg/cm^2/day) was 14 times higher than non-aged CPS (1.9 µg/cm^2/day). ≈3% $SrCO_3$ and ≈0.3% $SrCO_3$ test solution showed the lowest diffusivity. Both the ≈3% $SrCO_3$ and ≈0.3% $SrCO_3$ showed the similar rate of diffusivity after 21 days with initial higher diffusivity from ≈3% $SrCO_3$ sample. Similar trend in the diffusivity from ≈1.3% $CoCl_2$ CPS (11 µg/cm^2/day) and non-aged control CPS (11µg/cm^2/day) was observed, which was found to be 5 times lower than the aged ≈3% $SrCl_2$ (47 µg/cm^2/day) SO_4^{2-} diffusivity. The results obtained from open circuit diffusivity experiment did not show any similarities in diffusivity pattern in comparison with closed circuit diffusivity experiment. The

rates of diffusivity of SO_4^{2-} from encapsulated cation CPSs were similar (2.49 –

3.75 µg/cm^2/day) and ≈3 times higher than the average rate of diffusivity of SO_4^{2-}

from control CPS (0.94 µg/cm^2/day) in open circuit diffusivity experiment.

Table 4.8 Concentration of SO_4^{2-} calculated in BFS:OPC in mmoles

BFS:OPC CPS	SO_4^{2-} concentration (mmoles)
Control	18
≈ 3% SrCl$_2$	19
≈ 3% CsCl	19
≈ 1.3% CoCl$_2$	19
combined metal	19.4
≈ 0.3% SrCl$_2$	17.5
≈ 0.3% CsCl	17.2
≈ 0.3% SrCO$_3$	17.1
≈ 3% SrCO$_3$	17.5

4.5   Conclusions

1   The make-up water composition affected the segregation of inherent/added cations in the cement paste samples.

2   Initial pH values for all samples except ≈3% $SrCO_3$ were in the range 9 to 13; the addition of strontium carbonate could be akin to adsorption of CO_2 i.e. carbonation.

3   The rate of decrease in the pH value could be a function of the cement chemistry occurring within the paste sample.

4   The rate of carbonation was insufficient to affect pH trends, but in some cases was sufficient to affect rate of diffusivity.

5   Strontium when added as a soluble salt to the make-up water influences the rate of diffusivity.

6   The concentration of the added salt to the make-up water also affects diffusivity.

7   The addition of cation salts to the make-up water affected the rate of diffusion of calcium ions from the cement paste samples and may not be influenced by the concentration of added salt.

8   Diffusivity of chloride ions from the cement paste samples is dependent on the concentration of chloride in the make-up water.

9   Aging of the cement paste samples influenced the diffusivity rate of sulphate.

10   More dilute make-up water i.e. ≈0.3% cation concentration had a greater effect on diffusivity of sodium than more concentrated make-up water.

11   Aging of the cement paste sample had little effect on sodium diffusivity.
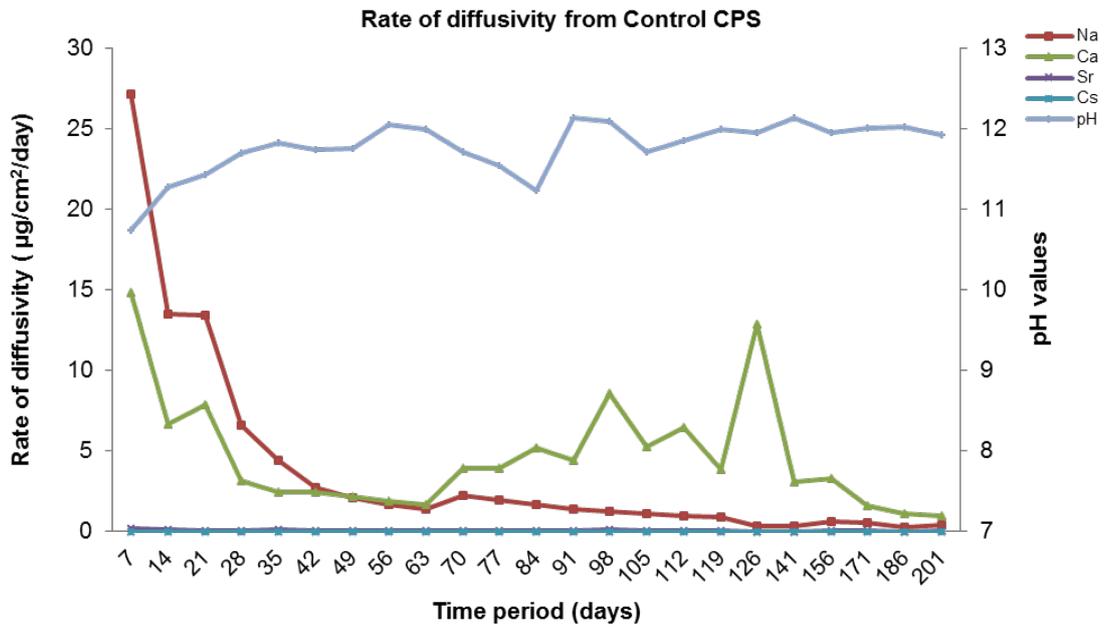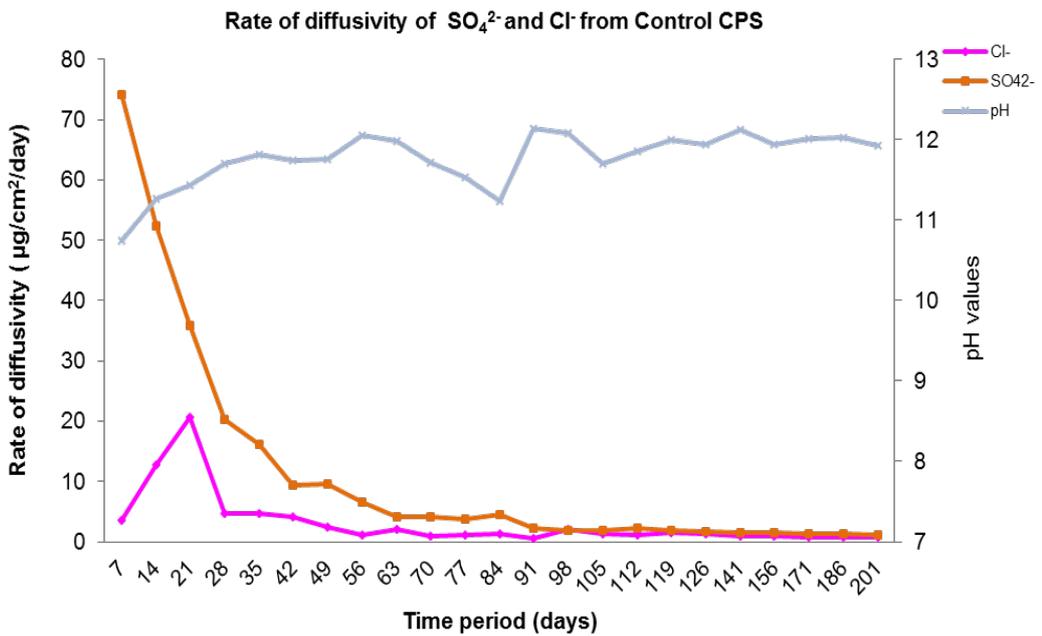
Figure 4.1 Rate of diffusivity of cations (a) and anions (b) from control BFS:OPC
CPS in DW
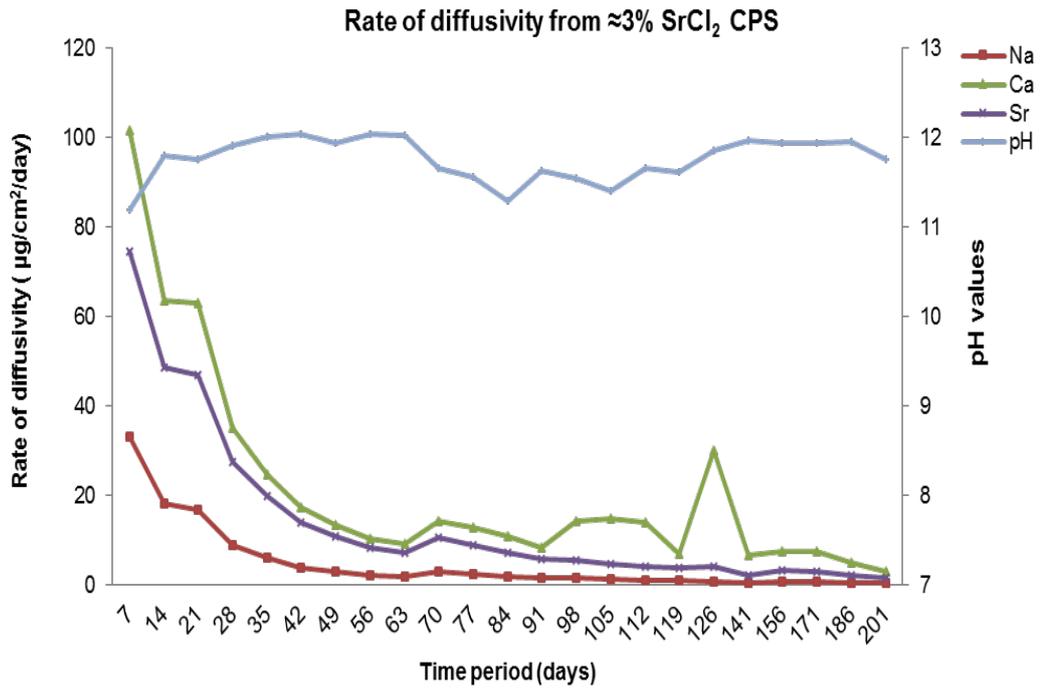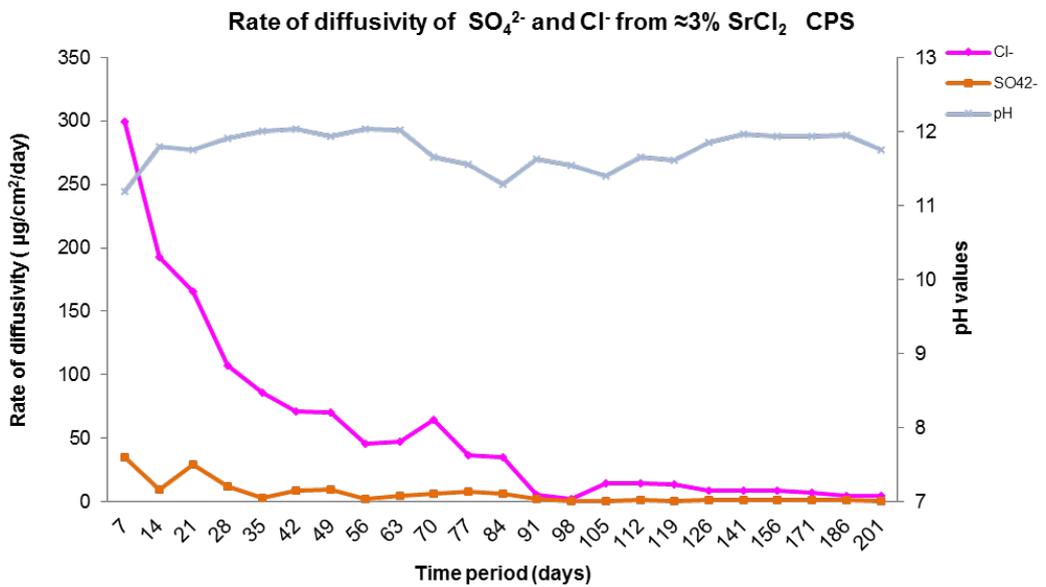
Figure 4.2 Rate of diffusivity of cations (a) anions (b) from ≈3% SrCl$_2$ BFS:OPC CPS in DW
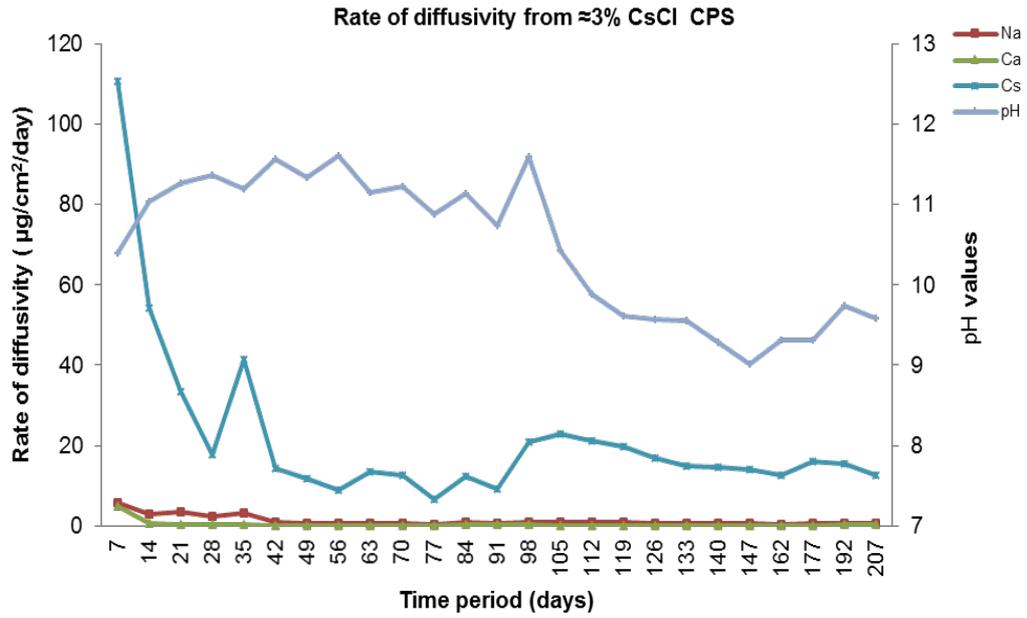
(a)
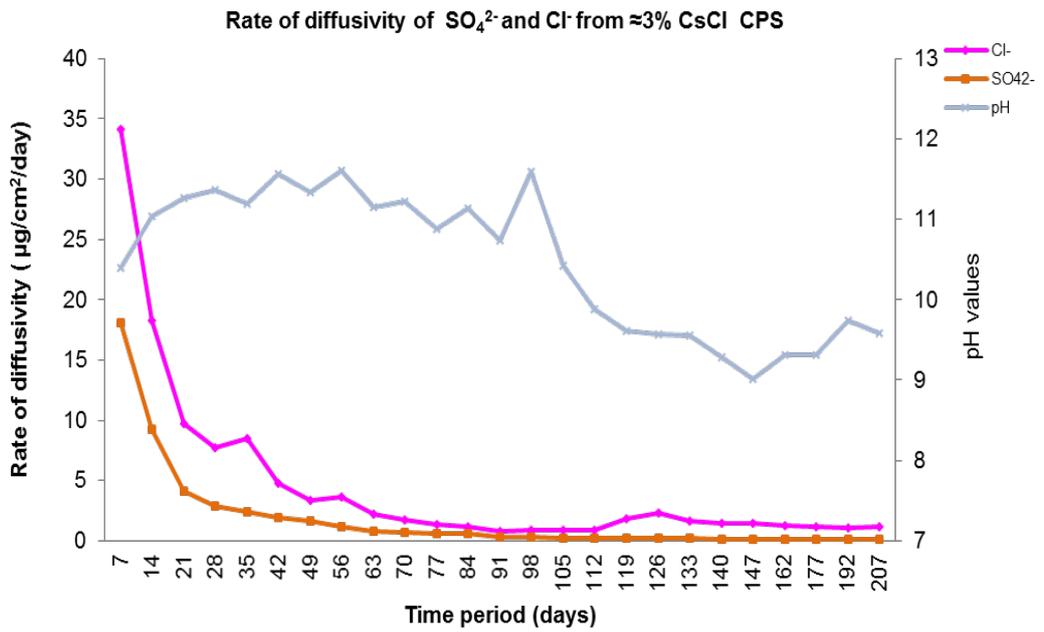
(b)

Figure 4.3 Rate of diffusivity of cations (a) and anions (b) from ≈3% CsCl BFS:OPC CPS in DW

(a)

(b)
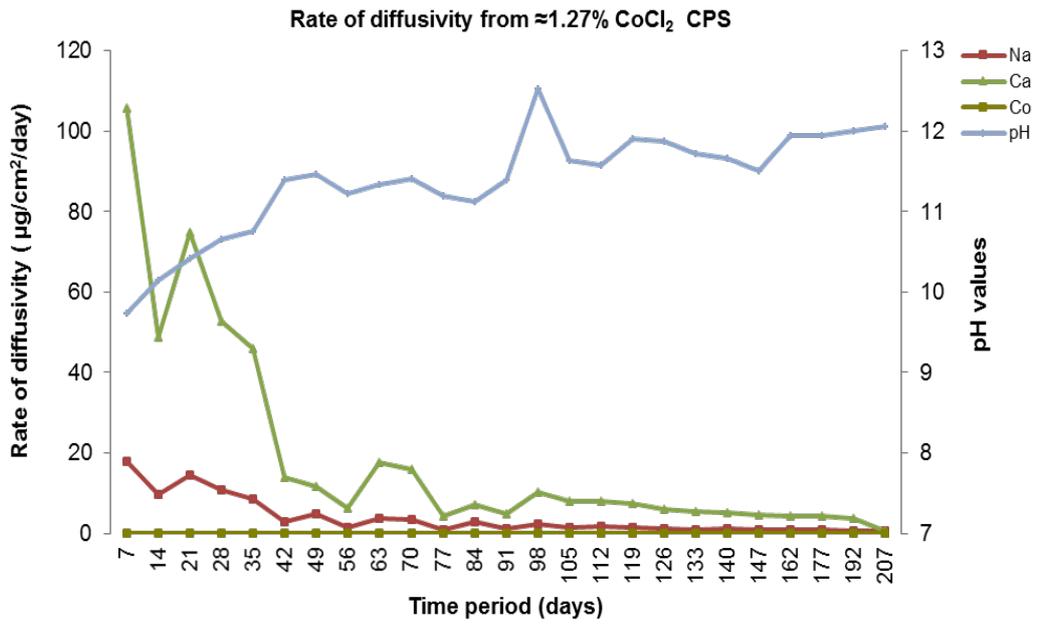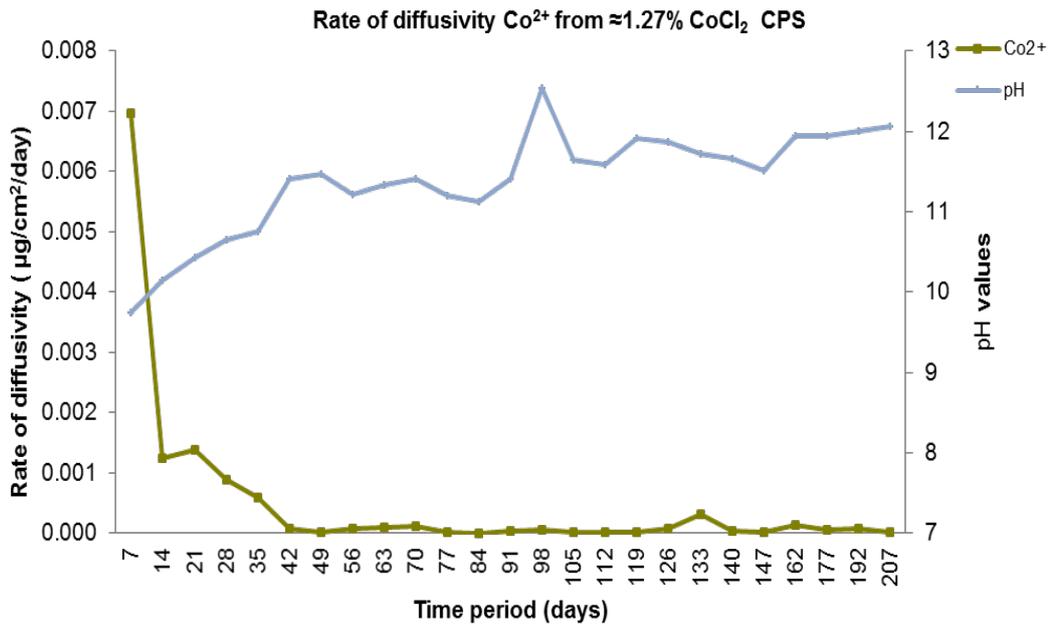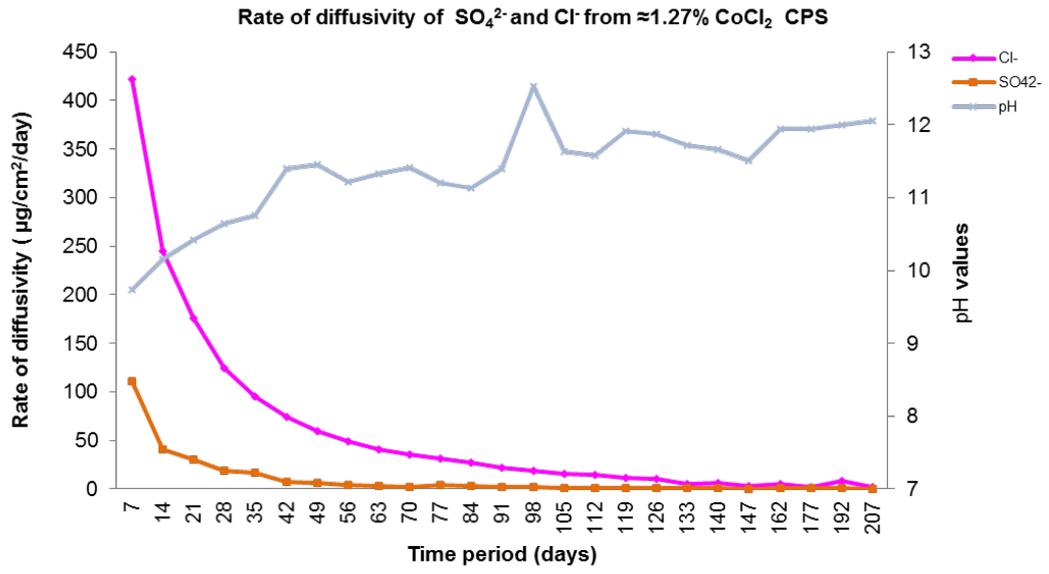
Figure 4.4 Rate of diffusivity of cations (a) Co^{2+} (b) and anions (c) from ≈1.27 % $CoCl_2$ BFS:OPC CPS in DW
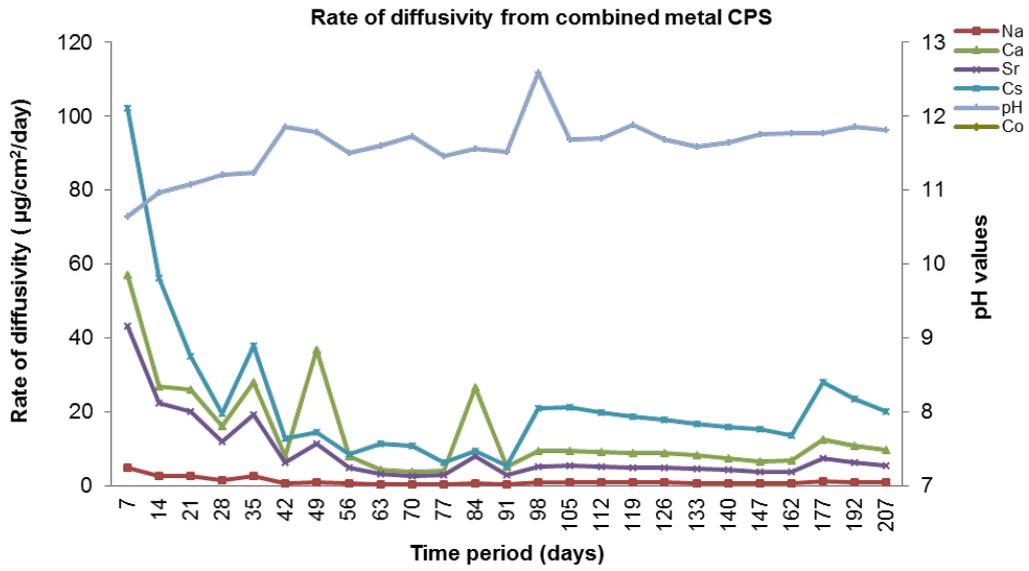
(a)
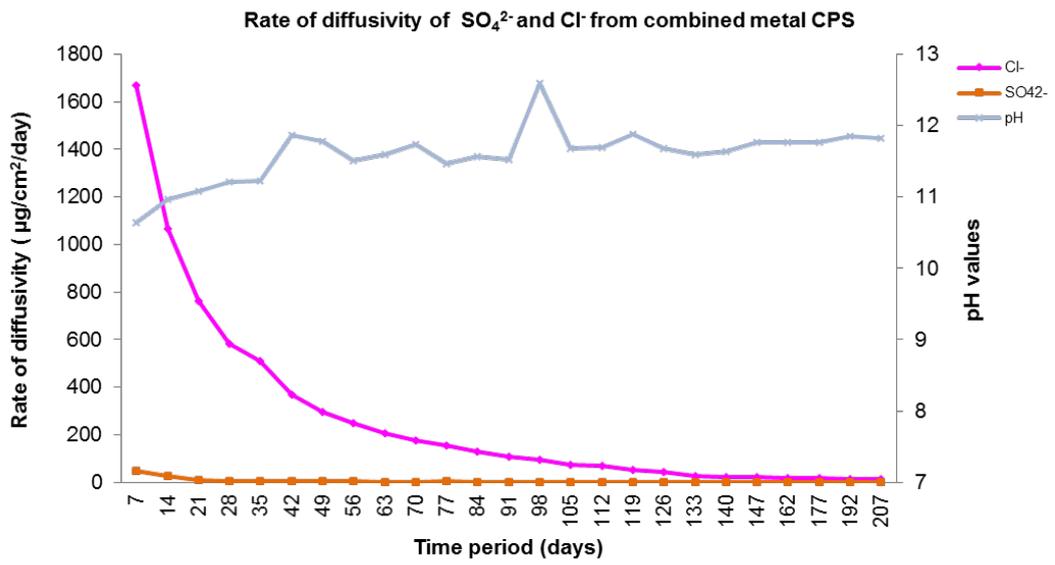
(b)

Figure 4.5 Rate of diffusivity of cations (a) and anions (b) from combined metal BFS:OPC CPS in DW
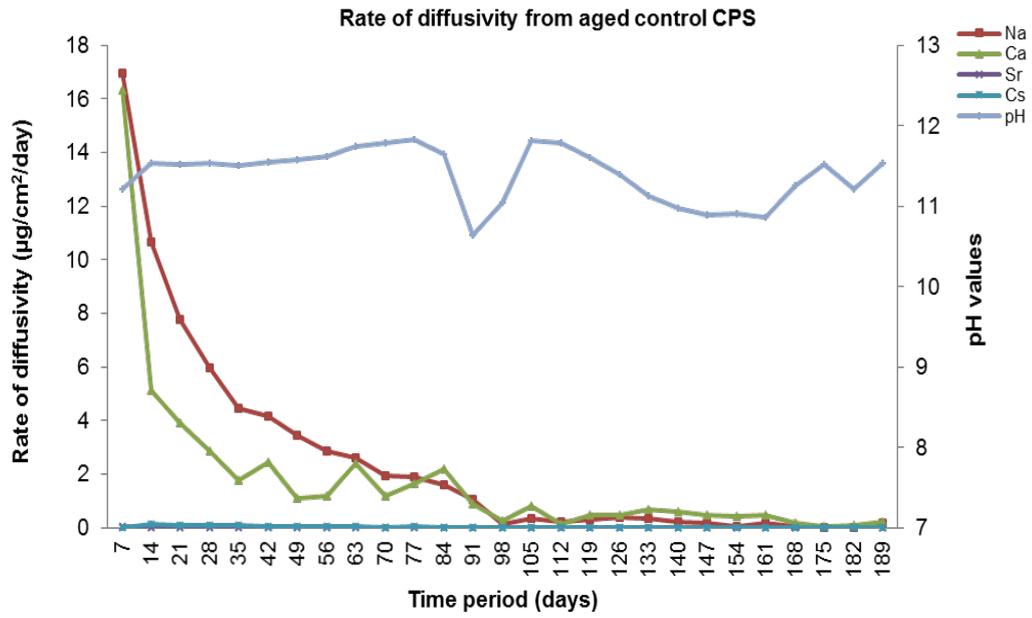
(a)
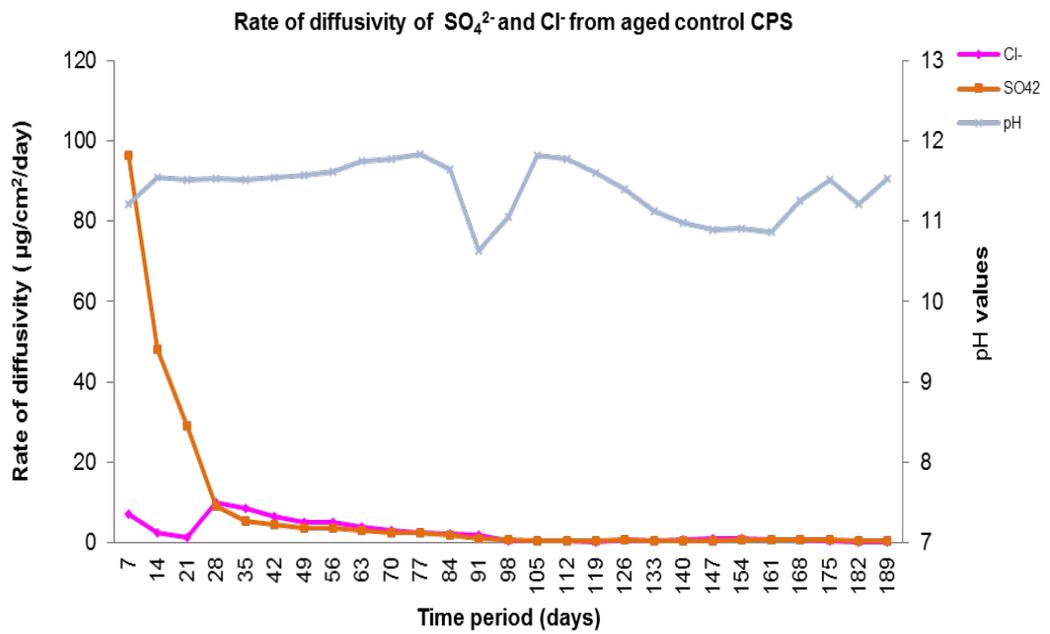
(b)

Figure 4.6 Rate of diffusivity of cations (a) and anions (b) from aged control BFS:OPC CPS in DW
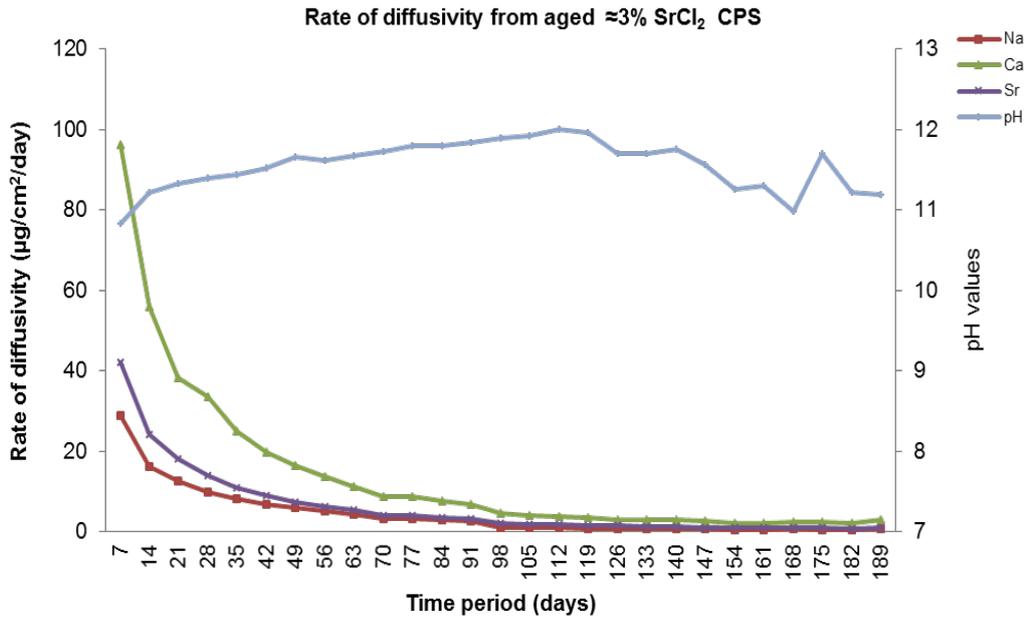
(a)
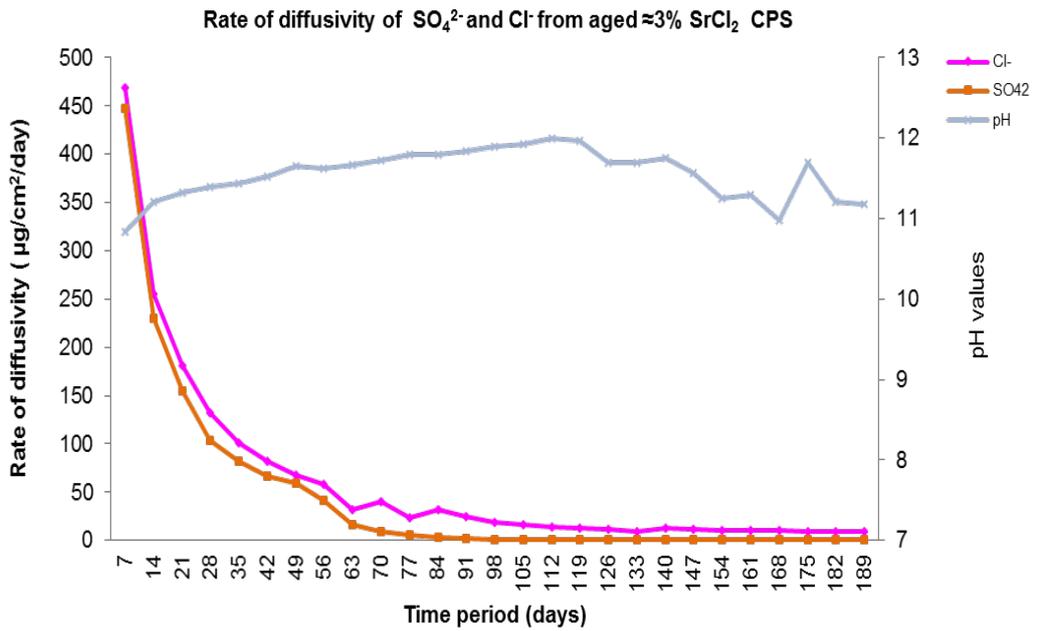
(b)

Figure 4.7 Rate of diffusivity of cations (a) anions (b) from aged ≈3% SrCl$_2$ BFS:OPC CPS in DW

Rate of diffusivity from aged ≈3% CsCl CPS

(a)

Rate of diffusivity from aged ≈3% CsCl CPS

(b)

Rate of diffusivity of SO$_4^{2-}$ and Cl$^-$ from aged ≈3% CsCl CPS
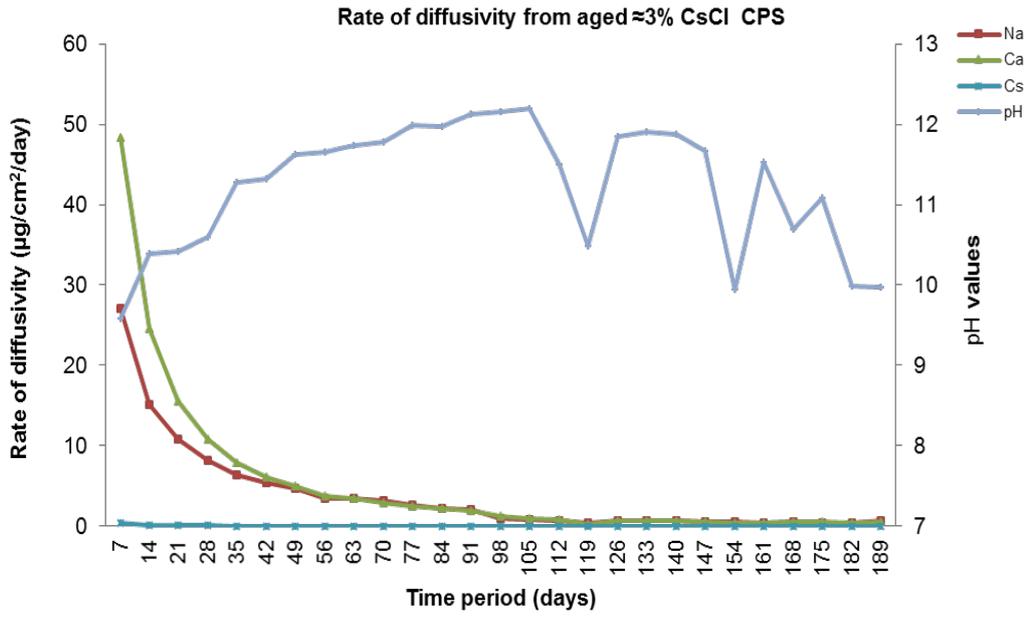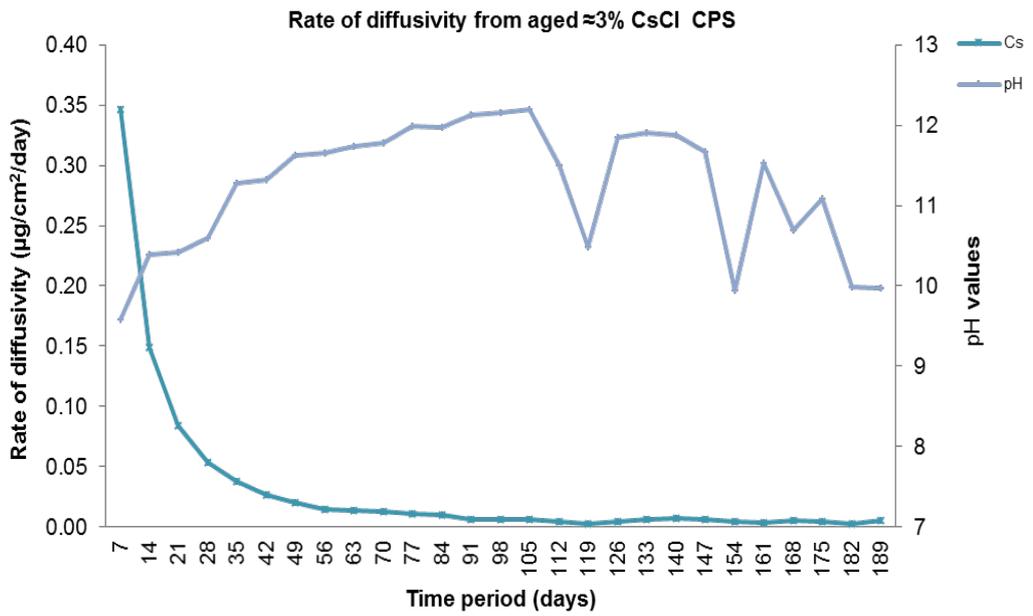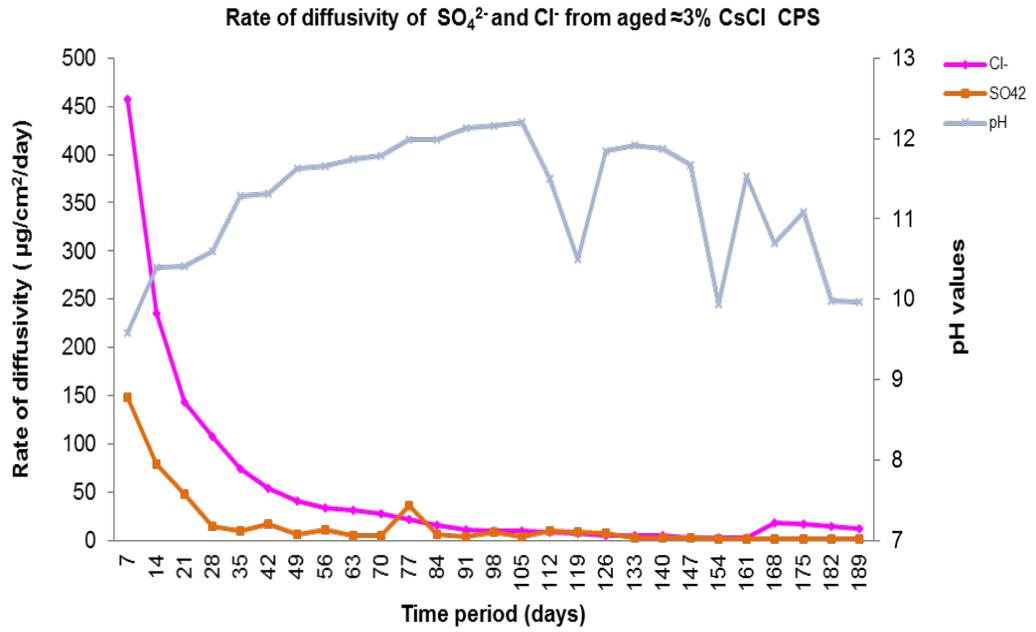
(c)

Figure 4.8 Rate of diffusivity of cations (a) Cs$^+$ (b) and anions (c) from aged ≈3% CsCl$_2$ BFS:OPC CPS in DW

(a)

(b)

135
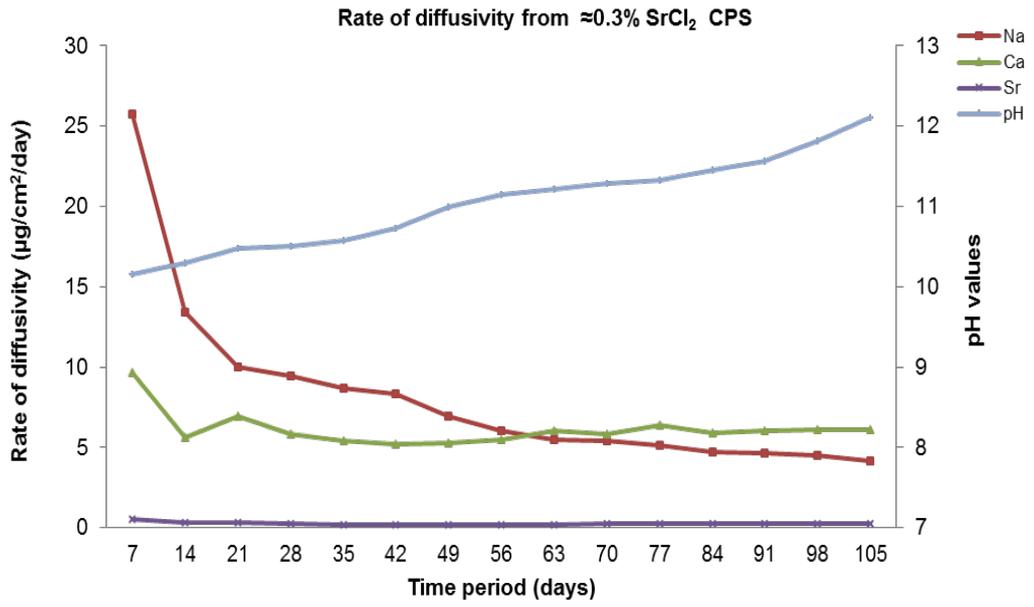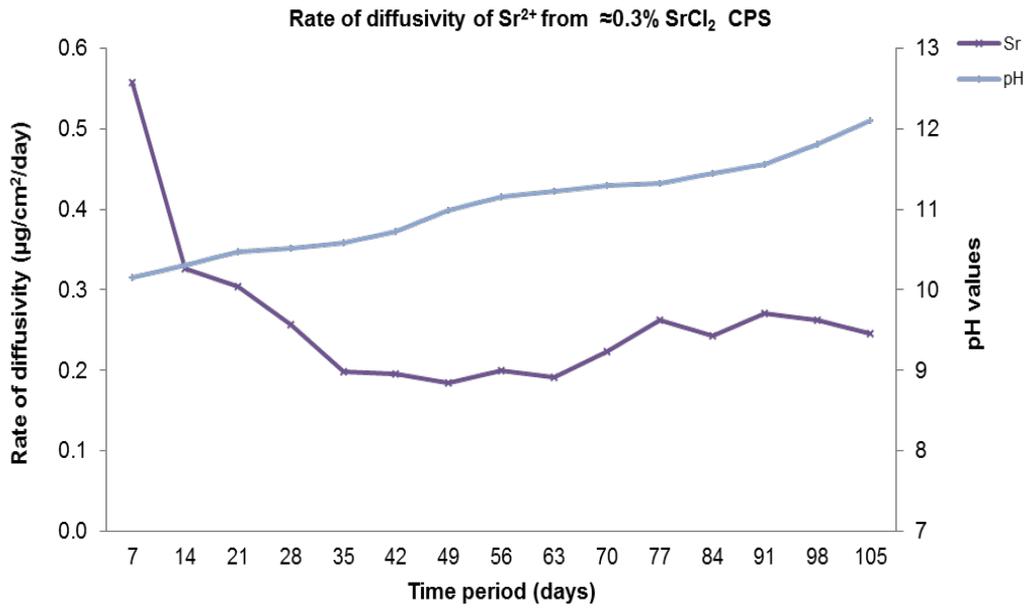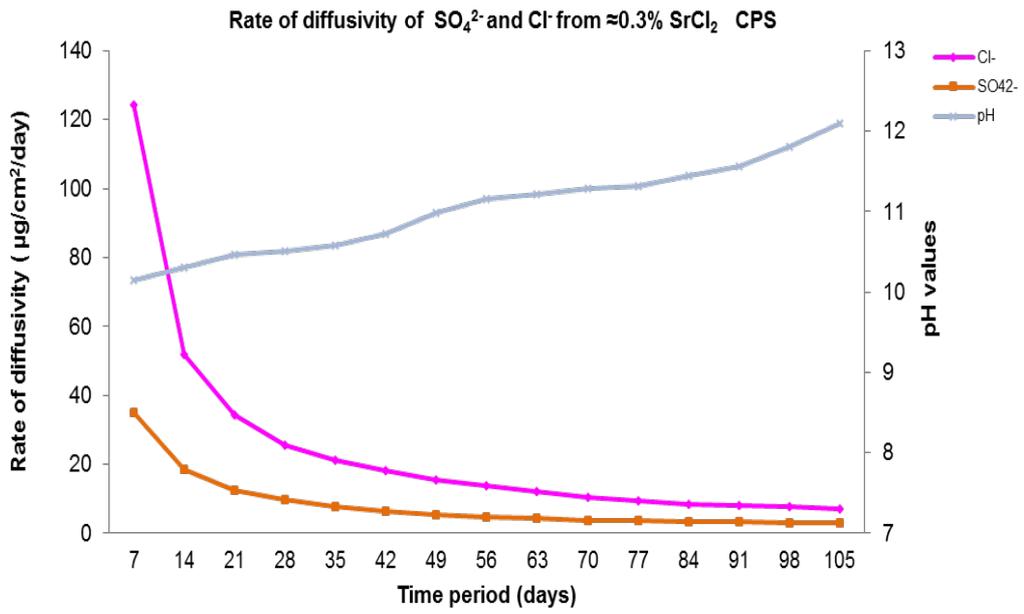
(c)

Figure 4.9 Rate of diffusivity of cations (a) Sr^{2+} (b) and anions (c) from ≈0.3% SrCl$_2$ BFS:OPC CPS in DW

Rate of diffusivity from ≈3% CsCl CPS

(a)

Rate of diffusivity of Cs⁺ from ≈3% CsCl CPS

(b)

137
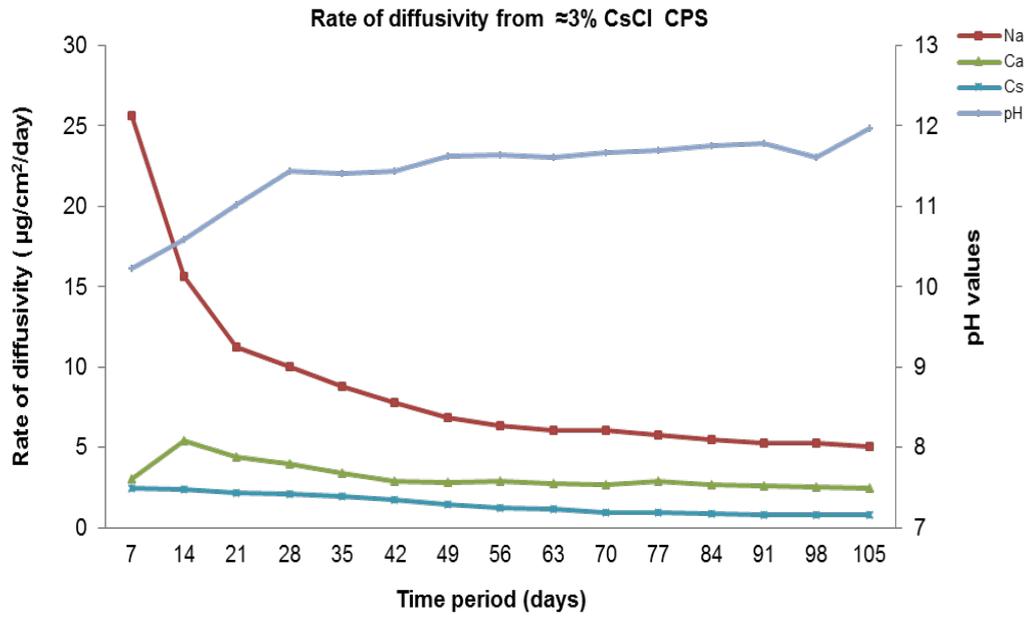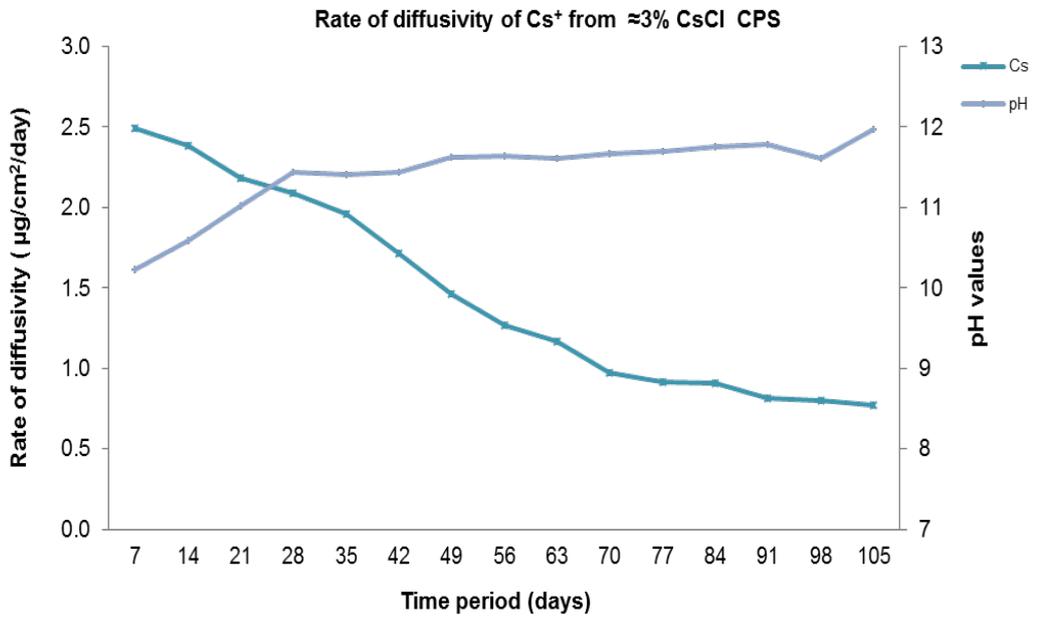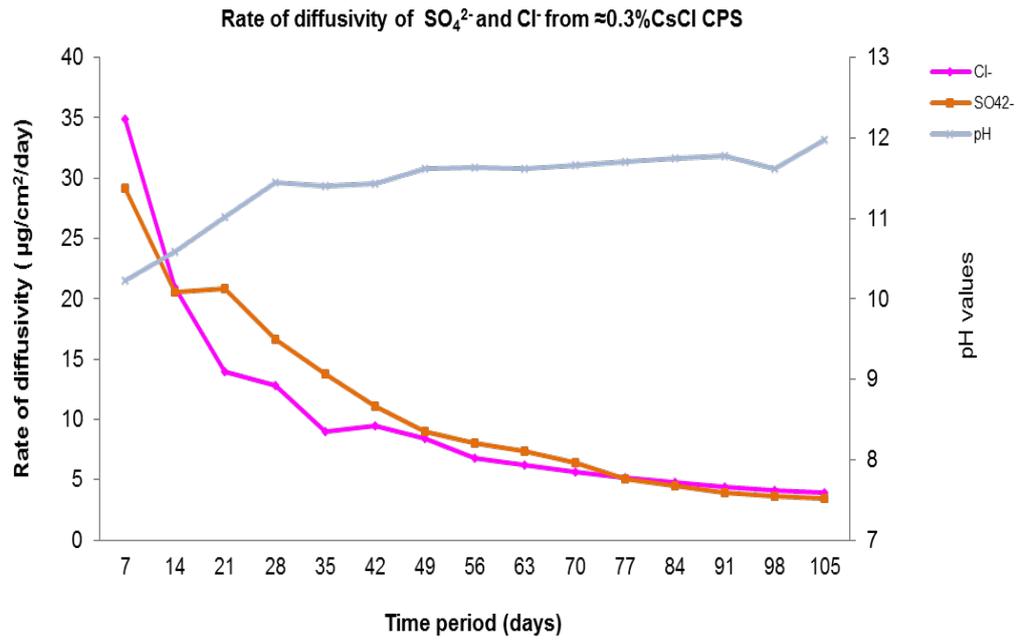
Figure 4.10 Rate of diffusivity of cations (a) Cs+ (b) and anions (c) from ≈0.3%
CsCl BFS:OPC CPS in DW

(a)

(b)

Rate of diffusivity of SO_4^{2-} and Cl^- from ≈0.3% $SrCO_3$ CPS
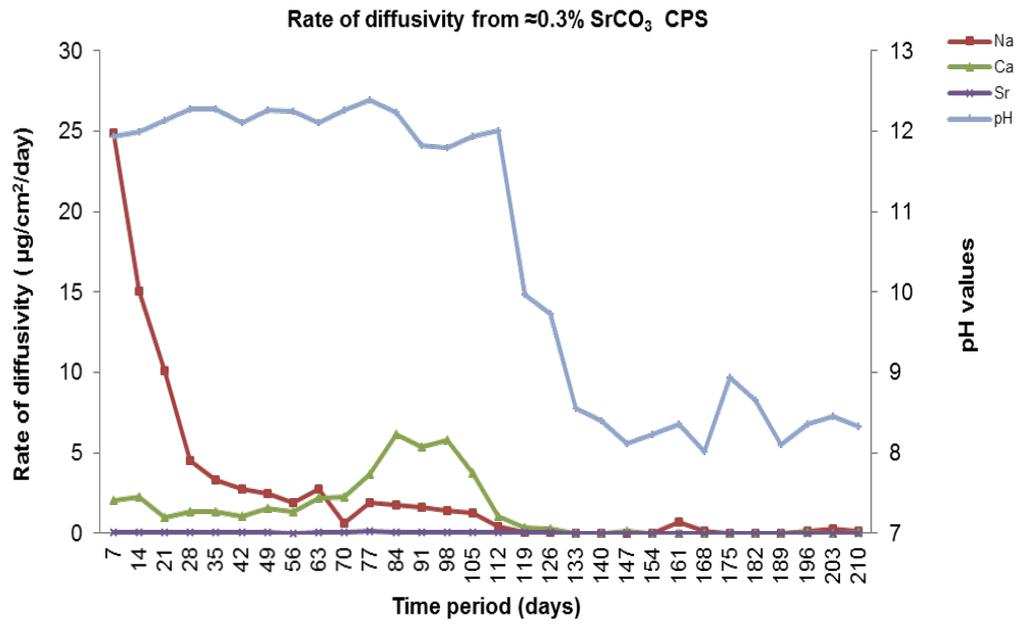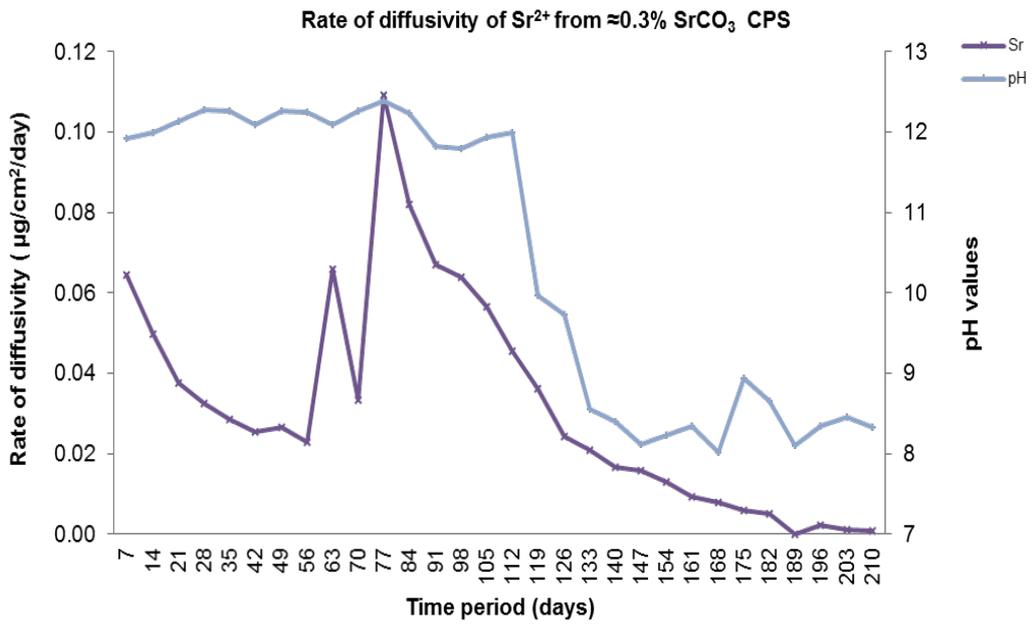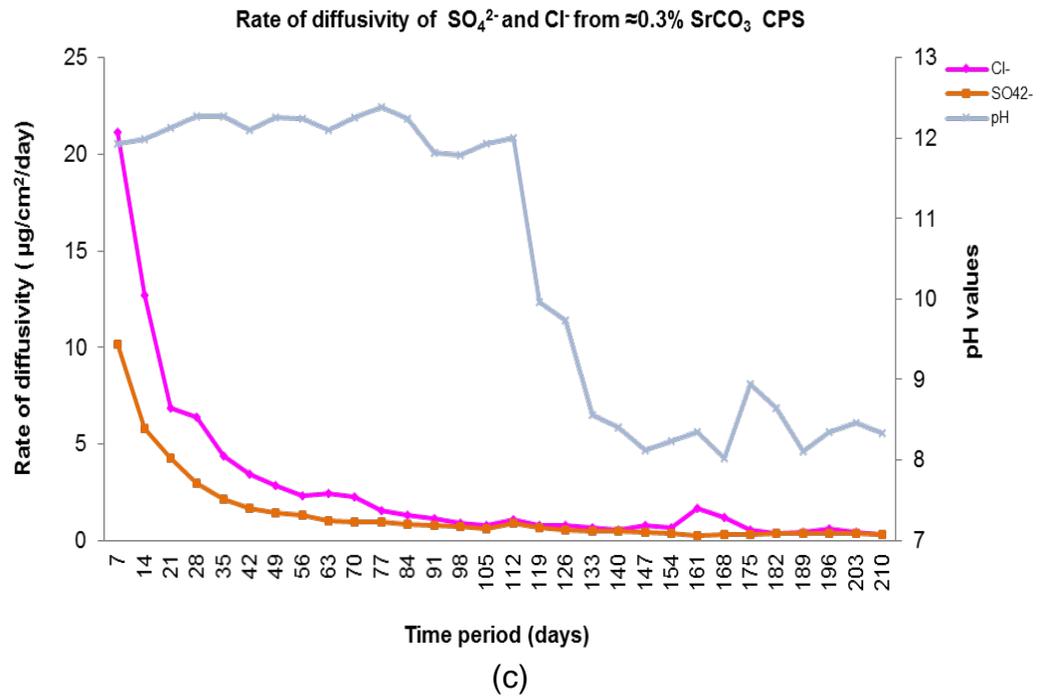
Figure 4.11 Rate of diffusivity of cations (a) Sr^{2+} (b) and anions (c) from ≈0.3% $SrCO_3$ BFS:OPC CPS in DW

Rate of diffusivity from ≈3% SrCO₃ CPS

(a)

Rate of diffusivity of Sr²⁺ from ≈3% SrCO₃ CPS

(b)

141
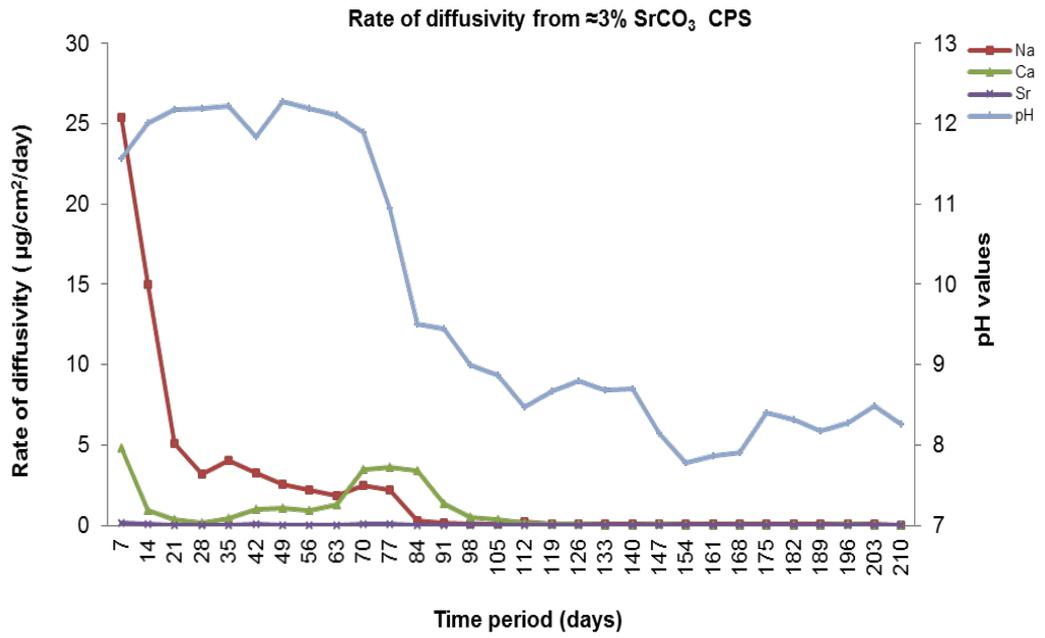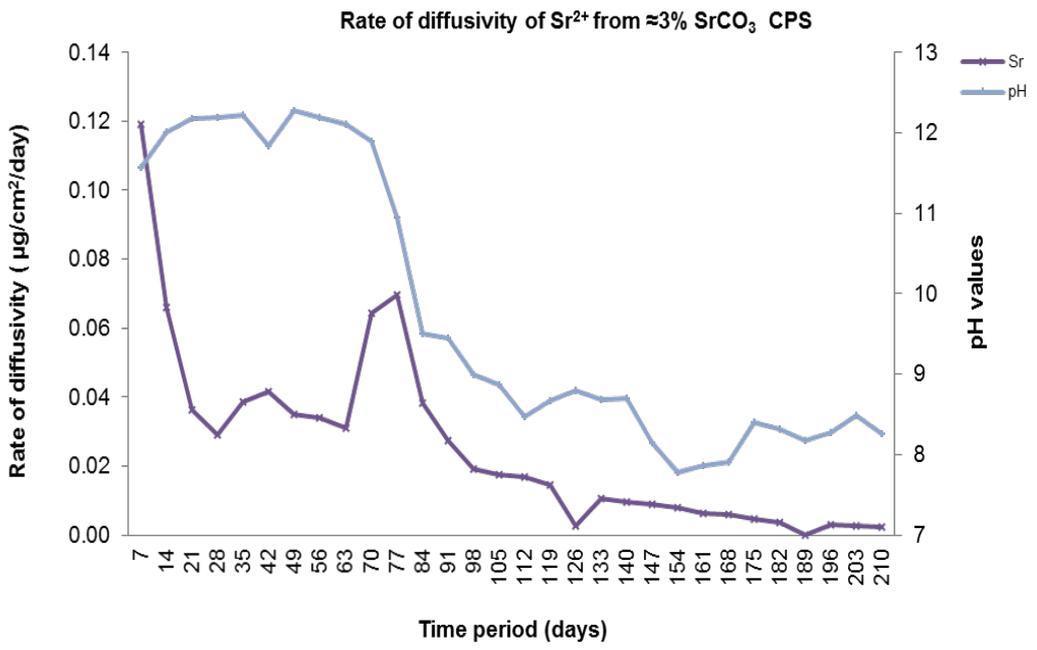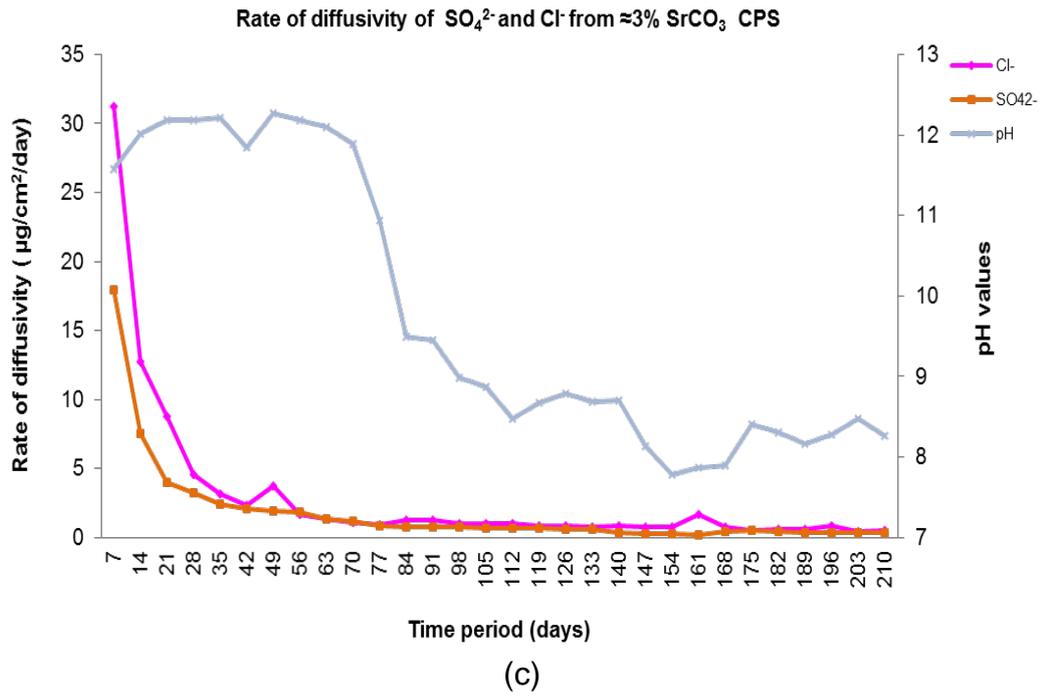
Figure 4.12 Rate of diffusivity of cations (a) Sr²⁺ (b) and anions (c) from ≈3% SrCO₃ BFS:OPC CPS in DW
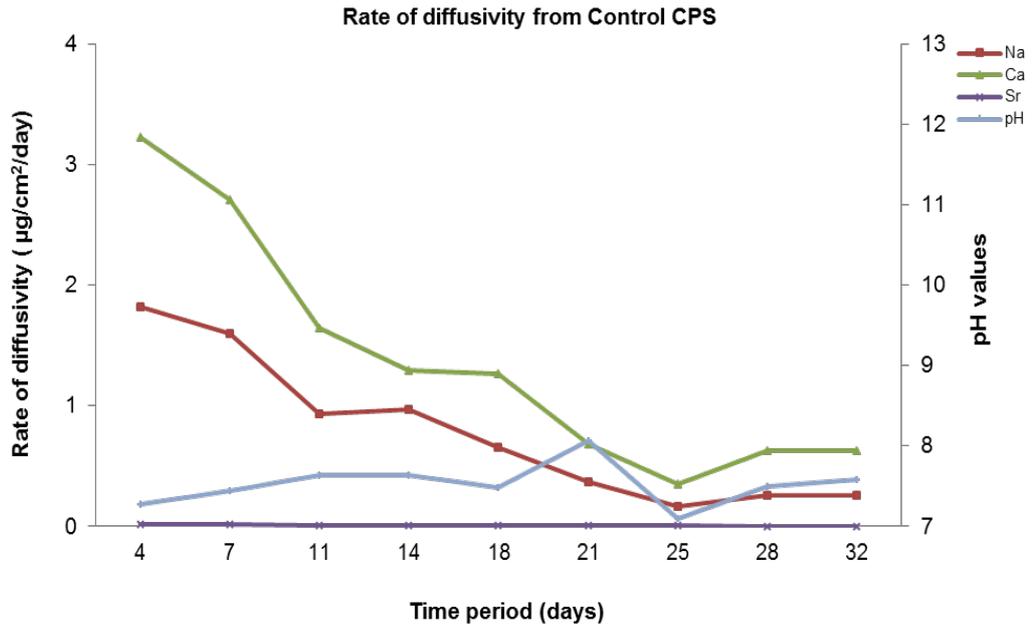
(a)
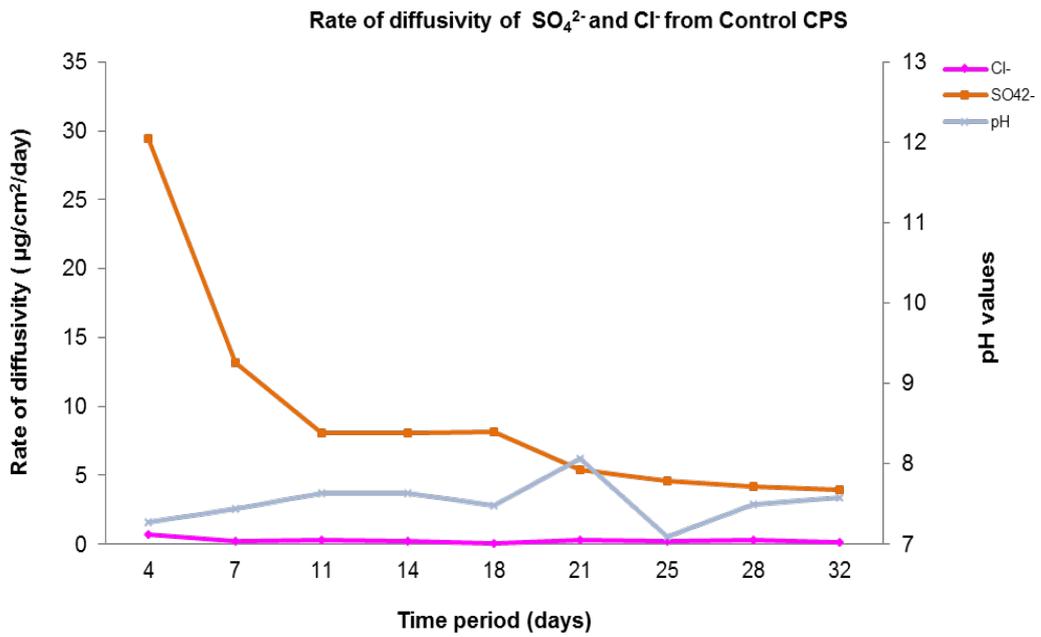
(b)

Figure 4.13 Rate of diffusivity of cations (a) and anions (b) from control BFS:OPC CPS in tap water (open circuit)

Rate of diffusivity from ≈3% SrCl$_2$ CPS

(a)

Rate of diffusivity of SO$_4^{2-}$ and Cl$^-$ from ≈3% SrCl$_2$ CPS
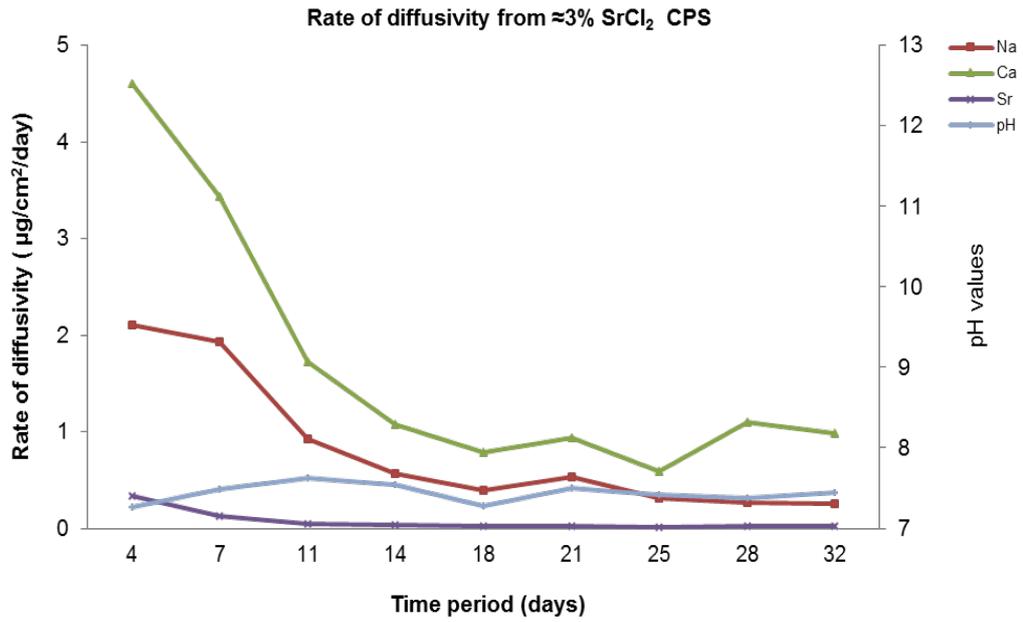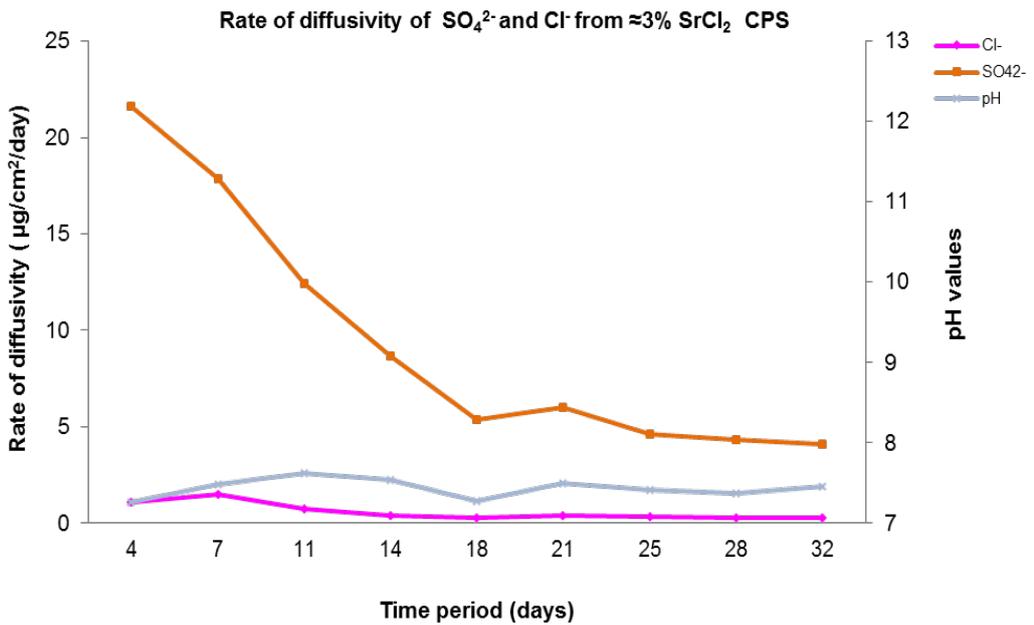
(b)

Figure 4.14 Rate of diffusivity of cations (a) and anions (b) from ≈3% SrCl$_2$ BFS:OPC CPS in tap water (open circuit)

144
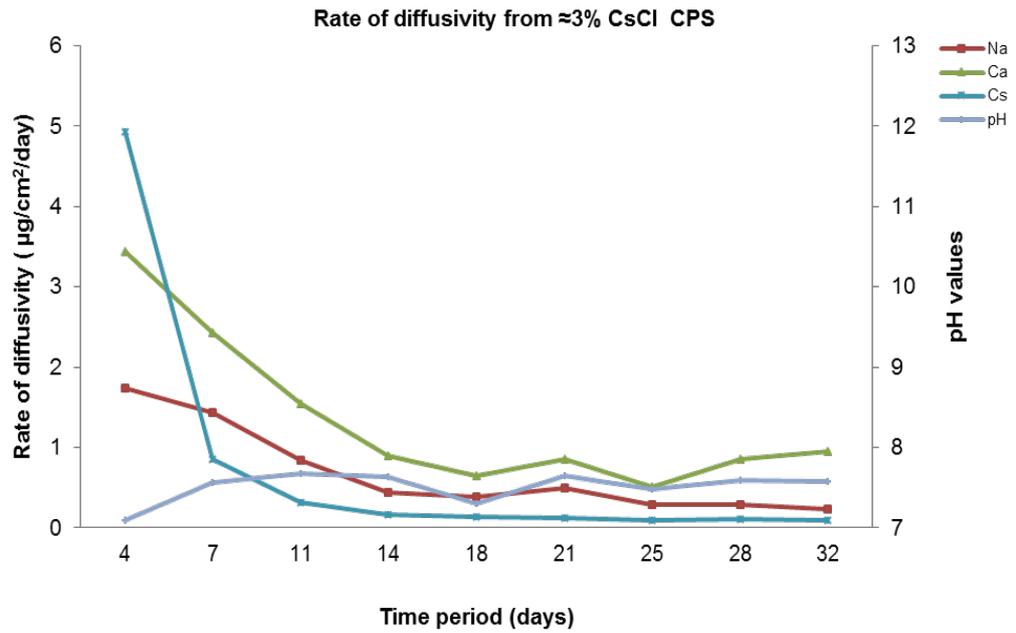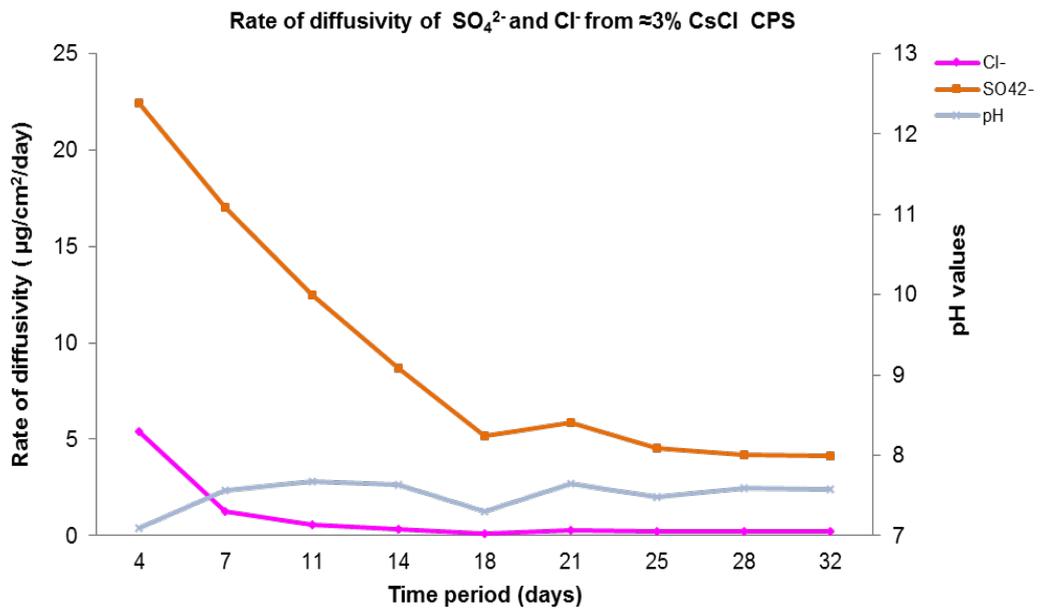
Figure 4.15 Rate of diffusivity of cations (a) and anions (b) from ≈3% CsCl BFS:OPC CPS in tap water (open circuit)

Rate of diffusivity from ≈3% SrCO₃CPS

(a)

Rate of diffusivity of SO₄²⁻ and Cl⁻ from ≈3% SrCO₃CPS
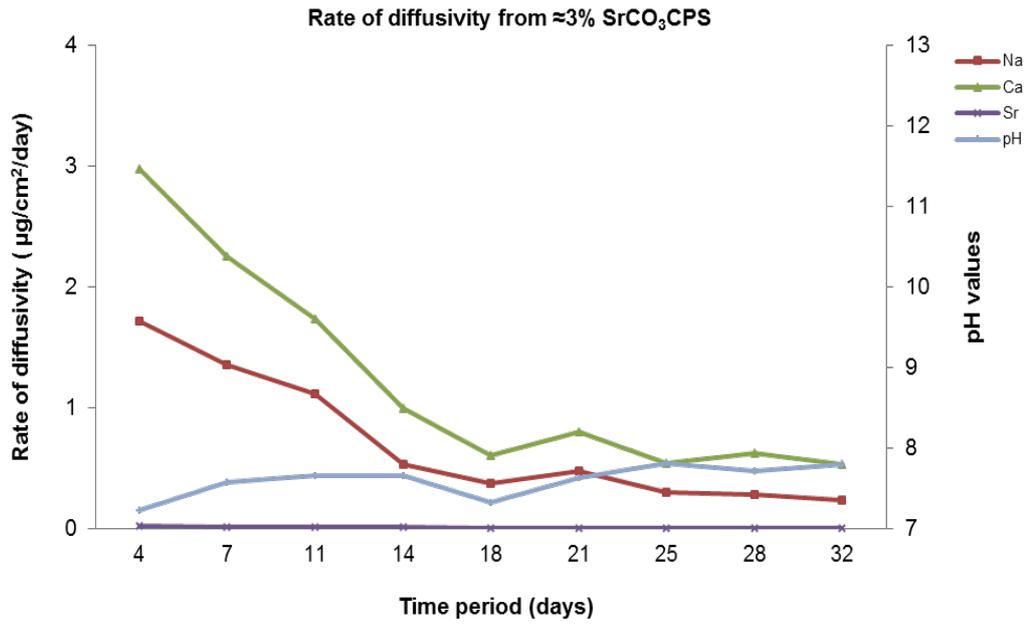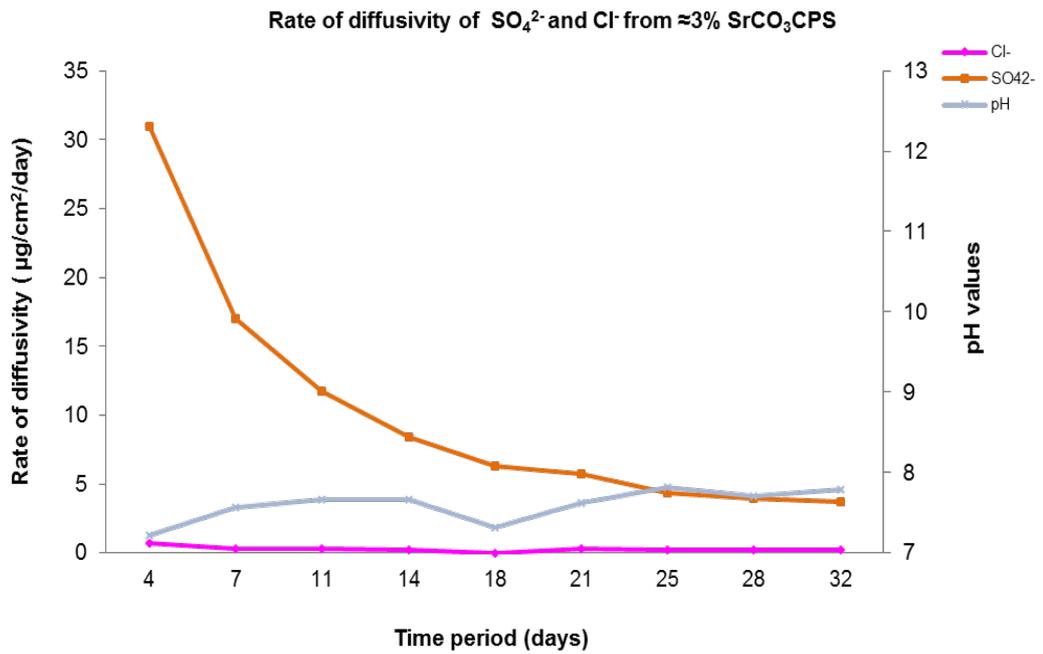
(b)

Figure 4.16 Rate of diffusivity of cations (a) and anions (b) from ≈3% SrCO₃ BFS:OPC CPS in tap water (open circuit)
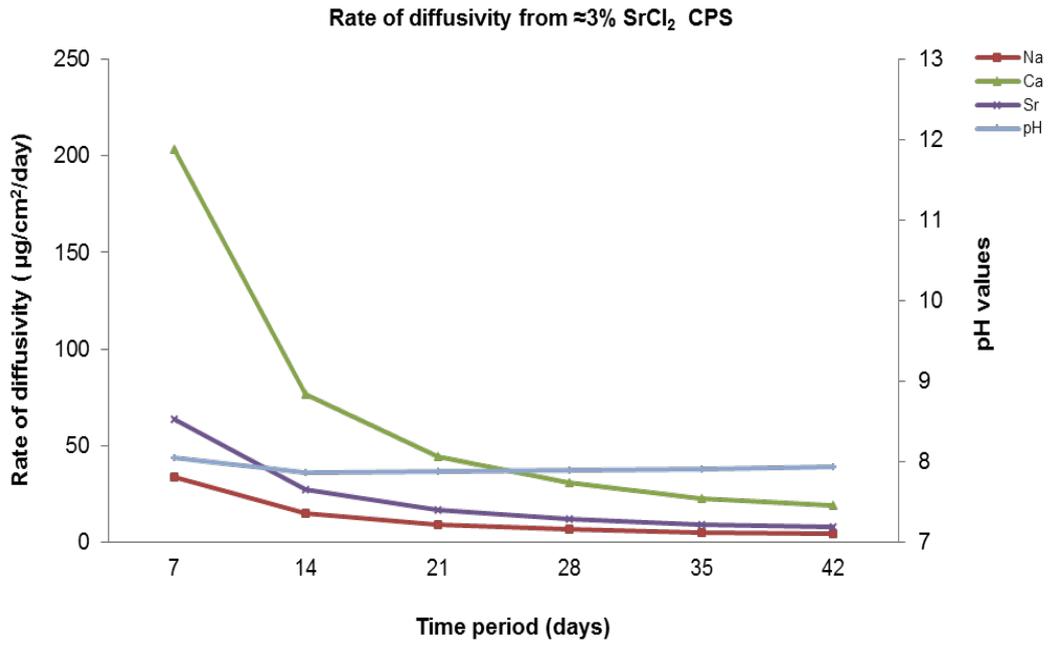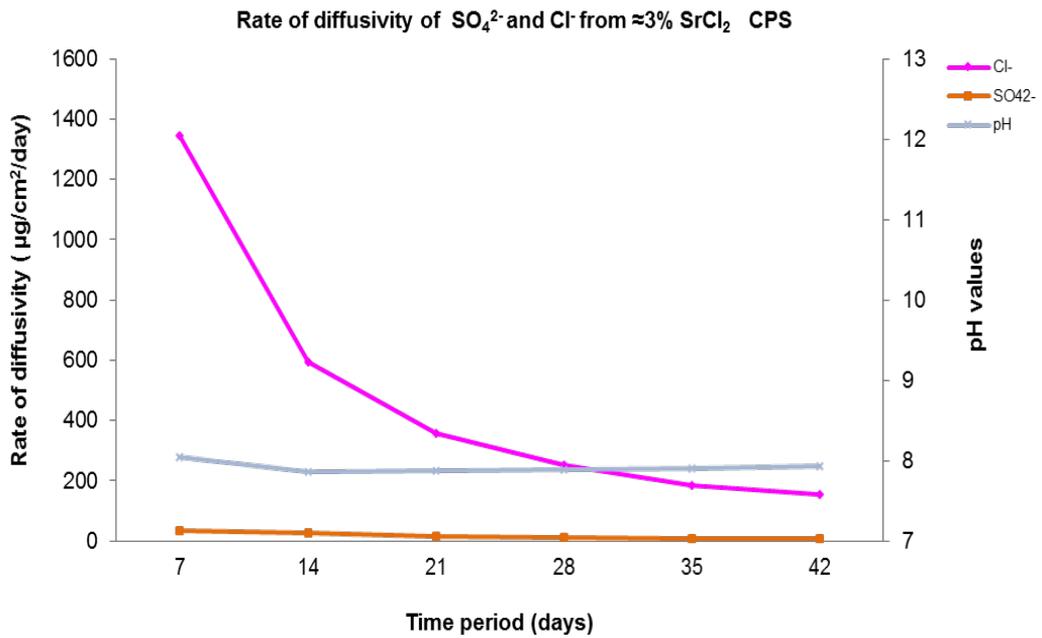
Figure 4.17 Rate of diffusivity of cations (a) and anions (b) from ≈3% SrCl$_2$ BFS:OPC CPS in tap water (closed circuit)

Chapter 5: Diffusivity from PFA:OPC CPSs with distilled water as a test solution

5.1 Aims of study

To evaluate the influence of concentration and nature of encapsulated cations in (PFA:OPC) formulations on their diffusivity when in contact with distilled water.

5.2 Introduction

Pulverised fuel ash (PFA) is another additive which is often used in formation of cement paste in nuclear waste encapsulation [210]. In this chapter, a series of closed and open circuit diffusivity experiments (section 2.4) have been carried out on PFA:OPC CPSs encapsulating caesium when added as chloride salt and strontium when added as chloride and carbonate salt (Table 5.1). The main purpose for carrying out these experiments was to confirm that the diffusivity of the encapsulated cations is dependent on their concentration and also to compare the rate of diffusivity between and BFS: OPC cement paste samples. The preparation of PFA: OPC CPSs and the formulation were kept identical with that of BFS:OPC CPS preparation (Table 2.1). Dynamic diffusivity tests were initiated 90 days after curing the PFA:OPC cement paste samples in the laboratory atmosphere. The experimental set-up consisted of two sets of diffusivity experiments with distilled water (Table 5.1) and one set consisted of tap water as a test solution for comparative purposes. Tap water was selected for the 'open' diffusivity experiments. Each experiment consisted of two to four sets of closed circulating diffusivity circuits with PFA:OPC cement paste and different cation characteristics.

5.3   Cement paste samples

The diffusivity experiments were carried out on 10 CPSs, of which 6 samples were subjected to diffusivity test using distilled water and 4 were subjected to open circuit tap water test (Table 5.1).

Table 5.1 Cement paste samples and test solutions used.

Experiment	PFA:OPC Cement paste samples	Test solution
1	(a) Control	Distilled water
	(b) $\approx 3\% SrCl_2$	
	(c) $\approx 3\%$ CsCl	
	(d) $\approx 3\%$ $SrCO_3$	
2	(a) $\approx 0.3\%$ $SrCl_2$	Distilled water
	(b) $\approx 0.3\%$ CsCl	
3	(a) Control	Tap water
	(b) $\approx 3\% SrCl_2$	
	(c) $\approx 3\%$ CsCl	
	(d) $\approx 3\%$ $SrCO_3$	

5.4   Results

The elemental analysis of the as received OPC and PFA from NNL were found to be similar with the other cement and fly ash used in the waste encapsulation (Table 5.2). The cement paste mixture preparation of PFA: OPC showed high fluidity in comparison to the BFS: OPC mixture. During the curing stage, the PFA: OPC cement paste samples lost less liquid (bleed) in contrary to BFS: OPC cement paste samples. The addition of Sr and Cs affected the surface finish of the cement paste sample. The samples containing $SrCO_3$ produced a rough

finish compared to the samples containing $SrCl_2$. Both the control and samples containing CsCl produced similar finish, which was less rough than the Sr containing cement paste samples.

Table 5.2 Analysis of as received OPC and PFA (%).

Material	Na^+	K^+	Cs^+	Ca^{2+}	Mg^{2+}	Sr^{2+}	Cl^-	SO_4^{2-}	moisture
OPC	0.6	0.63	0.06	42.64	1.36	4.61	0.11	1.37	26.2
PFA	1.10	2.00	0.06	1.30	0.89	4.50	not quoted	not quoted	0.1

5.4.1 Chemical analysis of cement paste sample

As previously reported, the chemical analysis of the dissected BFS: OPC CPSs showed segregation of the cation; although the average of the measured cation concentrations was approximately the same as the amount of cation added during the cement paste preparation. It is more than likely that the segregation will take place even in PFA:OPC cement paste samples, this may be inferred from the micro-pore and surface area values reported in Table 5.4. Based on this assumption it was decided that chemical analysis of PFA:OPC cement paste samples were not warranted as diffusivity rates could be similar from the cylindrical sample for all three sections i.e. top, middle and bottom i.e. the variation in concentration was not that significant.

5.4.2 Moisture content of CPS

The moisture content of PFA:OPC CPSs were in the range of 3.9 -7.8%. (Table 5.3). There was no significant difference in the moisture content of top, middle and bottom section, contrary to BFS:OPC CPSs.

Table 5.3 % moisture content of PFA:OPC CPS

	Control	≈3% $SrCl_2$	≈3% CsCl	≈3% $SrCO_3$
Top	4.5	7.8	4.9	5.6
Middle	3.9	7.0	5.2	4.6
Bottom	4.2	7.6	4.8	5.5

5.4.3 Micropore and surface area analysis of cement paste sample measured by BET method

Micropore and surface area results of the dissected CPSs are shown in the Table 5.4. The result shows that the micropore area of the middle layer of ≈ 3% $SrCl_2$ CPS was lower than top and bottom layer which is comparable with surface area, in contrast to ≈ 3% CsCl CPS; the middle layer showed higher micropore area than top and bottom layer. However, there was no significant difference observed in the micropore area of the top, middle and bottom layer of ≈ 3% $SrCO_3$ CPS. The average micropore areas of the CPSs used in this experiment were in the range of 3 – 3.9 m^2/g (Table 5.5). There was no significant difference observed in the micropore area of the PFA: OPC CPSs in contrast to BFS: OPC CPSs.

The surface area of the middle layer of ≈ 3% $SrCl_2$ CPS was lower than top and bottom layer, in contrast to ≈ 3% CsCl and ≈ 3% $SrCO_3$ CPS ; which did not show any significant difference in surface area measured in all three dissected layers. The average surface area of all the CPSs used in this experiment, were in the range of 21.7 – 40.6 m^2/g. However, the average surface area ≈ 3% $SrCl_2$ was found to be the highest of all the samples.

Table 5.4 Micropore and surface area analysis of dissected PFA:OPC cement paste samples measured by BET method

Dissected PFA:OPC CPS	≈ 3% SrCl$_2$ CPS		3% SrCO$_3$ CPS		≈ 3% CsCl CPS	
	Micro-pore area	Surface area	Micro-pore area	Surface area	Micro-pore area	Surface area
	m^2/g		m^2/g		m^2/g	
Top	3.4	43.8	3.8	22.9	3.0	28.6
Middle	2.2	33.9	3.5	24.5	4.2	27.2
Bottom	3.5	44.1	4.0	24.1	3.5	26.4

Table 5.5 Average micropore and surface area of PFA:OPC cement paste samples measured by BET method

Sample	Micropore area	Surface area
	m^2/g	
Control	3.9	22.7
≈3% SrCl$_2$	3.0	40.6
≈3% CsCl	3.6	27.4
≈3% SrCO$_3$	3.7	23.8
≈0.3% SrCl$_2$	3.7	22.2
≈0.3% CsCl$_2$	3.2	21.7

5.4.4 Test solution analysis

5.4.4.1 pH values

The pH values of the test solutions increased from 7.0 to 12.13 (Figure 5.1 to Figure 5.10) for the closed circuit distilled water experiments. Lower pH values were found in the test solutions with ≈3% SrCl$_2$. This could be due to the dissociation of SrCl$_2$ to Sr(OH)$_2$ and HCl. The HCl formed could be responsible for the lower pH values of test solutions from ≈3% SrCl$_2$. The pH values from all the test solutions of open circuit experiments were found to in similar range and there was no significant difference found among the test solutions.

5.4.4.2 Chemical analysis of test solution

The rates of diffusivity of all the experiments are shown in Figure 5.1 to Figure 5.10. All the diffusivity data have been normalised for comparative purposes. In the following sub sections the average diffusivity data have been used for comparative purposes. The rate of diffusivity values of each CPS are given in appendix 5.1 to 5.10.

5.4.4.2.1 *Strontium*

A significant higher rate of diffusivity of Sr^{2+} was measured for the ≈3% $SrCl_2$ (134 $\mu g/cm^2/day$) followed by ≈0.3% $SrCl_2$ (10 $\mu g/cm^2/day$) and ≈3% $SrCO_3$ CPSs (0.29 $\mu g/cm^2/day$) in the closed circuit experiments. Similar trend in diffusivity pattern was observed in open circuit diffusivity experiment; Sr^{2+} from ≈3% $SrCl_2$ diffused out at considerable faster rate than from ≈3% $SrCO_3$ CPS. The rate of diffusivity of Sr^{2+} from ≈3% $SrCl_2$ PFA: OPC CPS (134 $\mu g/cm^2/day$) was measured ≈4 times faster than ≈3% $SrCl_2$ BFS: OPC CPS (35 $\mu g/cm^2/day$). This demonstrates that the diffusivity of Sr^{2+} and other cations is dependent upon its concentration and cement additive used in the cement paste formulation.

5.4.4.2.2 *Caesium*

The rate of diffusivity of Cs^+ from ≈3% CsCl CPS was higher than the rest of the Cs CPS. Caesium from ≈0.3% CsCl CPS (21 $\mu g/cm^2/day$) diffused out 17 times slower than the rate of diffusivity Cs^+ from ≈3% CsCl CPS (363 $\mu g/cm^2/day$). Approximately similar difference in the rate of diffusivity in BFS: OPC was measured. The rate of diffusivity of Cs^+ was found to be 2-3 times higher than Sr^{2+} in both PFA: OPC and BFS: OPC CPS.

153

5.4.4.2.3 *Calcium*

The diffusivity of Ca^{2+} from $\approx 3\%$ $SrCl_2$ CPS (190 $\mu g/cm^2/day$) paste sample was measured as 163 times higher than control CPS (1.16 $\mu g/cm^2/day$), followed by $\approx 0.3\%$ $SrCl_2$ CPS (2.89 $\mu g/cm^2/day$) which was measured as 2 times higher the diffusivity of Ca^{2+} from control CPS. The diffusivity pattern of Ca^+ from $\approx 3\%$ CsCl (1.59 $\mu g/cm^2/day$) and control sample showed relatively similar ($p > 0.05$) trend in the diffusivity. The diffusion of Ca^{2+} from 3% $SrCO_3$ (0.73 $\mu g/cm^2/day$) CPS was 2 times slower than the rate of diffusivity from control CPS. The rate of diffusivity of Ca^{2+} from $\approx 0.3\%$ CsCl CPS (0.24 $\mu g/cm^2/day$) was found to be lowest of all the samples and was measured as 7 times slower than $\approx 3\%$ CsCl CPS (1.59 $\mu g/cm^2/day$). The diffusion of Ca^{2+} from open circuit experiment showed a similar pattern of diffusivity in comparison with closed circuit experiment with higher rate of Ca^{2+} diffusivity from $\approx 3\%$ $SrCl_2$ CPS compared to control sample. However, the rate of diffusivity of Ca^{2+} from control was found lowest in contrast with closed circuit experiment. There was no significant difference in the rate of diffusivity of Ca^{2+} from $\approx 3\%$ CsCl CPS and control sample. In both PFA: OPC and BFS:OPC cement paste samples, the diffusivity of Ca^{2+} from strontium encapsulated CPS was higher than caesium encapsulated CPS. The enhanced diffusivity of calcium from CPS can be attributed to Cl^- concentration in particular for $\approx 3\%$ $SrCl_2$ CPS. The $\approx 3\%$ $SrCl_2$ CPS had the highest Cl^- concentration (≈ 26 mmoles) compared with the $\approx 3\%$ CsCl CPS (≈ 15.4 mmoles) and control CPS (0.36 mmoles).

5.4.4.2.4 *Sodium*

The rate of diffusivity of Na^+ from $\approx 3\%$ $SrCl_2$ CPS (63 $\mu g/cm^2/day$) was found to be highest of all the samples and was measured as 3 times higher than control CPS (24 $\mu g/cm^2/day$). There was no significant difference found in the diffusivity

of Na^+ from ≈0.3% $SrCl_2$ (22 µg/cm^2/day), ≈0.3% CsCl (21 µg/cm^2/day),   ≈3% CsCl (21 µg/cm^2/day) and   ≈3% $SrCO_3$ CPS (20 µg/cm^2/day). The data obtained from open circuit experiment, showed highest diffusivity of sodium from ≈3% $SrCl_2$ CPS. However there was no significant difference in the diffusivity pattern of Na^+ found in ≈3% $SrCO_3$, ≈3% CsCl CPS, and control sample. The diffusivity of Na^+ in BFS: OPC showed different sequence in comparison with PFA: OPC.

5.4.4.2.5   *Chloride*

The sequence of diffusivity of Cl^- in our study was: ≈3% $SrCl_2$> ≈3% CsCl > ≈0.3% $SrCl_2$>≈0.3% CsCl >≈3% SrCO3 >Control. This could be due to the concentration effect, the concentration of Cl^- in ≈3% $SrCl_2$ (25.8 mmoles) was higher than all other CPS (Table 5.6). Chloride from ≈3% $SrCl_2$ CPS (1303 µg/cm^2/day) diffused out at higher rate than rest of the CPSs and was measured 268 times higher than control CPS (4.9µg/cm^2/day). However, Cl^- from ≈3% CsCl CPS (243 µg/cm^2/day) was measured 50 times higher than the rate of diffusivity of Cl^- from control CPS. The rate of diffusivity of Cl^- from closed circuit experiment showed a similar sequence of diffusivity in comparison with open circuit experiment with higher rate of Cl^- diffusivity from ≈3% $SrCl_2$ compared to control sample. Chloride from strontium encapsulated cement paste sample was higher than caesium encapsulated cement paste sample in both PFA: OPC and BFS:OPC CPSs. These studies demonstrate that Cl^- is the most mobile of all anions and confirms previous published data [102, 103].

Table 5.6 Concentration of Cl⁻ calculated in PFA:OPC CPS in mmoles

CPS	Cl⁻ concentration (mmoles)
Control	0.36
≈ 3% $SrCl_2$	25.8
≈ 3% CsCl	15.4
≈ 3% $SrCO_3$	0.36

5.4.4.2.6 *Sulphate*

The rate of diffusivity of sulphate from ≈0.3% CsCl CPS (38 µg/cm²/day) was ≈3 times higher than ≈3% $SrCl_2$ CPS (13 µg/cm²/day); that diffused out lowest of all the CPSs. There was no significant difference in the diffusivity pattern observed in ≈0.3% CsCl CPS, control and ≈3% CsCl CPS. Sulphate from ≈3% $SrCO_3$ CPS and ≈0.3% $SrCl_2$ CPS diffused out at similar rate. A similar grouping of diffusivity pattern was measured in open circuit diffusivity experiments. The diffusivity of SO_4^{2-} in BFS: OPC showed different sequence in comparison with PFA: OPC. The diffusion of SO_4^{2-} is from inherent anion in the OPC and/or BFS and was not added to the CPS (Table 5.7).

Table 5.7 Concentration of SO_4^{2-} calculated in PFA:OPC CPS in mmoles.

PFA:OPC CPS	SO_4^{2-} concentration (mmoles)
Control	9.1
≈ 3% $SrCl_2$	9.7
≈ 3% CsCl	9.7
≈ 3% $SrCO_3$	9.1

5.5 Conclusions

1   The composition of make-up water affects both the bleed water volume and physical characteristics of the cement paste samples.

2   The micropore area values for all PFA:OPC CPSs were similar and not significantly different from BFS:OPC CPSs of the same formulation. ≈ 3% strontium chloride contaminated samples had greater surface area values but were not significantly different to other contaminated strontium cement pastes.

3   The initial pH range was consistent for most samples and slightly lower than the BFS:OPC values. These lower pH values could be a consequence of the much lower calcium content of PFA:OPC CPSs.

4   Strontium concentration of the make-up water and the nature of the added strontium salt influences the cation diffusivity.

5   Similarly to conclusion 4, caesium concentration influences its diffusivity, but more importantly diffuses more quickly than other cations, respective of cement formulation.

6   Both caesium and strontium influence calcium diffusion when compared with the corresponding control CPS. This is not surprising for strontium as it will be a good surrogate for calcium and hence take part in some of the hydrates produced during curing. Caesium has a lower impact on calcium diffusivity.

7   Strontium appeared to have the greater influence on chloride diffusivity but this could be largely dependent on the mass of the anion in the PFA: OPC CPS compared with other CPSs.

8   The diffusivity of sulphate was influenced by the nature of the cation added to the make-up water. Strontium had the greatest effect on lowering the diffusion primarily due to the formation of sparingly soluble strontium sulphate.

9   Strontium influenced sodium diffusivity.

10   The diffusivity of Sr^{2+} and other cations is dependent upon its concentration and cement additive used in the cement paste formulation.

11   Cl^- is the most mobile of all anions.
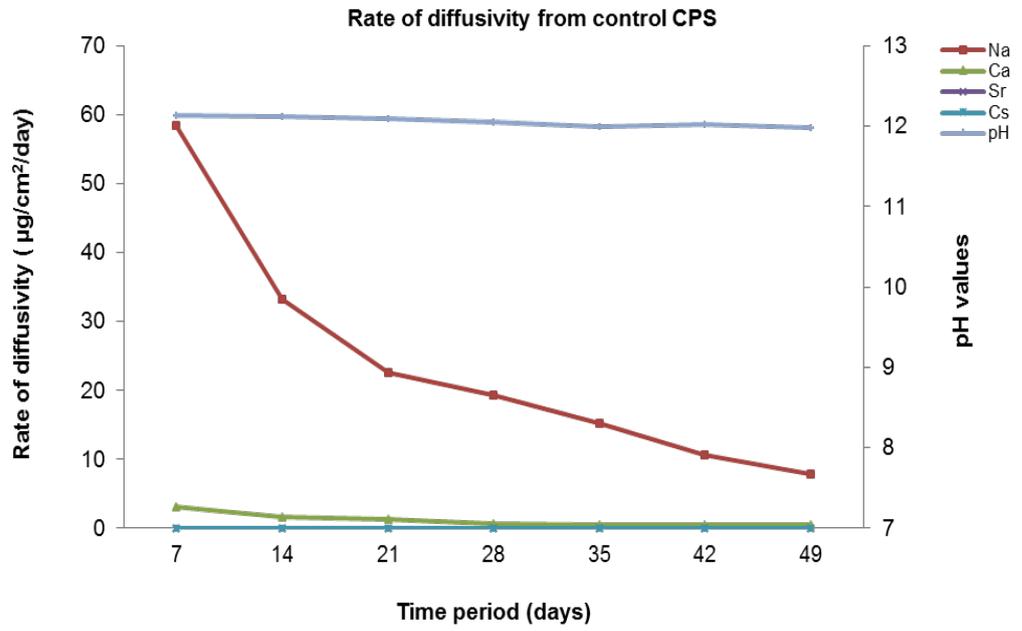
(a)
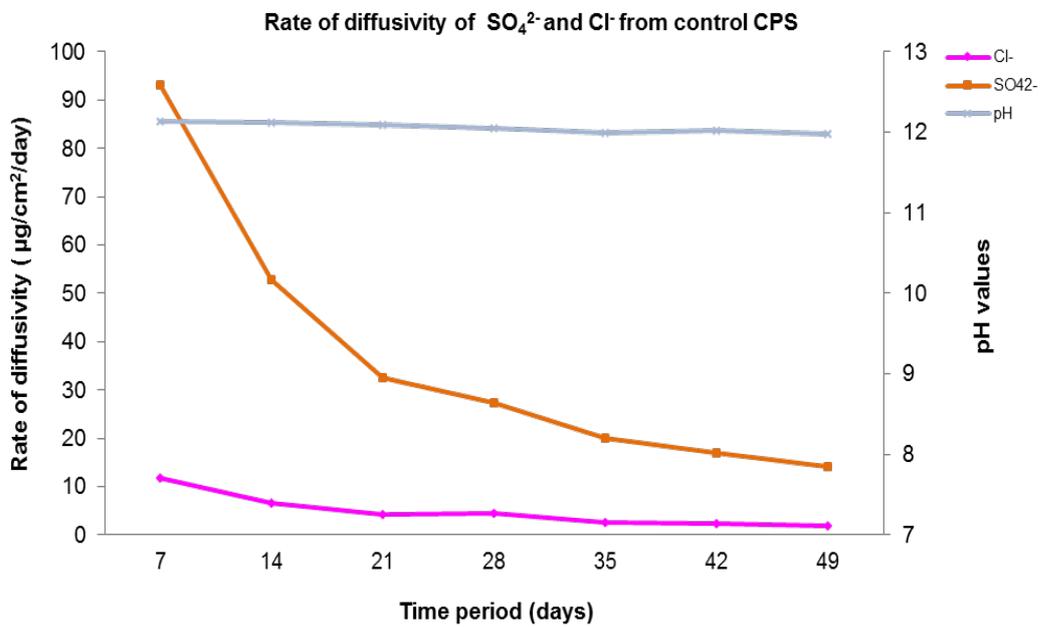
(b)

Figure 5.1 Rate of diffusivity of cations (a) and anions (b) from control PFA:OPC CPS in DW
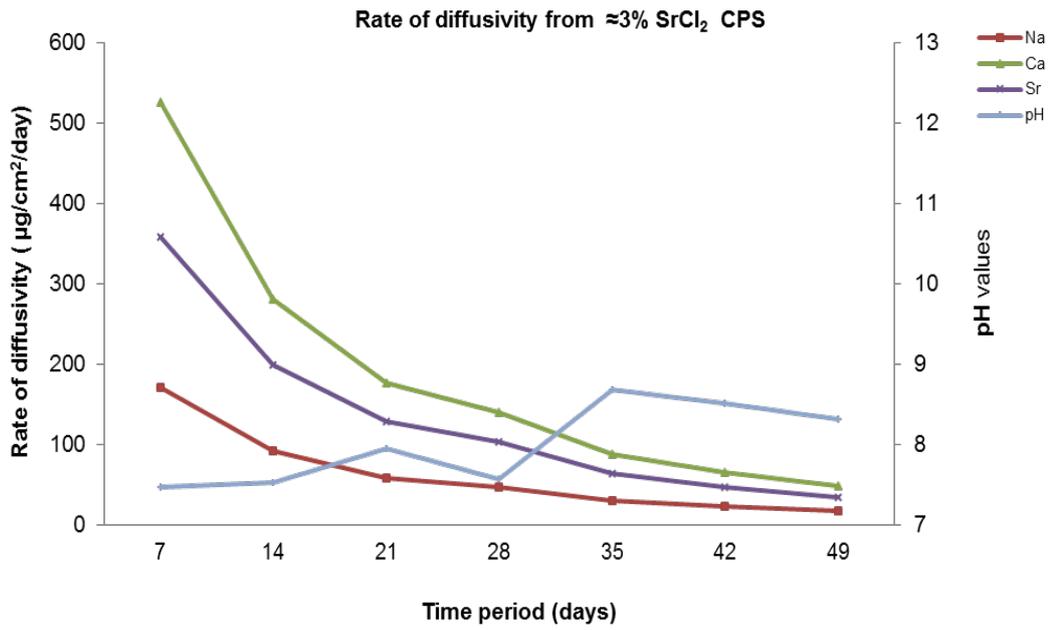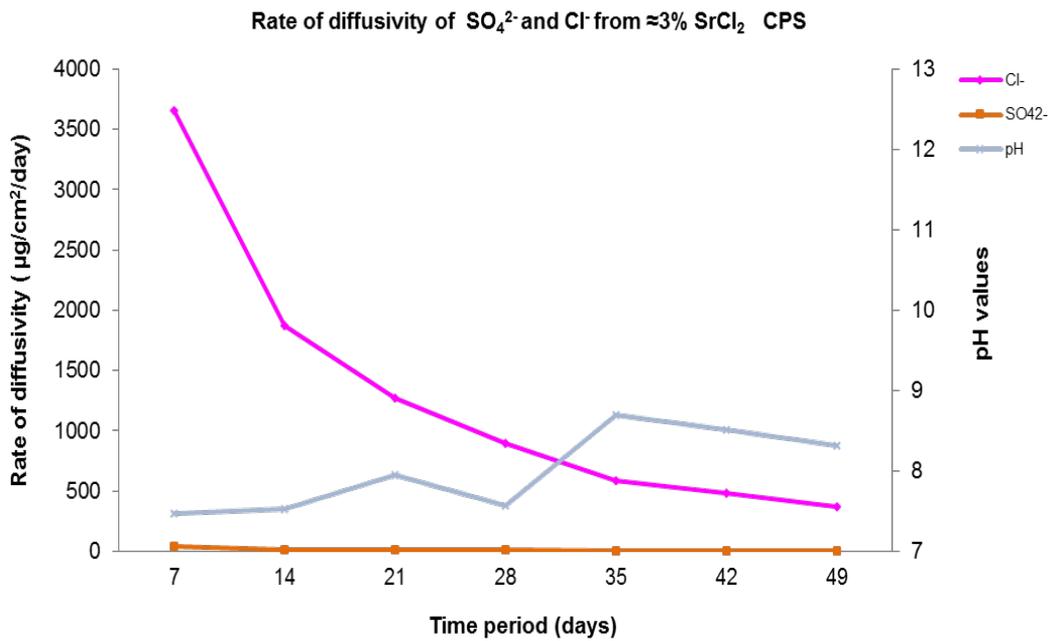
Figure 5.2 Rate of diffusivity of cations (a) and anions (b) from ≈ 3% SrCl₂ PFA:OPC CPS in DW
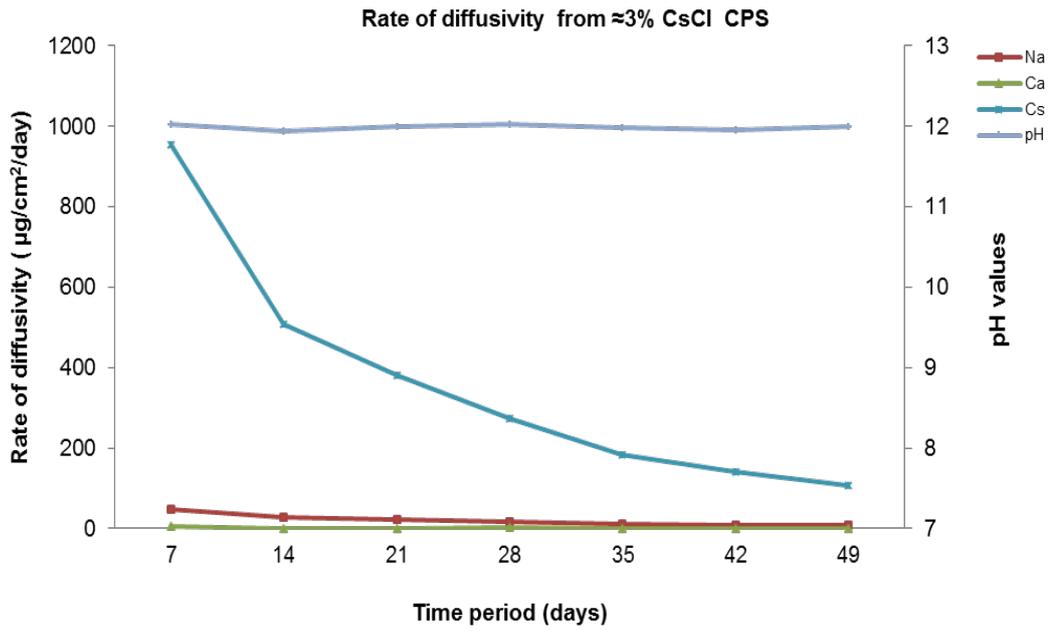
(a)
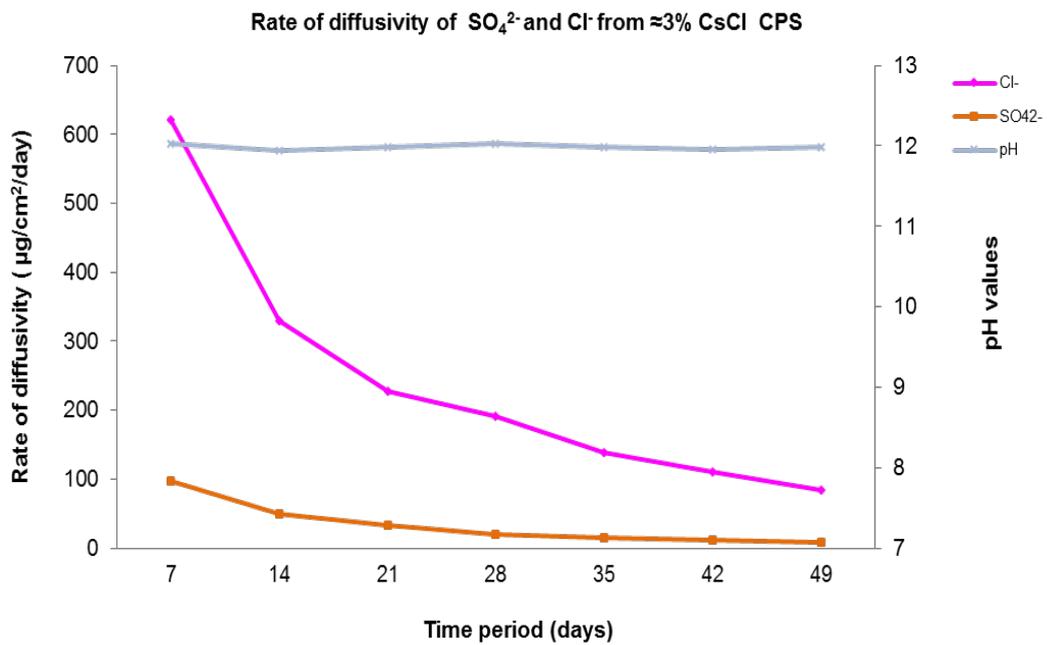
(b)

Figure 5.3 Rate of diffusivity of cations (a) and anions (b) from ≈ 3% CsCl PFA:OPC CPS in DW
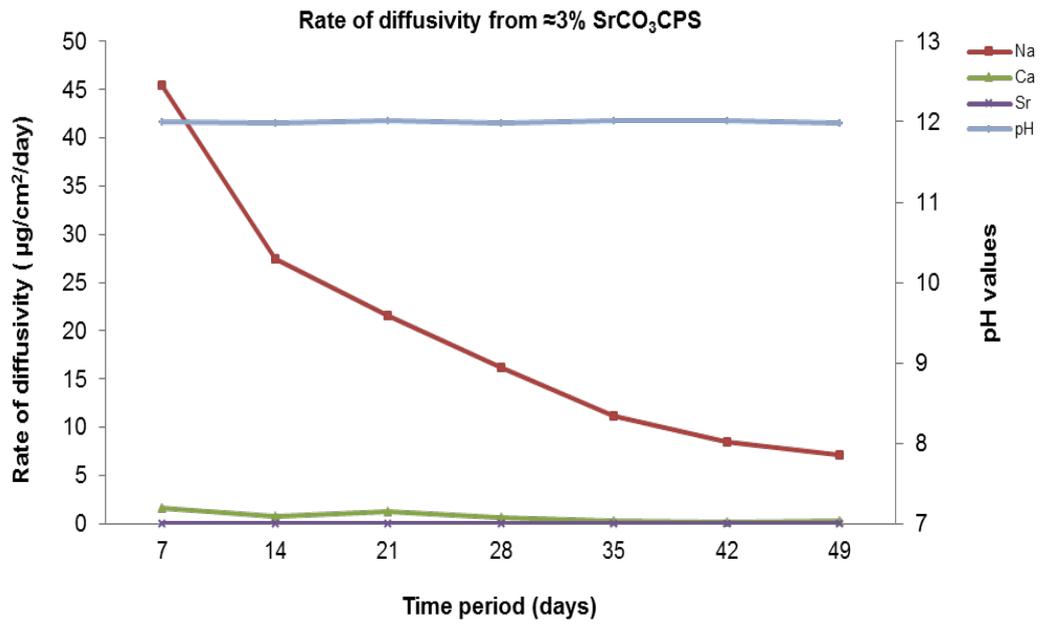
(a)
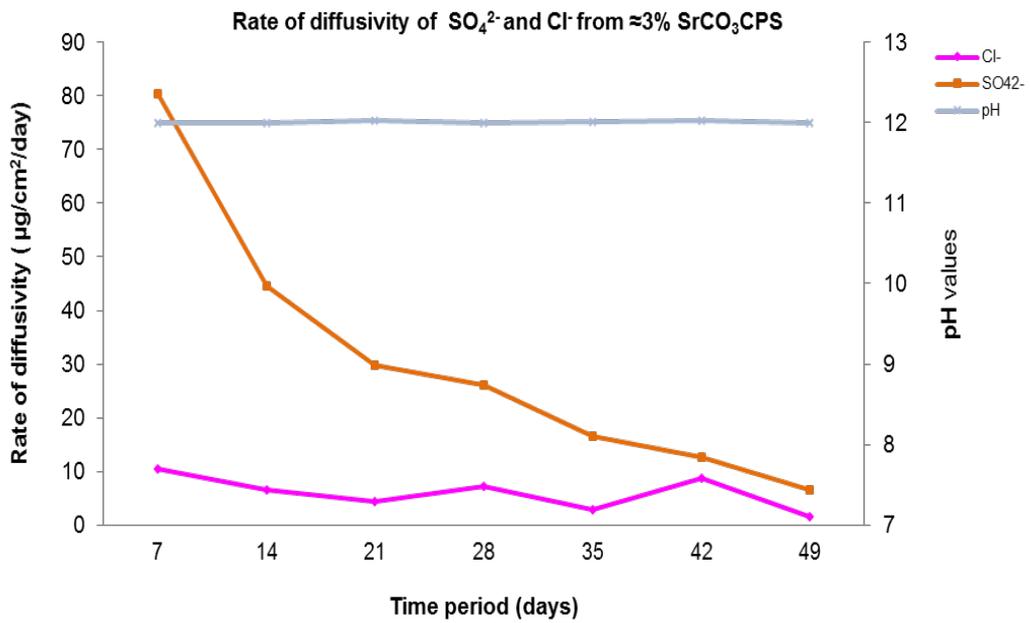
(b)

Figure 5.4 Rate of diffusivity of cations (a) and anions (b) from ≈3% SrCO$_3$ PFA:OPC CPS in DW
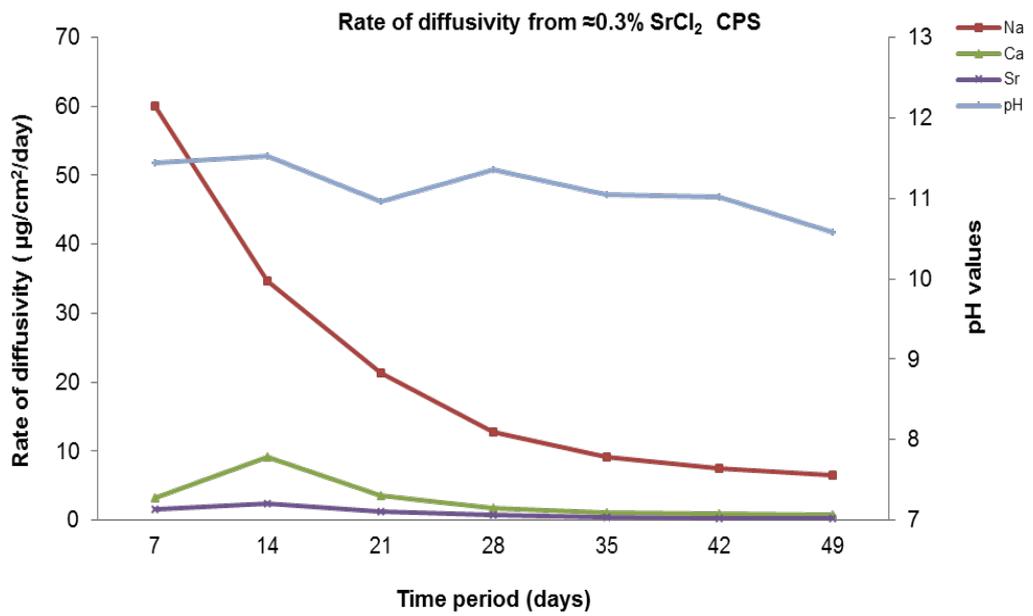
(a)
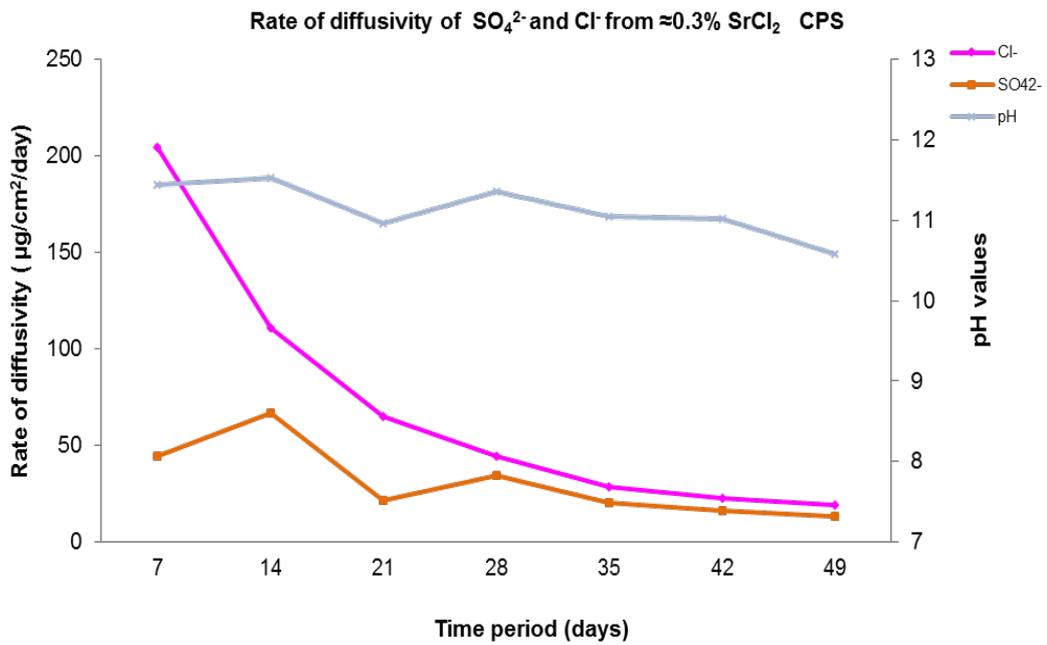
(b)

Figure 5.5 Rate of diffusivity of cations (a) and anions (b) from ≈0.3% SrCl$_2$ PFA:OPC CPS in DW
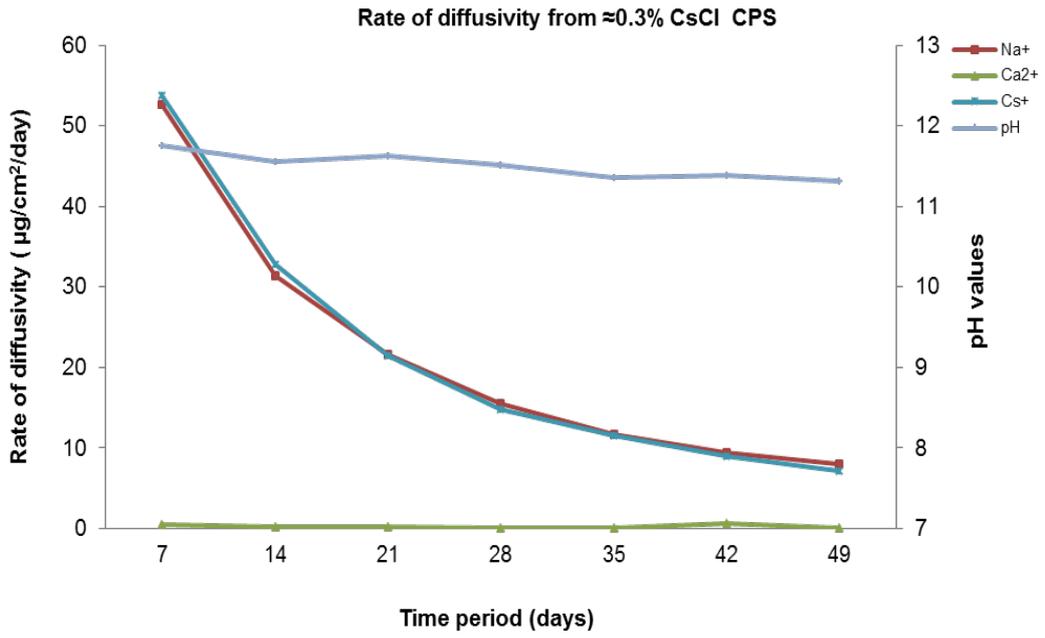
(a)
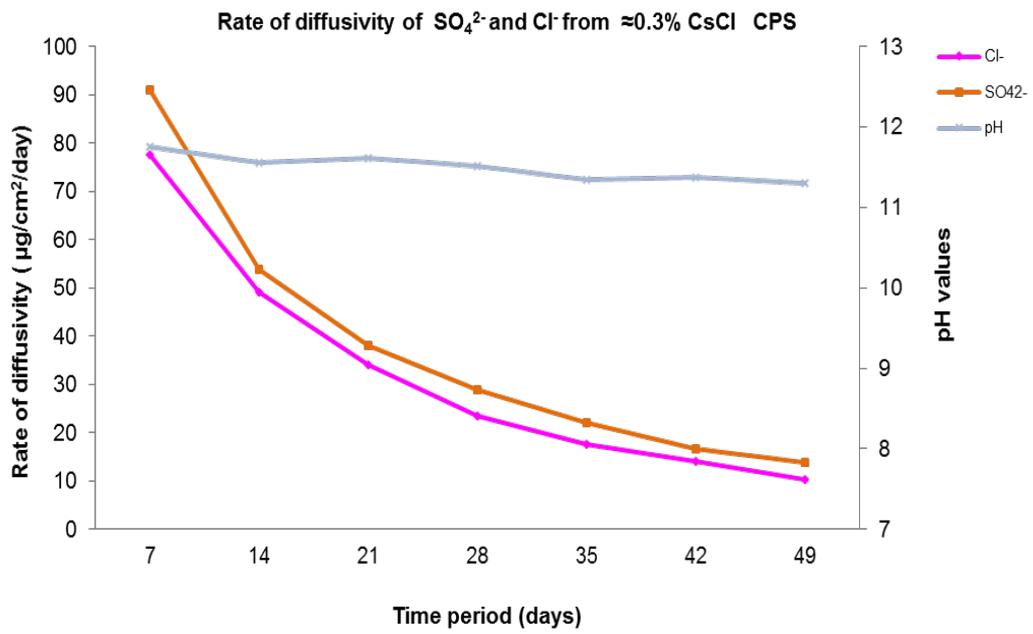
(b)

Figure 5.6 Rate of diffusivity of cations (a) and anions (b) from ≈0.3% CsCl PFA:OPC CPS in DW
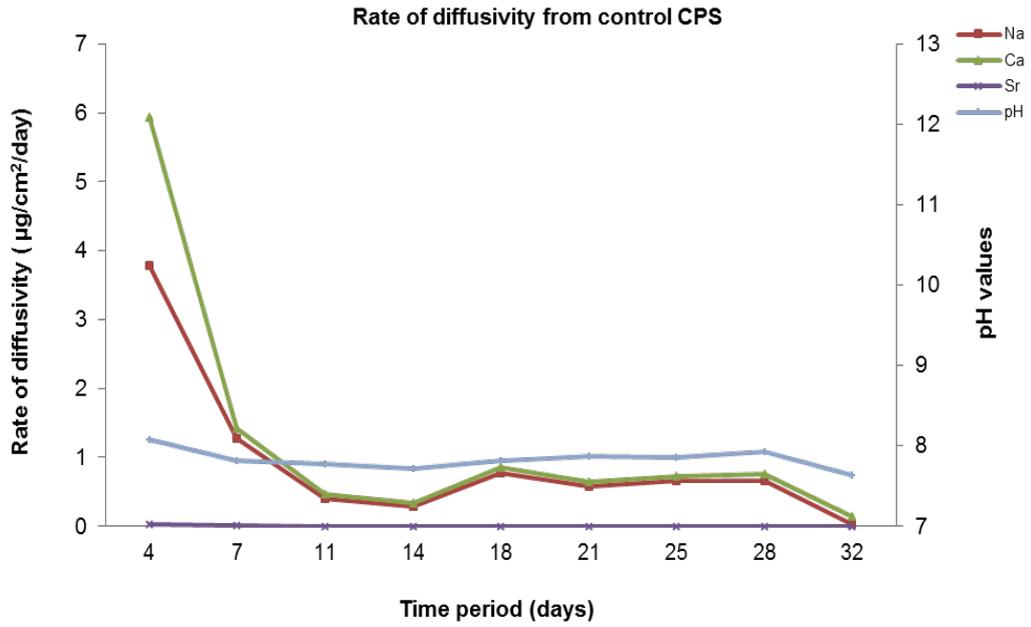
(a)
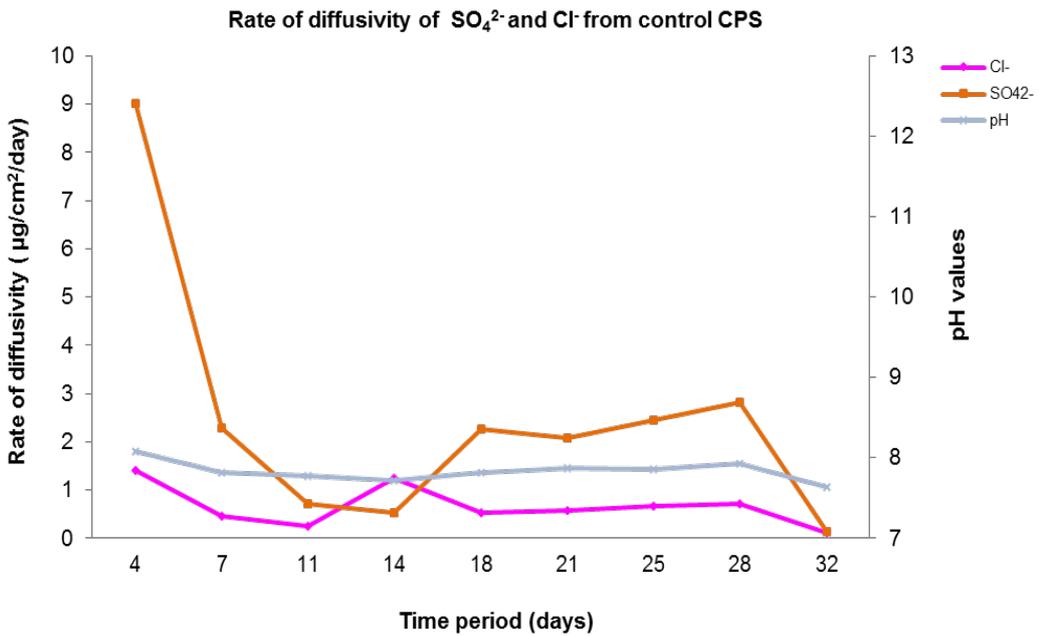
(b)

Figure 5.7 Rate of diffusivity of cations (a) and anions (b) from control PFA:OPC CPS in tap water (open circuit)

Rate of diffusivity from ≈3% SrCl₂ CPS

(a)

Rate of diffusivity of SO₄²⁻ and Cl⁻ from ≈3% SrCl₂ CPS
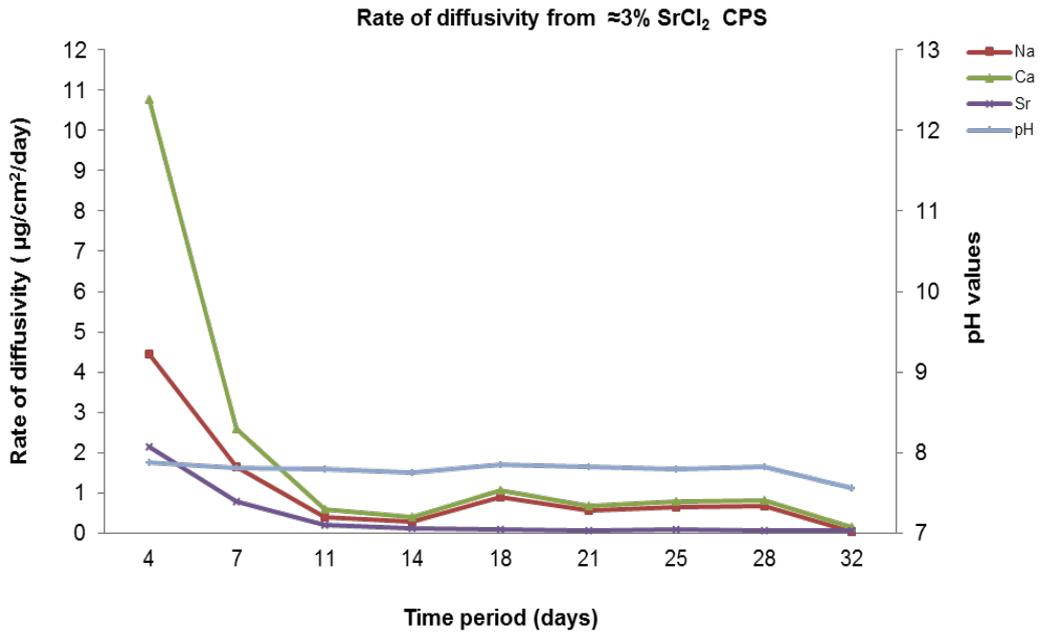
(b)

Figure 5.8 Rate of diffusivity of cations (a) and anions (b) from ≈3% SrCl₂ PFA:OPC CPS in tap water (open circuit)

166
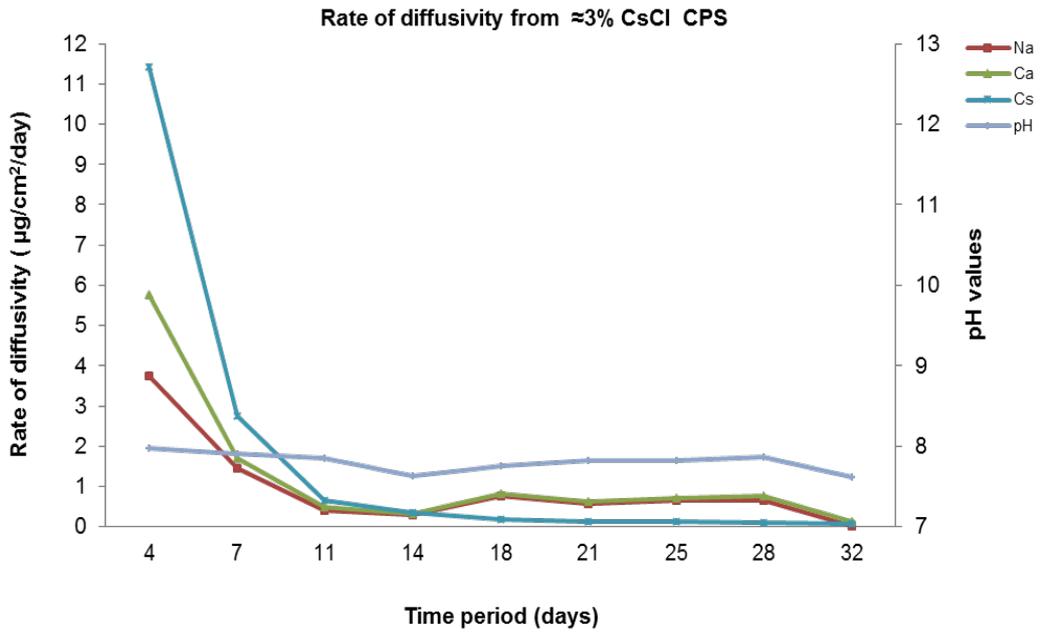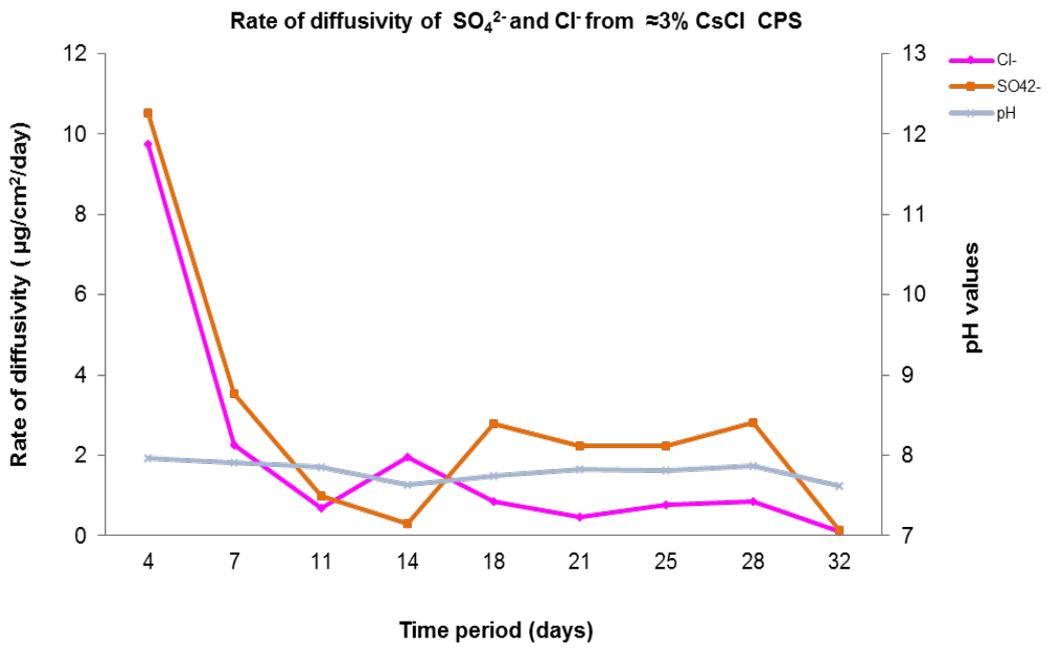
Figure 5.9 Rate of diffusivity of cations (a) and anions (b) from ≈3% CsCl PFA:OPC CPS in tap water (open circuit)
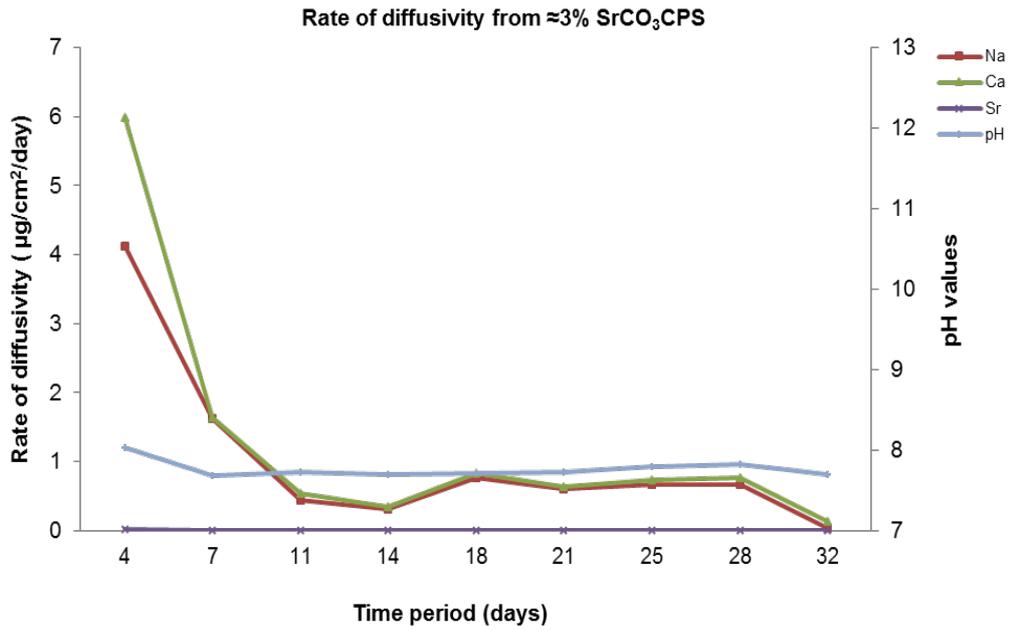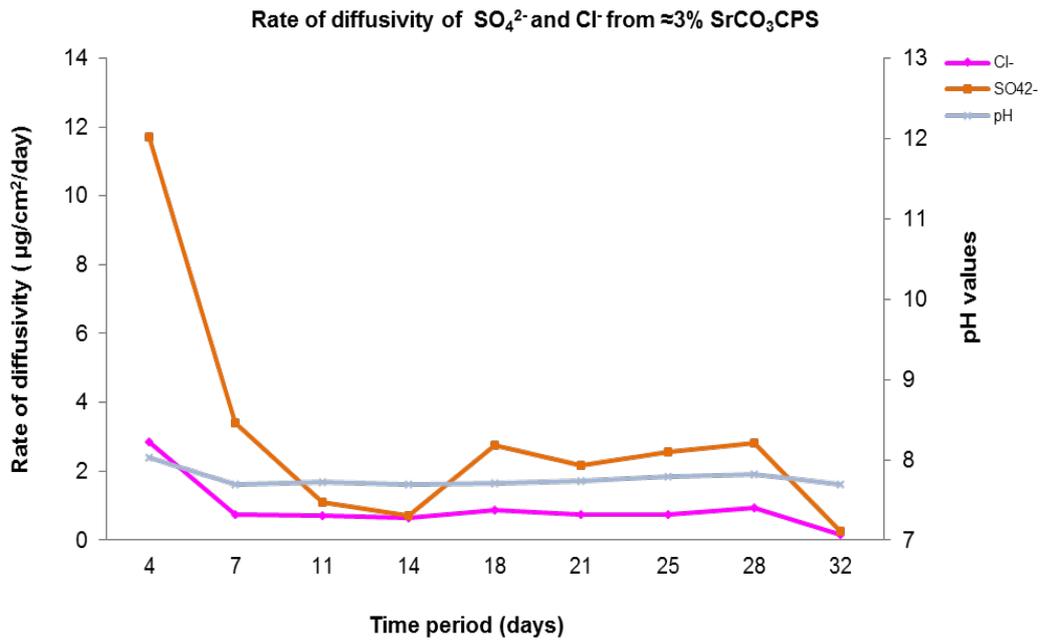
Figure 5.10 Rate of diffusivity of cations (a) and anions (b) from ≈3% SrCO₃ PFA:OPC CPS in tap water (open circuit)

Chapter 6: Diffusivity from BFS:OPC CPSs with Sellafield pore water as a test solution

6.1 Aims of study

The aim of this chapter is to evaluate the influence of simulated ground pore water, nature of cation and their concentration on the diffusivity of cations when encapsulated in BFS: OPC.

6.2 Introduction

The present study investigates the effect of simulated ground water on the diffusivity of encapsulated waste when under simulated Geological Disposal Facility (GDF) conditions. The stability of the cementitious waste was assessed by subjecting the encapsulated CPSs under closed circuit diffusivity experiments using Sellafield pore water as test solution. Two simulated groundwater solutions, concentrated Sellafield pore water (CSPW) and diluted Sellafield pore water (DSPW) (Table 6.1), were used as test solution in experiment 1 and experiment 2 respectively (Table 6.2). The simulated pore waters were prepared in accordance with compositions reported by King et al. [65].

Table 6.1 *Nominal composition of the test solution used [65]*

Parameter	salts used	Units	Concentrated Sellafield pore water (CSPW)	Diluted Sellafield pore water (DSPW)
			Sellafield BH3, DET1	*Sellafield BH9B, SPFT3*
pH		pH	6.8	6.8
Na^+	NaCl	mg/L	71600	19.3
K^+	KCl	mg/L	327	1.47
Mg^{2+}	$MgCl_2$	mg/L	696	13
Ca^{2+}	$CaCl_2$	mg/L	300	40.7
SiO_4^{4-}	-	mg/L	2.67	5.24
Cl^-	$NaCl/MgCl_2$	mg/L	108000	14.5
SO_4^{2-}	Na_2SO_4	mg/L	4910	4.01

6.3 Cement paste samples

The diffusivity experiments were carried out on 2 sets of 7 different CPSs, using CSPW in experiment 1 and DSPW in experiment 2.

Table 6.2 BFS: OPC cement paste samples and test solution used

Experiment	BFS:OPC Cement paste samples		Test solution
1	(a)	Control	Concentrated
	(b)	≈3% $SrCl_2$	Sellafield pore water
	(c)	≈3% CsCl	(CSPW)
	(d)	≈0.3% $SrCl_2$	
	(e)	≈0.3% CsCl	
	(f)	≈3% $SrCO_3$	
	(g)	≈0.3% $SrCO_3$	
2	(a)	Control	Diluted
	(b)	≈3% $SrCl_2$	Sellafield pore water
	(c)	≈3% CsCl	(DSPW)
	(d)	≈0.3% $SrCl_2$	
	(e)	≈0.3% CsCl	
	(f)	≈3% $SrCO_3$	
	(g)	≈0.3% $SrCO_3$	

6.4 Results and discussion

The duration of the dynamic diffusivity experiments was 105 days. The rate of diffusivity values of each cement paste sample are given in table appendix 6.1 to 6.14.

6.4.1 Micropore and surface area analysis of cement paste sample measured by BET method

The average micropore and surface area of the cement paste samples are shown in Table 6.3. The micropore values of the cement paste samples prior to the diffusivity experiment were in the range of 1.4 – 8.5 m^2/g. The highest values were measured in ≈3% $SrCl_2$ (8.5 m^2/g) and the lowest micropore area was

observed in ≈3% CsCl (1.4 m^2/g). However, the micropore area of control, ≈3% SrCl$_2$, ≈0.3% CsCl, ≈3% SrCO$_3$, ≈0.3% SrCO$_3$ was fairly in similar range (3.1- 4.8 m^2/g).

The average surface areas of the cement paste sample were measured in the range of 13.1 – 31.8 m^2/g. The highest surface area was measured in control CPS (31.8 m^2/g), whereas the lowest values were measured in ≈3% CsCl (13.1 m^2/g). Both the micropore and surface area of ≈3% CsCl CPS were found to be lowest than for all other CPS.

Table 6.3 Average micropore and surface area of cement paste samples measured by BET method

CPS	Average micropore area	Average surface area
	m^2/g	
Control	4.4	31.8
≈3% SrCl$_2$	8.5	22.3
≈3% CsCl	1.4	13.1
≈0.3% SrCl$_2$	3.1	19.2
≈0.3% CsCl	4.2	19.2
≈3% SrCO$_3$	5.3	22
≈0.3% SrCO$_3$	4.8	23

6.4.2 Test solution analysis

6.4.2.1 pH values

The pH values of the CSPW test solutions after few days of the diffusivity experiments increased from 6.8 (natural pH of CSPW) to 7.41-11.35. The lowest pH values were recorded in the test solutions of ≈3% SrCl$_2$ and ≈ 3% CsCl CPS (Figure 6.1 and 6.5). Highest range in pH values with increasing trend was measured in the CSPW from ≈ 0.3% counterpart and CPSs with carbonate.

The simulated pore waters have no or little inherent buffering capacity and therefore will change significantly with the duration of the experiments. This was more evident for the DSPW. The pH values in the DSPW for all the CPS excluding $\approx 3\%$ SrCl$_2$ and $\approx 3\%$ CsCl showed higher pH values and were fairly close to the pH values measured in the DW experiment.

6.4.2.2 Chemical analysis of test solution

The rates of diffusivity of the cations and anions are presented in Figure 6.1 to Figure 6.14. All the diffusivity data have been normalised for dilution effect and cation/anion composition of CSPW. The average rate of diffusivity data of 105 days from DW BFS: OPC experiment have been utilised for comparative purpose.

6.4.2.2.1 *Strontium*

The diffusivity of Sr^{2+} from CSPW and DSPW experiments showed similar trend in the diffusivity i.e. $\approx 3\%$ SrCl$_2$ > $\approx 0.3\%$ SrCl$_2$ > $\approx 3\%$ SrCO$_3$ > $\approx 0.3\%$ SrCO$_3$. The diffusivity of Sr^{2+} was found to be slowest of all cations within individual CPS except in case of CSPW for $\approx 3\%$ SrCl$_2$ CPS. The difference in the diffusion of Sr^{2+} between two experiments is notable. The average rate of diffusivity of Sr^{2+} in CSPW from $\approx 3\%$ SrCl$_2$ CPS (25 µg/cm^2/day), $\approx 0.3\%$ SrCl$_2$ CPS (3 µg/cm^2/day), $\approx 3\%$ SrCO$_3$ CPS (1 µg/cm^2/day) and $\approx 0.3\%$ SrCO$_3$ CPS (0.3 µg/cm^2/day) was 6, 10, 71 and 16 times higher than the rate of diffusivity of Sr in DSPW from $\approx 3\%$ SrCl$_2$ CPS (4.3 µg/cm^2/day), $\approx 0.3\%$ SrCl$_2$ CPS (0.27 µg/cm^2/day), $\approx 3\%$ SrCO$_3$ CPS (0.032 µg/cm^2/day) and $\approx 0.3\%$ SrCO$_3$ CPS (0.018 µg/cm^2/day) respectively. The dependence of Sr^{2+} diffusivity on the type of aqueous solution, concentration and nature of Sr^{2+} added to cement paste mixture is explained in the previous chapter, section 3.3.

6.4.2.2.2 *Caesium*

Caesium diffused out at faster rate from ≈3% CsCl CPS than ≈0.3% CsCl CPS in both the experiments. The diffusivity of Cs^+ from ≈3% CsCl CPS (840 µg/cm^2/day) and ≈0.3% CsCl CPS (77 µg/cm^2/day) in CSPW experiment was ≈ 45 times faster than the diffusivity of Cs^+ from ≈3% CsCl CPS (19 µg/cm^2/day) and ≈0.3% CsCl CPS (1.72 µg/cm^2/day) CPSs in DSPW experiment. This could be due to the pH effect. The pH range of CSPW for 3% and 0.3% CsCl CPS was in the range of 7.18 – 9.05. However, the pH range measured in DSPW for 3% and 0.3% CsCl CPS was in the range of 7.7 -12.01. In comparison with DW diffusivity data; Cs^+ in CSPW diffused out 32 and 53 times faster for ≈3% CsCl and ≈0.3% CsCl CPS respectively. This suggests that the encapsulated metal ion may have faster diffusivity rate when subjected to a leaching process with higher ionic strength test solution with pH values in the range of 7 - 9.

6.4.2.2.3 *Calcium*

Calcium diffused out at faster rate from ≈3% $SrCl_2$ CPS in both the DSPW and CSPW test solutions. In CSPW, Ca^+ from ≈3% contaminated CPSs diffused out faster in comparison with ≈0.3% contaminated CPSs. The sequence of diffusivity of Ca^+ observed in CSPW test solution was ≈3% $SrCl_2$> control > ≈3% CsCl > ≈3% $SrCO_3$> ≈0.3% $SrCl_2$ > ≈0.3% CsCl > ≈0.3% $SrCO_3$.

Contrary to CSPW, the results of DSPW showed the sequence of diffusivity as ≈3% $SrCl_2$> ≈0.3% $SrCl_2$ >≈3% $SrCO_3$> ≈3% CsCl > ≈0.3% CsCl > ≈0.3% $SrCO_3$>control. The diffusivity of Ca^+ from ≈0.3% CsCl was faster compared to all the CPS in DSPW. Calcium from control in DSPW diffused out slowest of all the CPS.

The average rate of diffusivity of Ca^+ in CSPW experiment was higher than DW and DSPW experiment. There was no significant difference in the rate of diffusivity between DW and DSPW from all the 0.3% CPSs. However, the average rate of diffusivity of Ca^+ from ≈3% CsCl CPS (4.3 µg/cm^2/day) and ≈3% $SrCO_3$ CPS (4.7 µg/cm^2/day) was ≈7 times higher compared to DW experiment (≈3% CsCl CPS (0.6 µg/cm^2/day); ≈3% $SrCO_3$ CPS (0.8 µg/cm^2/day).

6.4.2.2.4 *Sodium*

Sodium diffused out at fairly similar and higher rate from control, ≈3% $SrCl_2$, and ≈3% CsCl CPS compared to ≈0.3% $SrCl_2$, ≈0.3% CsCl, ≈0.3% $SrCO_3$ and ≈3% $SrCO_3$ in CSPW experiment. This could be due to higher concentration of Na in 200 ml CSPW i.e. 623 mmoles compared to the maximum Na^+ can diffuse at its highest concentration i.e. 23 mmoles from CPS. The rate of diffusivity of sodium from all the CPSs in DSPW was significantly similar except from ≈3% $SrCO_3$.

In comparison with DW experiment, the diffusivity of sodium from all the CPSs in CSPW was considerably higher than the DW and DSPW.

6.4.2.2.5 *Chloride*

The difference in the rate of diffusivity of the anion between the two experiments was observed. The diffusivity of Cl^- from all the CPSs in CPSW showed a significant similar rate of diffusivity. The CSPW test solution contains much more Cl^- ion than the DSPW (Table 6.1). It is highly unlikely that the concentration of diffused Cl^- can be measured. The concentration of Cl^- present in 200 ml CPSW is 609 mmoles, which is significantly higher than the maximum concentration of Cl^- could be leached out i.e. 60 mmoles. There could be back diffusion of Cl^- due to reverse concentration gradient.

In case of DSPW, Cl^- from ≈3% $SrCl_2$ CPS (177 μg/cm^2/day) diffused out at faster rate followed by ≈3% CsCl CPS (154 μg/cm^2/day), ≈0.3% $SrCl_2$ CPS (26 μg/cm^2/day) and ≈0.3% $SrCl_2$ CPS (26 μg/cm^2/day). There was no significant difference observed in the diffusivity Cl^- between ≈3% CsCl CPS (13 μg/cm^2/day), control CPS (12 μg/cm^2/day) ≈3% $SrCO_3$ CPS (9 μg/cm^2/day) and ≈0.3% $SrCO_3$ CPS (8 μg/cm^2/day).

In comparison with DW experiment, the average rate of diffusivity of Cl^- from ≈3% CsCl CPS (154 μg/cm^2/day) in DSPW was ≈23 times higher than the average rate of diffusivity in DW (7 μg/cm^2/day). Contrary to its 0.3% counterpart; the average rate of diffusivity in DSPW was 1.8 times lower in comparison with DW diffusivity.

In case of ≈3% $SrCl_2$, the average rate of diffusivity was ≈2 times higher in DSPW (177 μg/cm^2/day) in comparison with DW diffusivity (83 μg/cm^2/day). However, the average rate of diffusivity was measured 9 times higher from its 0.3% counterpart in DSPW (26 μg/cm^2/day) in comparison with DW (2.9 μg/cm^2/day).

6.4.2.2.6   *Sulphate*

The rate of diffusivity of SO_4^{2-} was faster from ≈0.3% $SrCO_3$ CPS compared to all the CPSs in the CSPW. There was no significant difference in the rate of diffusivity of SO_4^{2-} from ≈3% CsCl, ≈3% $SrCl_2$, and ≈0.3% CsCl and control CPS. The concentration of SO_4^{2-} in CSPW was twice as high as in the CPSs, which may have created inverse concentration gradient in favour of test solution. In DSPW experiment, the diffusivity of SO_4^{2-} from ≈3% CsCl was faster compared to all the CPSs in the DSPW. There was no significant difference observed in the rate of diffusivity of SO_4^{2-} from ≈3% $SrCl_2$, ≈0.3% $SrCO_3$, ≈0.3% CsCl and control

CPS. The average rate of diffusivity of SO_4^{2-} from control in DW (16 µg/cm^2/day) and DSPW (16 µg/cm^2/day) experiments was found to be similar.

Comparing the results obtained from DW experiments; the average rate of diffusivity of SO_4^{2-} from CSPW was 2-17 times higher compared to diffusivity measured in DW experiment from all the CPSs. In case of DSPW; there was no significant difference observed in the diffusivity of SO_4^{2-} from control ≈3% $SrCl_2$ ≈0.3% $SrCl_2$, ≈0.3% CsCl. However, the average rate of diffusivity of SO_4^{2-} from ≈3% CsCl (35 µg/cm^2/day), ≈ 3% $SrCO_3$ (22 µg/cm^2/day) in DSPW was ≈ 6 and ≈4 times higher in comparison with DW experiment from ≈3% CsCl (6 µg/cm^2/day), ≈ 3% $SrCO_3$ (6 µg/cm^2/day).

6.5 Conclusions

1 Although the ionic strength of the CSPW was significantly higher than other test solution (≈3 compared with ≈0.1), it had little or no effect on pH values; however for the DSPW the values decreased slightly by one unit.

2 Strontium diffusivity depends on concentration and nature of strontium salt added to the make-up water.

3 The concentration of cations and anions in the test solution influenced strontium diffusivity. A similar situation was observed for caesium diffusion.

4 Calcium diffusion was affected by both nature of the cation added to make-up water and its concentration. This effect was less marked for caesium contaminated CPSs.

5 These test solutions had the least impact on chloride diffusivity, but this could be attributed to the high concentration of chloride in the test solution in particular for CSPW.

6 The diffusivity of sulphate was hindered by the presence of strontium.

7 The changes in the rate of sulphate diffusivity could be attributed to the changing chemistry of hydrates and pore water compositions with time.

8 The impact of cement paste and test solution composition had little influence of sodium diffusion.
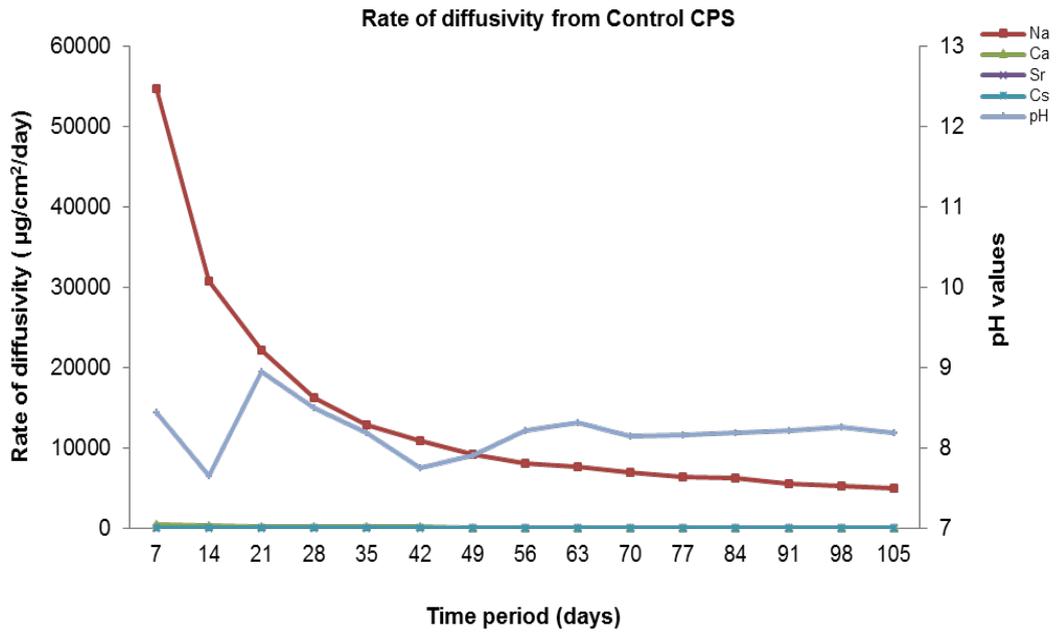
(a)

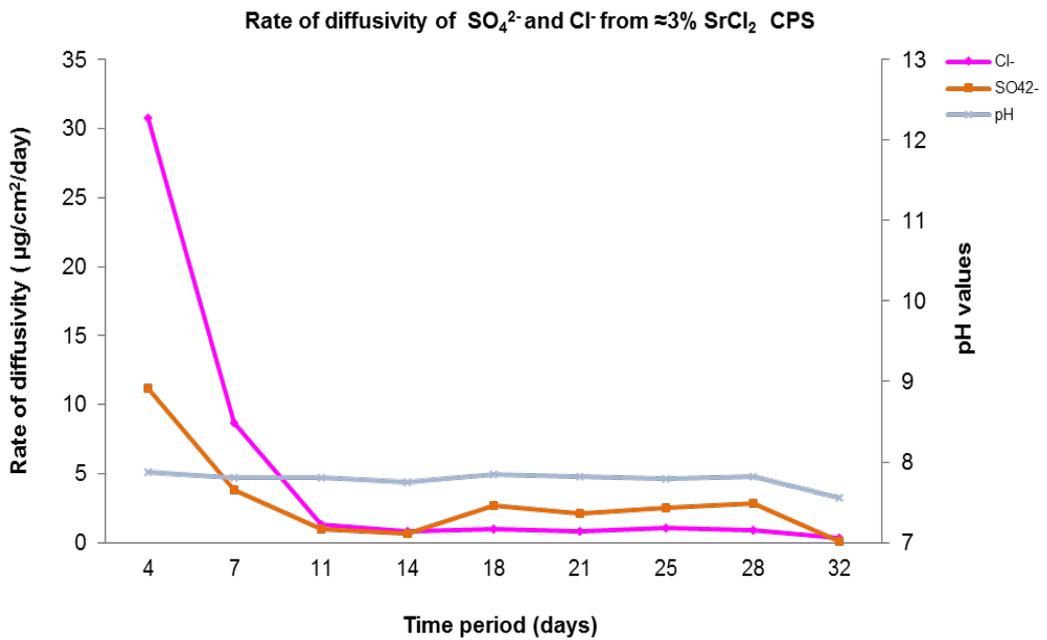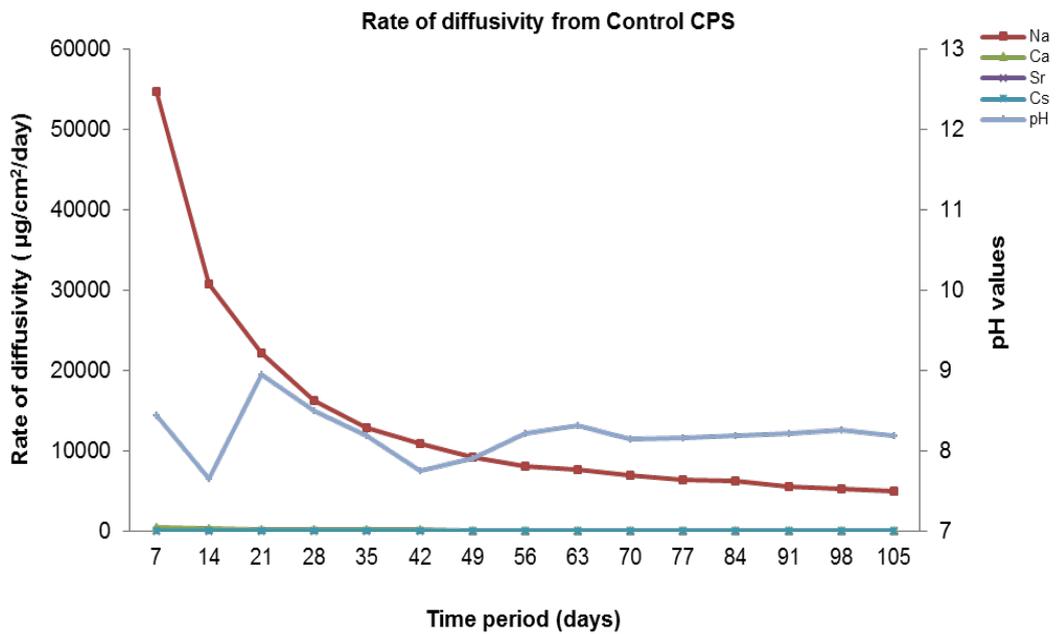**(b)**

Figure 6.1 Rate of diffusivity of cations (a) and anions (b) from control BFS:OPC CPS in CSPW
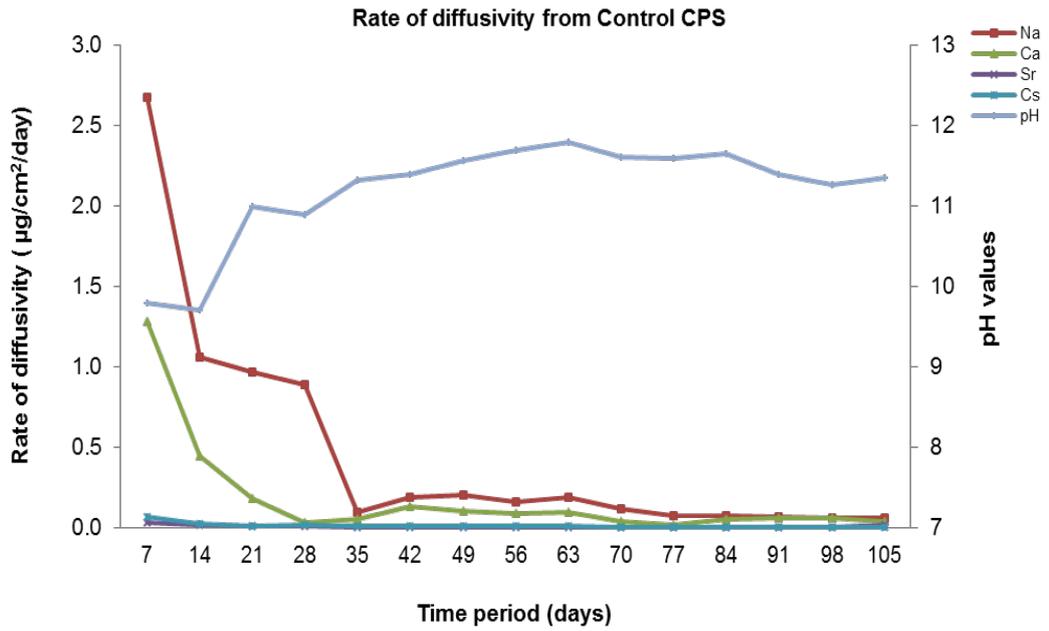
(a)
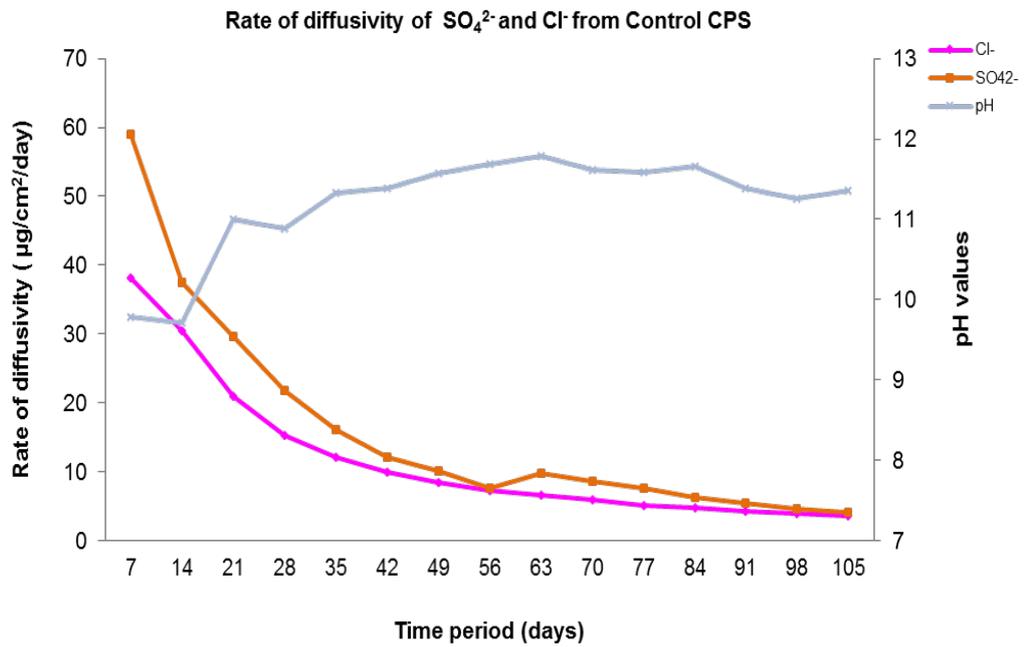
(b)

Figure 6.2 Rate of diffusivity of cations (a) and anions (b) from control BFS:OPC CPS in DSPW
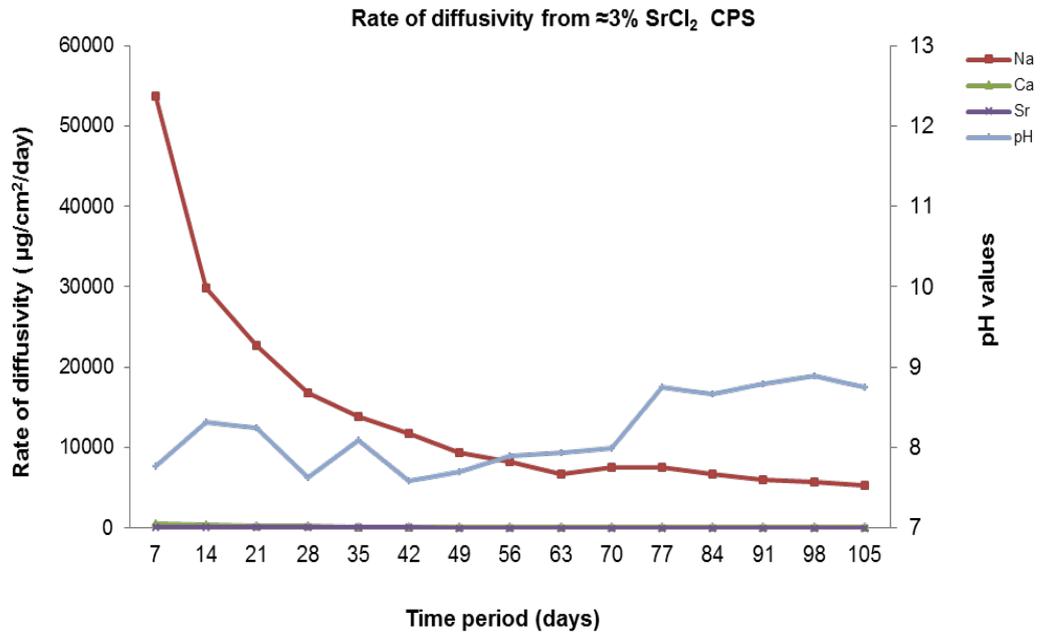
(a)
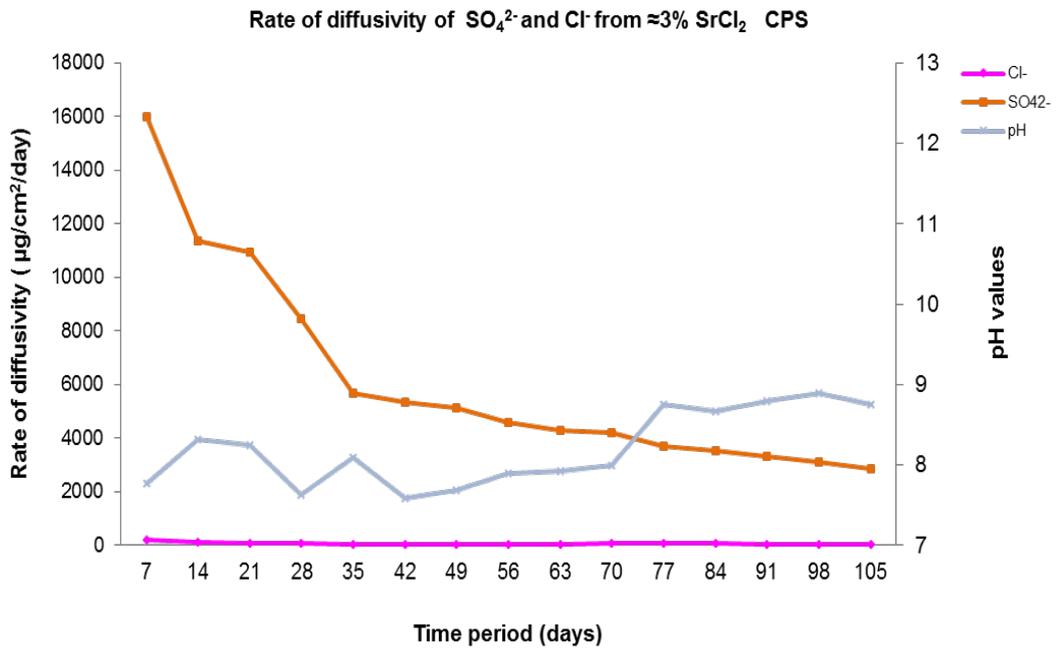
(b)

Figure 6.3 Rate of diffusivity of cations (a) anions (b) from ≈3% SrCl$_2$ BFS:OPC CPS in CSPW
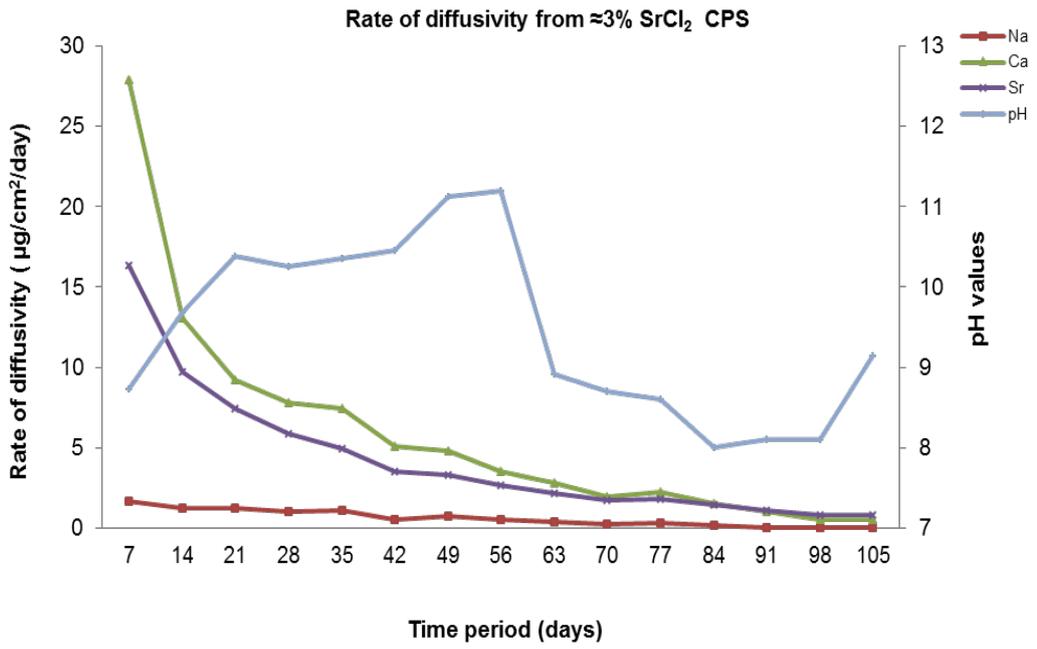
(a)
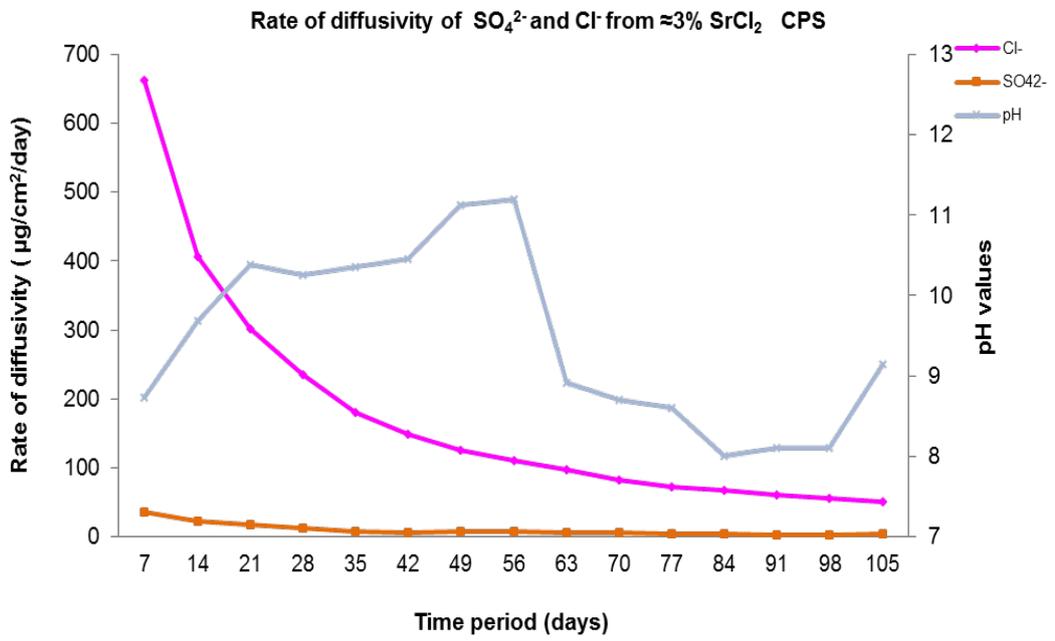
(b)

Figure 6.4 Rate of diffusivity of cations (a) anions (b) from ≈3% SrCl₂ BFS:OPC CPS in DSPW

181
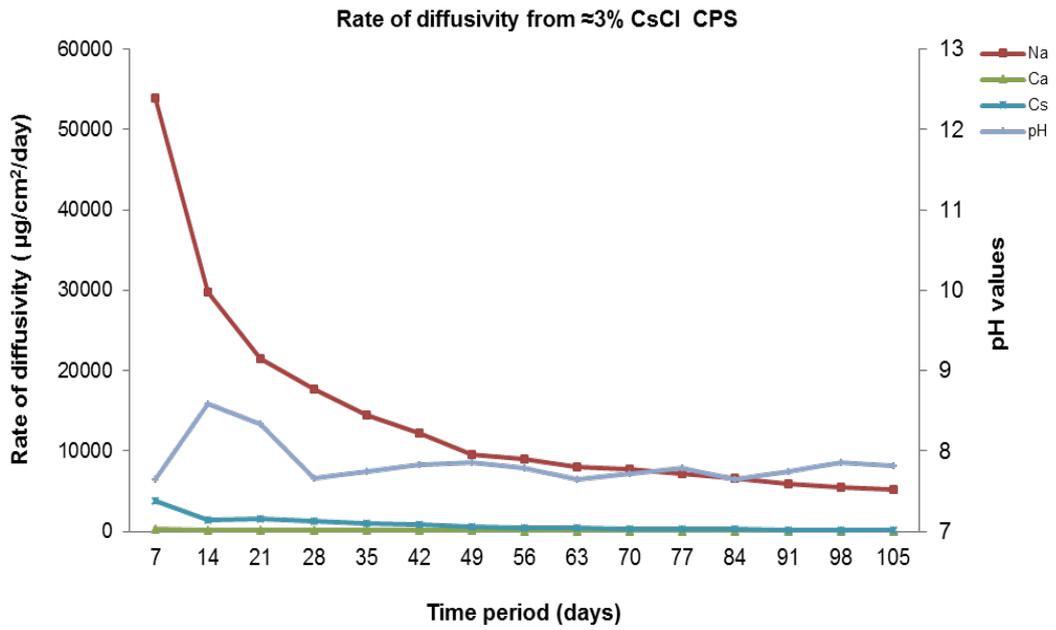
(a)
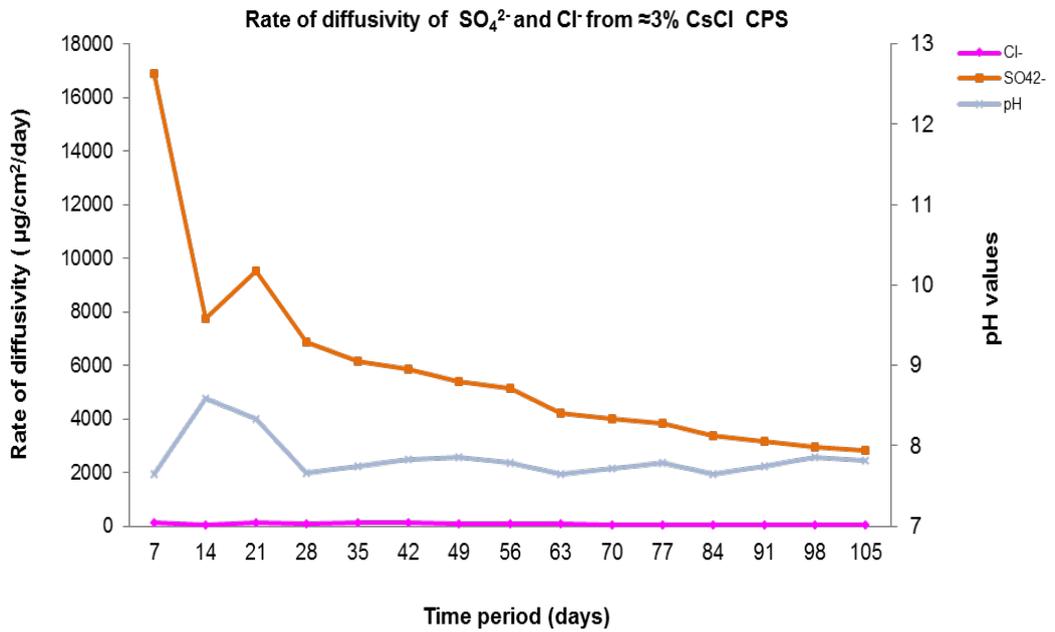
(b)

Figure 6.5 Rate of diffusivity of cations (a) anions (b) from ≈3% CsCl BFS:OPC CPS in CSPW
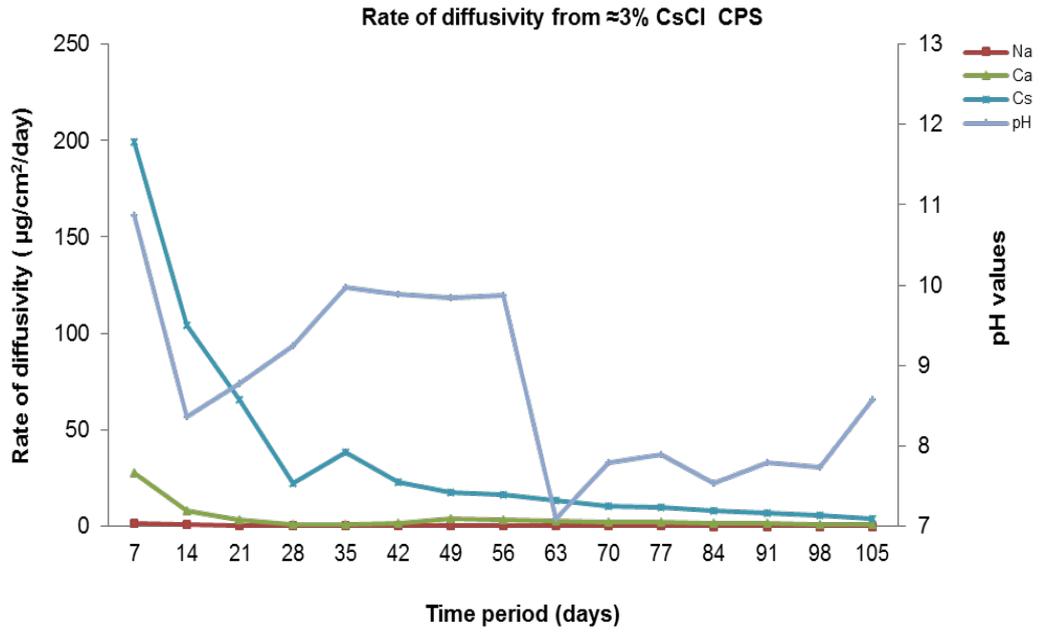
(a)
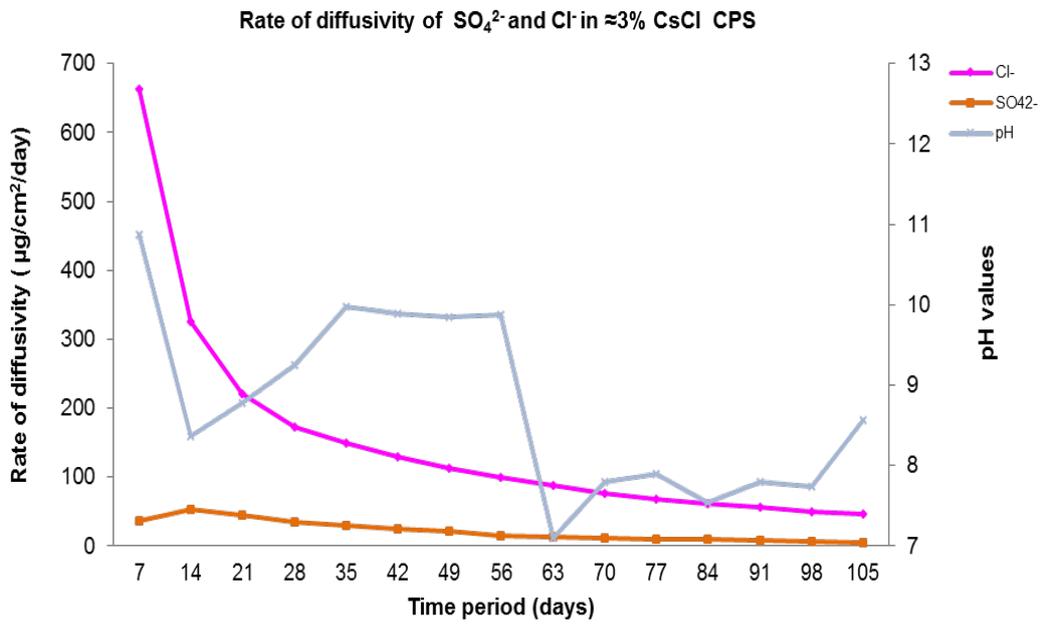
(b)

Figure 6.6 Rate of diffusivity of cations (a) anions (b) from ≈3% CsCl BFS:OPC CPS in DSPW
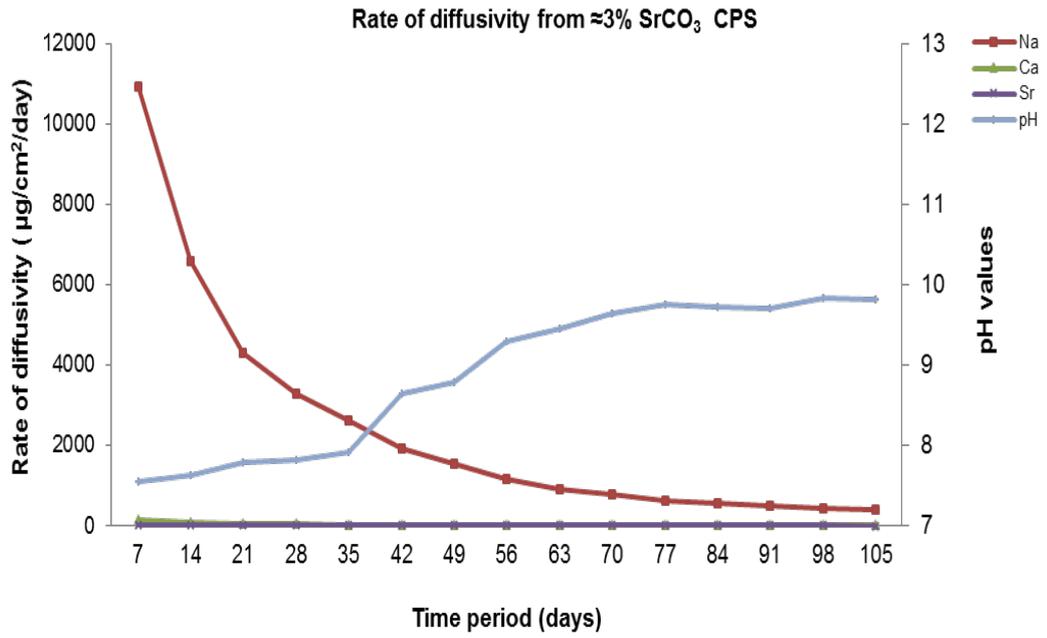
(a)
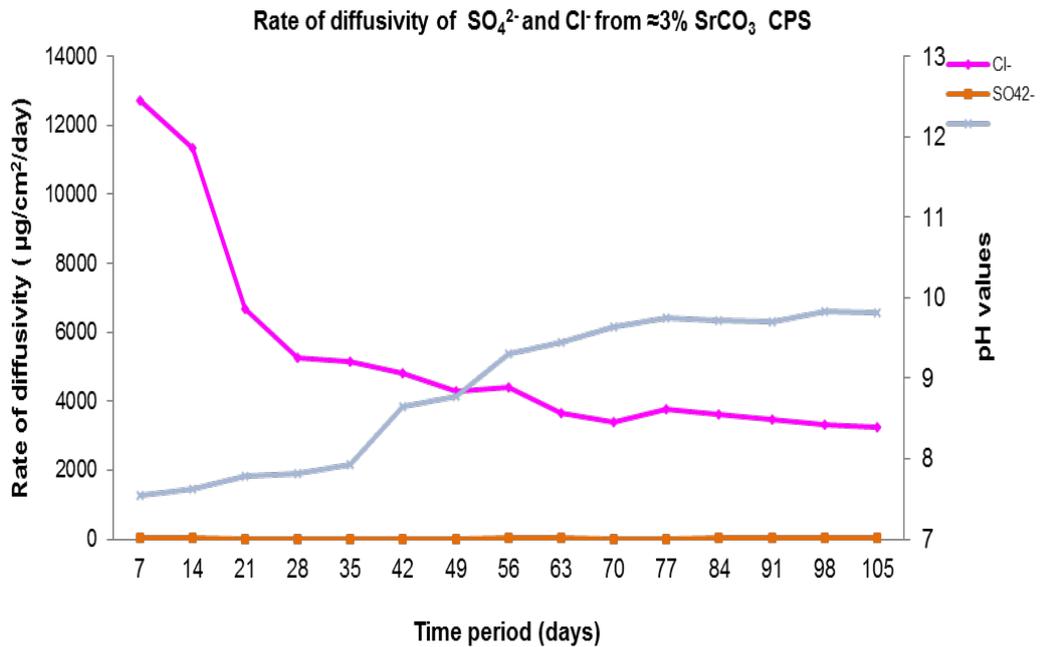
(b)

Figure 6.7 Rate of diffusivity of cations (a) anions (b) from ≈3% SrCO$_3$ BFS:OPC CPS in CSPW

Rate of diffusivity from ≈3% SrCO₃ CPS

(a)

Rate of diffusivity of SO₄²⁻ and Cl⁻ in ≈3% SrCO₃ CPS
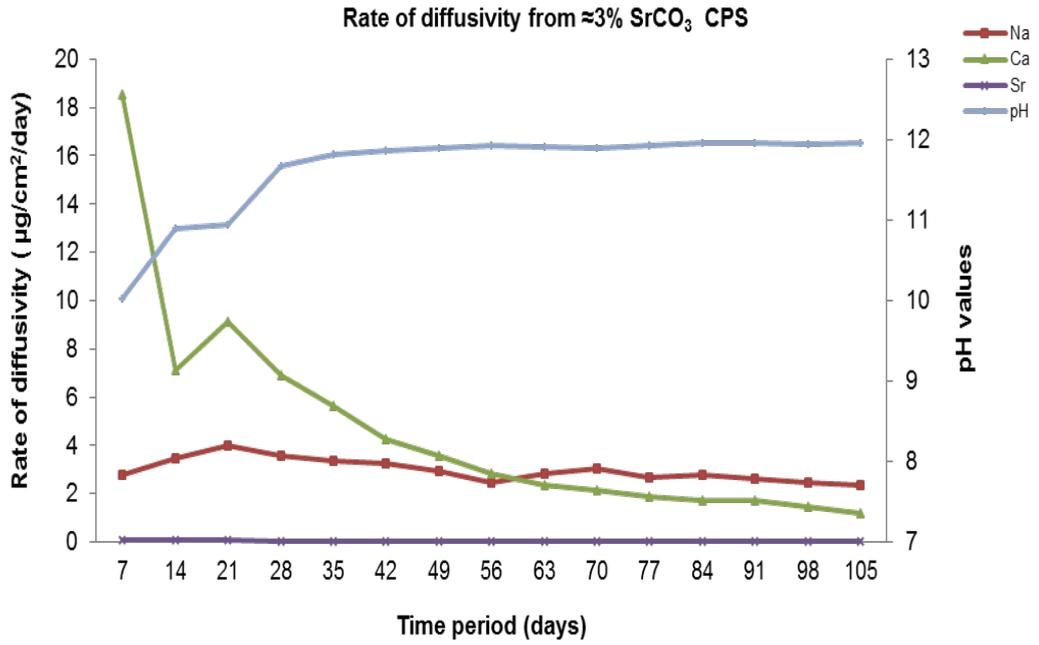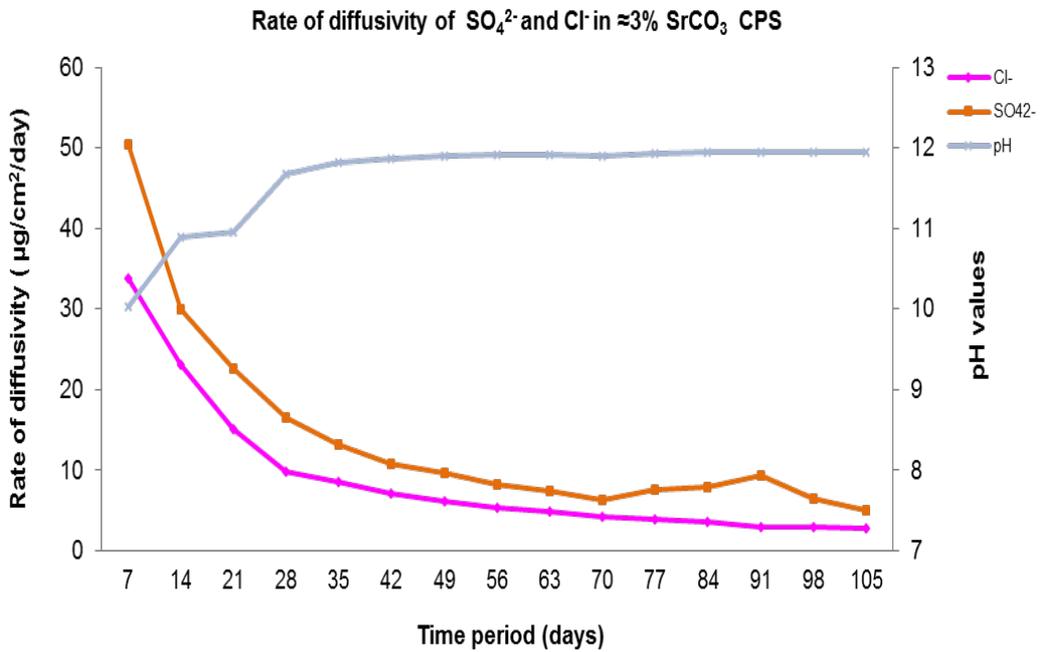
Figure 6.8 Rate of diffusivity of cations (a) anions (b) from ≈3% SrCO₃ BFS:OPC CPS in DSPW

185
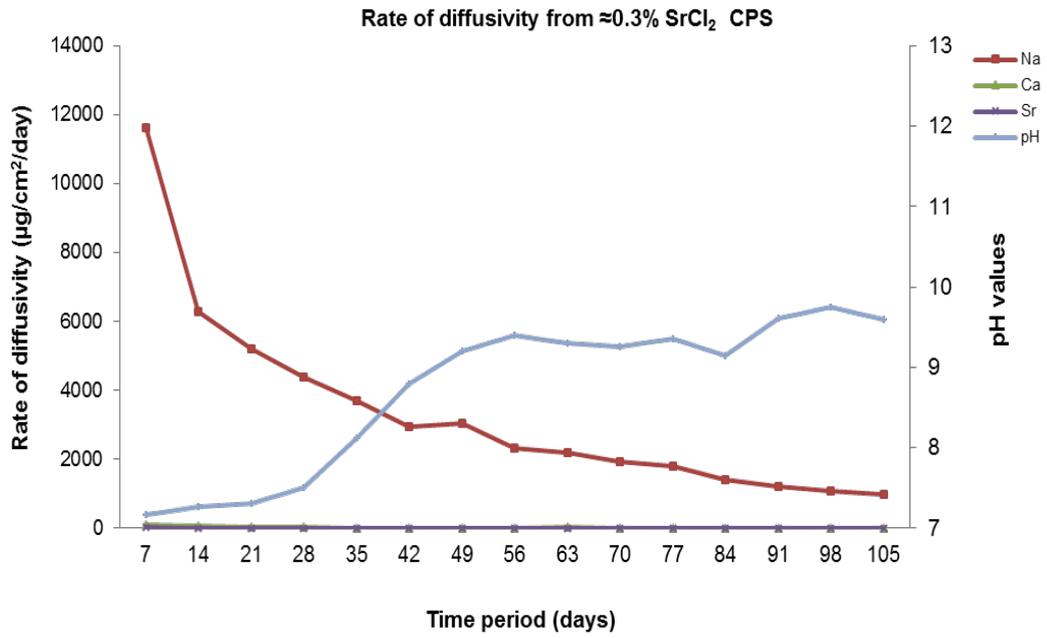
(a)
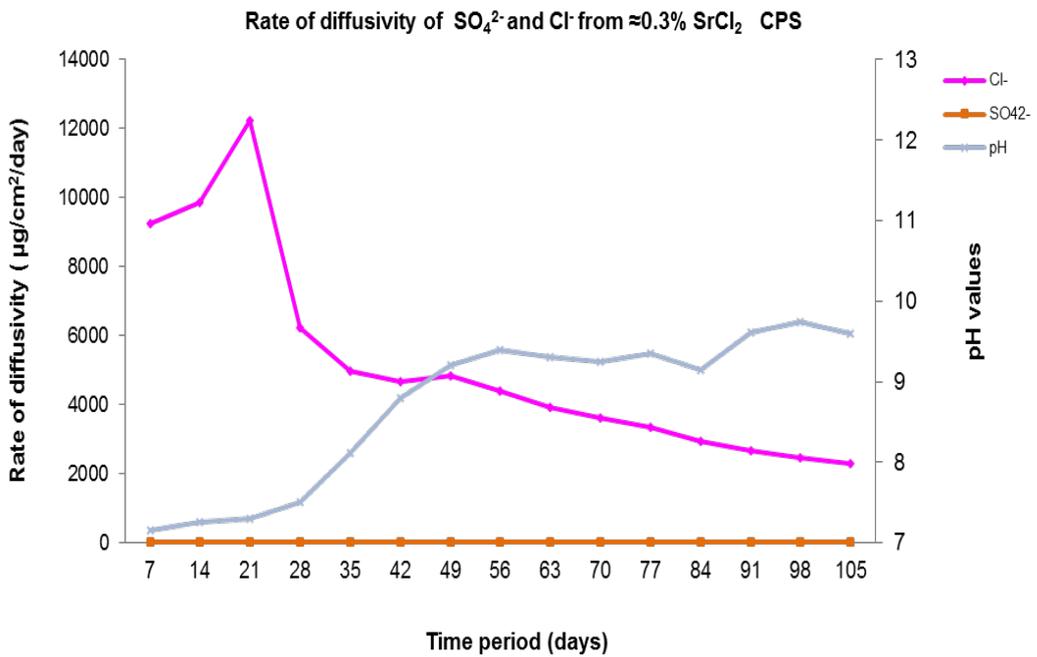
(b)

Figure 6.9 Rate of diffusivity of cations (a) anions (b) from ≈0.3% SrCl$_2$ BFS:OPC CPS in CSPW
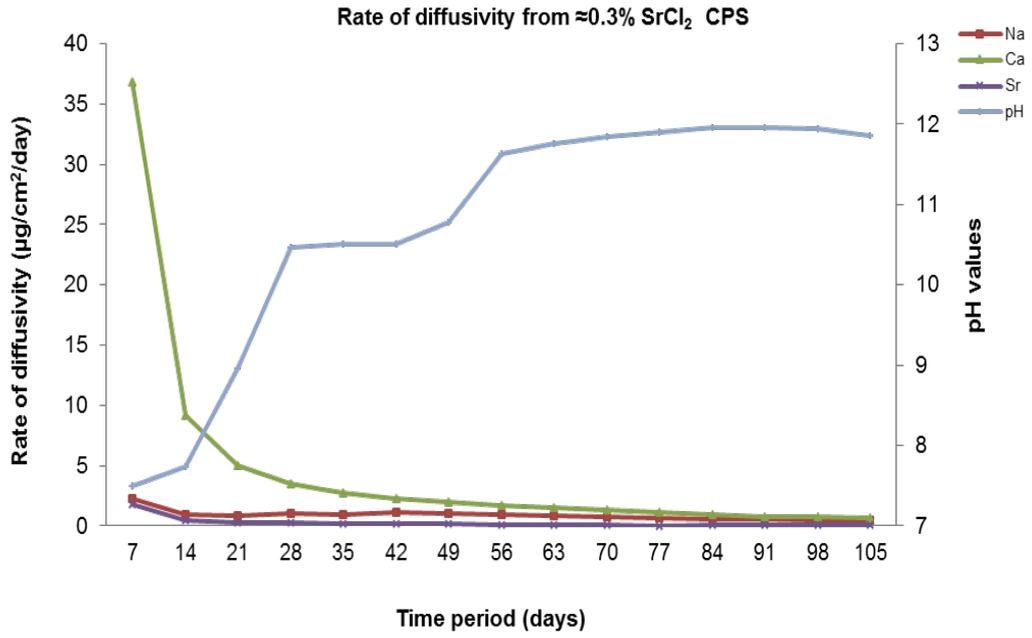
(a)
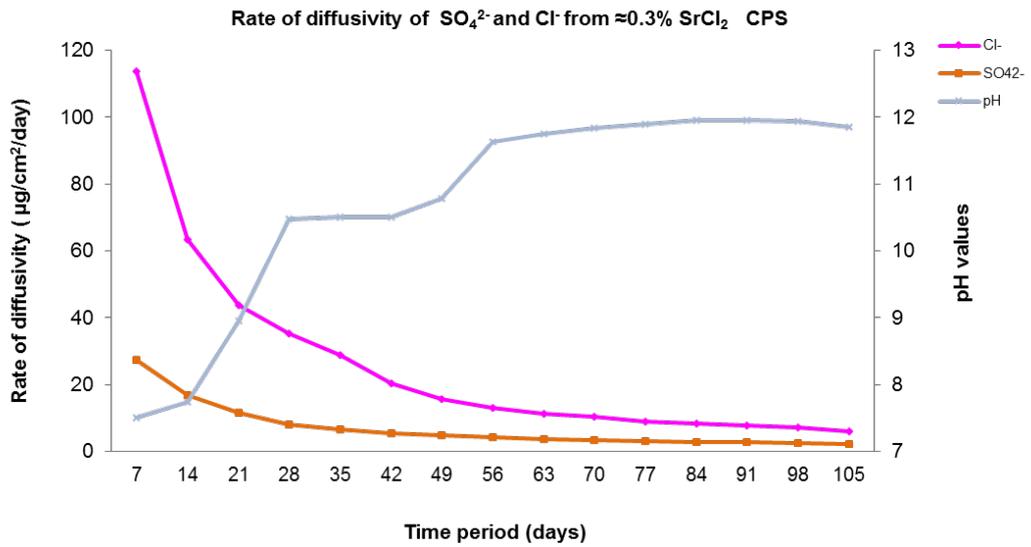
(b)

Figure 6.10 Rate of diffusivity of cations (a) anions (b) from ≈0.3% SrCl$_2$ BFS:OPC CPS in DSPW
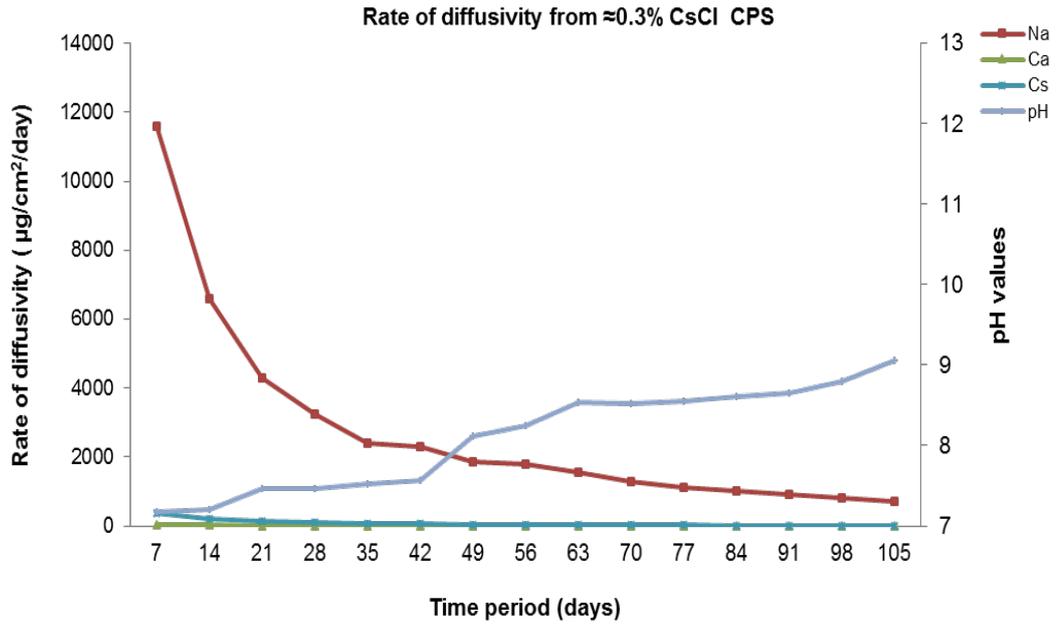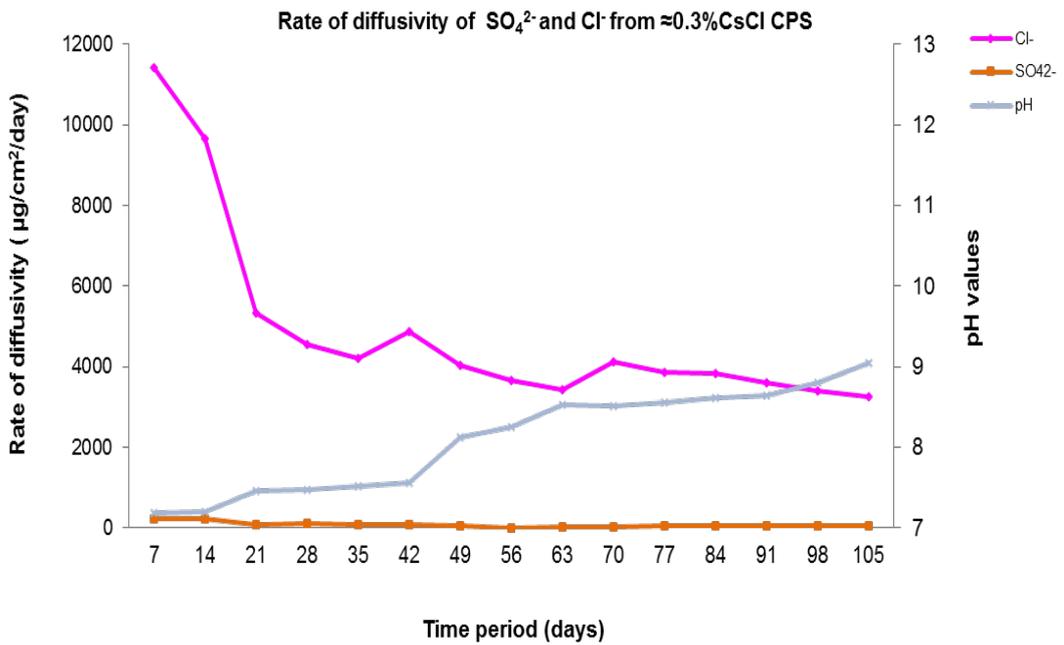
Figure 6.11 Rate of diffusivity of cations (a) anions (b) from ≈0.3% CsCl BFS:OPC CPS in CSPW
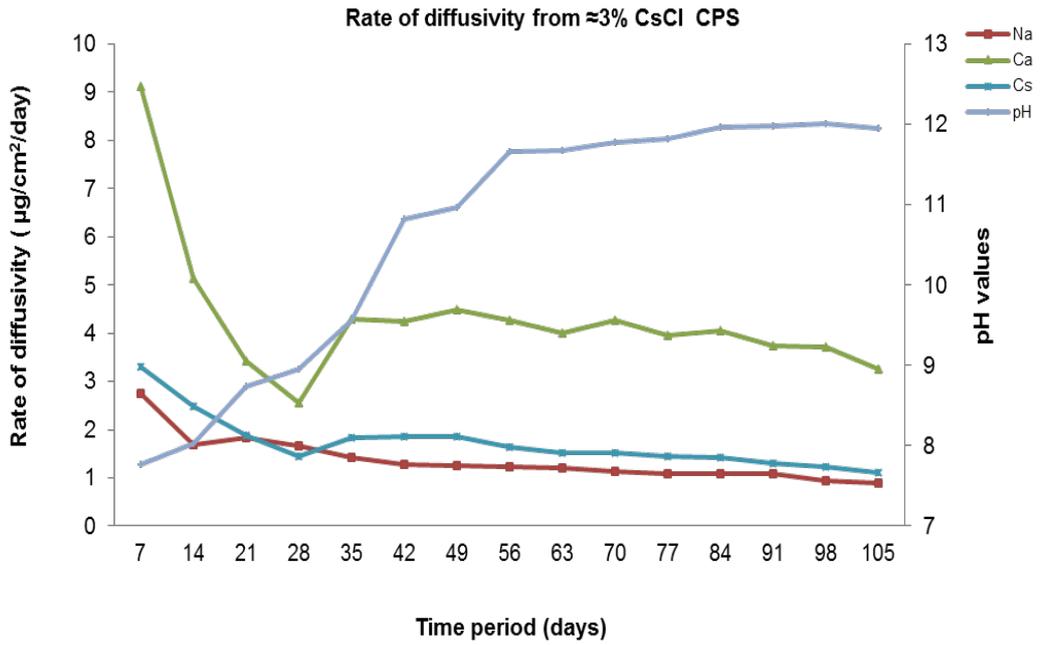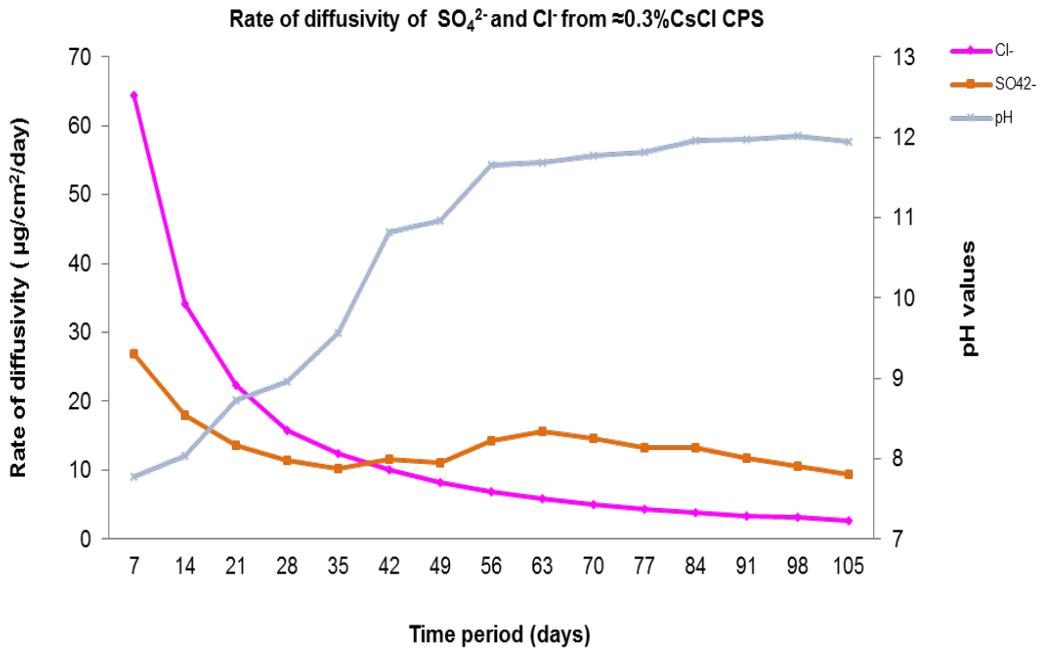
Figure 6.12 Rate of diffusivity of cations (a) anions (b) from ≈0.3% CsCl BFS:OPC CPS in DSPW
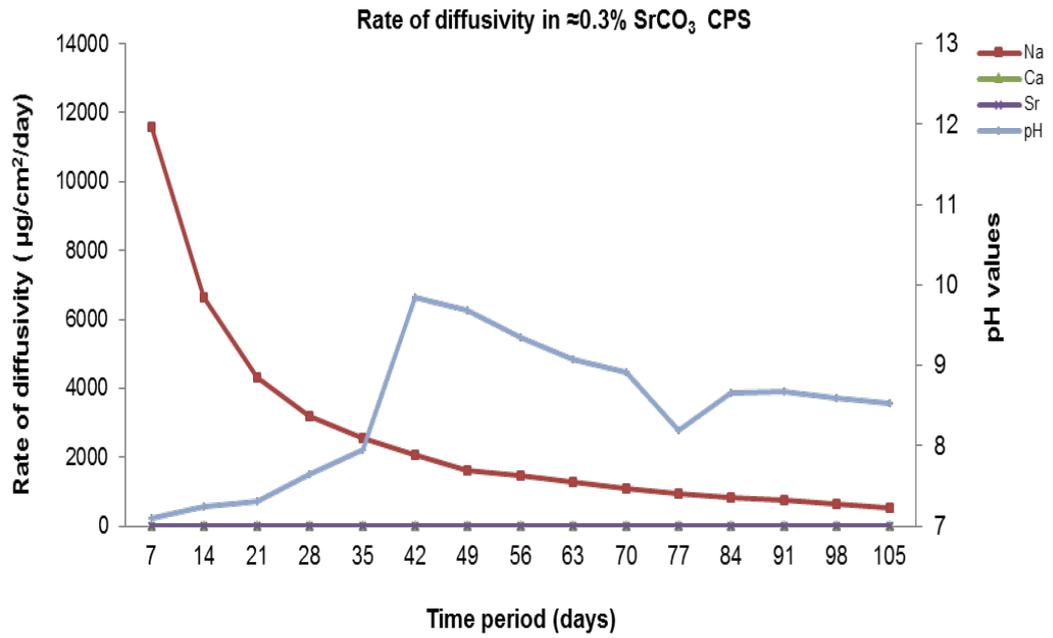
(a)
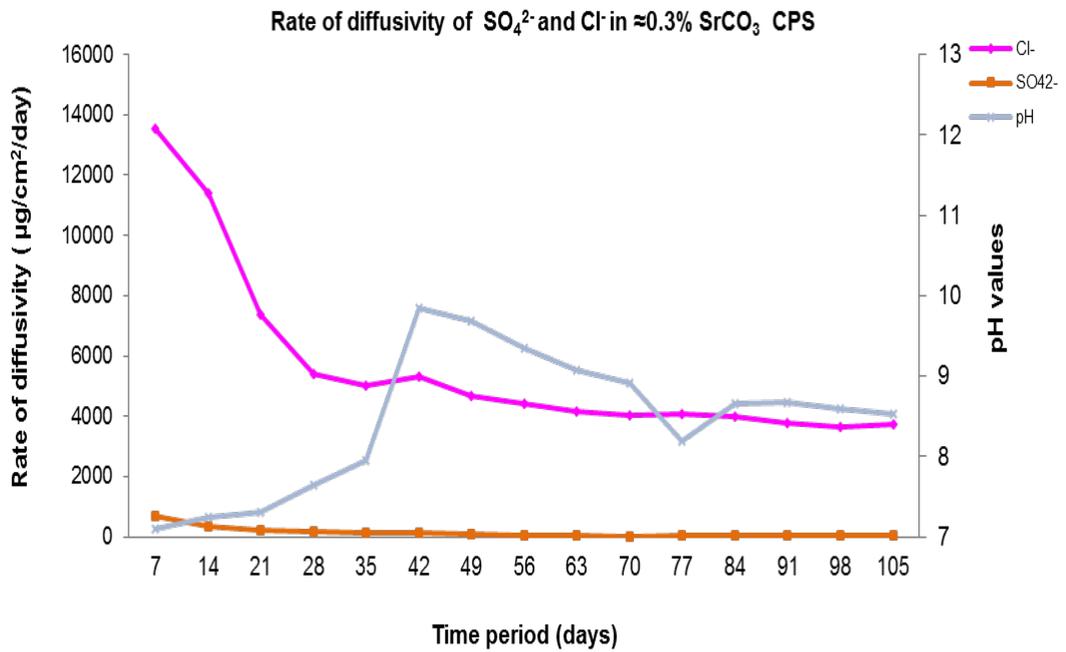
(b)

Figure 6.13 Rate of diffusivity of cations (a) anions (b) from ≈0.3% SrCO3 BFS:OPC CPS in CSPW

(a)

(b)

191
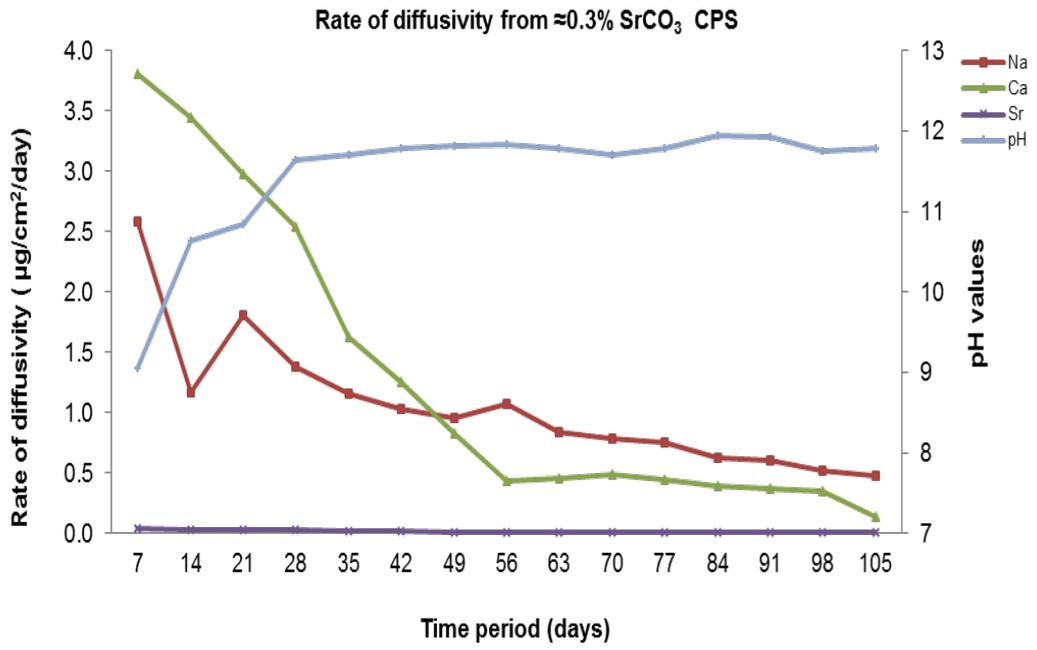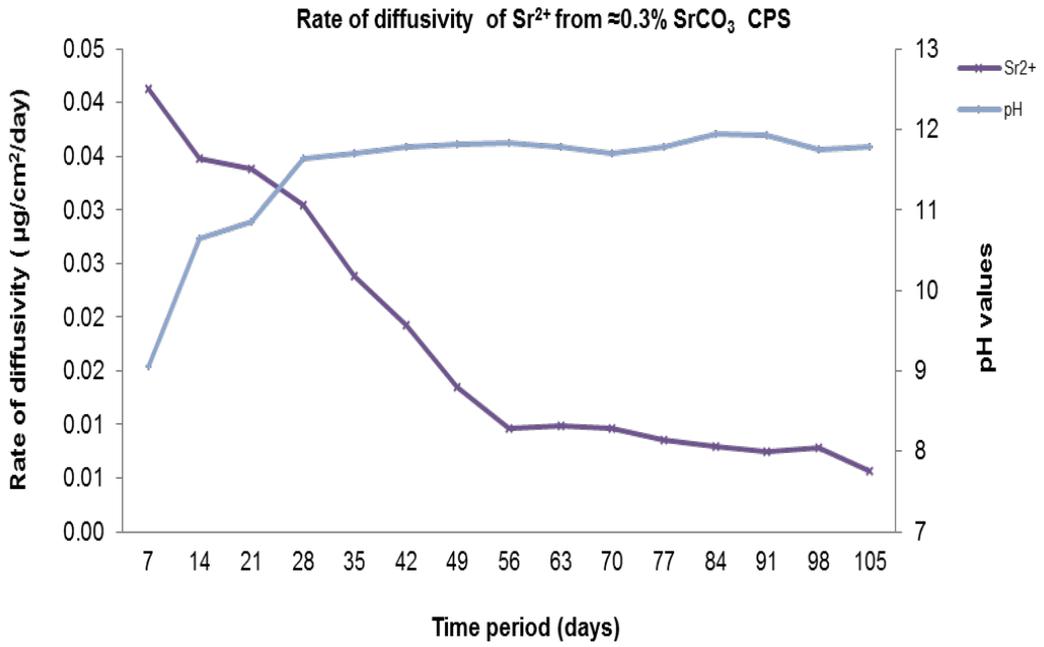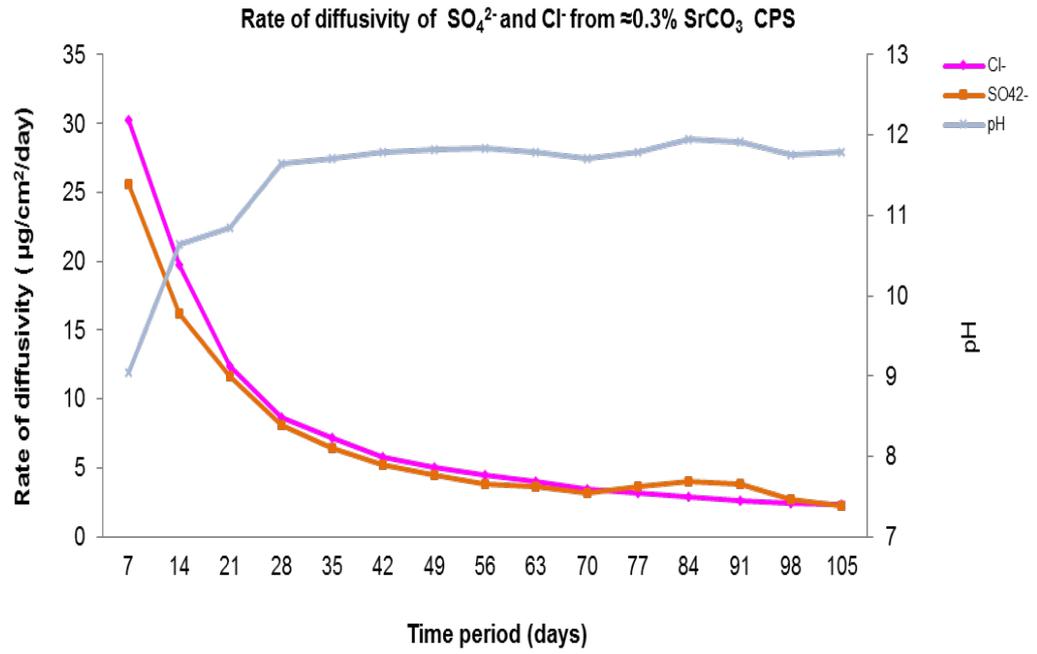
Figure 6.14 Rate of diffusivity of cations (a) anions (b) and Sr²⁺ (c) from ≈0.3% SrCO₃ BFS:OPC CPS in DSPW

Chapter 7:   **Diffusivity from PFA: OPC CPSs with Sellafield pore water as a test solution**

7.1 Aims of study

To evaluate the influence of simulated ground water, nature of cations and their concentration on the diffusivity of cations when encapsulated in PFA: OPC.

7.2 Introduction

This chapter addresses diffusivity experiments involving PFA: OPC CPSs with simulated ground water to compare the rates of diffusivity with that of BFS: OPC ground water diffusivity data (chapter 6). The diffusivity studies with concentrated Sellafield pore water (CSPW) (composition reported in Table 6.2) were carried out on PFA: OPC CPSs that had been cured for 90 days. The experimental setup consisted of four sets of closed circuit diffusivity experiments with PFA:OPC CPSs with different cation characteristics (Table 7.1). Diffusivity studies on PFA CPS with DSPW were not carried out because of time constraints and DSPW diffusivity from BFS: OPC was closer to the diffusivity of DW BFS: OPC diffusivity.

The DSPW diffusivity of BFS: OPC was measured to be in similar range of diffusivity rate as measured in DW BFS: OPC experiments. It is more than likely that the similar diffusivity pattern with DSPW and DW will take place even in PFA: OPC CPSs.

7.3 Cement paste samples

The diffusivity experiments were carried out on 4 different CPSs using CSPW.

Table 7.1 PFA: OPC cement paste samples and test solutions used

Experiment	PFA:OPC cement paste samples		Test solution
1	(a)	Control	Concentrated
	(b)	≈3% $SrCl_2$	Sellafield pore water
	(c)	≈3% CsCl	(CSPW)
	(f)	≈3% $SrCO_3$	

7.4 Results

The duration of the dynamic diffusivity experiments (closed system) was 35 days. The rates of diffusivity values of each CPS are given in Appendix 7.1 to 7.4.

7.4.1 Micropore and surface area analysis of cement paste sample

The average micropore areas of the PFA: OPC CPSs used in this experiment were in the similar range $3 - 3.9$ m^2/g (Table 7.2). There was no significant difference observed in the micropore area of the PFA: OPC CPSs. The average surface area of all the CPSs used in this experiment, were in the range of $21.7 - 40.6$ m^2/g. However, only the average surface area ≈ 3% $SrCl_2$ was found to be the highest of all the samples.

Table 7.2 Average micropore and surface area of PFA: OPC cement paste samples measured by BET method

CPS	Micropore area	Surface area
	m^2/g	
Control	3.9	22.7
≈3% SrCl$_2$	3.0	40.6
≈3% CsCl	3.6	27.4
≈3% SrCO$_3$	3.7	23.8
≈0.3% SrCl$_2$	3.7	22.2
≈0.3% CsCl$_2$	3.2	21.7

7.4.2 Test solution analysis

7.4.2.1 pH values

The pH values of the CSPW test solution increased from 6.8 (natural pH of CSPW) to 7.41 -11.35 after few days of the diffusivity experiments. The lowest values were recorded in the test solution of ≈3% SrCl$_2$ (7.41-7.54) (Figure 7.2) which were fairly close to the pH values measured in the CSPW from control CPS until day 28 (7.69-7.80) (Figure 7.1) and increased thereafter to day 35 (9.10). Highest pH values were recorded in CSPW from ≈3% CsCl and ≈3% SrCO$_3$ (8.14-11.35). In both the CSPW test solutions from ≈3% CsCl and ≈3% SrCO$_3$; pH values showed a gradual increase in pH from day 14 to day 35. (Figure 7.3 to 7.4)

7.4.2.2 Chemical analysis of test solution

The rates of diffusivity of the cations and anions are presented in Figure 7.2 to 7.4. All the diffusivity data have been normalised for dilution effect and cation/anion composition of CSPW. The average rate of diffusivity data at 35 days from CSPW BFS: OPC experiment have been utilised for comparative purpose.

7.4.2.2.1 *Strontium*

The average rate of diffusivity of Sr^{2+} in CSPW from $\approx$3% $SrCl_2$ (35 $\mu g/cm^2/day$) was 24 times higher than $\approx$3% $SrCO_3$ (1.5 $\mu g/cm^2/day$). However, the average rate of diffusivity from Sr^{2+} contaminated BFS: OPC CPS ($\approx$3% $SrCl_2$=53, $\approx$3% $SrCO_3$= 3 $\mu g/cm^2/day$) was $\approx$ 2 times higher than PFA: OPC CPS at fairly similar pH range in case of $\approx$3% $SrCl_2$. Comparing the results from DW with CSPW PFA: OPC diffusivity experiments; the average rate of diffusivity of Sr^{2+} from $\approx$3% $SrCl_2$ (171 $\mu g/cm^2/day$) was measured 5 times higher than the average rate of diffusivity of Sr^{2+} from $\approx$3% $SrCl_2$ (35 $\mu g/cm^2/day$) respectively. However, the pH range of DW was higher (7.47 – 8.69) in comparison with CPSW (7.41 – 7.54).

7.4.2.2.2 *Caesium*

Caesium diffusivity rate from PFA: OPC $\approx$3% CsCl CPS in CSPW was slower in comparison with BFS: OPC $\approx$3% CsCl CPS. The average rate of diffusivity of Cs^+ from BFS: OPC $\approx$3% CsCl CPS (1811 $\mu g/cm^2/day$) was 3.5 times higher than the average rate of diffusivity of Cs^+ from PFA: OPC $\approx$3% CsCl (516 $\mu g/cm^2/day$). However, the pH of CPSW from BFS: OPC $\approx$3% CsCl CPS was measured in the rage of 7.66 -8.59 compared to PFA: OPC CPS $\approx$3% CsCl which was in the range of 8.14 – 10.56. There was no significant difference observed in the rate of diffusivity between CSPW and DW diffusivity experiments ($p>0.05$).

7.4.2.2.3 *Calcium*

Calcium from $\approx$3% $SrCl_2$ diffused out at faster rate compared to the other CPS in CSPW. The sequence of diffusivity of Ca^{2+} observed in CSPW was $\approx$3% $SrCl_2$ >

≈3% CsCl > ≈3% $SrCO_3$ > control. The average rate of diffusivity of Ca^{2+} from ≈3% $SrCl_2$ (116 µg/cm^2/day) at pH (7.41-7.54), was ≈8 times higher than the average rate of diffusivity of Ca^{2+} from control (14 µg/cm^2/day) at pH (7.69 -9.10). However, there was no significant difference in the diffusivity of Ca^{2+} from ≈3% CsCl and ≈3% $SrCO_3$ and control CPS (p>0.05). Comparing the results of BFS: OPC with PFA: OPC in CSPW, the rate of diffusivity of Ca^{2+} from PFA: OPC CPSs was considerably lower than the rate of diffusivity of Ca^{2+} from BFS: OPC CPSs. This is due to the difference in Ca^{2+} content of BFS:OPC and PFA:OPC CPS. However, faster diffusivity of Ca^{2+} was also observed from ≈3% $SrCl_2$ in CSPW from BFS: OPC and in DW from PFA: OPC CPSs.

7.4.2.2.4 *Sodium*

The diffusivity of Na^+ in CSPW from all the PFA: OPC CPSs did not show any significant difference. Sodium diffused out at fairly similar rate. This is due to higher concentration of Na^+ in CSPW test solution compared to maximum quantity of Na^+ could diffuse out as explained in previous chapter 6. However, the average rate of diffusivity of Na^+ from all the PFA: OPC CPSs was considerably lower than BFS: OPC CPSs.

7.4.2.2.5 *Chloride*

The rate of diffusivity of Cl^- from all PFA: OPC CPSs in CSPW were in a fairly similar range (8729- 12431 µg/cm^2/day). Similar observations were noted in the case of CSPW BFS: OPC CPS experiments (4007- 6166 µg/cm^2/day). This is due to similar reason as sodium in test solution.

7.4.2.2.6 *Sulphate*

The rate of diffusivity of SO_4^{2-} from ≈3% CsCl and ≈3% $SrCO_3$ was similar (p>0.05) and higher compared to the rate of diffusivity of SO_4^{2-} from control and ≈3% $SrCl_2$. The average rate of diffusivity of ≈3% $SrCl_2$ (21 $\mu g/cm^2/day$) was 3-7 times lower than all the CPSs (56 - 140 $\mu g/cm^2/day$) in CSPW. Similar sequence of diffusivity was observed in DW PFA: OPC diffusivity experiment. The average rate of diffusivity of SO_4^{2-} from ≈3% $SrCl_2$ (17 $\mu g/cm^2/day$) was 2.5 times lower than all the CPSs (39-45 $\mu g/cm^2/day$) in DW experiment. Contrary to PFA: OPC CSPW diffusivity, the average rate of diffusivity of BFS: OPC ≈3% $SrCO_3$ (16 $\mu g/cm^2/day$) was 6-8 time lower than all the CPSs (99-129 $\mu g/cm^2/day$) in CSPW experiments. A notable lower range of pH values (7.41 – 8.69) was observed in the test solutions with lowest diffusivity of SO_4^{2-} compared to all the test solutions which were measured to be on higher side.

7.5 Conclusions

1. In general the pH values were lower primarily due to the ionic strength of the make-up water hindering diffusion of calcium ions, concentration of calcium of the cement paste but again with both pore water and hydrate composition changing with time, pH values were influenced accordingly.

2. Strontium diffusivity was dependent on the cation concentration of the make-up water and the nature of the salt used. The composition of the cement paste had a slight impact with BFS:OPC CPS favouring a more rapid diffusion. Similar trends were observed for caesium paste samples.

3. Calcium concentration and the surrogate behaviour of strontium influenced its leachability.

4. Sodium diffusivity was relatively similar for most experimental conditions.

5. Chloride concentration of the CSPW overshadowed any real effect of added chloride as cation salt and/or the inert chloride in the CPSs.

6. The formation of sparing soluble sulphate salts affected sulphate diffusion.
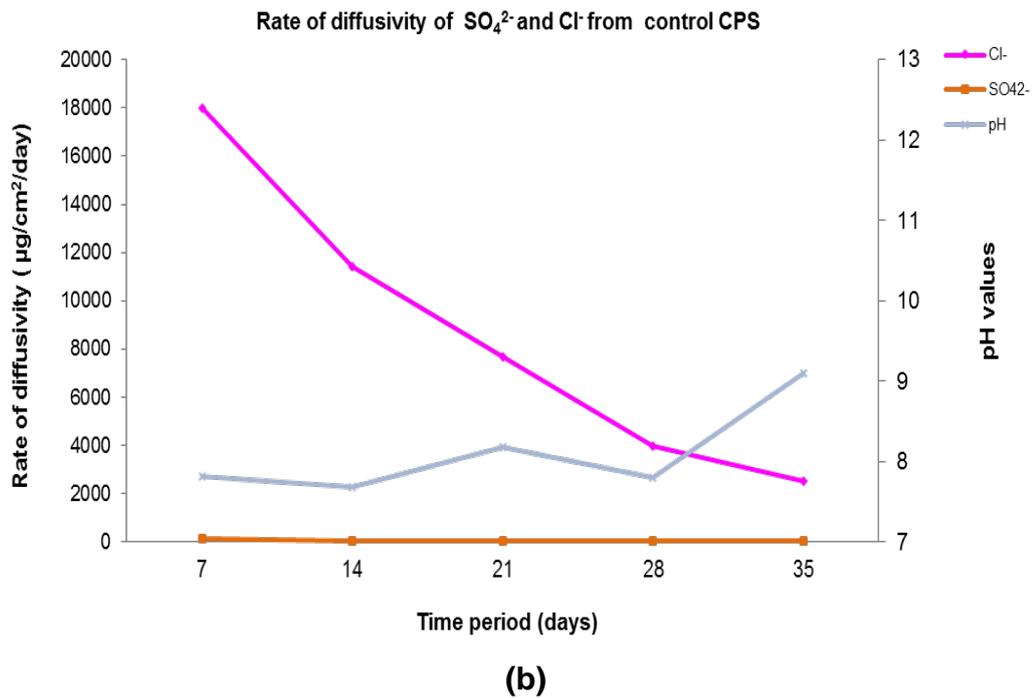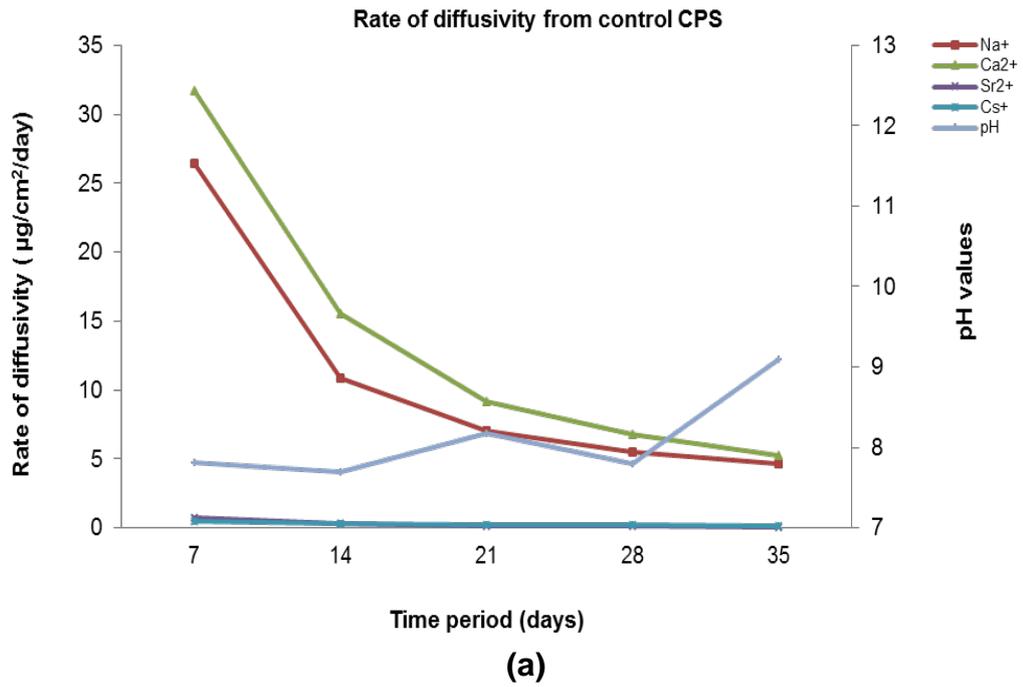
Figure 7.1 Rate of diffusivity of cations (a) and anions (b) from control PFA: OPC CPS in CSPW
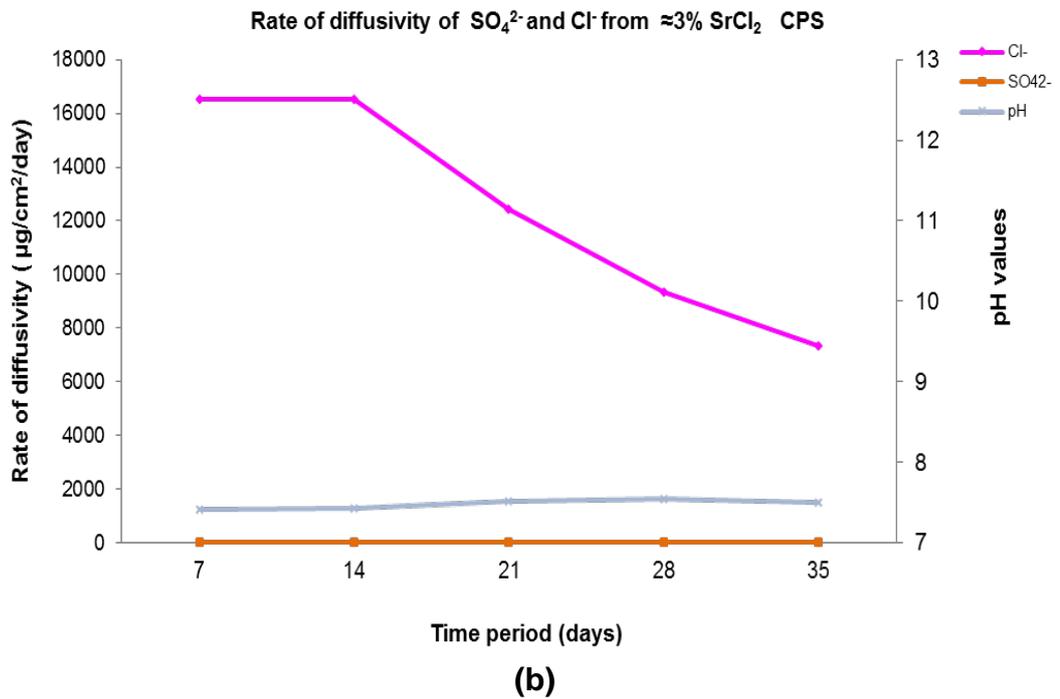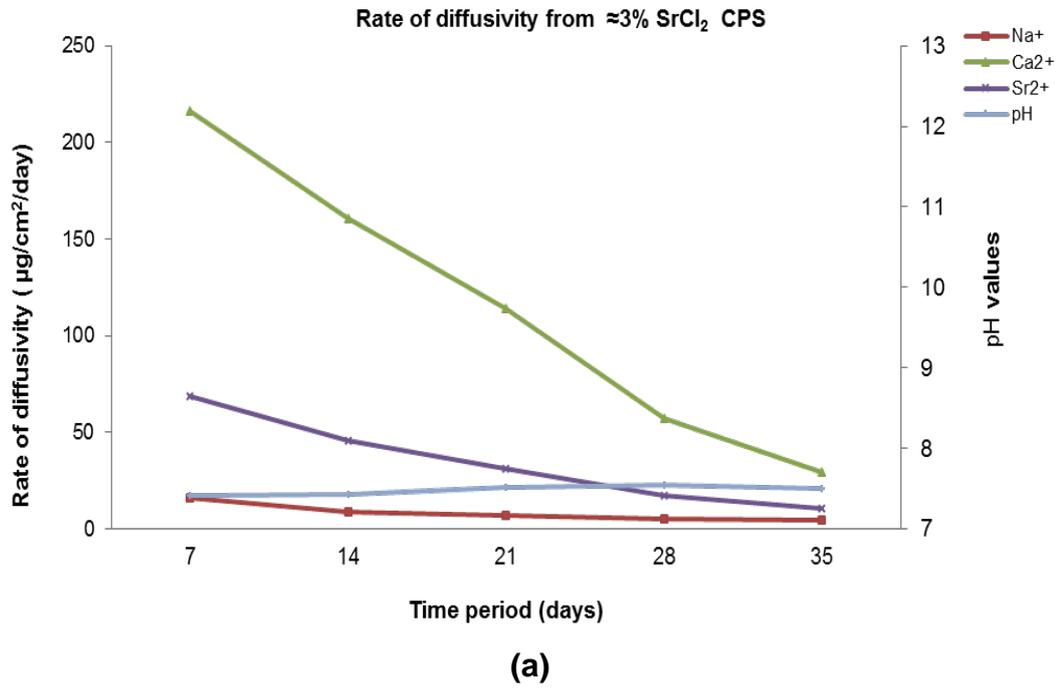
Figure 7.2 Rate of diffusivity of cations (a) and anions (b) from ≈3% SrCl$_2$ PFA: OPC CPS in CSPW

(a)

(b)
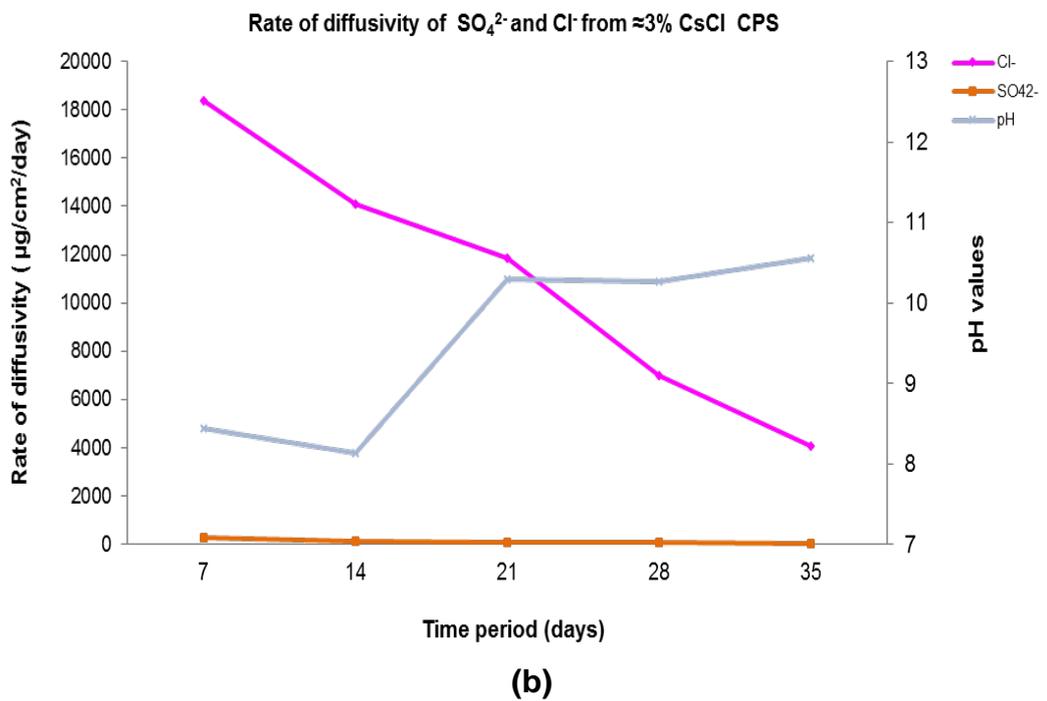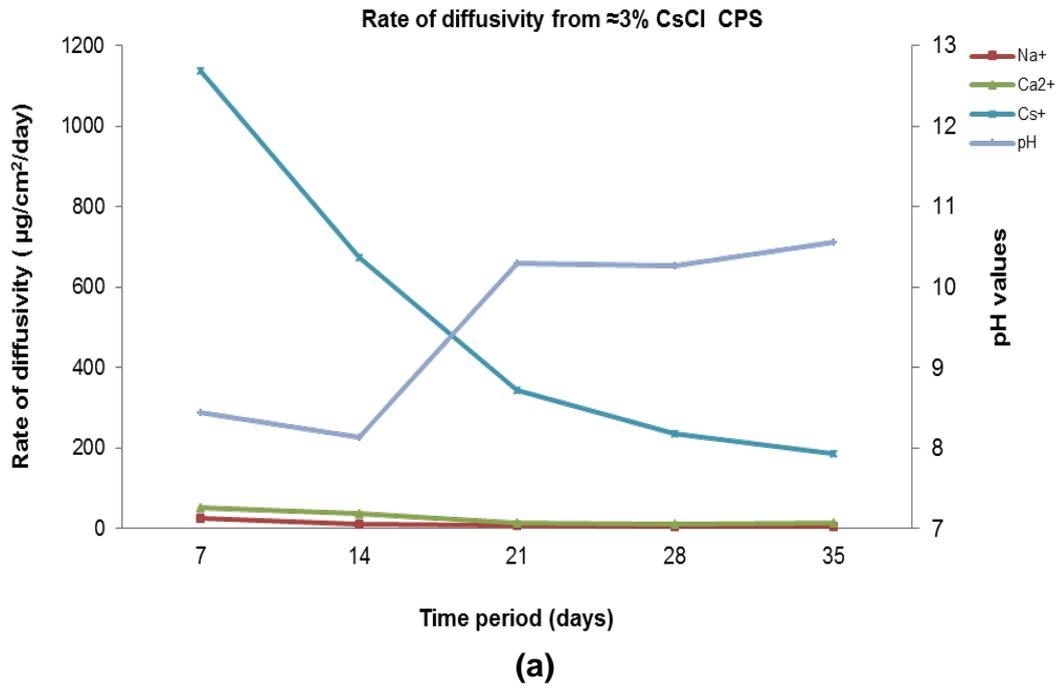
Figure 7.3 Rate of diffusivity of cations (a) and anions (b) from ≈3% CsCl PFA: OPC CPS in CSPW

202

(a)
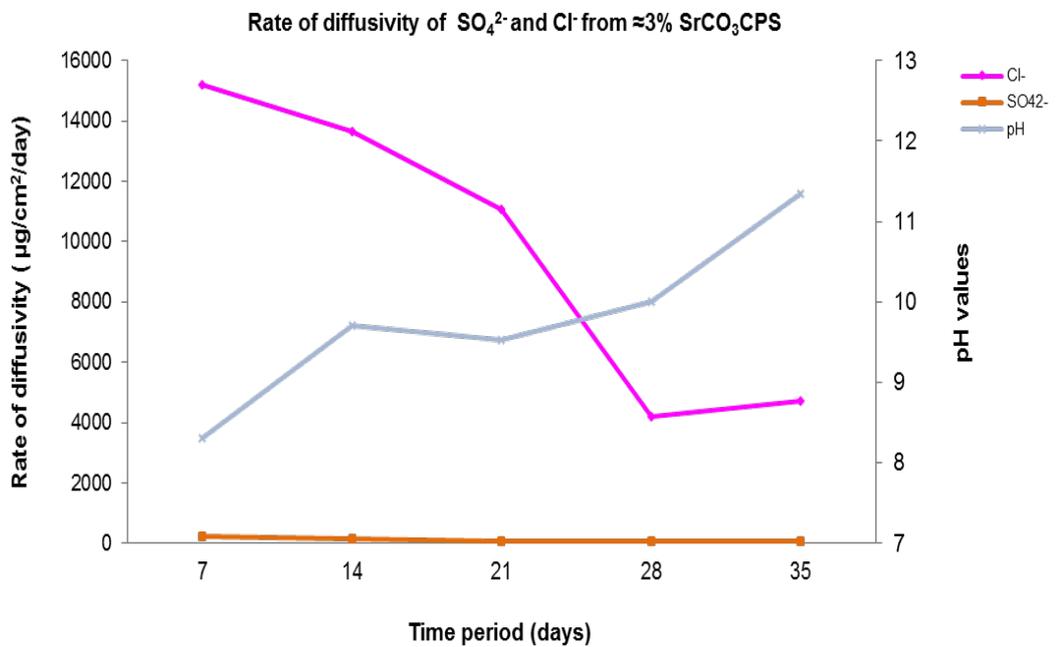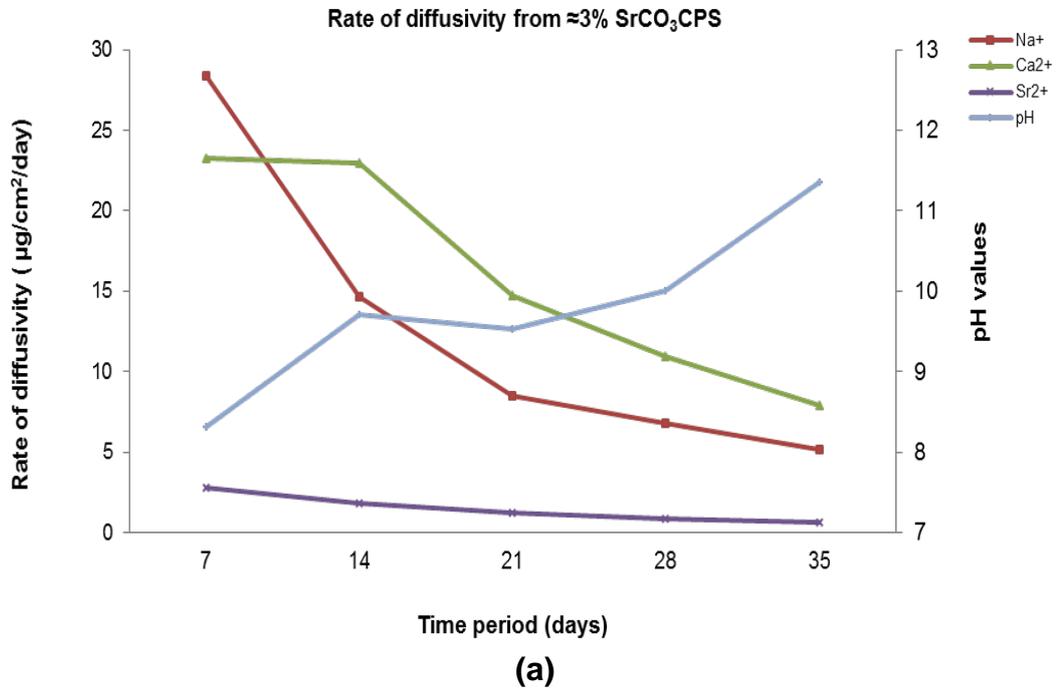
Figure 7.4 Rate of diffusivity of cations (a) and anions (b) from ≈3% SrCO₃ PFA: OPC CPS in CSPW

Chapter 8: Diffusivity from BFS:OPC CPSs with John Innes soil solution as a test solution

8.1   Aims of study

To evaluate the influence of microorganisms present in the John Innes soil solution (JISS) on diffusivity of cations when encapsulated in BFS: OPC and to compare the data from other diffusivity experiments.

8.2   Introduction

The present study investigated microbial influenced diffusivity of encapsulated simulated waste when replicating conditions pertinent to GDF under aerobic condition. The stability of the cementitious waste was assessed by subjecting the encapsulated cement paste samples in closed circuit diffusivity experiments using a test solution (JISS) containing microorganisms extracted from John Innes No 3 soil. The JISS was prepared according to the protocol mentioned in section 2.5. John Innes compost is a set of four formulae for growing medium, developed at the former John Innes Horticultural Institution (JIHI) in the 1930s. The formulae contain loam, peat, sand or grit, and fertiliser in varying ratios for specific purposes. John Innes Potting Compost No.3 is a richer mixture for final re-potting of gross feeding vegetable plants and for mature foliage plants and shrubs in interior planters or outdoor containers [124]. It was selected on the advice of Prof G Morton, Principal Microbiologist (UCLan) [211] as this soil formula would provide a typical microbial population that could reside in the vicinity of a GDF site in the UK. It was also sufficiently rich in nutrients to sustain growth of microorganisms in the JISS extract.

8.3   Cement paste samples

Diffusivity experiments were carried out on 4 different BFS:OPC CPSs, details of which are mentioned in Table 8.1

Table 8.1 BFS:OPC cement paste samples and test solution used

Experiment	BFS:OPC CPS		Test solution
	(a)	Control	John Innes soil
1	(b)	≈3% $SrCl_2$	solution (JISS)
	(c)	≈3% CsCl	
	(f)	≈3% $SrCO_3$	

8.4 Results and discussion

The duration of dynamic diffusivity experiments (closed system) was 49 days. The rate of diffusivity values of each cement paste sample are given in appendix 8.1 to 8.4.

8.5 Micropore and surface area analysis of CPS measured by BET method

The average micropore and surface area results of the cement paste samples are shown in Table 8.2. The average values (top, middle and bottom) of micropore area of the CPSs prior to the JISS diffusivity experiments were in the range of 1.3 – 5.4 m^2/g. The highest micropore area was measured with ≈3% $SrCl_2$ CPS. There was no significant difference in the micropore area of control and ≈3% $SrCO_3$. The cement paste sample containing ≈3% CsCl had the lowest micro-pore area.

The average values (top, middle and bottom) of surface area of the CPSs were in the range of 11.6 – 24.2 m^2/g. The surface area of ≈3% $SrCl_2$, control and ≈3% $SrCO_3$ CPS were in fairly similar range (21.2 – 24.2 m^2/g). However, the average surface area of ≈3% CsCl (11.6 m^2/g) CPS was found to be lowest of all the CPSs.

Table 8.2 *Average micropore and surface area of cement paste samples measured by BET method*

CPS	Micropore area	Surface area
	(m^2/g)	
Control	2.7	24.2
≈ 3% SrCl$_2$	5.4	22.8
≈ 3% CsCl	1.3	11.6
≈ 3% SrCO$_3$	2.7	21.2

8.5.1 Test solution analysis

8.5.1.1 pH values

The pH values of JISS from control CPS after first few days of diffusivity increased from 7.21 (natural pH value of JISS) to 10.73 – 11.2. (Figure 8.1). However, the pH values of JISS from contaminated CPSs (≈ 3% SrCl$_2$, ≈3% CsCl, and ≈ 3% SrCO$_3$) were measured in the range of 6.77 – 8.09 (Figure 8.2 to 8.4). The lowest pH value (6.77) was measured in JISS from ≈3% CsCl on day 14.

8.5.1.2 Chemical analysis of test solutions

All the diffusivity data have been normalised for dilution effect and cation/anion composition of JISS (Table 8.3). The diffusivity data of first 49 days from BFS:OPC DW experiment have been utilised to validate the effect of JISS on rates of diffusivity. The rates of diffusivity of cations and anions are presented in Figure 8.1 to 8.4.

Table 8.3 Analysis of JISS

Sample	Concentration in ppb							pH
	Na$^+$	Mg^{2+}	K$^+$	Ca^{2+}	Fe^{3+}	Cl$^-$	SO$_4^{2-}$	
JISS	1541	1009	3576	29	442	62	8588	7.21

8.5.1.2.1 *Strontium*

The average rate of diffusivity of Sr^{2+} (19 $\mu g/cm^2/day$) in JISS from $\approx$ 3% $SrCl_2$ at pH 7.29 – 8.09 was $\approx$2 times lower than the average rate of diffusivity of Sr^{2+} (35 $\mu g/cm^2/day$) in DW from $\approx$ 3% $SrCl_2$ at pH 11.19 – 12.03 However, the effect of JISS was more pronounced in $\approx$ 3% $SrCO_3$. There was a $\approx$16 fold increase in the average rate of diffusivity of Sr^{2+} from $\approx$ 3% $SrCO_3$ in JISS (0.82 $\mu g/cm^2/day$) at pH 7.53 – 7.93 in comparison with DW (0.052 $\mu g/cm^2/day$) ay pH 11.57 – 12.27.

8.5.1.2.2 *Caesium*

The effect of JISS on the diffusivity of added cation was more prominent in case of $\approx$3% CsCl in comparison with $\approx$ 3% $SrCl_2$ CPS. The average rate of diffusivity of Cs^+ in JISS (191 $\mu g/cm^2/day$) was $\approx$ 4.7 times higher than the average rate of diffusivity in DW (41 $\mu g/cm^2/day$). However, the pH range of JISS from $\approx$3% CsCl was lower (6.77 – 7.8) compared to DW from $\approx$3% CsCl CPS (10.4 – 11.57).

8.5.1.2.3 *Calcium*

Calcium from $\approx$ 3% $SrCl_2$ CPS diffused out at faster rate compared to all the other CPSs. The average rate of diffusivity of Ca^{2+} from $\approx$ 3% $SrCO_3$ (18 $\mu g/cm^2/day$) was 3 times lower than the average rate of diffusivity of Ca^{2+} from $\approx$ 3% $SrCl_2$ (60 $\mu g/cm^2/day$). The lowest diffusivity of Ca^{2+} was measured in control CPS. It is interesting to note that the pH values in JISS from control CPS were higher (10.73 – 11.2) in comparison with JISS from contaminated CPSs (6.77 – 8.09). Comparing the results from DW BFS:OPC with JISS BFS:OPC diffusivity experiments; the average rate of diffusivity of Ca^{2+} from $\approx$3% CsCl (0.99 $\mu g/cm^2/day$) at pH (11.19 – 12.03) was measured 32 times lower than the average rate of diffusivity of Ca^{2+} from $\approx$3% CsCl (32 $\mu g/cm^2/day$) at pH (6.77 –

7.87) respectively. Similarly, the average rate of diffusivity of Ca^{2+} from $\approx 3\%$ $SrCO_3$ (1.26 µg/cm^2/day) was measured 14.5 times lower than the average rate of diffusivity of Ca^{2+} from $\approx 3\%$ CsCl (18.3 µg/cm^2/day) respectively. However, the difference was less prominent in case of $\approx 3\%$ $SrCl_2$, and control CPS.

8.5.1.2.4 *Sodium*

Sodium from $\approx 3\%$ $SrCl_2$ CPS diffused out at highest rate compared to all the other CPSs in JISS diffusivity experiment. The sequence of diffusivity shown by sodium was $\approx 3\%$ $SrCl_2$ > $\approx 3\%$ CsCl > $\approx 3\%$ $SrCO_3$ > control. There was no significant difference ($p > 0.05$) observed in the rate of diffusivity of Na^+ between control and $\approx 3\%$ $SrCO_3$ CPS; however, the pH range of JISS from control was higher (10.73 – 11.2) compared to $\approx 3\%$ $SrCO_3$ (7.53 – 7.93). The average rate of diffusivity of Na^+ from $\approx 3\%$ CsCl (9.9 µg/cm^2/day) in JISS was ≈ 4 times higher than the average rate of diffusivity of Na^+ from $\approx 3\%$ CsCl (2.8 µg/cm^2/day) in DW. However there was no significance difference in the rate of diffusivity of Na^+ between JISS and DW from $\approx 3\%$ $SrCl_2$ ($p > 0.05$), $\approx 3\%$ $SrCO_3$ ($p > 0.05$) and control ($p > 0.05$).

8.5.1.2.5 *Chloride*

The highest rate of diffusivity was measured from $\approx 3\%$ $SrCl_2$ CPS, followed by $\approx 3\%$ CsCl, $\approx 3\%$ $SrCO_3$ and control. The average rate of diffusivity of Cl^- from control (4.2 µg/cm^2/day) was 65 times lower than the average rate of diffusivity of Cl^- from $\approx 3\%$ $SrCl_2$ (270 µg/cm^2/day). There was no significance difference ($p > 0.05$) between the rate of diffusivity of Cl^- from $\approx 3\%$ $SrCO_3$ and control CPS. In comparison with DW diffusivity experiment, the average rate of diffusivity of Cl^- from $\approx 3\%$ $SrCl_2$, in JISS (270 µg/cm^2/day) was approximately twice as high as measured in DW (142 µg/cm^2/day). The effect of JISS on diffusivity of Cl^- was

more prominent in case of ≈3% CsCl in comparison with DW. The average rate of diffusivity of Cl$^-$ from ≈3% CsCl (206 µg/cm^2/day) in JISS was ≈ 17 times higher than the average rate of diffusivity of Cl$^-$ from ≈3% CsCl (12.4 µg/cm^2/day) in DW. However, Cl$^-$ from ≈3% SrCO$_3$ (5 µg/cm^2/day) and control (4.17 µg/cm^2/day) diffused out two times lower in JISS than in DW (9.5 and 8, respectively).

8.5.1.2.6   *Sulphate*

The sequence of diffusivity of SO$_4^{2-}$ shown in JISS was ≈3% SrCO$_3$ > ≈3% CsCl > control > ≈3% SrCl$_2$.   Sulphate from ≈3% SrCO$_3$ diffused out at highest rate compared to all the other CPS in JISS diffusivity experiment. The average rate of diffusivity of SO$_4^{2-}$ from ≈3% SrCO$_3$ (112 µg/cm^2/day) was 6 times higher than the average rate of diffusivity of SO$_4^{2-}$ from ≈3% SrCl$_2$ (20 µg/cm^2/day). Sulphate from ≈3% CsCl (75 µg/cm^2/day) diffused out 1.5 times lower in comparison with ≈3% SrCO$_3$ (112 µg/cm^2/day). Comparing the results from DW BFS:OPC with JISS BFS:OPC diffusivity experiments; the average rate of diffusivity of SO$_4^{2-}$ from ≈3% SrCO$_3$ (6 µg/cm^2/day) was 20 times lower than the average rate of diffusivity of SO$_4^{2-}$ from ≈3% SrCO$_3$ (112 µg/cm^2/day); 13 times lower in DW (6 µg/cm^2/day) compared to JISS (75 µg/cm^2/day) from ≈3% CsCl. However, there was no significant difference in the rate of diffusivity observed between DW and JISS from ≈3% SrCl$_2$ (p>0.05) and control CPS (p>0.05).

8.5.2 Microbial community profile

All methods employed in this section were carried out as described in section 2.6 to 2.9

8.5.2.1 Total viable count of John Innes soil solution

John Innes No: 3 soil solution of different ratios of soil to water were prepared and tested to achieve the best viable microbial population for the diffusivity experiment. The spread plate method gave a bacterial count of 5×10^4 cfu/g of soil present in JISS, which was considered adequate to carry out the microbial induced diffusivity experiments [212].

8.5.2.2 Microbial analysis of test solution

The results of microbial analysis of the test solutions are shown in the Table 8.4. The total viable counts measured on final day were in the range of $3 – 4.7 \times 10^7$ cfu. The highest viable count was measured in the JISS from ≈3% $SrCl_2$ (4.7 x 10^7 cfu), followed by ≈3% CsCl (1.9 x 10^7 cfu) and ≈3% $SrCO_3$ (9.1 x 10^4 cfu) CPS. There was no significant viable population measured in the JISS from control CPS. The results of primary identification of the bacteria isolated from the test solutions of the CPS are summarised in Table 8.4. The data show that both motile and non-motile Gram positive (G+ve) bacilli bacteria were present in the JISS from ≈3% CsCl and ≈3% $SrCO_3$. However, only non-motile G+ve bacteria were present in in the JISS from ≈3% $SrCl_2$. Genus level identification of bacteria showed the presence of *Actinomyces spp* in JISS from ≈3% CsCl and *Streptomyces spp.* in JISS from ≈3% $SrCO_3$.

The Fungi isolated from JISS were identified using taxonomical keys [91], on the basis of their morphology, hyphal nature and patterns of spore formation. The presence of *Cladosporium macrocarpom* was prominent in all the circulating systems, excluding the control. There was no fungal growth observed in the JISS circulation system control sample.

Table 8.4 Summary table showing total viable count measured in JISS.

Experiment	BFS:OPC CPS		Total viable count (cfu)
1	(a)	Control	3
	(b)	≈3% $SrCl_2$	4.7×10^7
	(c)	≈3% CsCl	1.9×10^7
	(f)	≈3% $SrCO_3$	9.1×10^4

Table 8.5 Summary table showing bacteria isolated from JISS

Experiment	BFS:OPC PS		Primary identification test	
			Gram stain	**motility**
1	(a)	Control	NR*	NR*
	(b)	≈3% $SrCl_2$	G+ve	-
	(c)	≈3% CsCl	G+ve	+ -
	(f)	≈3% $SrCO_3$	G+ve	+ -

*none recorded

8.6 Conclusion

1. Make-up water salts e.g. strontium; caesium chlorides had a significant impact on the JISS test solution pH in comparison with the control cement paste sample.

2. Test solution composition (JISS extract) retard strontium diffusivity but accelerated caesium diffusion in comparison with distilled water values.

3. Although the calcium diffusivity values were affected by the added cation to the make-up water the values for strontium were marginal but more exaggerated for caesium.

4. Strontium had the greatest impact on the rate of sodium diffusion.

5. At the lower pH values of JISS test solution leaching at the solid cement surface in addition to diffusion through pore water may be a contributory factor.

6. Caesium or strontium has a similar effect on the average rate of chloride diffusivity.

7. Strontium carbonate enhanced the diffusivity of sulphate ions.

8. Growth of microorganisms in control CPS was negligible in comparison to contaminated CPSs.

9. The concentrations of Sr^{2+} and Cs^+ in the JISS influenced the growth of microorganisms ($\approx 3 \times 10^7$ cfu).

10. There was a far greater amount of ions (Sr^{2+} and Cs^+) in the JISS from 3% $SrCl_2$ and 3% CsCl CPS, in comparison from $\approx$3% $SrCO_3$ CPSs which has contributed to the lesser growth of microorganism ($\approx 10^5$ cfu).
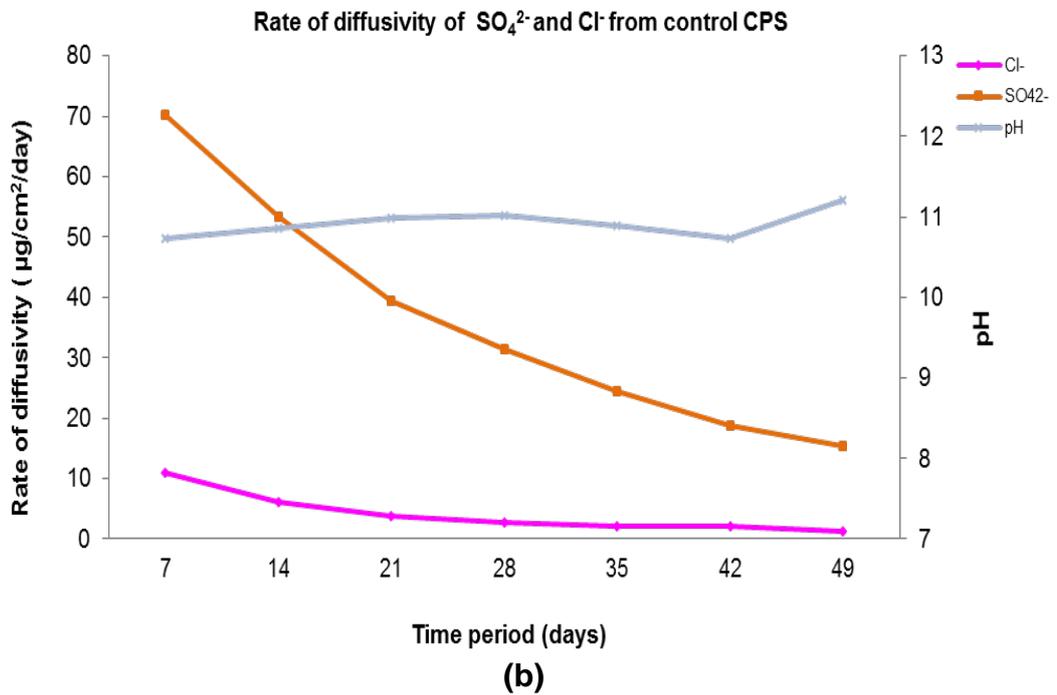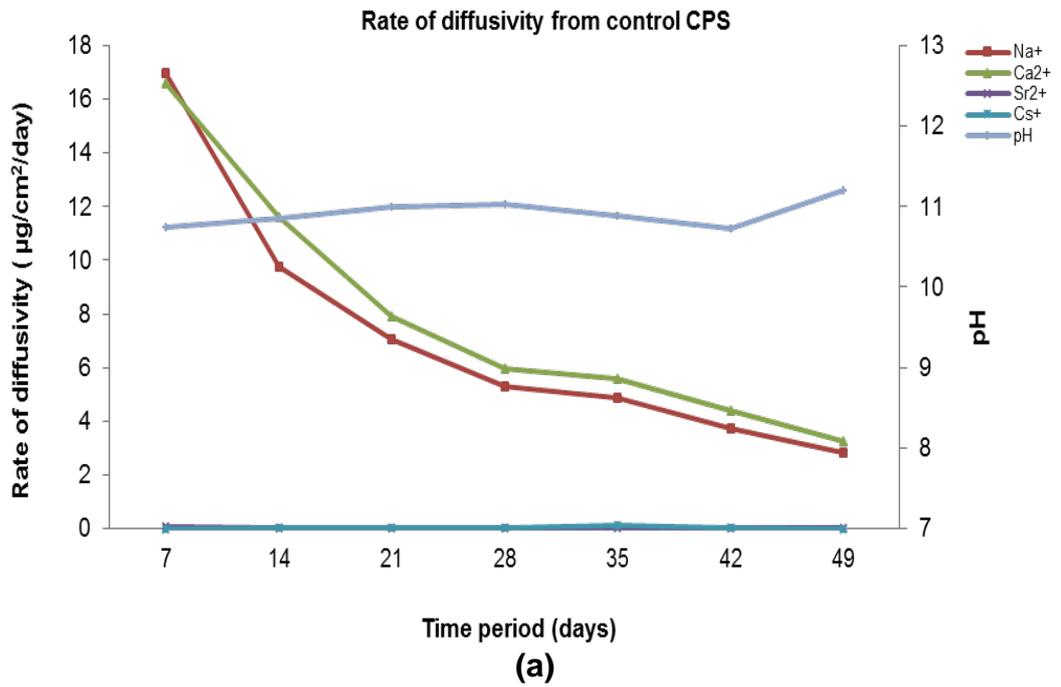
Figure 8.1 Rate of diffusivity of cations (a) and anions (b) from control CPS in JISS

213
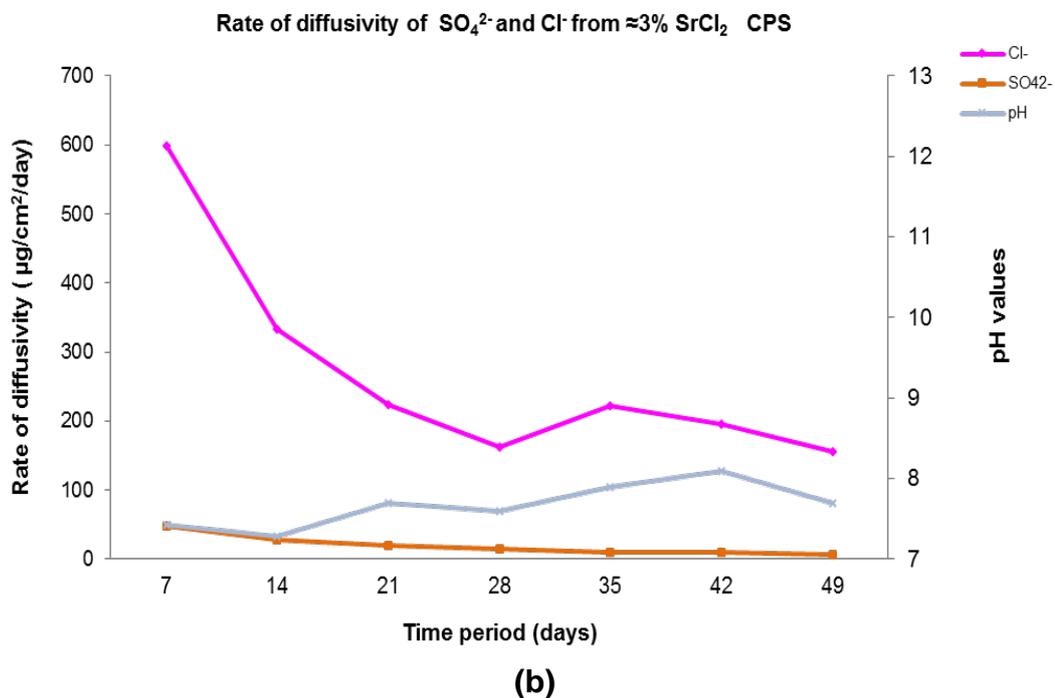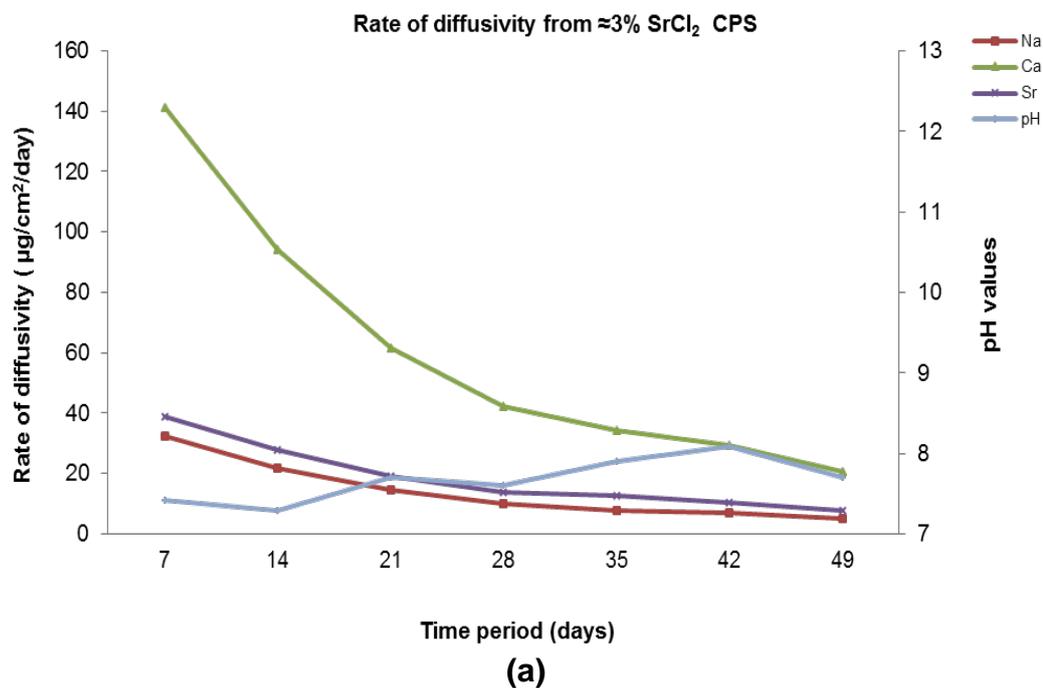
Figure 8.2 Rate of diffusivity of cations (a) and anions (b) from ≈3% SrCl₂ CPS in JISS
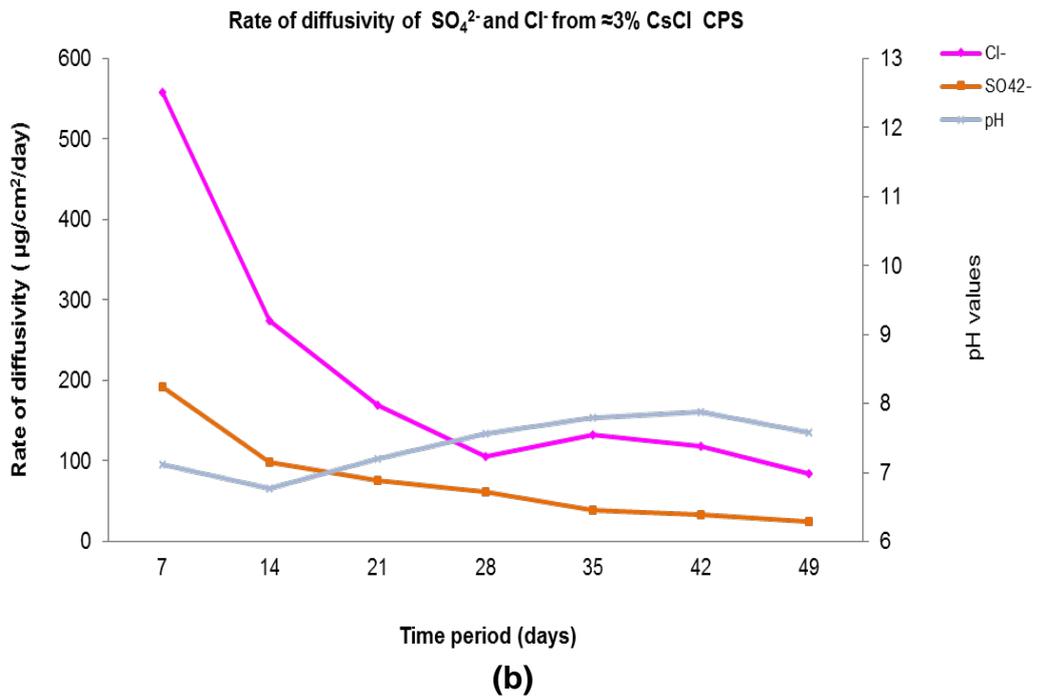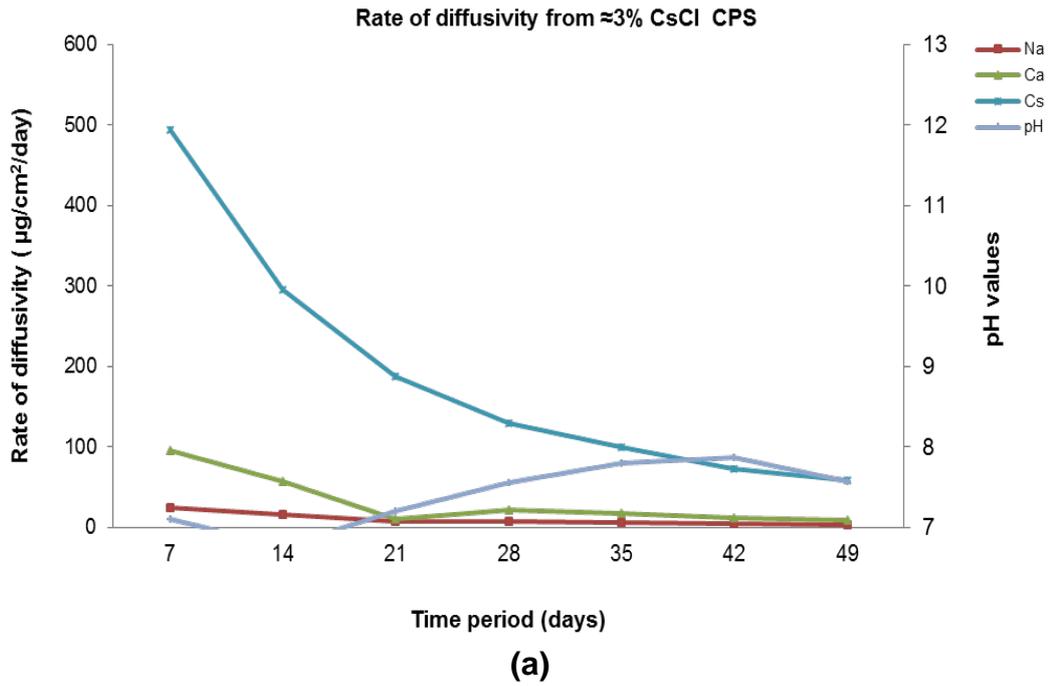
Figure 8.3 Rate of diffusivity of cations (a) and anions (b) from ≈3% CsCl CPS in JISS
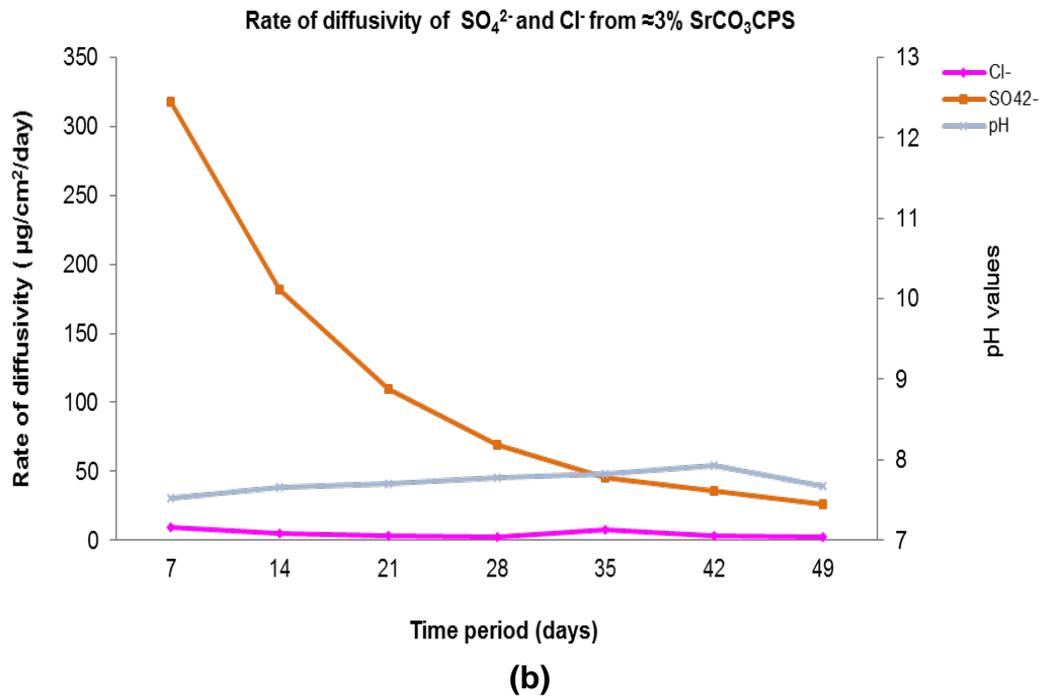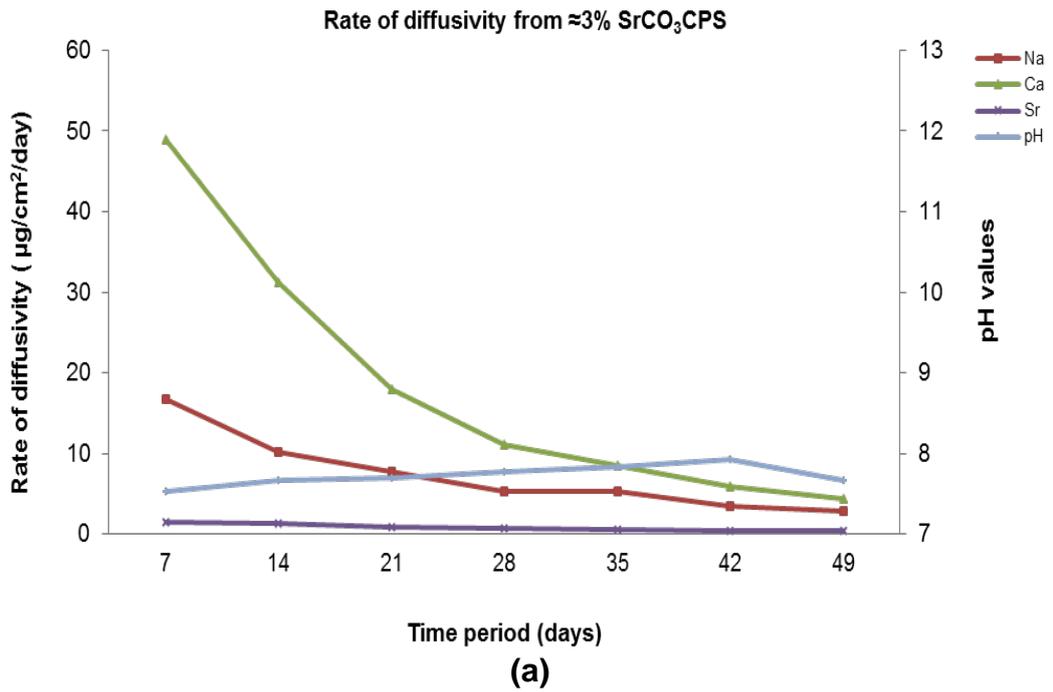
Figure 8.4 Rate of diffusivity of cations (a) and anions (b) from ≈3% SrCO$_3$ CPS in JISS

Chapter 9: Diffusivity from PFA:OPC CPSs with John Innes soil solution as a test solution

9.1 Aims of study

To evaluate the influence of microorganism present in the John Innes soil solution (JISS) on diffusivity of cations when encapsulated in PFA: OPC and to compare the data from other diffusivity experiments.

9.2 Introduction

This chapter addresses diffusivity experiments involving PFA:OPC CPSs with John Innes soil solution (JISS). The main purpose for carrying out these experiments were to compare the rates of diffusivity with that of BFS:OPC JISS diffusivity data (chapter 8) and other data sets. Both the PFA:OPC DW and JISS diffusivity experiments were initiated after the samples had been cured for 90 days. The experimental setup consisted of four sets of closed circuit diffusivity experiments with PFA:OPC CPSs with different cation characteristics (Table 9.1)

9.3 Cement paste samples

Diffusivity experiments were carried out on 4 different PFA: OPC CPSs, details of which are mentioned in Table 9.1.

Table 9.1 BFS:OPC cement paste samples and test solution used.

Experiment	PFA:OPC CPS		Test solution
	(a)	Control	John Innes soil
1	(b)	≈3% $SrCl_2$	solution (JISS)
	(c)	≈3% CsCl	
	(f)	≈3% $SrCO_3$	

9.4 Result and discussion

The closed circuit dynamic diffusivity experiments were carried out for 49 days. The rate of diffusivity values of each cement paste sample are given in appendix 9.1 to 9.4.

9.4.1 Micropore area and surface area analysis of CPS

The average micropore and surface area results of the dissected CPSs are shown in the Table 9.2. The average micropore area of the CPSs prior to the diffusivity experiments were in the range of $3 - 3.9$ m^2/g. The highest micropore area was measured in control CPS. There was no significant difference observed in the micropore area of $\approx 3\%$ CsCl and $\approx 3\%$ $SrCO_3$ CPS. The CPS containing $\approx 3\%$ $SrCl_2$ had the lowest micropore area compared to all the other CPSs in the present experiment.

The average surface area of cement paste samples were in the range of $22.7 - 40.6$ m^2/g. The average surface area $\approx 3\%$ $SrCl_2$ was found to highest of all the CPSs. The lowest surface area was measured in control CPS.

Table 9.2   Average micropore and surface area of cement paste samples measured by BET method

Sample	Micropore area	Surface area
	m^2/g	
Control	3.9	22.7
$\approx 3\%$ $SrCl_2$	3	40.6
$\approx 3\%$ CsCl	3.6	27.4
$\approx 3\%$ $SrCO_3$	3.7	23.8

9.5 Test solution analysis

9.5.1 pH values

The pH values of JISS after the first few days of the diffusivity experiment increased from 7.21 (natural pH of JISS) to 8.07 - 12.27 (Figure 9.2 to 9.5). Lower pH values (8.07- 8.47) were measured in the JISS from ≈3% $SrCl_2$. The pH values of JISS from control and ≈ 3% $SrCO_3$ CPSs were found to be in similar range. Similar trend of pH values were observed in case of PFA: OPC DW diffusivity experiments. There was no significant difference in the trend of pH values observed in PFA: OPC JISS and DW diffusivity experiments contrary to BFS: OPC JISS and DW diffusivity comparative studies.

9.5.2 Chemical analysis of test solution

All the diffusivity data have been normalised for comparative purpose. The diffusivity data from PFA: OPC DW experiment have been utilised to validate the effect of JISS on rates of diffusivity of PFA: OPC CPSs. The rates of diffusivity of cations and anions are presented in Figure 9.2 to 9.5.

9.5.2.1.1 *Strontium*

The average rate of diffusivity of Sr^{2+} in JISS from ≈ 3% $SrCl_2$ (103 µg/cm^2/day) was considerably higher than the average rate of diffusivity of Sr^{2+} from ≈ 3% $SrCO_3$ (0.032 µg/cm^2/day). However, there was no significant difference (p>0.05) measured in the rate of diffusivity between JISS and DW diffusivity experiment. The average rate of diffusivities of Sr^{2+} from ≈ 3% $SrCl_2$ CPS (103 µg/cm^2/day) and ≈ 3% $SrCO_3$ (0.032 µg/cm^2/day) in JISS were in fairly similar range with that of DW diffusivity (≈ 3% $SrCl_2$ (134 µg/cm^2/day), ≈ 3% $SrCO_3$ (0.036 µg/cm^2/day) in similar range of pH values. Comparing the results from JISS BFS: OPC with

JISS PFA: OPC diffusivity experiments; the average rate of diffusivity of Sr^{2+} was measured 5.5 times lower from ≈ 3% $SrCl_2$ (18.6 $\mu g/cm^2$/day) and 25 times higher from 3% $SrCO_3$ (0.82$\mu g/cm^2$/day) than the average rate of diffusivity of Sr^{2+} from ≈ 3% $SrCl_2$ (103 $\mu g/cm^2$/day) and ≈ 3% $SrCO_3$ (0.032 $\mu g/cm^2$/day) respectively. However, the pH values of JISS from ≈ 3% $SrCO_3$ PFA: OPC CPS were in the range of 11.99 – 12.19 compared to JISS from ≈ 3% $SrCO_3$ BFS: OPC CPS, which were measured in the range of 7.53 – 7.93.

9.5.2.1.2 *Caesium*

There was no significant difference (p>0.05) observed in the rate of diffusivity between JISS and DW diffusivity experiments. The average rate of diffusivity of Cs^+ from ≈ 3% CsCl (310 $\mu g/cm^2$/day) in JISS was similar with DW diffusivity of Cs^+ from ≈ 3% CsCl (363 $\mu g/cm^2$/day) at similar range of pH values. In comparison with JISS BFS:OPC diffusivity results; the average rate of diffusivity of Cs from PFA:OPC ≈ 3% CsCl (310 $\mu g/cm^2$/day) in JISS was 1.6 times higher than the BFS:OPC diffusivity (191 $\mu g/cm^2$/day). However, the pH values of JISS from ≈ 3% CsCl PFA: OPC CPS were in the range of 11.63 – 11.98 compared to JISS from ≈ 3% CsCl BFS: OPC CPS, which were in the range of 6.77 – 7.87.

9.5.2.1.3 *Calcium*

Calcium from ≈ 3% $SrCl_2$ CPS diffused out at faster rate compared to all the other CPSs in JISS diffusivity experiments. In comparison with control (2.1 $\mu g/cm^2$/day) CPS; the average rate of diffusivity of Ca from ≈ 3% $SrCl_2$ (158 $\mu g/cm^2$/day) was 76 times higher and 1.6 times higher than ≈ 3% CsCl (3.2 $\mu g/cm^2$/day) CPS. Calcium from ≈ 3% $SrCO_3$ diffused out at slower rate compared to all the other CPS. The average rate of diffusivity of Ca from ≈3% CsCl (3.2 $\mu g/cm^2$/day) and control (2.1 $\mu g/cm^2$/day) in JISS was ≈2 times higher than the average rate of

diffusivity of Ca^{2+} in DW (($\approx$3% CsCl (1.6 µg/cm^2/day) and control (1.2 µg/cm^2/day)) respectively. However there was no significant difference in the rate of diffusivity of Ca^{2+} between JISS and DW from $\approx$3% $SrCl_2$ ($p>0.05$) and $\approx$3% $SrCO_3$ ($p>0.05$). Comparing the results of BFS: OPC with PFA: OPC in JISS, the rate of diffusivity of Ca^{2+} from PFA: OPC CPSs was considerably lower than the rate of diffusivity of Ca^{2+} from all the BFS: OPC CPSs excluding $\approx$3% $SrCl_2$. The average rate of diffusivity of Ca from PFA: OPC $\approx$3% $SrCl_2$ (158 µg/cm^2/day) in JISS was 2.6 times higher than the BFS: OPC diffusivity (60 µg/cm^2/day) at similar range of pH values, although the concentration of Ca^{2+} in BFS:OPC CPSs (565 -602 mmoles) is higher than PFA:OPC CPS (138 - 148 mmoles).

9.5.2.1.4 *Sodium*

The average rate of diffusivity of Na^+ from $\approx$3% $SrCl_2$ (49 µg/cm^2/day) CPS was found to be highest of all the samples and was measured as $\approx$2 times higher than control (22 µg/cm^2/day) CPS. However, there was no significant difference found in the diffusivity of Na^+ from control (22 µg/cm^2/day), $\approx$3% CsCl (18 µg/cm^2/day) and $\approx$3% $SrCO_3$ (24 µg/cm^2/day) cps. The average rates of diffusivity of Na^+ from all the CPSs in JISS was relatively similar with DW diffusivity of Na^+ from all the CPSs. Comparing the results of BFS: OPC with PFA:OPC in JISS, the rate of diffusivity of Na^+ from PFA:OPC CPSs was $\approx$3 times higher than the rate of diffusivity of Na^+ from all the BFS:OPC CPSs. This could be due to the concentration of Na^+ present in PFA:OPC CPSs (25.1 -27 mmoles) in comparison with BFS:OPC CPSs (11.9 – 12.7 mmoles)

9.5.2.1.5 *Chloride*

The highest rate of diffusivity was measured from $\approx$3% $SrCl_2$, followed by $\approx$3% CsCl, control and $\approx$3% $SrCO_3$. The average rate of diffusivity of Cl^- from $\approx$3%

SrCl$_2$ (1405 µg/cm^2/day) was 4 times higher than the average rate of diffusivity of Cl$^-$ from ≈3% CsCl (352 µg/cm^2/day). There was no significance difference (p>0.05) between the rate of diffusivity of Cl$^-$ from ≈3% SrCO$_3$ and control CPS. The rates of diffusivity of Cl$^-$ from all the CPSs in JISS were similar with DW diffusivity rates of Cl$^-$ from all the CPSs. In comparison with BFS: OPC JISS diffusivity experiment, the rate of diffusivity of Cl$^-$ from PFA:OPC CPSs were ≈2 times higher the rate of diffusivity of Cl$^-$ from all the BFS:OPC CPSs excluding ≈3% SrCl$_2$; which was 5.2 times higher than the BFS: OPC diffusivity (270 µg/cm^2/day) at fairly similar range of pH values.

9.5.2.1.6   *Sulphate*

The average rate of diffusivity of SO$_4^{2-}$ form control (46 µg/cm^2/day), ≈3% CsCl (53 µg/cm^2/day) and ≈3% SrCO$_3$ (46 µg/cm^2/day) was similar and ≈ 3.5 higher than the average rate of diffusivity of SO$_4^{2-}$ from ≈3% SrCl$_2$ CPS. A similar grouping of diffusivity pattern was measured in PFA: OPC DW diffusivity experiments (Figure 9.1). Comparing the results from DW PFA: OPC with JISS PFA: OPC diffusivity experiments; the average rate of diffusivity of SO$_4^{2-}$ from ≈3% CsCl (34 µg/cm^2/day) and ≈3% SrCO$_3$ (31 µg/cm^2/day) was measured ≈ 1.7 times lower than the average rate of diffusivity of SO$_4^{2-}$ from ≈3% CsCl (53 µg/cm^2/day) and ≈3% SrCO$_3$ (54 µg/cm^2/day) respectively. However, there was no significant difference in the rate of diffusivity of SO$_4^{2-}$ between JISS and DW from control (p>0.05) and ≈3% SrCl$_2$ (p>0.05). BFS:OPC JISS SO$_4^{2-}$ diffusivity rates of all the CPS were relatively similar to PFA:OPC JISS diffusivity rates, except in case of ≈3% SrCO$_3$; which was twice as high compared to PFA:OPC.
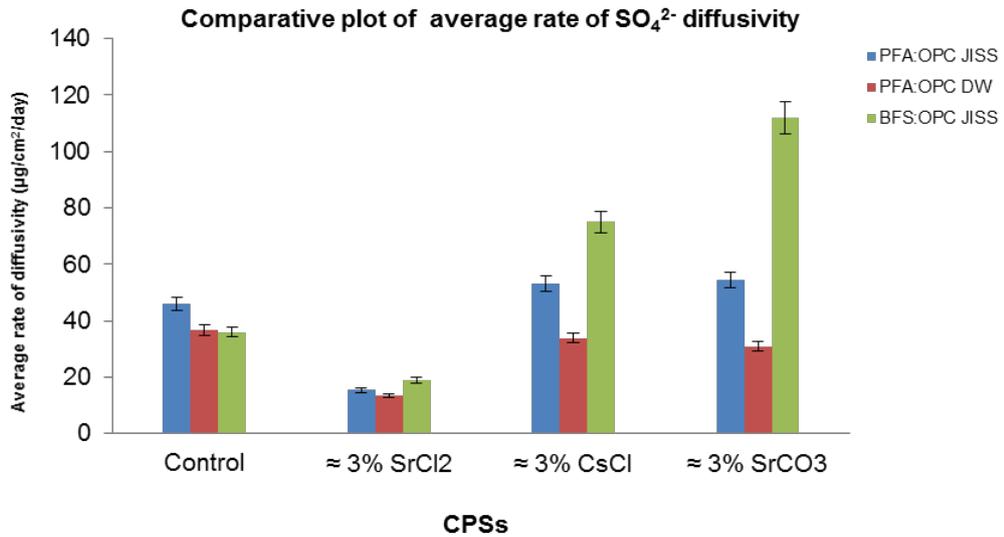
Figure 9.1 comparative plot of average rate of diffusivity of sulphate from PFA:OPC in JISS, PFA:OPC in DW and BFS:OPC in JISS

9.6 Microbial community profile

All methods/procedures employed in this section were carried out as described in Section 2.6 – 2.9.

9.6.1.1 Microbial analysis of test solution

The results of microbial analysis of the test solutions are shown in the Table 9.3. The total viable counts measured on final day were in the range of 2.3×10^3– 0.57×10^7 cfu. The highest viable count was measured in the JISS from ≈3% $SrCl_2$ (0.57×10^7 cfu) followed by ≈3% $SrCO_3$ ($< 2.3 \times 10^3$ cfu) CPS. There was no significant viable population measured in the JISS from control CPS and ≈3% CsCl. The results of primary identification of the bacteria isolated from the test solutions of the CPS are summarised in Table 9.4. The data show that non-motile Gram positive (G+ve) bacilli bacteria were present in the JISS from ≈3% $SrCl_2$

223

and ≈3% $SrCO_3$. There was no occurrence of fungi observed in the JISS of all the CPSs.

Table 9.3 Summary table showing total viable count measured in JISS

Experiment	PFA:OPC CPS	Total viable count (cfu)
1	(a) Control	NR*
	(b) ≈3% $SrCl_2$	0.57×10^7
	(c) ≈3% CsCl	NR*
	(f) ≈3% $SrCO_3$	2.3×10^3

* None recorded

Table 9.4 Summary table showing bacteria isolated from JISS

Experiment	PFA:OPC CPS	Primary identification test	
		Gram stain	motility
1	(a) Control	NR*	NR*
	(b) ≈3% $SrCl_2$	G+ve	-
	(c) ≈3% CsCl	NR	NR*
	(f) ≈3% $SrCO_3$	G+ve	-

* None recorded

9.7 Conclusions

1 Strontium chloride 'buffered' the pH value of the initial test solution to around 8.5 compared with the control, caesium chloride and strontium carbonate cement paste samples pH values were nearer to 12.

2 Comparative trends for strontium chloride and strontium carbonate cement paste samples with JISS and DW were similar.

3 The cement paste formulation influenced the strontium diffusion rate.

4 Caesium diffused quicker from PFA:OPC CPS than the BFS:OPC counterpart, but pH values differed significantly.

5 Strontium added as chloride enhances calcium diffusion unlike caesium that had a marginal effect on calcium diffusion.

6 Calcium diffusion is greater from BFS:OPC than PFA:OPC CPS which could be attributed to the higher concentration of calcium in the cement paste sample.

7 Although strontium chloride influenced sodium diffusion, the impact on the rates was comparatively small.

8 Diffusivity from strontium chloride cement pastes were the highest, which could be attributed to the higher chloride of the cement paste.

9 Diffusion rates of sulphate from all PFA cement paste samples were small in comparison with diffusion rates for BFS:OPC CPSs.

10 The encapsulated 3% CsCl caused Na^+ and K^+ to leach out at very early stage in the experiment resulting in the lack of or poor growth of microorganisms in PFA:OPC CPSs.
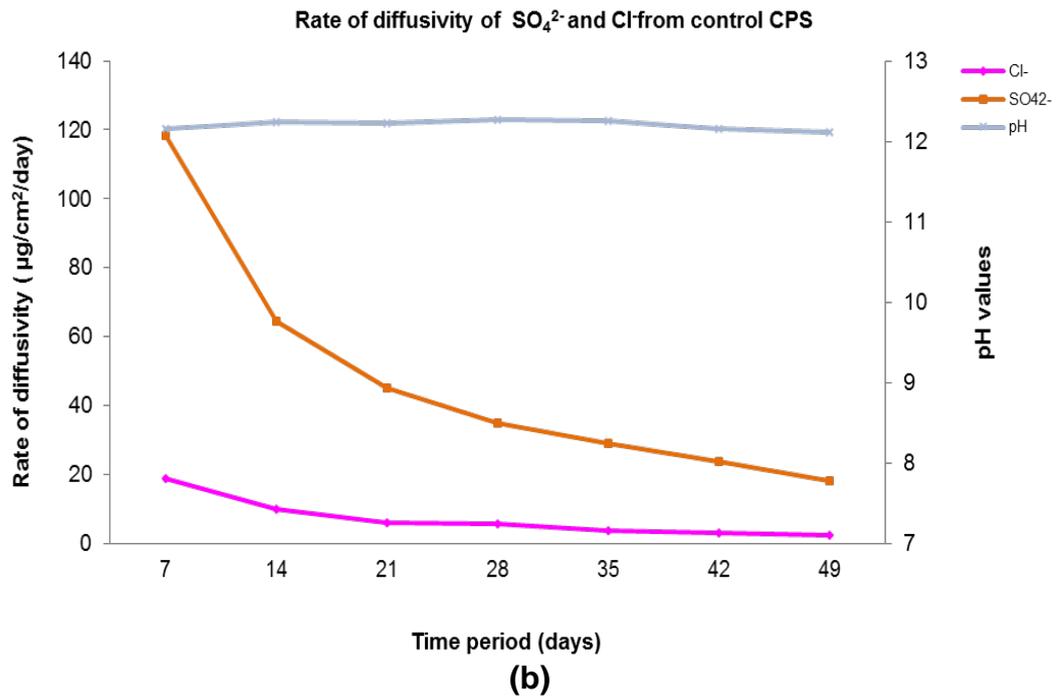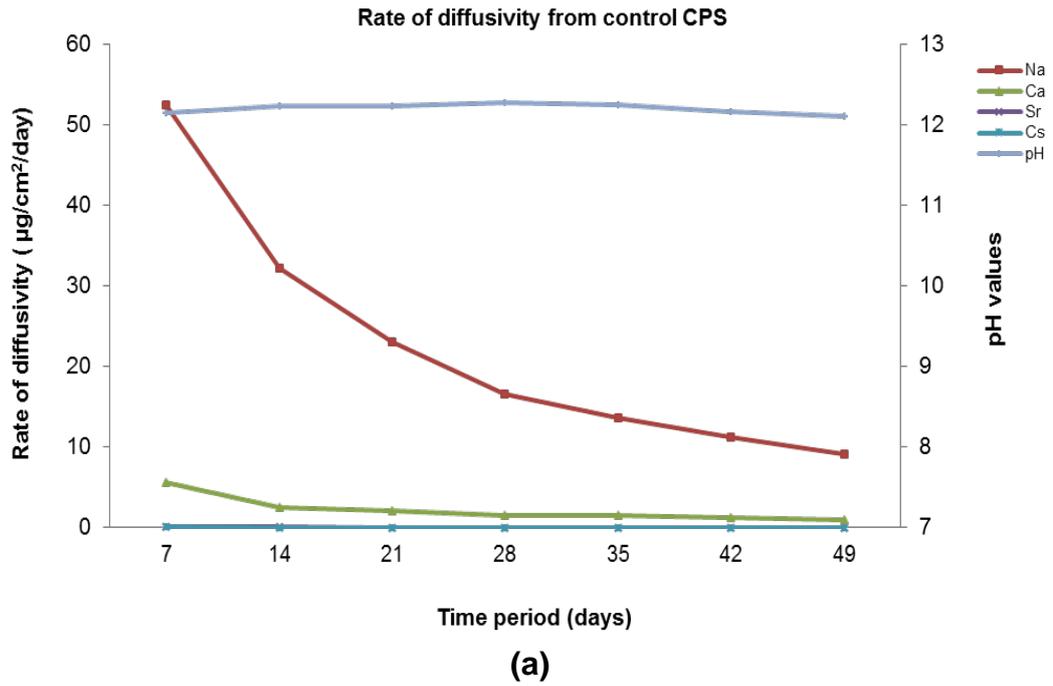
Figure 9.2 Rate of diffusivity of cations (a) and anions (b) from control CPS in JISS
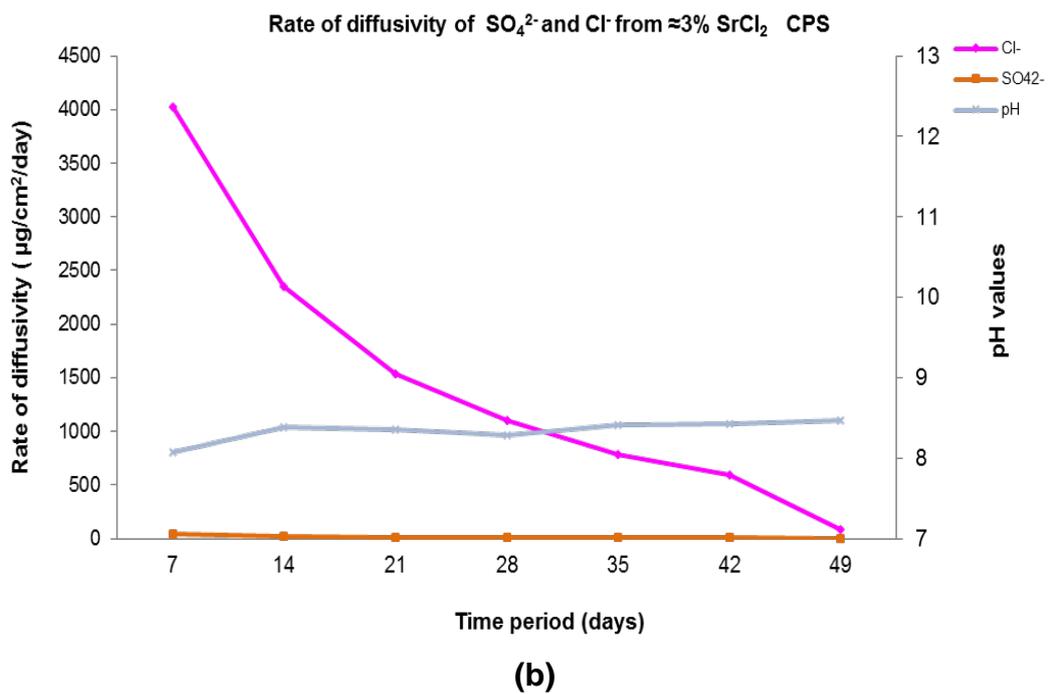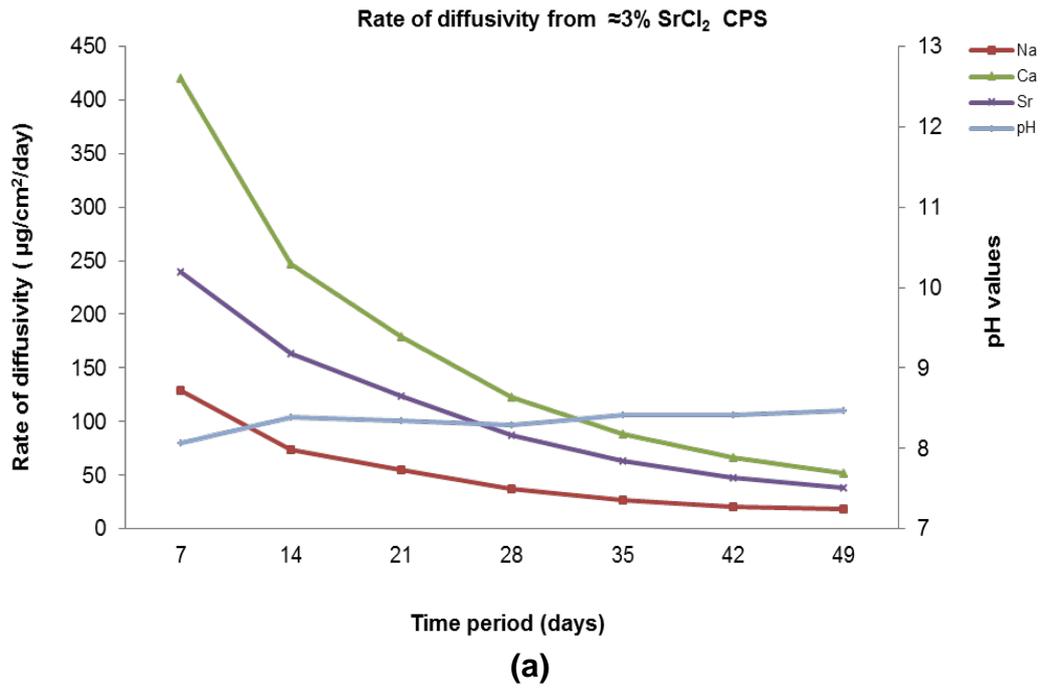
Figure 9.3 Rate of diffusivity of cations (a) and anions (b) from ≈3% SrCl₂ CPS in JISS
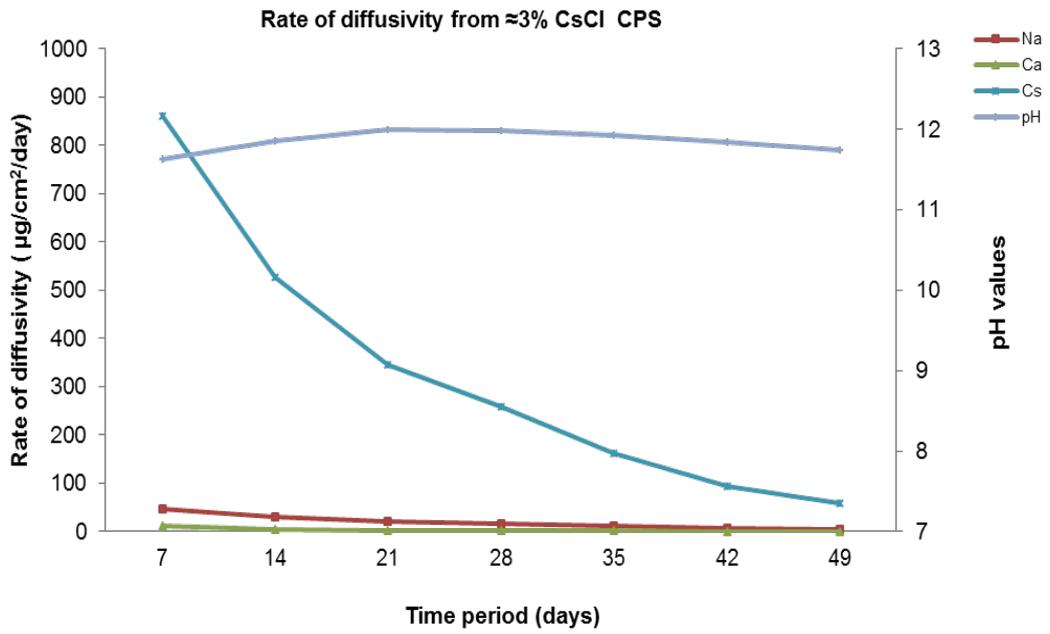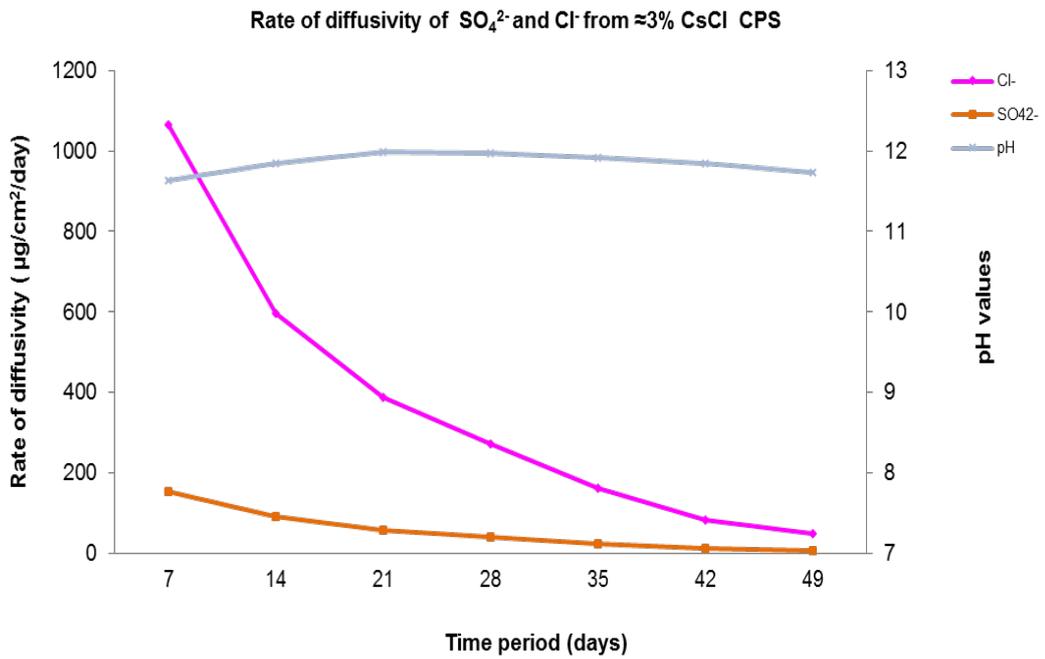
Figure 9.4 Rate of diffusivity of cations (a) and anions (b) from ≈3% CsCl CPS in JISS
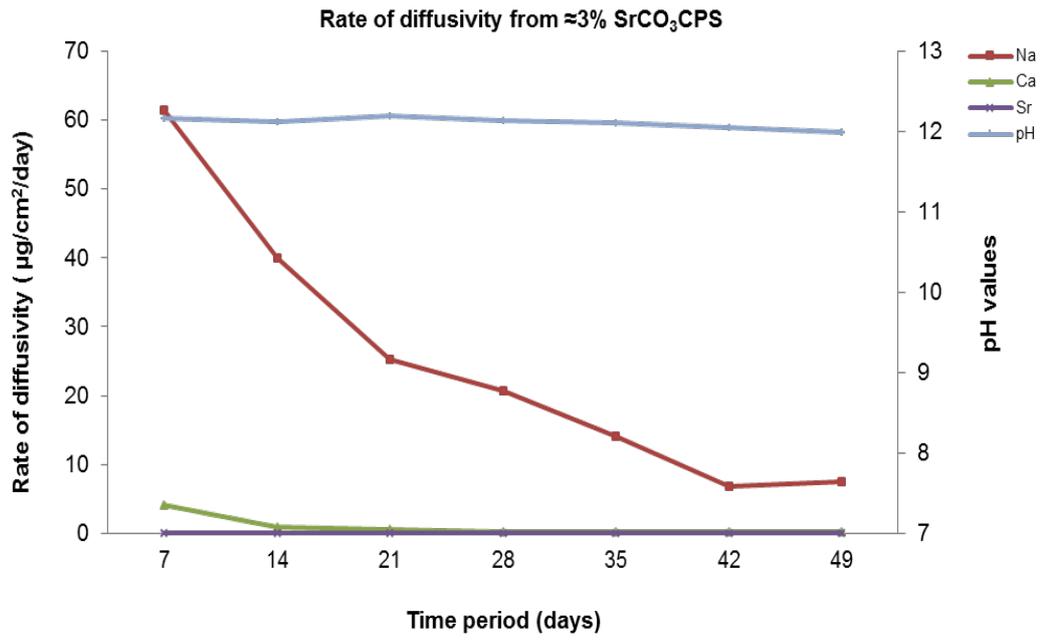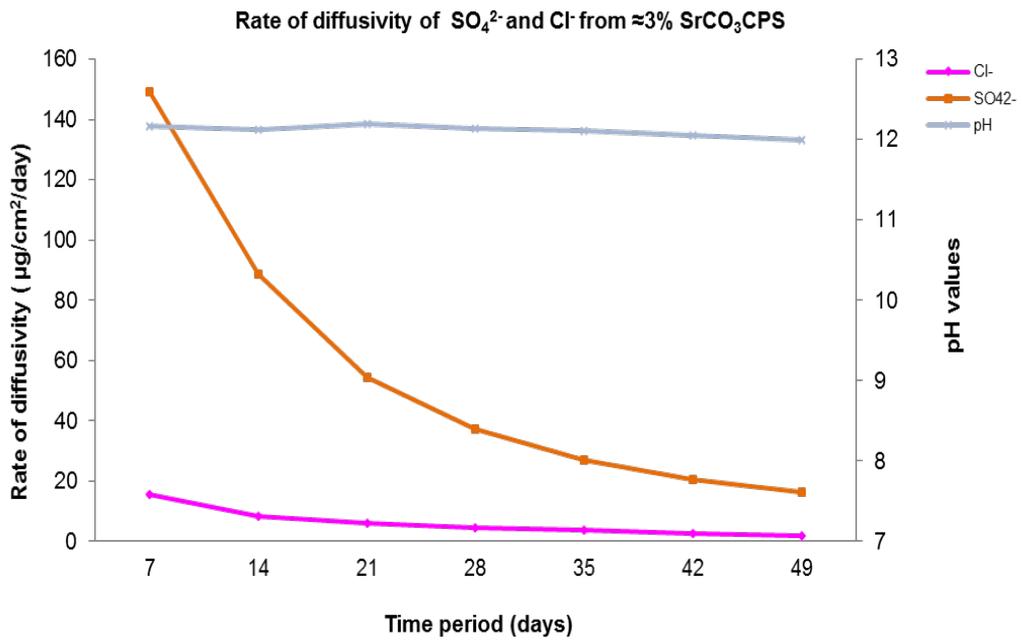
Figure 9.5 Rate of diffusivity of cations (a) and anions (b) from ≈3% SrCO₃ CPS in JISS

Chapter 10:   Conclusions

10.1 Generic conclusion

The main aim of this project was to evaluate the diffusivity of strontium, caesium and cobalt when added as inactive forms to OPC:BFS and PFA:OPC cement composition. Additional aims were to investigate the effects physic-chemical parameters on the diffusivity of cement paste samples. This work significantly contributes to the knowledge of factors influencing the diffusivity of encapsulated cations i.e. composition of cement paste (BFS:OPC and PFA:OPC), hydration of cement, added salt to the makeup water, pore water chemistry and, nature of leachant/aqueous solution and its condition (stagnant or mobile). The aims of these studies have therefore been achieved and the following conclusions have been drawn on at least one occasion in chapters 4 to 9 and can therefore be regarded as generic.

1. The make-up water composition affected the segregation of inherent/added cations in the cement paste samples and also both the bleed water volume and physical characteristics of the cement paste samples.

2. Strontium when added as a soluble salt to the make-up water influences the rate of diffusivity. The composition of the cement paste had a slight impact with PFA:OPC favouring a more rapid diffusion. Similar trends were observed for caesium paste samples.

3. The diffusivity of Sr^{2+} and other cations is dependent upon its concentration and cement additive used in the cement paste formulation.

4. The concentration of the added salt to the make-up water also affects diffusivity.

5. Diffusivity of chloride ions from the cement paste sample is dependent on the concentration of chloride in the make-up water.

6. Both caesium and strontium influence calcium diffusion when compared with the corresponding control CPS. This is not surprising for strontium as it will be a good surrogate for calcium and hence take part in some of the hydrates produced during curing. Caesium has a lower impact on calcium diffusivity.

7. The diffusivity of sulphate was influenced by the nature of the cation added to the make-up water. Strontium had the greatest effect on lowering the diffusion primarily due to the formation of sparingly soluble strontium sulphate.

8. Calcium diffusion was affected by both nature of the cation added to make-up water and its concentration. This effect was less marked for caesium contaminated CPSs. Calcium diffusion is greater from BFS:OPC CPS than PFA:OPC which could be attributed to the higher concentration of calcium in the cement paste sample.

9. In general, the pH values were lowered primarily due to the ionic strength of the make-up water hindering diffusion of calcium ions, concentration of calcium of the cement paste but again with both pore water and hydrate composition changing with time pH values were influenced accordingly.

10. The JISS test solution composition retard strontium diffusivity but accelerated caesium diffusion in comparison with distilled water values, this retardation could be due to the inherent sulphate content ($\approx$8600 ppb) of the JISS test solution.

11. Growth of microorganisms in control CPS was negligible in comparison to contaminated CPSs.

12. The concentrations of Sr^{2+} and Cs^+ in the JISS influenced the growth of microorganisms ($\approx 3 \times 10^7$ cfu).

13. There was a far greater amount of ions (Sr^{2+} and Cs^+) in the JISS from $\approx 3\%$ $SrCl_2$ and $\approx 3\%$ CsCl BFS:OPC CPSs, in comparison from $\approx 3\%$ $SrCO_3$ CPSs which has contributed to the lesser growth of microorganism ($\approx 10^5$ cfu).

14. The encapsulated 3% CsCl causes Na^+ and K^+ to leach out at very early stage in the experiment resulting in the lack of or poor growth of microorganisms in PFA:OPC CPSs.

15. The cumulative effect of presence of motile bacteria, fungi and presence of humic substances might have lowered the pH and influenced the diffusivity of cation from BFS:OPC CPSs.

16. Diffusion rates of sulphate from all PFA cement paste samples were small in comparison with diffusion rates for BFS:OPC CPSs.

Controlling the compositions of the make-up water and cement paste can be made to influence the diffusivity of strontium ions. Cement pastes with a high sulphate content will also retard the diffusivity. No conditions/additives studied in these experiments were able to control caesium diffusion.

10.2 Implication of findings to nuclear industry

In most leach experiments cement paste samples are contacted with a solution (normally distilled water) for a period of time, usually 20 days; the samples are removed and contacted with fresh distilled water for a further period. All subsequent solutions (DW) are analysed for the appropriate target. This approach unlike ours ensures that:

(a) the sample approximates a semi-infinite medium, which in practise means that no material is leached out of locations farthest away from the exposed surfaces

(b)   the concentration gradients at the surface of the cement sample and leach solution are virtually zero i.e. zero boundary concentration

(c)   the solubilities of leached ions control diffusivity and leaching

(d)   re-adsorption of ions is low.

It is unlikely however that this scenario will replicate ground water seepage into an underground nuclear repository and subsequently come in to contact with encapsulated wastes. The scheme i.e. closed circuit recirculation adopted in this research would be more fitting of the real situation i.e. stagnation followed by percolation and therefore diffusivity of ions will be greatly influenced by the test solution chemistry and composition. In all other aspects our experimental arrangement confers with ANSI/ANS 16.1 standard [213], namely:

(a)   the cations were well mixed in the cement formulation prior to leaching

(b)   the cement surface is continuously exposed to the test solution

(c)   temperature is kept relatively constant

(d)   the cement formulation is homogeneous (this may not be the case for $SrCO_3$ contaminated cement formulations)

10.2.1 Diffusion of ions from encapsulated waste

In cement paste, the diffusive transport of ions takes place in the micropores as long as they maintain a continuous pathway. The rather large ratio of micropore diameter to the diameter of the hydrated ions such as cations, chloride etc. encountered in cement paste allows for a continuum description of diffusive transport of ions through the saturated pores. The leaching process consists of physic-chemical phenomena in which diffusion plays a crucial role. Fick's law alone is not always sufficient for a reasonable full description of the fundamental

processes involved in the kinetics of leaching. Factors that have an important effect on the elution process are:

a.   the heterogeneity of the cement paste sample including the pore structure and the changes that take place when calcium hydroxide is lost to the test solution

b.   physic-chemical mechanisms through which the retention properties of the cement sample might be impaired under the prolonged contact with test solution.

It is known that for sparingly soluble salts, strontium carbonate is a good example in our case, a low rate of salt dissolution in the embedding hydrophobic matrix leads to completely different release kinetics.

The depth of dissolution studies in this research indicated that the diffusivity of Sr^{2+} when added as carbonate salt revealed diffusion of few micron from the surface of the CPS. Reference studies have shown that addition of calcium carbonate serves two functions; one as an active participant in the hydration process of cement paste, affecting the amount of free calcium hydroxide, and AFm and AFt phases [44]. The sulphate ions that are released from AFm in the course of carbonation reacts with water and $Ca(OH)_2$ leading to formation of ettringite. This ettrigite formation increases the molar volume of the solids present in paste enhancing the space-filling of paste, resulting in reduction of porosity and permeability of hardened cement pastes [44]. Encapsulation of cations as carbonate salt may lower the diffusivity of some cations; however, may not be the case for caesium. Caesium carbonate is very soluble in comparison with sparingly soluble strontium carbonate. Therefore, lowered diffusivity of caesium when added as carbonate salt will have to be due to reduced porosity of hardened

cement paste and not due to any changes in the binding mechanism of Cs^+ when added as carbonate salt. Caesium is highly soluble in alkaline pore water of cement paste sample along with the other inherent soluble cations Na^+, K^+. Based on the solubility, cations/radionuclides encapsulated in cement paste fall under two categories; the ones which are soluble in alkaline pore water of hardened cement paste such as caesium and Iodine, whereas insoluble cations include nickel and cobalt which remain immobilised as long as the pH of the pore water remains alkaline. Data generated from ≈1.3% $CoCl_2$ BFS:OPC CPS showed correlation of test solution pH values and cumulative concentration of Co^{2+} leached in the test solution. However, the fact that Sr^{2+} replaces Ca^{2+} in the cement paste mixture, our studies have shown direct correlation between diffusivity of Sr^{2+} and total amount of Ca^{2+} present in the CPS; depending on the type of formulation (BFS:OPC, PFA:OPC). The rate of diffusivity and the depth of cation diffusion was significantly higher in ≈3% $SrCl_2$ PFA:OPC having 147 mmoles of Ca^{2+} compared to its BFS counterpart having 602 mmoles of Ca^{2+}. Thus it can be deduced that maintaining Ca:Sr cations ratio play an important role for encapsulation of Sr^{2+}. This also indicates that the PFA:OPC formulation may not be suitable for Sr^{2+} encapsulation due to lower wt% of calcium present in PFA (1.30) in comparison with BFS (38.22). The percentage of Ca^{2+} in PFA can be increased by incorporation of calcium chloride in PFA:OPC mixture to improve the binding capacity of Sr^{2+} in PFA:OPC hardened cement paste. Calcium chloride has been used as an accelerator for hydration of calcium silicates (C_3S) for many decades in cement industry [214]. Calcium chloride has been shown to increase the resistance to the weathering of the cementitious material and faster cure rate than plain concrete [16]. Studies have shown that the final concrete set time is reduced by two-thirds upon addition of two per cent

calcium chloride to cement paste mix [52]. A wealth of information is available on the usage of $CaCl_2$ in cement paste mixtures [52, 214, 215].

10.2.2 Diffusion of caesium ions from cement matrix

The faster diffusivity of Cs^+ in our studies (calculated $D_e = 1.06 \times 10^{-5}$ cm^2/day), which increases with increase in ionic concentration of leach/test solution (DSPW, CSPW) may have potential impact on environment taking into consideration its transport from near to far-field and subsequent accumulation in food web originating from microorganisms. Attention towards the fate and accumulation of radiocaesium deepened since the Chernobyl nuclear accident, 1986; which indicated a high potential of bioavailability and mobility of ^{137}Cs and [134]Cs [67, 216, 217]. The accumulation and the levels of radiocaesium in the soils, waters and living species in the UK since May 1986, after the Chernobyl accident have been well documented [217]. A number of studies have been performed to measure its concentration in abiotic (soil, sediment, water) and biotic systems of terrestrial and aquatic ecosystem. These studies revealed that the accumulation of radioacaesium in biosphere depends on number of factors, few of which reported, include its mineral content of the solid substrate and the abundance of monovalent cations [217]. The partitioning of Cs^+ between abiotic (i.e. soils, sediments, water) and biotic components of terrestrial and aquatic ecosystems is complex and dependent on a number of factors, e.g. inorganic mineral content of the solid substrates and the abundance of monovalent cations. Reference studies have shown that Cs^+ has equal or greater affinity for transport in comparison with K^+ in some organisms which is greatly influenced by the presence of external K^+, $NH4^+$, and Na^+[216]. Cs^+ is monovalent and most electropositive metal having high water solubility than other radioisotopes. It is

also a weak Lewis acid having lower tendency to form complex with ligands, however, this facilitates bioaccumulation of Cs^+ via intracellular monovalent transport system located in the plasma membrane of an organism. This transport is accompanied by stoichiometric exchange for intracellular K^+ [216]. Radiocaesium remains active in the biosphere for many years owing to the relative longer half-life of ^{137}Cs ($\approx$30years). The challenges of Caesium radio-isotopes is now a major concern for the clean-up the FUKUSHIMA Daiichi nuclear plant site. Although more locally distributed in comparison to Chernobyl it is never the less a major nuclear waste commitment requiring a final waste disposal outcome.

There have been several attempts to improve the immobilisation of highly soluble Cs^+ in cement paste. One of such attempt showed that incorporation of 20% by weight densified silica fumes (DSF) in cement paste mixture (w/c= 0.45) greatly improved the immobilisation of Cs^+. The incorporation of DSF to cement paste mixture forms a DSF agglomerates which absorbs Cs^+, thus reducing its leachability. Furthermore, this work also indicated that during the pozzolanic reaction, a hydrated rim develops around the agglomerate that acts as an additional diffusion barrier for the Cs^+, resulting in an increased efficiency of Cs^+ immobilization [31]. DSF is an agglomerated raw silica fume, which has larger particle diameter than raw silica fume (0.1 µm). Silica fume is considered as very effective pozzolanic material due to its extreme fineness and high silica content. Silica fumes are used in cement mixture according to the ASTM standard ASTM C1240 [218]. During hydration process, amorphous silica reacts with $Ca(OH)_2$ to form additional CSH gel which has lower Ca:Si ratio compared to CSH originating

from the hydration of cement [219]. Research evidence indicate that the Cs^+ retention increases with decrease in Ca:Si ratio [31, 220, 221]

10.2.3 Impact of microorganisms

The depth of dissolution studies and rates of diffusivity have shown that highest diffusivity of Na^+ and K^+ from the test solutions of contaminated CPS (3% $SrCl_2$, 3% CsCl and 3% $SrCO_3$), in the presence of viable communities in the circulating system, in comparison with control CPS where no viable communities were reported; such correlation have not been reported previously. Most studies have been carried out on cement pastes either encapsulated with cation/radionuclides or added to microbial media to investigate the viable communities. Although such studies have isolated the group of concrete colonising microorganism, however failed to represent the actual GDF scenario. In our studies, the colonisation and subsequent influence on the diffusivity of cations from CPS was carried out using filtered soil compost (John Innes No.3) solution, no additional growth media was added to the JISS solution. This may represents the actual GDF scenario in a condition where seepage of water will take place. As indicated by Humphreys [70], the GDF will have indigenous population of microorganism which may be in active or dormant form raises a concern about the durability of immobilised waste. Although the maximum care will be taken to prevent the mobilisation of cations/radionuclides from the cement paste, the interaction of encapsulated cations/radionuclides and microorganism either in mobile or stationary aqueous media will certainly affect the encapsulated wasteform primarily by lowering the pH as indicated from our studies, ultimately affecting the integrity of CSH leading to the dissolution of solidified waste.

Chapter 11:   Future Work

The work reported in this thesis has made a significant contribution to the understanding of the challenges of encapsulating nuclear wastes with OPC formulations. The work as demonstrated, in particular, that few if any conditions influence (retard) the diffusivity of the Cs cation. Consequently further work is required to address this major challenge, the areas worthy of further investigation are:

1   **Pore water;** this plays a crucial role in the migration of ions from cement paste into surrounding environments. Expression of this liquor from cement paste samples during the various stages of experiments to demonstrate the time dependence of ion migration would be extremely valuable. It would also confirm the success or otherwise of the effectiveness of additives to OPC (replacing BFS or PFA for example) in reducing the diffusivity of caesium cation. Monitoring the composition of this water would also identify if for example chloride ion plays a key role in conveying caesium into this environment.

2   **Waste form;** caesium wastes will largely be in the form of sludges, solids or loaded ion exchange resins/absorbers. Understanding how caesium could be released from these wastes will be important to the success of achieving the objective of reduced diffusivity. With loaded ion exchange resins then diffusion from these will be largely dependent on the pore water chemistry, i.e. capable of initially leaching the cation from the functional site. This could well be a slow process influenced by external considerations such as the flow of ground water over/around the encapsulated waste.

3   **Other additives to OPC**; BFS and PFA are the most common additive to OPC mixture for encapsulation purposes, however although they may achieve many of the properties required of encapsulation such as low cost, contribute to cement's physical attributes e.g. strength, durability, heat resistant etc. they enhance OPC's caesium retention properties very little. Silica fume and other materials are being considered largely from the physical property aspects but this interest needs to be extended to the chemical behaviour of radionuclide retention.

4   **Make-up water;** both its composition and volume to cement affects diffusivity. Generally restricted *w/c* (≈0.3 to ≈0.7) is used. As this make-up water influences pore water evaluating lower water make-up ratios may be of value. Addition of low cost chemicals may be worthy of consideration such as sodium hydroxide that would disturbed the pH changes that occur with curing, would this be advantageous? Equally to complement 3 above incorporating pore blockers into the cement paste recipe should have some impact on diffusional processes.

5   **Radio-tracers**; We chose not to use radio-tracers for a variety of reasons not least the number of experiments underway at any one time would have imposed a major challenge for the small radio-lab at UCLan. Incorporating radio-tracers could have provided a wealthy of addition information such as the progression of ions from cement paste into pore water, the potential for back diffusion from the test solution into the cement paste sample and influence inherent cations on added cations; caesium is a good example as OPC and some additives have low caesium content.

6   **Experimental arrangement**; The closed circuit experiments provided some interesting challenges, not least accounting for dilution effects on

240

adding fresh test solution after samples (20ml) had been withdrawn. Without this protocol then studying the influence of microorganisms on the diffusivity of ions would have been compromised. For non-microbial work smaller samples could have been removed but then a direct comparison may have been difficult. The open circuit experiments overcame many of these difficulties but the logistics of accommodated more than a few experiments in a laboratory would have been a challenge. The closed circuit arrangement we believe is likely to replicate what happens in and around a GDF with ground water flow. The diffusivity values calculated from our experimental data may be more difficult to replicate and other arrangements, dual cell type may provide this consistency. The major drawback with our experimental arrangement was not being able to study the influence of temperature on the diffusional processes.

7   **Other analysis**; due to time and work load constraints analytical techniques such as TGA, NMR, FT-IR etc. were not employed. It is appreciated that these techniques would have provide other additional information that would have shed light on how pore water interacts with cement paste, formation of cement paste hydrates and their changing phase etc.

8   **Modelling;** although our diffusion coefficients are similar to previously published values, the experimental arrangements that were used to collect this data were different. Modelling diffusivity that incorporates make-up water, various and different additives including pore deformers, coupled with external near field conditions that replicate both flowing and stagnant ground water could provide some added value to radioactive waste cement encapsulation.

241

Many if not all of the above suggestions are likely to be considered when the final disposal form of Cs^+ loaded ION-SIV being used in the clean-up of the FUKUSHIMA Daiichi nuclear plant site. This material is being used to remove caesium from ground water that has entered the damaged reactor building. Currently the loaded ION-SIV is being stored on site awaiting a decision on how best to reach the final waste management end point. OPC type encapsulation is likely to be one consideration.

References

1. Krauskopf, K., *Radioactive waste disposal and geology*. Vol. 1. 2013, New York Springer Science & Business Media.

2. World Nuclear Association. *The Nuclear Fuel Cycle*. 2015 [cited 2015 May]; Available from: http://www.world-nuclear.org/info/Nuclear-Fuel-Cycle/Introduction/Nuclear-Fuel-Cycle-Overview/.

3. World Nuclear Association. *Nuclear Power in the United Kingdom*. 2015 [cited 2015 May]; Available from: http://www.world-nuclear.org/info/Country-Profiles/Countries-T-Z/United-Kingdom/.

4. Ojovan, M.I. and W.E. Lee, *An introduction to nuclear waste immobilisation*. Second ed. 2014: Elsevier, UK.

5. Abu-Khader, M.M., *Recent advances in nuclear power: A review.* Progress in Nuclear Energy, 2009. **51**(2): p. 225-235.

6. MacKenzie, A.B., *Environmental radioactivity: experience from the 20th century — trends and issues for the 21st century.* Science of The Total Environment, 2000. **249**(1–3): p. 313-329.

7. Atomic Energy Regulatory Board, *Classification of radioactive waste*. 2011, Atomic Energy Regulatory Board, Mumbai (India).

8. World Nuclear Association. *Waste Management: Overview*. 2012; Available from: http://www.world-nuclear.org/info/Nuclear-Fuel-Cycle/Nuclear-Wastes/Waste-Management-Overview/.

9. NDA. *The 2013 Inventory: Nuclear Decommisioning Authority*. 2013 [cited 2015 January]; Available from: https://www.nda.gov.uk/ukinventory/the-2013-inventory/2013-uk-data/.

10. Alexander, W.R. and L. McKinley, *Deep geological disposal of radioactive waste*. Vol. 9. 2011: Elsevier.

11. Miller B, Tooley J, and G. Thomson. *Storage and Disposal of ILW and HLW in the UK: Implications for Copeland.* A REPORT FOR COPELAND BOROUGH COUNCIL 2006; Available from: http://www.copelandbc.gov.uk/sites/default/files/attachments/CIS/pdf/180 107_nwg8a.pdf.

12. McKinney, J. and S. Barlow, *Graphite waste treatment and disposal—A UK perspective on the current opportunities and issues.* 2010, IAEA-TECDOC-1647, International Atomic Energy Agency, Vienna, Austria.

13. Nirex, *viability of a phased geological repository concept for the long-term management of the UK's radioactive waste.* Nirex report N/122, 2005.

14. Glasser, F.P., *Application of inorganic cements to the conditioning and immobilisation of radioactive wastes.* Handbook of Advanced Radioactive Waste Conditioning Technologies, Woodhead, Oxford, 2011: p. 67-135.

15. Duxson, P., et al., *The role of inorganic polymer technology in the development of 'green concrete'.* Cement and Concrete Research, 2007. **37**(12): p. 1590-1597.

16. Neville, A.M., *Properties of concrete.* Vol. Fourth edition. 2003: Harlow : Longman Group

17. British Geological Survey. *Cement: Mineral Planning Factsheet.* 2005 [cited 2013 November]; Available from: https://www.bgs.ac.uk/downloads/start.cfm?id=1353.

18. Borges., P.H.R., et al., *Carbonation of CH and C–S–H in composite cement pastes containing high amounts of BFS.* Cement and Concrete Research, 2010. **40**(2): p. 284-292.

19. Harris, A.W., *An assessment of the pH buffering provided by the Nirex reference vault backfill within a radioactive waste repository.* Nirex Report NSS, 1998. **323**: p. 1998.

20. Malhotra, V.M., *Durability of concrete incorporating high-volume of low-calcium (ASTM Class F) fly ash.* Cement and Concrete Composites, 1990. **12**(4): p. 271-277.

21. Wang, X.-Y. and H.-S. Lee, *A model for predicting the carbonation depth of concrete containing low-calcium fly ash.* Construction and Building Materials, 2009. **23**(2): p. 725-733.

22.   Papadakis, V.G., *Effect of fly ash on Portland cement systems: Part I. Low-calcium fly ash.* Cement and Concrete Research, 1999. **29**(11): p. 1727-1736.

23.   Pavía, S. and E. Condren, *Study of the durability of OPC versus GGBS concrete on exposure to silage effluent.* Journal of Materials in Civil Engineering, 2008. **20**(4): p. 313-320.

24.   Bogue, R.H., *The chemistry of Portland cement.* Soil Science, 1955. **79**(4): p. 322.

25.   Joshi, R.C. and R.P. Lohita, *Fly ash in concrete: production, properties and uses.* 1997: CRC Press.

26.   Faucon, P., et al., *Long-term behaviour of cement pastes used for nuclear waste disposal: review of physico-chemical mechanisms of water degradation.* Cement and Concrete Research, 1998. **28**(6): p. 847-857.

27.   Glasser, F.P., J. Marchand, and E. Samson, *Durability of concrete—degradation phenomena involving detrimental chemical reactions.* Cement and Concrete Research, 2008. **38**(2): p. 226-246.

28.   Abou-Mesalam, M.M., *Leaching behavior of some radionuclides from cement matrix incorporating exhausted polymeric resins.* Journal of Radioanalytical and Nuclear Chemistry, 2002. **251**(1): p. 123-128.

29.   Akers, D.W., N.C. Kraft, and J.W. Mandler, *Release of radionuclides and chelating agents from cement-solidified decontamination low-level radioactive waste collected from the Peach Bottom Atomic Power Station Unit 3*, in *Other Information: PBD: Mar 1994.* 1994. p. Medium: ED; Size: 129 p.

30.   Alexander, M., A. Bertron, and N. De Belie, *Performance of Cement-based Materials in Aggressive Aqueous Environments.* 2013: Springer.

31.   Bar-Nes, G., et al., *The mechanism of cesium immobilization in densified silica-fume blended cement pastes.* Cement and Concrete Research, 2008. **38**(5): p. 667-674.

32.   Carde, C., R. François, and J.-M. Torrenti, *Leaching of both calcium hydroxide and CSH from cement paste: Modeling the mechanical behavior.* Cement and concrete research, 1996. **26**(8): p. 1257-1268.

33.   Fuhrmann, M., et al. *The effects of temperature on the leaching behavior of cement waste forms: The cement/sodium sulfate system*. in *MRS Proceedings*. 1989.

34.   Aviam, O., et al., *Accelerated biodegradation of cement by sulfur-oxidizing bacteria as a bioassay for evaluating immobilization of low-level radioactive waste.* Applied and environmental microbiology, 2004. **70**(10): p. 6031-6036.

35.   Bertos, M.F., et al., *Investigation of accelerated carbonation for the stabilisation of MSW incinerator ashes and the sequestration of CO2.* Green Chemistry, 2004. **6**(8): p. 428-436.

36.   Saito, H. and A. Deguchi, *Leaching tests on different mortars using accelerated electrochemical method.* Cement and Concrete Research, 2000. **30**(11): p. 1815-1825.

37.   Hidalgo, A., C. Andrade, and C. Alonso, *An accelerated leaching test to evaluate the long term behaviour of concrete in waste disposal.* L'Industria Italiana del Cemento, 2001. **766**: p. 498-507.

38.   Hermansson, H.-P. and S. Eriksson, *Corrosion of the copper canister in the repository environment.* SKI Report, 1999. **99**: p. 52.

39.   Ekström, T., *Leaching of concrete: experiments and modelling*, in *Report TVBM 3090*. 2001.

40.   Heikola, T., *Dynamic leach testing of low-and medium-pH injection grouts to be used in deep repositories: cementitious materials in deep geological repositories.* Working Reports - Posiva, 2008.

41.   Fick, A., *V. On liquid diffusion.* The London, Edinburgh, and Dublin Philosophical Magazine and Journal of Science, 1855. **10**(63): p. 30-39.

42.   Cau Dit Coumes, C., et al., *Formulating a low-alkalinity, high-resistance and low-heat concrete for radioactive waste repositories.* Cement and Concrete Research, 2006. **36**(12): p. 2152-2163.

43.   Miller, W., et al., *Geological disposal of radioactive wastes and natural analogues.* Vol. 2. 2000: Elsevier.

44. Matschei, T., B. Lothenbach, and F.P. Glasser, *The role of calcium carbonate in cement hydration.* Cement and Concrete Research, 2007. **37**(4): p. 551-558.

45. Richardson, M.G., *Carbonation of reinforced concrete: Its causes and management.* 1988, Dublin, London and New York: CITIS LTD.

46. Silva, C.A., et al., *Carbonation-Related Microstructural Changesin Long-Term Durability Concrete.* Materials Research, 2002. **5**(3): p. 287-293.

47. Hills, C.D., R.E.H. Sweeney, and N.R. Buenfeld, *Microstructural study of carbonated cement-solidified synthetic heavy metal waste.* Waste Management, 1999. **19**(5): p. 325-331.

48. Lange, L.C., C.D. Hills, and A.B. Poole, *Preliminary investigation into the effects of carbonation on cement-solidified hazardous wastes.* Environmental science & technology, 1995. **30**(1): p. 25-30.

49. Walton, J.C., et al., *Role of Carbonation in Transient Leaching of Cementitious Wasteforms.* Environmental Science & Technology, 1997. **31**(8): p. 2345-2349.

50. Sanchez, F., et al., *Leaching of inorganic contaminants from cement-based waste materials as a result of carbonation during intermittent wetting.* Waste Management, 2002. **22**(2): p. 249-260.

51. Hill, J., et al., *The effect of sodium chloride on the dissolution of calcium silicate hydrate gels.* Waste Management, 2006. **26**(7): p. 758-768.

52. Kishar, E.A., et al., *Effect of calcium chloride on the hydration characteristics of ground clay bricks cement pastes.* Beni-Suef University Journal of Basic and Applied Sciences, 2013. **2**(1): p. 20-30.

53. Lagerblad, B. and J. Trägårdh, *Conceptual model for concrete long time degradation in a deep nuclear waste repository.* 1994, Svensk Kärnbränslehantering AB: Swedish Cement and Concrete Research Institute.

54. Gascoyne, M., *Influence of grout and cement on groundwater composition.* 2002, POSIVA Working Report: Helsinki

55. Holgersson, S., et al., *Effects of gluco-isosaccharinate on Cs, Ni, Pm and Th sorption onto, and diffusion into cement.* Radiochimca Acta, 1998. **82**(Supplement): p. 393-398.

56. Wolfaardt, G.M. and D.R. Korber, *Near-field Microbiological Considerations Relevant to a Deep Geological Repository for used Nuclear Fuel–State of Science Review.* Report NWMO TR-2012-02. Nuclear Waste Management Organization, Toronto, 2012.

57. Pedersen, K., *Microbial processes in radioactive waste disposal.* 2000, Svensk Kärnbränslehantering AB/Swedish Nuclear Fuel and Waste Management Company.

58. Grant W G, et al., *The survival of micro-organisms in a deep cementitious repository under alkaline, high temperature conditions.* AEA Technology Report, 2001. **AEAT/R/ENV/0227**.

59. Sand, W. and E. Bock, *Biodeterioration of mineral materials by microorganisms—biogenic sulfuric and nitric acid corrosion of concrete and natural stone.* Geomicrobiology Journal, 1991. **9**(2-3): p. 129-138.

60. Sand, W., *Microbial mechanisms of deterioration of inorganic substrates—A general mechanistic overview.* International Biodeterioration & Biodegradation, 1997. **40**(2–4): p. 183-190.

61. Gadd, G.M., *Microbial influence on metal mobility and application for bioremediation.* Geoderma, 2004. **122**(2–4): p. 109-119.

62. Kieft, T.L. and T.J. Phelps, *Life in the slow lane: activities of microorganisms in the subsurface.* The microbiology of the terrestrial deep subsurface, 1997: p. 137-163.

63. Olmstead, W. and H. Hamlin, *Converting portions of the Los Angeles outfall sewer into a septic tank.* Eng News, 1900. **44**(19): p. 317-318.

64. Kappler, U., et al., *Sulfite: Cytochrome c Oxidoreductase fromThiobacillus novellus purification, characterization, and molecular biology of a heterodimeric member of the sulfite oxidase family.* Journal of Biological Chemistry, 2000. **275**(18): p. 13202-13212.

65. King, F., P. Humphreys, and R. Metcalfe, *A Review of the Information Available to Assess the Risk of Microbiologically Influenced Corrosion in Waste Packages.* 2011, Quintessa Ltd, Henley-on-Thames, UK.

66. Gadd, G.M., *Fungal Production of Citric and Oxalic Acid: Importance in Metal Speciation, Physiology and Biogeochemical Processes*, in *Advances in Microbial Physiology*, R.K. Poole, Editor. 1999, Academic Press. p. 47-92.

67. Zhdanova, N.N., et al., *Fungi from Chernobyl: mycobiota of the inner regions of the containment structures of the damaged nuclear reactor.* Mycological Research, 2000. **104**(12): p. 1421-1426.

68. Gaylarde, C.C. and L.G. Morton, *Deteriogenic biofilms on buildings and their control: a review.* Biofouling, 1999. **14**(1): p. 59-74.

69. Wei, S., et al., *Microbiologically induced deterioration of concrete: a review.* Brazilian Journal of Microbiology, 2014(AHEAD): p. 0-0.

70. Humphreys, P., J. West, and R. Metcalfe, *Microbial effects on repository performance.* Quintessa contractors report prepared for the Nuclear Decommissioning Authority (Radioactive Waste Management Directorate), Harwell, Didcot, Oxfordshire, UK, 2010.

71. Santo Domingo, J.W., et al., *Microbiology of spent nuclear fuel storage basins.* Current microbiology, 1998. **37**(6): p. 387-394.

72. Diosi, G., et al., *Corrosion influenced by biofilms during wet nuclear waste storage.* International biodeterioration & biodegradation, 2003. **51**(2): p. 151-156.

73. Chicote, E., et al., *Biofouling on the walls of a spent nuclear fuel pool with radioactive ultrapure water.* Biofouling, 2004. **20**(1): p. 35-42.

74. Tanji, Y., et al., *Structural analysis of a biofilm which enhances carbon steel corrosion in nutritionally poor aquatic environments.* Journal of bioscience and bioengineering, 1999. **88**(5): p. 551-556.

75. Sarró, M.I., et al., *Biofouling on austenitic stainless steels in spent nuclear fuel pools.* Materials and Corrosion, 2003. **54**(7): p. 535-540.

76. Busscher, H.J. and H.C. van der Mei, *Microbial adhesion in flow displacement systems.* Clinical microbiology reviews, 2006. **19**(1): p. 127-141.

77. Eccles, H., *Process for the treatment of contaminated material.* U.S. Patent No. 5,840,191, 1999.

78. OlSiwbiillOn, O.F., *An assessment of the important radionuclides in nuclear waste.* 1985.

79. Evans, N.D.M., *Binding mechanisms of radionuclides to cement.* Cement and Concrete Research, 2008. **38**(4): p. 543-553.

80. Atkins, M. and F.P. Glasser, *Application of Portland cement-based materials to radioactive waste immobilization.* Waste Management, 1992. **12**(2): p. 105-131.

81. Bonen, D. and S.L. Sarkar. *Environmental attack on concrete.* in *Proc 16th Eng Found Conf, Am Soc Civil Eng* 1994. New York.

82. Noshita, K., T. Nishi, and M. Matsuda, *Improved Sorption Ability for Radionuclides by Cementitious Materials.* WM, 1998. **98**: p. 1880-1886.

83. El-Kamash, A., A. El-Dakroury, and H. Aly, *Leaching kinetics of 137 Cs and 60 Co radionuclides fixed in cement and cement-based materials.* Cement and concrete research, 2002. **32**(11): p. 1797-1803.

84. Colombo, P. and D. Dougherty, *Leaching Mechanisms of Solidified Low-level Waste: The Literature Survey.* 1985: Nuclear Waste Research Group, Department of Nuclear Energy, Brookhaven National Laboratory, Associated Universities.

85. Aggarwal, S., et al., *Radionuclide concentration in cementitious pore-fluids extracted under high pressure.* 2001, AEAT/R/ENV/0231.

86. Brunauer S, E.P.H.T.E., *Adsorption of gases in multimolecular layers.* Journal of the American Chemical Society, 1938. **60**: p. 309-19.

87. Thomas, J.J., Jennings, H. M. and A. J.Allen *The surface area of hardened cement paste as measured by various techniques.* Concrete Science and Engineering, 1999. **1**(1): p. 45 - 64.

88. Odler, I., *The BET-specific surface area of hydrated Portland cement and related materials.* Cement and Concrete Research, 2003. **33**(12): p. 2049-2056.

89. Madigan, M.T., et al., *Brock Biology of microorganisms, 12th edn.* 2008: Pearson Benjamin Cummings, San Francisco, CA, USA.

90. Barrow, G. and R.K.A. Feltham, *Cowan and Steel's manual for the identification of medical bacteria*. 2004: Cambridge university press.

91. Bessey, E.A., *Morphology and Taxonomy of Fungi*. Soil Science. Vol. 71. 1951: London, Constable & Company Limited; Philadelphia,. 79.

92. Zar, J.H., *Biostatistical analysis. 2nd.* Prentice Hall USA, 1984.

93. Gutierrez, N., et al. *Effects of carbonation on the long-term leaching performance of cementitious wasteforms*. in *Proc. 1996 HSRC/WERC Joint Conf. on the Environ*. 1996. Albuquerque, New Mexico: Kansas State Univ., Manhattan, KS (United States).

94. Kinoshita, H., et al., *Carbonation of composite cements with high mineral admixture content used for radioactive waste encapsulation*. Minerals Engineering, 2014. **59**: p. 107-114.

95. Chen, W., *Hydration of slag cement: theory, modeling and application*. Ph.D. Thesis,. 2006, University of Twente, The Netherlands.

96. Song, S., et al., *Hydration of alkali-activated ground granulated blast furnace slag*. Journal of Materials Science, 2000. **35**(1): p. 249-257.

97. Provis, J.L., et al., *X-ray microtomography shows pore structure and tortuosity in alkali-activated binders*. Cement and Concrete Research, 2012. **42**(6): p. 855-864.

98. Khokhar, I.A. *Hydration of Cement*. 2013 [cited 2015 January]; Available from: http://www.slideshare.net/rizwansamor/hydration-of-cement.

99. Radwan, M. and H.S. El, *Hydration characteristics of tetracalcium alumino-ferrite phase in the presence calcium carbonate*. Ceramics-Silikaty, 2011. **55**(4): p. 337-342.

100. Mohran, M.A.A.H. *Cement Hydration*. (n.d) [cited 2015 January]; Available from: http://www.mohran.com/wp-content/uploads/2014/10/Hydration-of-Portland-Cement.pdf.

101. Matschei, T., B. Lothenbach, and F.P. Glasser, *The AFm phase in Portland cement*. Cement and Concrete Research, 2007. **37**(2): p. 118-130.

102. Theissing, E.M., P.V. Hest-Wardenier, and G. De Wind, *The combining of sodium chloride and calcium chloride by a number of different hardened cement pastes.* Cement and Concrete Research, 1978. **8**(6): p. 683-691.

103. Arya, C., N.R. Buenfeld, and J.B. Newman, *Factors influencing chloride-binding in concrete.* Cement and Concrete Research, 1990. **20**(2): p. 291-300.

104. Wan, X.-m., et al., *Chloride content and pH value in the pore solution of concrete under carbonation.* Journal of Zhejiang University SCIENCE A, 2013. **14**(1): p. 71-78.

105. Lafhaj, Z., et al., *Correlation between porosity, permeability and ultrasonic parameters of mortar with variable water/cement ratio and water content.* Cement and Concrete Research, 2006. **36**(4): p. 625-633.

106. Živica, V., *Effects of the very low water/cement ratio.* Construction and Building Materials, 2009. **23**(12): p. 3579-3582.

107. Felekoğlu, B., S. Türkel, and B. Baradan, *Effect of water/cement ratio on the fresh and hardened properties of self-compacting concrete.* Building and Environment, 2007. **42**(4): p. 1795-1802.

108. Prokopski, G. and B. Langier, *Effect of water/cement ratio and silica fume addition on the fracture toughness and morphology of fractured surfaces of gravel concretes.* Cement and concrete research, 2000. **30**(9): p. 1427-1433.

109. Fujita, H., et al., *Concentration and Molecular Weight of Superplasticizer Contained in Pore Solution Extracted from Hardened Cement Pastes.* Journal of Advanced Concrete Technology, 2008. **6**(3): p. 389-395.

110. Adjoudj, M.h., et al., *Evaluation of rheological parameters of mortar containing various amounts of mineral addition with polycarboxylate superplasticizer.* Construction and Building Materials, 2014. **70**(0): p. 549-559.

111. Tasdemir, C., *Combined effects of mineral admixtures and curing conditions on the sorptivity coefficient of concrete.* Cement and Concrete Research, 2003. **33**(10): p. 1637-1642.

112. Young, A.J., et al., *Behaviour of radionuclides in the presence of superplasticiser.* Advances in Cement Research, 2013. **25**(1): p. 32-43.

113. McCulloch, C.E., et al., *Cements in radioactive waste disposal: some mineralogical considerations.* Mineralogical Magazine, 1985. **49**(351): p. 211-221.

114. Gruyaert, E., et al., *Investigation of the influence of blast-furnace slag on the resistance of concrete against organic acid or sulphate attack by means of accelerated degradation tests.* Cement and Concrete Research, 2012. **42**(1): p. 173-185.

115. Bordallo, H.N., L.P. Aldridge, and A. Desmedt, *Water dynamics in hardened ordinary portland cement paste or concrete: From quasielastic neutron scattering.* The Journal of Physical Chemistry B, 2006. **110**(36): p. 17966-17976.

116. Jensen, O.M. and P.F. Hansen, *Water-entrained cement-based materials: I. Principles and theoretical background.* Cement and Concrete Research, 2001. **31**(4): p. 647-654.

117. Milestone, N.B. and J.P. Gorce, *Determining how water is held in composite cement binders.* Journal of the Australian Ceramic Society, 2012. **48**(2): p. 244-248.

118. Lothenbach, B. and F. Winnefeld, *Thermodynamic modelling of the hydration of Portland cement.* Cement and Concrete Research, 2006. **36**(2): p. 209-226.

119. Bentz, D., et al., *Drying/hydration in cement pastes during curing.* Materials and Structures, 2001. **34**(9): p. 557-565.

120. Ravindrarajah, R.S. *Bleeding of fresh concrete containing cement supplementary materials.* in *9th East Asia-Pacific Conference on Structural Engineering and Construction.* 16-18 December, 2003. Bali, Indonesia, .

121. Persson, B., D.P. Bentz, and G. Fagerlund. *Self-desiccation and its importance in concrete technology.* in *Proceedings of the fourth international research seminar, Gaithersburg, .* 2005. Maryland, USA: Div Building Materials, LTH, Lund university.

122. Maltais, Y., E. Samson, and J. Marchand, *Predicting the durability of Portland cement systems in aggressive environments—laboratory validation.* Cement and Concrete Research, 2004. **34**(9): p. 1579-1589.

123. Samson, E. and J. Marchand, *Modeling the effect of temperature on ionic transport in cementitious materials.* Cement and Concrete Research, 2007. **37**(3): p. 455-468.

124. John Innes Manufacturers Association. *About John Innes.* (n.d) [cited 2014 June]; Available from: http://www.johninnes.info/about.htm.

125. Wolf-Gladrow, D.A., et al., *Total alkalinity: The explicit conservative expression and its application to biogeochemical processes.* Marine Chemistry, 2007. **106**(1–2): p. 287-300.

126. Berner, U., *Concentration limits in the cement based Swiss repository for long-lived, intermediate-level radioactive wastes (LMA).* 1999, Paul Scherrer Inst., CH-5232 Villigen PSI (Switzerland).

127. Tits, J., et al., *Strontium binding by calcium silicate hydrates.* Journal of colloid and interface science, 2006. **300**(1): p. 78-87.

128. Evans, N., *Binding mechanisms of radionuclides to cement.* Cement and concrete research, 2008. **38**(4): p. 543-553.

129. Abotsi, G., D. Bostick, and D. Beck, *Evaluation of interim and final waste forms for the newly generated liquid low-level waste flowsheet.* 1996, Oak Ridge National Lab., TN (United States). Funding organisation: USDOE, Washington, DC (United States).

130. Zha, X., et al., *Numerical modeling of supercritical carbonation process in cement-based materials.* Cement and Concrete Research, 2015. **72**(0): p. 10-20.

131. Johannesson, B. and P. Utgenannt, *Microstructural changes caused by carbonation of cement mortar.* Cement and concrete Research, 2001. **31**(6): p. 925-931.

132. Song, H.-W. and S.-J. Kwon, *Permeability characteristics of carbonated concrete considering capillary pore structure.* Cement and Concrete Research, 2007. **37**(6): p. 909-915.

133. Collins, F. and J. Sanjayan, *Microcracking and strength development of alkali activated slag concrete.* Cement and Concrete Composites, 2001. **23**(4): p. 345-352.

134.   Silva, A., R. Neves, and J. de Brito, *Statistical modelling of carbonation in reinforced concrete.* Cement and Concrete Composites, 2014. **50**: p. 73-81.

135.   Castellote, M., et al., *Accelerated carbonation of cement pastes in situ monitored by neutron diffraction.* Cement and concrete research, 2008. **38**(12): p. 1365-1373.

136.   Bertos, M.F., et al., *A review of accelerated carbonation technology in the treatment of cement-based materials and sequestration of CO 2.* Journal of Hazardous Materials, 2004. **112**(3): p. 193-205.

137.   Sanchez, F., et al., *Leaching of inorganic contaminants from cement-based waste materials as a result of carbonation during intermittent wetting.* Waste Management, 2002. **22**(2): p. 249-260.

138.   Bertos, M.F., et al., *Investigation of accelerated carbonation for the stabilisation of MSW incinerator ashes and the sequestration of CO 2.* Green Chemistry, 2004. **6**(8): p. 428-436.

139.   Shafique, M.S.B., et al., *Influence of carbonation on leaching of cementitious wasteforms.* Journal of Environmental Engineering, 1998. **124**(5): p. 463-467.

140.   Atkinson, A., K. Nelson, and T.M. Valentine, *Leach test characterisation of cement-based nuclear waste forms.* Nuclear and Chemical Waste Management, 1986. **6**(3-4): p. 241-253.

141.   Voglis, N., et al., *Portland-limestone cements. Their properties and hydration compared to those of other composite cements.* Cement and Concrete Composites, 2005. **27**(2): p. 191-196.

142.   Lothenbach, B., et al., *Influence of limestone on the hydration of Portland cements.* Cement and Concrete Research, 2008. **38**(6): p. 848-860.

143.   Rahman, R.A., D.Z. El Abidin, and H. Abou-Shady, *Cesium binding and leaching from single and binary contaminant cement–bentonite matrices.* Chemical Engineering Journal, 2014. **245**: p. 276-287.

144.   Mahoney, J.D. and A.D. Elaine. *Radiochemical studies of the leaching of metal ions from sludge bearing concrete.* in *Third Conference On Advanced Pollution Control For The Metal Finishing Industry* 1981. Orlando Hyatt House, Kissimmee, FL.

145. Faucon, P., et al., *Behaviour of crystallised phases of Portland cement upon water attack.* Materials and Structures, 1997. **30**(8): p. 480-485.

146. Haga, K., et al., *Effects of porosity on leaching of Ca from hardened ordinary Portland cement paste.* Cement and Concrete Research, 2005. **35**(9): p. 1764-1775.

147. Mainguy, M., et al., *Modelling of leaching in pure cement paste and mortar.* Cement and Concrete Research, 2000. **30**(1): p. 83-90.

148. Kuhl, D., F. Bangert, and G. Meschke, *Coupled chemo-mechanical deterioration of cementitious materials. Part I: Modeling.* International Journal of Solids and Structures, 2004. **41**(1): p. 15-40.

149. Holt, E., *Durability of low-pH injection grout. A literature survey.* 2008, Posiva Oy, Helsinki (Finland).

150. Goñi, S. and A. Guerrero, *Accelerated carbonation of Friedel's salt in calcium aluminate cement paste.* Cement and Concrete Research, 2003. **33**(1): p. 21-26.

151. Ouyang, C., A. Nanni, and W.F. Chang, *Internal and external sources of sulfate ions in Portland cement mortar: two types of chemical attack.* Cement and Concrete Research, 1988. **18**(5): p. 699-709.

152. Al-Amoudi, O.S.B., *Attack on plain and blended cements exposed to aggressive sulfate environments.* Cement and Concrete Composites, 2002. **24**(3): p. 305-316.

153. Fu, Y., J. Ding, and J. Beaudoin, *Expansion of portland cement mortar due to internal sulfate attack.* Cement and Concrete Research, 1997. **27**(9): p. 1299-1306.

154. Rozière, E., et al., *Durability of concrete exposed to leaching and external sulphate attacks.* Cement and Concrete Research, 2009. **39**(12): p. 1188-1198.

155. Neville, A., *The confused world of sulfate attack on concrete.* Cement and Concrete Research, 2004. **34**(8): p. 1275-1296.

156. Estokova, A., et al., *Sulphur oxidizing bacteria as the causative factor of biocorrosion of concrete.* Chem. Eng. Trans, 2011. **24**: p. 1-6.

157.   Li, V.C. and E.-H. Yang, *Self healing in concrete materials*, in *Self Healing Materials*. 2007, Springer. p. 161-193.

158.   Guppy, R., *Autogenous healing of cracks in concrete and its relevance to radwaste repositories*. 1988, United Kingdom Nirex, Ltd.

159.   Harr, M.E., *Ground water and seepage*, in *The Civil Engineering Handbook, Second Edition*, W.F. Chen and J.Y.R. Liew, Editors. 2002, CRC Press. p. 18.3 -18.26.

160.   Samson, E., J. Marchand, and K. Snyder, *Calculation of ionic diffusion coefficients on the basis of migration test results.* Materials and Structures, 2003. **36**(3): p. 156-165.

161.   Ahmad, A. and A. Kumar, *Chloride ion migration/diffusion through concrete and test methods.* International Journal of Advanced Scientific and Technical Research, 2013. **6**(3).

162.   Johannesson, B., et al., *Multi-species ionic diffusion in concrete with account to interaction between ions in the pore solution and the cement hydrates.* Materials and structures, 2007. **40**(7): p. 651-665.

163.   Batchelor, B., *Leach models: Theory and application.* Journal of Hazardous Materials, 1990. **24**(2–3): p. 255-266.

164.   Park, J.-Y. and B. Batchelor, *General chemical equilibrium model for stabilized/solidified wastes.* Journal of environmental engineering, 2002. **128**(7): p. 653-661.

165.   Rogers, R., et al., *Development of test methods for assessing microbial influenced degradation of cement-solidified radioactive and industrial waste.* Cement and concrete research, 2003. **33**(12): p. 2069-2076.

166.   West, J.M. and I.G. Mckinley, *Radioactive Waste Disposal, Geomicrobiology of*. 2002: Wiley Online Library.

167.   House, M. and W. Weiss, *Review of Microbially Induced Corrosion and Comments on Needs Related to Testing Procedures.* 2014.

168.   Haferburg, G. and E. Kothe, *Microbes and metals: interactions in the environment.* Journal of basic microbiology, 2007. **47**(6): p. 453-467.

169. Eccles, H., *Personal communication with Prof Eccles.* 2011.

170. Pedersen, K. and F. Karlsson, *Investigations of subterranean microorganisms: their importance for performance assessment of radioactive waste disposal.* 1995: SKB.

171. DEFRA, BERR, and D. ADMINISTRATIONS, *Managing Radioactive Waste Safely: A Framework for Implementing Geological Disposal.* Vol. cm 7386. 2008, The Stationery Office, London.

172. Horn, J.M., et al., *Bacterial growth dynamics, limiting factors, and community diversity in a proposed geological nuclear waste repository environment.* Geomicrobiology Journal, 2004. **21**(4): p. 273-286.

173. Perfettini, J.V., E. Revertegat, and N. Langomazino, *Evaluation of cement degradation induced by the metabolic products of two fungal strains.* Experientia, 1991. **47**(6): p. 527-533.

174. Molnár, M., et al., *Study of gas generation in real L/ILW containers.* Journal of radioanalytical and nuclear chemistry, 2010. **286**(3): p. 745-750.

175. Gadd, G.M., *Metals, minerals and microbes: geomicrobiology and bioremediation.* Microbiology, 2010. **156**(3): p. 609-643.

176. Silver, S. and T.K. Misra, *Plasmid-mediated heavy metal resistances.* Annual Reviews in Microbiology, 1988. **42**(1): p. 717-743.

177. Giannantonio, D.J., et al., *Effects of concrete properties and nutrients on fungal colonization and fouling.* International Biodeterioration & Biodegradation, 2009. **63**(3): p. 252-259.

178. Magniont, C., et al., *A new test method to assess the bacterial deterioration of cementitious materials.* Cement and Concrete Research, 2011. **41**(4): p. 429-438.

179. Önal, M.M., *Reinforcement of Beam by Using Carbon Fiber Reinforced Polymer in Concrete Buildings.* Sci. Res. Essay, 2009. **4**(10): p. 1136-1145.

180. Lahav, O., et al., *Modeling hydrogen sulfide emission rates in gravity sewage collection systems.* Journal of environmental engineering, 2004. **130**(11): p. 1382-1389.

181. Vollertsen, J., et al., *Corrosion of concrete sewers—The kinetics of hydrogen sulfide oxidation.* Science of the total environment, 2008. **394**(1): p. 162-170.

182. Ghafoori, N. and R. Mathis, *Sulfate resistance of concrete pavers.* Journal of materials in civil engineering, 1997. **9**(1): p. 35-40.

183. Lajili, H., et al., *Alteration of a cement matrix subjected to biolixiviation test.* Materials and structures, 2008. **41**(10): p. 1633-1645.

184. Warscheid, T. and J. Braams, *Biodeterioration of stone: a review.* International Biodeterioration & Biodegradation, 2000. **46**(4): p. 343-368.

185. Setareh, M. and R. Javaherdashti, *Evaluation of sessile microorganisms in pipelines and cooling towers of some Iranian industries.* Journal of materials engineering and performance, 2006. **15**(1): p. 5-8.

186. Edwards, K.J., et al., *Geomicrobiology of pyrite (FeS2) dissolution: case study at Iron Mountain, California.* Geomicrobiology Journal, 1999. **16**(2): p. 155-179.

187. Gazsó, L.G., *The key microbial processes in the removal of toxic metals and radionuclides from the environment.* Central European Journal of Occupational and Environmental Medicine, 2001. **7**(3/4): p. 178-185.

188. Bousserrhine, N., et al., *Bacterial and chemical reductive dissolution of Mn-, Co-, Cr-, and Al-substituted goethites.* Geomicrobiology journal, 1999. **16**(3): p. 245-258.

189. Lloyd, J.R., *Microbial reduction of metals and radionuclides.* FEMS microbiology reviews, 2003. **27**(2-3): p. 411-425.

190. Barkay, T. and J. Schaefer, *Metal and radionuclide bioremediation: issues, considerations and potentials.* Current opinion in microbiology, 2001. **4**(3): p. 318-323.

191. Bryan, N.D., et al., *The effects of humic substances on the transport of radionuclides: recent improvements in the prediction of behaviour and the understanding of mechanisms.* Applied Geochemistry, 2012. **27**(2): p. 378-389.

192.	Gadd, G.M., *Fungal production of citric and oxalic acid: importance in metal speciation, physiology and biogeochemical processes.* Advances in microbial physiology, 1999. **41**: p. 47-92.

193.	Ramsay, L., J. Sayer, and G. Gadd, *Stress responses of fungal colonies towards toxic metals.* The Fungal Colony, 1999: p. 178-200.

194.	Burgstaller, W., et al., *Solubilization of zinc oxide from filter dust with Penicillium simplicissimum: bioreactor leaching and stoichiometry.* Environmental science & technology, 1992. **26**(2): p. 340-346.

195.	Haas, H., *Molecular genetics of fungal siderophore biosynthesis and uptake: the role of siderophores in iron uptake and storage.* Applied Microbiology and Biotechnology, 2003. **62**(4): p. 316-330.

196.	Saha, R., et al., *Microbial siderophores: a mini review.* Journal of basic microbiology, 2013. **53**(4): p. 303-317.

197.	Birch, L. and R. Bachofen, *Complexing agents from microorganisms.* Experientia, 1990. **46**(8): p. 827-834.

198.	Lloyd, J.R. and D.R. Lovley, *Microbial detoxification of metals and radionuclides.* Current Opinion in Biotechnology, 2001. **12**(3): p. 248-253.

199.	Gadd, G.M., *Heavy metal accumulation by bacteria and other microorganisms.* Experientia, 1990. **46**(8): p. 834-840.

200.	Dighton, J., T. Tugay, and N. Zhdanova, *Fungi and ionizing radiation from radionuclides.* FEMS microbiology letters, 2008. **281**(2): p. 109-120.

201.	Gadd, G.M., *Microbial Bioremediation of Metals and Radionuclides.* Encyclopedia of Environmetrics, 2013.

202.	Keith-Roach, M.J. and F.R. Livens, *Microbial interactions with metals/radionuclides: the basis of bioremediation.* Interactions of microorganisms with radionuclides, 2002: p. 179.

203.	Pinheiro, S., M. Silva, and F. dos Santos Souza, *The Influence of Biodeterioration on Concrete Durability.* ACI Special Publication, 2005. **229**.

204. Dighton, J., T. Tugay, and N. Zhdanova, *Interactions of fungi and radionuclides in soil*, in *Microbiology of Extreme Soils*. 2008, Springer. p. 333-355.

205. Padan, E., et al., *Alkaline pH homeostasis in bacteria: new insights.* Biochimica et biophysica acta (BBA)-biomembranes, 2005. **1717**(2): p. 67-88.

206. Roger, G.M., et al., *Effect of ionic condensation and interactions between humic substances on their mobility: An experimental and simulation study.* Colloids and Surfaces A: Physicochemical and Engineering Aspects, 2013. **436**: p. 408-416.

207. Ephraim, J.H. and B. Allard, *Metal ion binding by humic substances.* Modelling in Aquatic Chemistry, 1997: p. 207-244.

208. Shaban, I.S. and F. Macášek, *Influence of humic substances on sorption of cesium and strontium on montmorillonite.* Journal of radioanalytical and nuclear chemistry, 1998. **229**(1): p. 73-78.

209. Dumat, C. and S. Staunton, *Reduced adsorption of caesium on clay minerals caused by various humic substances.* Journal of Environmental Radioactivity, 1999. **46**(2): p. 187-200.

210. Rice, G., N. Miles, and S. Farris, *Approaches to control the quality of cementitious PFA grouts for nuclear waste encapsulation.* Powder Technology, 2007. **174**(1–2): p. 56-59.

211. Morton, L.H.G., *Personal communication with Prof Morton.* 2012.

212. Somdee, T., et al., *Degradation of [Dha(7)]MC-LR by a Microcystin Degrading Bacterium Isolated from Lake Rotoiti, New Zealand.* ISRN Microbiology, 2013. **2013**: p. 596429.

213. ANSI/ANS-16.1-2003, *Measurement of the Leachability of Solidified Low-Level Radioactive Wastes by a Short-Term Test Procedure.* American Nuclear Society, ANS, 2003. **http://www.ans.org/**.

214. Ramachandran, V.S., *Calcium chloride in concrete.* Mag Concr Res, 1977. **29**: p. 1-216.

215. Bortoluzzi, E.A., et al., *The Influence of Calcium Chloride on the Setting Time, Solubility, Disintegration, and pH of Mineral Trioxide Aggregate and*

White Portland Cement with a Radiopacifier. Journal of Endodontics, 2009. **35**(4): p. 550-554.

216.   Avery, S.V., *Caesium accumulation by microorganisms: uptake mechanisms, cation competition, compartmentalization and toxicity.* Journal of industrial microbiology, 1995. **14**(2): p. 76-84.

217.   Chaplow, J.S., N.A. Beresford, and C.L. Barnett, *Post Chernobyl surveys of radiocaesium in soil, vegetation, wildlife and fungi in Great Britain.* Earth System Science Data Discussions, 2014. **7**(2): p. 693-711.

218.   ASTM C1240-14, *Standard Specification for Silica Fume Used in Cementitious Mixtures.* ASTM International, West Conshohocken, PA, 2014. **www.astm.org**.

219.   V.S. Ramachandran, et al., *Supplementary Cementing Materials and other additions.* Handbook of Thermal Analysis of Construction Materials. 1987, USA: Noyes Publications. 300 - 302.

220.   Bagosi, S. and L.J. Csetenyi, *Caesium immobilisation in hydrated calcium-silicate-aluminate systems.* Cement and concrete research, 1998. **28**(12): p. 1753-1759.

221.   Hong, S.-Y. and F.P. Glasser, *Alkali binding in cement pastes: Part I. The C-S-H phase.* Cement and Concrete Research, 1999. **29**(12): p. 1893-1903.

Appendices

Appendix 2.1: summary of cement paste mixture proportions, CPS dimentions, cations concentration of BFS:OPC CPSs

| CPS | cement paste mixture proportions | | | | | CPS weight | CPS dimensions | Cation concentration of CPS |
| | OPC | BFS | Volume of cation soln added | SG of cation soln | Cation soln composition | | | |
	(g)	(g)	(mL)	(g/cm^3)	(g/L)	(g)	(dia x h cm)	(g/g)
control	300	900	440 (DI water)	1	-	83.7088	3.2 X 5	-
≈3% SrCl$_2$	400	1200	674.37 (590)	1.143	304.2	84.3944	3.2 X 5	0.094 [2.91%]
≈3% CsCl	400	1200	639.56 (590)	1.084	126.27	87.2456	3.2 X 5.2	0.04 [3.01%]
≈1.27% CoCl$_2$	400	1200	640 (600)	1..067	216.83 ***	91.8604	3.2 X 5.6	[1.27%]
mixed	400	1200	767 (590)	1.3	304.2 (Sr) 126.27 (Cs) prepared in 5% CoCl$_2$	97.8814	3.2 X 5.7	0.11Sr Sr[2.66%] 0.04 (Cs) [2.67%] Co [1.12%]
≈0.3% SrCl$_2$	200	600	300 (DI water)	**	(9.126 g)** 3.01gSr	82.0506	3.2 X 5	0.01 [0.27%]
≈0.3% CsCl	200	600	300 (DI water)	**	(3.788 g) ** 2.98gCs	81.468	3.2 X 5.2	0.003 [0.27%]
≈3% Sr CO$_3$	200	600	300 (DI water)	**	(50.486 g) ** 31.00g Sr	82.5966	3.2 X 5	0.046 [2.7%]
≈0.3% SrCO$_3$	200	600	300 (DI water)	**	(5.0486 g)** 3.10g Sr	84.9904	3.2 X 5.3	0.005 [0.27%]

** Required amount of salts (Sr^{2+} and Cs$^+$) was added directly to DI water prior to the addition of OPC and BFS

*** The appropriate percentage of CoCl$_2$ solution i.e 3% could not be achieved because of the solubility of cobalt chloride in the water

Appendix 2.2 summary of cement paste mixture proportions, CPS dimentions, cations concentration of PFA:OPC CPSs

| CPS | cement paste mixture proportions | | | | | CPS weight | CPS dimensions | Cation concentration of CPS |
| | OPC | PFA | Volume of cation soln added | SG of cation soln | Cation soln composition | | | |
	(g)	(g)	(mL)	(g/cm^3)	(g/L)	(g)	(dia x h cm)	(g/g)
control	200	600	300 (DI water)	1	-	73.477	3.2 X 5.5	-
≈3% SrCl$_2$	200	600	300 (DI water)	**	(91.26 g)** 30.02g Sr^{2+}	73.9296	3.2 X 5.5	0.083 [2.52%]
≈3% CsCl	200	600	300 (DI water)	**	(37.881 g)** 29.85 g Cs$^+$	72.0874	3.2 X 5.4	0.034 [2.62%]
≈0.3% SrCl$_2$	200	600	300 (DI water)	**	(9.126 g)** 2.5 g Sr	73.3911	3.2 X 5.6	0.008 [0.25%]
≈0.3% CsCl	200	600	300 (DI water)	**	(3.788 g)** 2.6 g Cs$^+$	70.6848	3.2 X 5.5	0.003 [0.26%]
≈3% Sr CO$_3$	200	600	300 (DI water)	**	(50.486 g)** 31.00g Sr^{2+}	76.8034	3.2 X 5.5	0.046 [2.70%]
≈0.3% SrCO$_3$	200	600	300 (DI water)	**	(5.0486 g)** 3.10g Sr^{2+}	72.1403	3.2 X 5.6	0.005 [0.27%]

** Required amount of salts (Sr^{2+} and Cs$^+$) was added directly to DI water prior to the addition of OPC and PFA

Appendix 4.1 Rate of diffusivity from control BFS:OPC CPS in DW

Days	Na$^+$	Ca^{2+}	Sr^{2+}	Cs$^+$	Cl$^-$	SO$_4$$^{2-}$	pH
			Rate of diffusivity (µg/cm^2/day)				
7	27.13	14.84	0.1631	0.0000	3.49	74.14	10.74
14	13.47	6.69	0.0933	0.0000	12.83	52.39	11.27
21	13.42	7.85	0.0562	0.0010	20.72	35.79	11.43
28	6.63	3.18	0.0598	0.0001	4.77	20.30	11.7
35	4.39	2.45	0.1136	0.0015	4.67	16.12	11.82
42	2.75	2.43	0.0341	0.0001	4.06	9.42	11.74
49	2.09	2.15	0.0191	0.0000	2.42	9.60	11.76
56	1.63	1.86	0.0165	0.0000	1.07	6.59	12.05
63	1.40	1.67	0.0142	0.0013	2.08	4.14	11.99
70	2.25	3.94	0.0206	0.0008	0.92	4.12	11.72
77	1.96	3.89	0.0172	0.0005	1.14	3.79	11.54
84	1.65	5.21	0.0206	0.0017	1.38	4.51	11.24
91	1.38	4.39	0.0161	0.0013	0.55	2.17	12.14
98	1.23	8.56	0.0967	0.0013	2.03	1.83	12.09
105	1.09	5.26	0.0291	0.0066	1.38	1.78	11.71
112	0.95	6.47	0.0251	0.0009	1.22	2.16	11.86
119	0.88	3.83	0.0156	0.0027	1.53	1.90	12
126	0.36	12.87	0.0066	0.0090	1.22	1.75	11.95
141	0.35	3.11	0.0068	0.0011	0.96	1.48	12.13
156	0.58	3.30	0.0112	0.0050	0.85	1.42	11.95
171	0.53	1.58	0.0104	0.0044	0.71	1.35	12.01
186	0.24	1.13	0.0081	0.0033	0.68	1.28	12.03
201	0.38	0.99	0.0488	0.0030	0.67	1.15	11.93

Appendix 4.2 Rate of diffusivity from ≈3% SrCl₂ BFS:OPC CPS in DW

Days	Na$^+$	Ca^{2+}	Sr^{2+}	Cl$^-$	SO$_4^{2-}$	pH
	Rate of diffusivity (µg/cm^2/day)	
7	33.23	101.54	74.60	299.47	34.98	11.19
14	18.12	63.49	48.50	192.73	9.24	11.8
21	16.72	62.89	46.84	165.16	28.87	11.75
28	8.84	34.98	27.33	106.88	11.95	11.91
35	5.95	24.74	19.94	85.58	3.29	12.01
42	3.93	17.30	13.90	71.19	9.00	12.03
49	2.84	13.29	10.77	70.29	9.83	11.93
56	2.13	10.19	8.24	45.39	2.03	12.03
63	1.88	9.29	7.30	47.24	4.92	12.02
70	2.84	14.29	10.52	64.89	6.49	11.65
77	2.49	12.90	8.98	36.35	7.44	11.56
84	1.95	10.78	7.23	34.51	6.48	11.29
91	1.58	8.35	5.90	5.11	1.86	11.62
98	1.53	14.32	5.51	2.07	0.81	11.54
105	1.35	14.66	4.70	14.07	0.68	11.4
112	1.11	13.94	4.22	14.38	0.99	11.66
119	1.01	6.96	3.76	13.89	0.66	11.61
126	0.80	29.89	4.13	8.95	1.13	11.85
141	0.46	6.74	2.12	8.57	1.21	11.97
156	0.71	7.54	3.20	8.69	1.17	11.93
171	0.66	7.40	3.03	7.23	1.08	11.94
186	0.50	4.93	2.23	4.47	0.96	11.95
201	0.36	2.97	1.69	4.65	0.74	11.75

Appendix 4.3 Rate of diffusivity from ≈3% CsCl BFS:OPC CPS in DW

Days	Na$^+$	Ca^{2+}	Cs$^+$	Cl$^-$	SO$_4^{2-}$	pH
			Rate of diffusivity (µg/cm^2/day)			
7	5.85	4.93	110.60	34.17	18.05	10.40
14	3.00	0.75	54.17	18.23	9.23	11.04
21	3.38	0.38	33.39	9.75	4.16	11.27
28	2.24	0.43	17.87	7.72	2.86	11.36
35	3.20	0.33	41.47	8.53	2.40	11.20
42	1.00	0.09	14.20	4.81	1.97	11.57
49	0.72	0.05	11.76	3.33	1.69	11.34
56	0.56	0.04	8.85	3.65	1.16	11.60
63	0.77	0.12	13.43	2.20	0.76	11.15
70	0.78	0.07	12.50	1.73	0.68	11.22
77	0.41	0.06	6.51	1.37	0.57	10.88
84	0.97	0.37	12.36	1.20	0.60	11.14
91	0.60	0.27	9.35	0.81	0.36	10.74
98	0.92	0.30	20.96	0.85	0.31	11.59
105	1.06	0.22	22.88	0.86	0.23	10.43
112	0.98	0.14	21.29	0.85	0.18	9.88
119	0.87	0.13	19.77	1.84	0.24	9.61
126	0.73	0.19	16.87	2.35	0.18	9.57
133	0.61	0.10	14.93	1.63	0.21	9.55
140	0.62	0.07	14.66	1.44	0.14	9.29
147	0.59	0.05	14.10	1.45	0.14	9.01
162	0.51	0.07	12.71	1.23	0.13	9.31
177	0.61	0.15	16.01	1.18	0.12	9.31
192	0.63	0.29	15.52	1.10	0.09	9.74
207	0.53	0.30	12.54	1.18	0.09	9.59

Appendix 4.4 Rate of diffusivity from ≈1.27% CoCl$_2$ BFS:OPC CPS in DW

Days	Na$^+$	Ca^{2+}	Co^{2+}	Cl$^-$	SO$_4^{2-}$	pH
			Rate of diffusivity (µg/cm^2/day)			
7	17.79	105.82	0.00697	421.85	111.36	9.74
14	9.73	48.86	0.00123	244.89	40.95	10.15
21	14.55	74.84	0.00138	175.43	30.44	10.42
28	10.68	52.81	0.00088	124.67	18.62	10.65
35	8.50	45.93	0.00059	95.62	16.97	10.75
42	2.72	13.93	0.00007	74.39	7.55	11.4
49	4.71	11.60	0.00001	59.82	6.15	11.46
56	1.53	6.21	0.00007	49.31	3.91	11.22
63	3.79	17.65	0.00009	41.06	2.86	11.33
70	3.39	15.87	0.00012	35.70	2.28	11.41
77	0.96	4.39	0.00001	31.21	4.20	11.2
84	2.90	7.16	0.00000	27.16	3.38	11.13
91	1.13	4.90	0.00004	21.62	2.02	11.4
98	2.34	10.33	0.00005	19.04	1.65	12.53
105	1.51	8.04	0.00000	15.38	1.40	11.64
112	1.76	8.09	0.00001	14.59	1.30	11.58
119	1.53	7.33	0.00002	11.60	1.23	11.91
126	1.17	6.05	0.00006	10.42	1.21	11.87
133	0.99	5.31	0.00031	5.23	0.93	11.72
140	1.02	5.06	0.00003	6.02	1.32	11.66
147	1.00	4.68	0.00001	2.66	0.43	11.51
162	0.79	4.18	0.00014	5.03	0.57	11.94
177	0.82	4.35	0.00006	2.20	0.52	11.94
192	0.71	3.83	0.00007	8.48	0.79	12
207	0.50	0.61	0.00001	2.29	0.47	12.06

Appendix 4.5 Rate of diffusivity from combined metal BFS:OPC CPS in DW

Days	Na$^+$	Ca^{2+}	Sr^{2+}	Co^{2+}	Cs$^+$	Cl$^-$	SO$_4$$^{2-}$	pH
				Rate of diffusivity (µg/cm^2/day)				
7	4.95	57.03	43.24	0.00005	102.10	1668	46.09	10.64
14	2.56	26.85	22.38	0.00003	56.34	1065	26.48	10.97
21	2.54	26.08	20.19	0.00000	35.16	760	7.69	11.08
28	1.55	16.09	12.05	0.00000	19.44	585	5.19	11.21
35	2.56	27.88	19.34	0.00004	37.80	509	4.85	11.23
42	0.76	7.88	6.27	0.00000	12.91	369	6.05	11.86
49	0.85	36.63	11.45	0.00000	14.42	298	4.08	11.78
56	0.54	8.04	4.84	0.00000	8.60	250	6.75	11.51
63	0.45	4.42	3.12	0.00002	11.37	206	2.37	11.6
70	0.42	3.90	2.75	0.00001	10.72	174	1.68	11.73
77	0.40	4.00	2.88	0.00000	6.30	153	4.62	11.46
84	0.56	26.55	7.89	0.00000	9.41	131	2.16	11.56
91	0.33	5.31	2.82	0.00000	5.39	107	2.07	11.52
98	0.91	9.30	5.31	0.00000	20.92	94	1.89	12.59
105	0.94	9.54	5.48	0.00000	21.13	74	1.86	11.68
112	0.90	9.23	5.27	0.00000	19.97	70	2.08	11.7
119	0.85	8.79	4.99	0.00000	18.83	51	1.46	11.88
126	0.82	8.77	4.83	0.00000	17.79	42	1.25	11.68
133	0.77	8.41	4.58	0.00000	16.84	27	1.03	11.59
140	0.72	7.56	4.19	0.00000	15.97	22	0.65	11.64
147	0.68	6.61	3.87	0.00000	15.20	22	0.92	11.76
162	0.62	6.75	3.65	0.00000	13.72	19	1.01	11.77
177	1.17	12.57	7.30	0.00005	27.97	16	0.83	11.77
192	0.99	10.91	6.26	0.00004	23.40	15	0.82	11.85
207	0.87	9.69	5.50	0.00004	20.14	14	0.69	11.82

Appendix 4.6 Rate of diffusivity from aged control BFS:OPC CPS in DW

Days	Na^+	Ca^{2+}	Sr^{2+}	Cs^+	Cl^-	SO_4^{2-}	pH
			Rate of diffusivity ($\mu g/cm^2/day$)				
7	16.96	16.32	0.059	0.017	7.04	96.31	11.21
14	10.68	5.14	0.027	0.136	2.48	48.01	11.54
21	7.78	3.91	0.022	0.088	1.33	29.18	11.52
28	5.95	2.85	0.016	0.094	9.99	9.12	11.53
35	4.48	1.78	0.011	0.097	8.62	5.48	11.51
42	4.17	2.45	0.011	0.055	6.41	4.49	11.55
49	3.45	1.09	0.008	0.044	5.01	3.73	11.57
56	2.87	1.20	0.008	0.047	4.99	3.53	11.62
63	2.62	2.39	0.010	0.046	3.97	3.06	11.74
70	1.93	1.18	0.007	0.023	3.18	2.37	11.78
77	1.88	1.65	0.008	0.033	2.58	2.53	11.83
84	1.60	2.19	0.008	0.020	2.26	1.88	11.65
91	1.06	0.89	0.005	0.022	1.94	1.12	10.64
98	0.12	0.25	0.001	0.003	0.45	0.65	11.05
105	0.36	0.81	0.004	0.016	0.34	0.48	11.82
112	0.22	0.12	0.002	0.009	0.41	0.43	11.78
119	0.32	0.47	0.003	0.013	0.30	0.38	11.6
126	0.37	0.49	0.004	0.007	0.63	0.68	11.4
133	0.33	0.66	0.004	0.006	0.33	0.37	11.13
140	0.23	0.59	0.003	0.008	0.78	0.60	10.98
147	0.18	0.49	0.003	0.008	1.16	0.57	10.89
154	0.03	0.41	0.000	0.004	0.90	0.74	10.91
161	0.17	0.45	0.003	0.004	0.83	0.65	10.87
168	0.04	0.16	0.001	0.012	0.76	0.75	11.25
175	0.02	0.05	0.001	0.005	0.42	0.73	11.52
182	0.02	0.09	0.000	0.005	0.30	0.57	11.21
189	0.16	0.20	0.001	0.004	0.09	0.51	11.53

Appendix 4.7 Rate of diffusivity from aged ≈3% SrCl₂ BFS:OPC CPS in DW

Days	Na$^+$	Ca^{2+}	Sr^{2+}	Cl$^-$	SO$_4$$^{2-}$	pH
	Rate of diffusivity (µg/cm^2/day)	
7	28.89	96.08	42.11	468.54	447.09	10.83
14	16.23	55.89	24.04	255.03	230.10	11.21
21	12.67	38.19	18.09	181.27	154.77	11.32
28	9.90	33.57	14.01	132.47	103.69	11.40
35	8.06	25.01	10.88	100.68	81.86	11.43
42	6.88	19.80	8.94	81.36	66.50	11.52
49	5.85	16.34	7.39	67.87	58.90	11.65
56	5.01	13.57	6.22	57.79	40.84	11.62
63	4.25	11.22	5.26	32.11	16.81	11.67
70	3.29	8.82	4.10	40.46	9.52	11.72
77	3.13	8.69	3.97	23.28	5.64	11.79
84	2.81	7.73	3.54	31.68	3.61	11.80
91	2.61	6.78	3.09	24.55	2.47	11.84
98	1.10	4.56	2.11	18.98	0.95	11.89
105	0.91	4.04	1.88	15.96	0.58	11.92
112	0.90	3.72	1.77	13.90	0.38	12.00
119	0.81	3.38	1.58	12.45	0.32	11.96
126	0.75	2.88	1.40	11.01	0.38	11.70
133	0.73	2.98	1.35	9.59	0.27	11.69
140	0.65	2.80	1.24	12.42	0.28	11.75
147	0.58	2.52	1.06	11.40	0.28	11.56
154	0.51	2.03	0.92	9.96	0.32	11.25
161	0.45	1.96	0.84	9.76	0.35	11.30
168	0.57	2.35	0.90	9.87	0.37	10.98
175	0.52	2.38	0.84	9.20	0.34	11.69
182	0.46	2.14	0.75	8.85	0.32	11.21
189	0.65	2.84	0.88	9.30	0.29	11.18

Appendix 4.8 Rate of diffusivity from aged ≈3% CsCl BFS:OPC CPS in DW

Elements	Na^+	Ca^{2+}	Cs^+	Cl^-	SO_4^{2-}	pH
	Rate of diffusivity ($\mu g/cm^2/day$)					
7	27.13	48.37	0.35	457.61	148.51	9.58
14	15.12	24.52	0.15	234.78	79.00	10.39
21	10.83	15.48	0.08	143.56	47.41	10.41
28	8.15	10.84	0.05	107.47	14.51	10.60
35	6.43	7.85	0.04	74.33	9.20	11.28
42	5.35	6.11	0.03	54.21	16.81	11.32
49	4.65	4.95	0.02	40.45	6.38	11.63
56	3.52	3.67	0.01	33.64	10.84	11.65
63	3.46	3.44	0.01	30.87	5.30	11.74
70	3.20	2.85	0.01	28.09	4.52	11.78
77	2.58	2.52	0.01	21.76	35.84	11.99
84	2.20	2.16	0.01	15.84	6.38	11.98
91	2.12	1.89	0.01	11.36	3.17	12.13
98	0.91	1.17	0.01	10.10	8.61	12.16
105	0.76	1.00	0.01	9.67	3.09	12.20
112	0.74	0.86	0.00	8.60	9.45	11.50
119	0.34	0.31	0.00	7.53	8.13	10.49
126	0.71	0.71	0.00	5.20	7.39	11.85
133	0.74	0.71	0.01	4.69	2.87	11.91
140	0.66	0.62	0.01	4.60	2.24	11.87
147	0.58	0.54	0.01	2.87	1.90	11.67
154	0.49	0.44	0.00	2.38	1.69	9.94
161	0.45	0.40	0.00	2.04	1.60	11.53
168	0.53	0.52	0.01	17.55	1.55	10.69
175	0.46	0.47	0.00	16.68	1.47	11.08
182	0.42	0.41	0.00	14.31	1.35	9.98
189	0.61	0.48	0.01	12.25	1.23	9.97

Appendix 4.9 Rate of diffusivity from aged ≈0.3% SrCl₂ BFS:OPC CPS in DW

Days	Na^+	Ca^{2+}	Sr^{2+}	Cl^-	SO_4^{2-}	pH
	Rate of diffusivity (µg/cm²/day)					
7	25.74	9.63	0.56	124.15	34.87	10.15
14	13.42	5.58	0.33	51.94	18.57	10.3
21	10.02	6.95	0.30	34.47	12.43	10.47
28	9.42	5.80	0.26	25.43	9.60	10.51
35	8.69	5.39	0.20	21.08	7.59	10.58
42	8.34	5.21	0.20	18.05	6.33	10.73
49	6.96	5.27	0.18	15.58	5.44	10.99
56	6.02	5.45	0.20	13.68	4.74	11.15
63	5.45	6.00	0.19	12.01	4.23	11.22
70	5.39	5.79	0.22	10.50	3.79	11.29
77	5.11	6.36	0.26	9.37	3.53	11.32
84	4.70	5.89	0.24	8.49	3.24	11.45
91	4.62	6.00	0.27	8.13	3.30	11.56
98	4.47	6.08	0.26	7.55	3.10	11.81
105	4.18	6.10	0.25	7.05	2.89	12.1

Appendix 4.10 Rate of diffusivity from aged ≈0.3% CsCl BFS:OPC CPS in DW

Elements	Na^+	Ca^{2+}	Cs^+	Cl^-	SO_4^{2-}	pH
	Rate of diffusivity (µg/cm²/day)					
7	25.65	3.07	2.49	34.85	29.16	10.22
14	15.60	5.40	2.38	20.95	20.59	10.59
21	11.21	4.41	2.18	13.96	20.82	11.02
28	10.03	3.96	2.09	12.84	16.59	11.44
35	8.82	3.39	1.95	9.01	13.79	11.4
42	7.81	2.88	1.72	9.51	11.07	11.43
49	6.86	2.84	1.46	8.43	8.96	11.62
56	6.35	2.90	1.27	6.79	7.99	11.63
63	6.07	2.71	1.17	6.25	7.41	11.61
70	6.04	2.67	0.97	5.69	6.36	11.66
77	5.76	2.93	0.92	5.18	5.06	11.7
84	5.50	2.65	0.91	4.81	4.46	11.75
91	5.29	2.58	0.82	4.44	3.91	11.78
98	5.24	2.57	0.80	4.10	3.60	11.61
105	5.05	2.47	0.77	3.88	3.41	11.97

Appendix 4.11 Rate of diffusivity from ≈0.3% SrCO₃ BFS:OPC CPS in DW

Days	Na$^+$	Ca^{2+}	Sr^{2+}	Cl$^-$	SO$_4$$^{2-}$	pH
	Rate of diffusivity (µg/cm^2/day)					
7	24.88	2.0456	0.0645	21.16	10.17	11.93
14	15.07	2.2518	0.0499	12.68	5.78	11.99
21	10.13	0.9728	0.0377	6.83	4.25	12.13
28	4.48	1.3644	0.0325	6.39	2.93	12.28
35	3.29	1.3246	0.0285	4.37	2.13	12.27
42	2.78	1.0478	0.0255	3.44	1.64	12.1
49	2.47	1.5342	0.0266	2.82	1.44	12.26
56	1.91	1.3146	0.0228	2.33	1.28	12.25
63	2.77	2.1804	0.0660	2.41	1.01	12.1
70	0.63	2.2724	0.0334	2.22	0.96	12.26
77	1.89	3.7009	0.1092	1.55	0.98	12.39
84	1.73	6.1338	0.0821	1.28	0.85	12.24
91	1.62	5.3652	0.0672	1.15	0.79	11.82
98	1.42	5.7818	0.0641	0.92	0.71	11.79
105	1.29	3.7728	0.0566	0.75	0.61	11.94
112	0.41	1.0416	0.0457	1.05	0.87	12
119	0.08	0.3461	0.0363	0.75	0.68	9.97
126	0.03	0.2379	0.0243	0.75	0.56	9.73
133	0.02	0.0000	0.0210	0.65	0.49	8.56
140	0.01	0.0000	0.0167	0.54	0.48	8.4
147	0.01	0.1590	0.0158	0.80	0.44	8.12
154	0.01	0.0000	0.0130	0.66	0.38	8.23
161	0.68	0.0000	0.0093	1.64	0.26	8.35
168	0.14	0.0000	0.0078	1.19	0.31	8.02
175	0.02	0.0000	0.0060	0.55	0.29	8.94
182	0.01	0.0000	0.0049	0.39	0.34	8.65
189	0.01	0.0000	0.0000	0.40	0.36	8.1
196	0.16	0.0558	0.0022	0.59	0.36	8.35
203	0.26	0.0000	0.0012	0.40	0.35	8.46
210	0.16	0.0338	0.0009	0.29	0.30	8.33

Appendix 4.12 Rate of diffusivity from ≈3% SrCO₃ BFS:OPC CPS in DW

Days	Na⁺	Ca²⁺	Sr²⁺	Cl⁻	SO₄²⁻	pH
	Rate of diffusivity (µg/cm²/day)	
7	25.42	4.78730	0.12	31.25	17.93	11.57
14	15.02	0.91363	0.07	12.75	7.54	12.01
21	5.08	0.34797	0.04	8.79	3.94	12.18
28	3.18	0.17997	0.03	4.60	3.20	12.19
35	4.01	0.45258	0.04	3.16	2.40	12.22
42	3.24	1.00915	0.04	2.34	2.07	11.84
49	2.55	1.09460	0.03	3.69	1.91	12.27
56	2.16	0.94097	0.03	1.70	1.87	12.19
63	1.83	1.30240	0.03	1.31	1.35	12.1
70	2.47	3.50241	0.06	1.09	1.19	11.89
77	2.20	3.59804	0.07	0.96	0.86	10.94
84	0.31	3.40126	0.04	1.22	0.77	9.5
91	0.11	1.31351	0.03	1.28	0.74	9.45
98	0.10	0.46806	0.02	0.99	0.73	8.99
105	0.06	0.32722	0.02	0.99	0.67	8.87
112	0.18	0.16841	0.02	0.96	0.67	8.47
119	0.11	0.10718	0.01	0.82	0.71	8.67
126	0.09	0.08474	0.00	0.83	0.56	8.79
133	0.09	0.00000	0.01	0.73	0.62	8.69
140	0.09	0.00000	0.01	0.83	0.32	8.7
147	0.10	0.05808	0.01	0.79	0.28	8.14
154	0.08	0.00000	0.01	0.75	0.26	7.78
161	0.09	0.00000	0.01	1.69	0.21	7.86
168	0.05	0.00000	0.01	0.73	0.40	7.9
175	0.05	0.00000	0.00	0.53	0.54	8.4
182	0.06	0.00000	0.00	0.62	0.43	8.31
189	0.05	0.00000	0.00	0.63	0.38	8.17
196	0.04	0.04579	0.00	0.80	0.35	8.28
203	0.04	0.00000	0.00	0.44	0.34	8.48
210	0.03	0.03282	0.00	0.49	0.33	8.26

Appendix 4.13 Rate of diffusivity from control BFS:OPC CPS in tap water (open circuit)

Days	Na^+	Ca^{2+}	Sr^{2+}	Cl^-	SO_4^{2-}	pH
	Rate of diffusivity ($\mu g/cm^2/day$)					
4	1.82	3.22	0.018	0.68	29.43	7.28
7	1.60	2.71	0.013	0.20	13.13	7.44
11	0.93	1.65	0.008	0.28	8.04	7.64
14	0.96	1.29	0.008	0.20	8.04	7.63
18	0.65	1.26	0.006	0.02	8.18	7.48
21	0.37	0.68	0.004	0.33	5.40	8.06
25	0.17	0.35	0.003	0.20	4.60	7.1
28	0.26	0.63	0.002	0.30	4.19	7.5
32	0.25	0.63	0.002	0.18	3.94	7.58

Appendix 4.14 Rate of diffusivity from ≈3% SrCl₂ BFS:OPC CPS in tap water (open circuit)

Days	Na^+	Ca^{2+}	Sr^{2+}	Cl^-	SO_4^{2-}	pH
	Rate of diffusivity ($\mu g/cm^2/day$)					
4	2.10	4.60	0.34	1.08	21.60	7.26
7	1.93	3.44	0.12	1.50	17.88	7.49
11	0.93	1.72	0.05	0.75	12.40	7.63
14	0.57	1.08	0.03	0.40	8.69	7.54
18	0.40	0.78	0.03	0.26	5.40	7.28
21	0.54	0.94	0.02	0.42	6.01	7.5
25	0.31	0.59	0.02	0.32	4.63	7.42
28	0.27	1.10	0.02	0.29	4.30	7.38
32	0.26	0.99	0.02	0.26	4.08	7.45

Appendix 4.15 Rate of diffusivity from ≈3% CsCl BFS:OPC CPS in tap water (open circuit)

Days	Na^+	Ca^{2+}	Cs^+	Cl^-	SO_4^{2-}	pH
	Rate of diffusivity ($\mu g/cm^2/day$)					
4	1.74	3.44	4.93	5.41	22.44	7.1
7	1.44	2.43	0.86	1.27	17.03	7.56
11	0.84	1.55	0.32	0.59	12.49	7.67
14	0.44	0.90	0.17	0.32	8.68	7.64
18	0.39	0.65	0.14	0.11	5.15	7.3
21	0.50	0.85	0.13	0.29	5.88	7.65
25	0.29	0.52	0.09	0.25	4.56	7.48
28	0.29	0.86	0.11	0.23	4.18	7.59
32	0.24	0.95	0.10	0.22	4.14	7.58

Appendix 4.16 Rate of diffusivity from ≈3% SrCO₃ BFS:OPC CPS in tap water (open circuit)

Days	Na$^+$	Ca^{2+}	Sr^{2+}	Cl$^-$	SO$_4$$^{2-}$	pH
	Rate of diffusivity (µg/cm^2/day)					
4	1.71	2.98	0.0200	0.69	30.92	7.22
7	1.35	2.25	0.0122	0.29	16.98	7.57
11	1.11	1.73	0.0088	0.31	11.77	7.66
14	0.53	0.99	0.0059	0.20	8.42	7.66
18	0.37	0.60	0.0037	0.02	6.28	7.32
21	0.47	0.80	0.0043	0.27	5.70	7.62
25	0.30	0.54	0.0031	0.22	4.34	7.81
28	0.28	0.62	0.0049	0.24	3.98	7.71
32	0.23	0.53	0.0042	0.18	3.74	7.79

Appendix 4.17 Rate of diffusivity from ≈3% SrCl₂ BFS:OPC CPS in tap water (closed circuit)

Days	Na$^+$	Ca^{2+}	Sr^{2+}	Cl$^-$	SO$_4$$^{2-}$	pH
	Rate of diffusivity (µg/cm^2/day)					
7	34	204	64	1346	35	8.05
14	15	76	27	593	27	7.86
21	9	44	17	357	17	7.88
28	7	31	12	254	12	7.89
35	5	23	9	186	9	7.91
42	4	19	8	154	8	7.93

Appendix 5.1 Rate of diffusivity from control PFA:OPC CPS in DW

Days	Na$^+$	Ca^{2+}	Sr^{2+}	Cs$^+$	Cl$^-$	SO$_4^{2-}$	pH
	Rate of diffusivity (µg/cm^2/day)						
7	58.48	3.06	0.0353	0.0373	11.83	93.18	12.13
14	33.22	1.66	0.0292	0.0422	6.67	52.86	12.12
21	22.56	1.33	0.0169	0.0360	4.33	32.53	12.09
28	19.33	0.66	0.0312	0.0442	4.40	27.30	12.05
35	15.26	0.53	0.0116	0.0415	2.62	20.04	11.99
42	10.59	0.49	0.0025	0.0197	2.28	16.97	12.02
49	7.91	0.42	0.0021	0.0468	1.92	14.05	11.98

Appendix 5.2 Rate of diffusivity from ≈3% SrCl$_2$ PFA:OPC CPS in DW

Days	Na$^+$	Ca^{2+}	Sr^{2+}	Cl$^-$	SO$_4^{2-}$	pH
	Rate of diffusivity (µg/cm^2/day)					
7	170.4	525.5	359	3650	39.7	7.47
14	92.5	280.3	199	1874	18.0	7.53
21	58.7	177.2	129	1267	12.1	7.95
28	47.5	140.5	103	897	8.8	7.57
35	30.3	88.1	64	586	6.1	8.69
42	22.7	65.8	47	479	5.3	8.51
49	17.1	49.3	35	368	4.5	8.32

Appendix 5.3 Rate of diffusivity from ≈3% CsCl PFA:OPC CPS in DW

Days	Na$^+$	Ca^{2+}	Cs$^+$	Cl$^-$	SO$_4^{2-}$	pH
	Rate of diffusivity (µg/cm^2/day)					
7	46.8	5.8	954	622	97.2	12.02
14	26.7	0.8	508	330	50.1	11.94
21	22.2	0.9	380	227	33.4	11.99
28	16.9	1.3	273	190	20.6	12.02
35	11.5	0.8	183	139	14.8	11.98
42	9.1	0.8	140	111	11.6	11.95
49	7.7	0.7	106	84	8.6	11.99

Appendix 5.4 Rate of diffusivity from ≈3% SrCO₃ PFA:OPC CPS in DW

Days	Na^+	Ca^{2+}	Sr^{2+}	Cl^-	SO_4^{2-}	pH
	Rate of diffusivity (µg/cm²/day)	
7	45.4	1.6	0.09	10.5	80.4	12.00
14	27.5	0.8	0.05	6.5	44.6	11.99
21	21.6	1.3	0.04	4.3	29.8	12.02
28	16.2	0.7	0.03	7.1	26.0	11.99
35	11.1	0.3	0.02	2.8	16.6	12.01
42	8.5	0.2	0.01	8.7	12.6	12.02
49	7.2	0.3	0.01	1.6	6.6	11.99

Appendix 5.5 Rate of diffusivity from ≈0.3% SrCl₂ PFA:OPC CPS in DW

Days	Na^+	Ca^{2+}	Sr^{2+}	Cl^-	SO_4^{2-}	pH
	Rate of diffusivity (µg/cm²/day)	
7	60	3.20	1.53	204	44	11.44
14	35	9.10	2.44	111	67	11.53
21	21	3.48	1.29	65	21	10.96
28	13	1.76	0.66	45	34	11.35
35	9	1.15	0.41	29	20	11.05
42	8	0.86	0.32	23	16	11.02
49	6	0.70	0.27	19	13	10.58

Appendix 5.6 Rate of diffusivity from ≈0.3% CsCl PFA:OPC CPS in DW

Days	Na^+	Ca^{2+}	Cs^+	Cl^-	SO_4^{2-}	pH
	Rate of diffusivity (µg/cm²/day)	
7	53	0.45	54	78	91	11.75
14	31	0.19	33	49	54	11.56
21	22	0.13	22	34	38	11.62
28	15	0.11	15	23	29	11.51
35	12	0.08	12	17	22	11.35
42	9	0.68	9	14	17	11.38
49	8	0.05	7	10	14	11.31

Appendix 5.7 Rate of diffusivity from control PFA:OPC CPS in tap water (open circuit)

Days	Na$^+$	Ca^{2+}	Sr^{2+}	Cl$^-$	SO$_4^{2-}$	pH
	Rate of diffusivity (μg/cm^2/day)	
4	3.79	5.94	0.020	1.40	9.02	8.08
7	1.28	1.42	0.006	0.46	2.28	7.81
11	0.40	0.47	0.003	0.25	0.71	7.78
14	0.29	0.33	0.002	1.25	0.53	7.72
18	0.77	0.85	0.003	0.53	2.25	7.81
21	0.58	0.64	0.002	0.56	2.08	7.87
25	0.66	0.72	0.003	0.65	2.45	7.85
28	0.66	0.75	0.003	0.72	2.82	7.93
32	0.03	0.14	0.001	0.10	0.12	7.63

Appendix 5.8 Rate of diffusivity from ≈3% SrCl$_2$ PFA:OPC CPS in tap water (open circuit)

Days	Na$^+$	Ca^{2+}	Sr^{2+}	Cl$^-$	SO$_4^{2-}$	pH
	Rate of diffusivity (μg/cm^2/day)	
4	4.44	10.76	2.15	30.76	11.21	7.87
7	1.63	2.59	0.79	8.65	3.84	7.81
11	0.40	0.59	0.20	1.32	0.96	7.8
14	0.29	0.40	0.13	0.80	0.62	7.75
18	0.89	1.06	0.10	1.02	2.66	7.85
21	0.57	0.67	0.07	0.85	2.13	7.82
25	0.65	0.77	0.09	1.06	2.51	7.79
28	0.66	0.80	0.07	0.87	2.81	7.82
32	0.02	0.15	0.05	0.30	0.10	7.56

Appendix 5.9 Rate of diffusivity from ≈3% CsCl PFA:OPC CPS in tap water (open circuit)

Days	Na$^+$	Ca^{2+}	Cs$^+$	Cl$^-$	SO$_4^{2-}$	pH
	Rate of diffusivity (µg/cm^2/day)	
4	3.75	5.77	11.42	9.75	10.52	7.97
7	1.44	1.70	2.76	2.27	3.54	7.91
11	0.42	0.48	0.64	0.69	0.99	7.85
14	0.28	0.31	0.34	1.96	0.32	7.63
18	0.75	0.82	0.18	0.86	2.79	7.75
21	0.58	0.62	0.12	0.48	2.22	7.83
25	0.65	0.70	0.14	0.77	2.23	7.82
28	0.67	0.77	0.11	0.87	2.81	7.87
32	0.02	0.12	0.07	0.10	0.12	7.62

Appendix 5.10 Rate of diffusivity from ≈3% SrCO$_3$ PFA:OPC CPS in tap water (open circuit)

Days	Na$^+$	Ca^{2+}	Sr^{2+}	Cl$^-$	SO$_4^{2-}$	pH
	Rate of diffusivity (µg/cm^2/day)	
4	4.12	5.98	0.0243	2.86	11.71	8.03
7	1.63	1.64	0.0092	0.75	3.42	7.69
11	0.43	0.55	0.0038	0.72	1.10	7.72
14	0.32	0.35	0.0026	0.63	0.71	7.7
18	0.77	0.83	0.0036	0.88	2.76	7.71
21	0.61	0.64	0.0028	0.75	2.18	7.73
25	0.67	0.72	0.0031	0.75	2.57	7.79
28	0.67	0.77	0.0032	0.94	2.83	7.82
32	0.03	0.13	0.0010	0.17	0.26	7.7

Appendix 6.1 Rate of diffusivity from control BFS:OPC CPS in CSPW

Days	Na^+	Ca^{2+}	Sr^{2+}	Cs^+	Cl^-	SO_4^{2-}	pH
	Rate of diffusivity ($\mu g/cm^2/day$)						
7	54681	469.31	2.21	0.27	264.76	12909	8.44
14	30657	246.13	1.45	0.49	146.63	9454	7.65
21	22082	183.37	1.20	1.11	78.47	5792	8.94
28	16268	142.27	0.89	0.89	90.56	4483	8.49
35	12853	118.86	0.68	0.80	65.82	3434	8.18
42	10901	116.09	0.57	1.21	53.49	3141	7.75
49	9121	80.89	0.46	0.52	53.94	3165	7.91
56	8002	62.72	0.38	0.43	48.76	3093	8.21
63	7600	64.27	0.34	0.37	13.86	2742	8.31
70	6970	47.38	0.30	0.44	12.00	2548	8.14
77	6351	49.75	0.27	0.23	14.42	1137	8.16
84	6216	52.04	0.27	0.28	8.94	2168	8.18
91	5546	50.93	0.22	0.26	12.19	2151	8.21
98	5235	46.33	0.20	0.20	14.99	1989	8.25
105	4908	34.89	0.17	0.54	13.26	1903	8.19

Appendix 6.2 Rate of diffusivity from control BFS:OPC CPS in DSPW

Days	Na^+	Ca^{2+}	Sr^{2+}	Cs^+	Cl^-	SO_4^{2-}	pH
	Rate of diffusivity ($\mu g/cm^2/day$)						
7	2.68	1.28	0.0298	0.0718	38.20	58.95	9.79
14	1.06	0.45	0.0181	0.0268	30.49	37.43	9.71
21	0.97	0.18	0.0112	0.0139	20.92	29.65	11
28	0.89	0.03	0.0087	0.0168	15.29	21.88	10.89
35	0.10	0.05	0.0076	0.0135	12.08	16.20	11.33
42	0.19	0.13	0.0064	0.0089	9.91	12.19	11.39
49	0.20	0.11	0.0056	0.0079	8.51	10.07	11.57
56	0.16	0.09	0.0048	0.0119	7.39	7.61	11.69
63	0.19	0.10	0.0044	0.0104	6.74	9.87	11.79
70	0.12	0.04	0.0053	0.0050	5.91	8.65	11.61
77	0.08	0.02	0.0037	0.0033	5.18	7.73	11.59
84	0.07	0.06	0.0040	0.0024	4.83	6.38	11.65
91	0.07	0.06	0.0034	0.0050	4.34	5.50	11.39
98	0.06	0.06	0.0022	0.0017	3.92	4.59	11.26
105	0.06	0.04	0.0204	0.0075	3.59	4.08	11.35

Appendix 6.3 Rate of diffusivity from ≈3% SrCl₂ BFS:OPC CPS in CSPW

Days	Na⁺	Ca²⁺	Sr²⁺	Cl⁻	SO₄²⁻	pH
	Rate of diffusivity (µg/cm²/day)		
7	53773	544.16	102.77	213.40	15994	7.77
14	29852	304.65	57.08	138.50	11365	8.31
21	22660	223.14	45.09	69.35	10950	8.24
28	16818	164.08	33.40	57.52	8440	7.63
35	13813	149.54	26.22	18.61	5677	8.09
42	11709	135.68	21.17	39.83	5340	7.58
49	9344	106.53	15.99	52.33	5109	7.69
56	8273	80.58	13.20	38.99	4600	7.89
63	6640	64.52	10.17	41.64	4290	7.93
70	7524	67.14	10.79	75.74	4214	7.99
77	7500	67.54	10.05	65.97	3704	8.75
84	6658	63.76	8.25	61.80	3535	8.67
91	6036	61.23	7.55	54.84	3301	8.79
98	5703	52.40	6.78	51.45	3099	8.89
105	5349	44.75	6.17	50.17	2864	8.75

Appendix 6.4 Rate of diffusivity from ≈3% SrCl₂ BFS:OPC CPS in DSPW

Days	Na⁺	Ca²⁺	Sr²⁺	Cl⁻	SO₄²⁻	pH
	Rate of diffusivity (µg/cm²/day)		
7	1.69	27.87	16.34	662.69	35.68	8.73
14	1.24	13.08	9.72	406.63	21.95	9.68
21	1.26	9.20	7.45	301.49	18.06	10.39
28	1.05	7.78	5.85	235.09	12.56	10.25
35	1.11	7.45	4.99	180.41	8.24	10.35
42	0.55	5.11	3.52	148.25	6.68	10.46
49	0.72	4.84	3.32	126.05	7.41	11.13
56	0.50	3.53	2.66	109.90	7.01	11.2
63	0.38	2.79	2.20	98.00	6.27	8.91
70	0.24	1.97	1.77	82.31	5.37	8.71
77	0.36	2.25	1.82	72.07	4.36	8.6
84	0.20	1.54	1.45	66.60	3.71	8
91	0.04	1.01	1.14	61.14	3.36	8.1
98	0.04	0.52	0.81	56.07	2.83	8.1
105	0.04	0.52	0.79	51.31	4.08	9.14

Appendix 6.5 Rate of diffusivity from ≈3% CsCl BFS:OPC CPS in CSPW

Days	Na^+	Ca^{2+}	Cs^+	Cl^-	SO_4^{2-}	pH
			Rate of diffusivity ($\mu g/cm^2/day$)			
14	29748	130.12	1378.40	63.09	7753	8.59
21	21508	168.88	1608.00	109.52	9511	8.34
28	17682	178.21	1307.02	104.55	6878	7.66
35	14405	162.38	1026.60	108.53	6139	7.75
42	12232	121.61	790.58	111.73	5868	7.83
49	9491	88.19	565.86	97.72	5412	7.86
56	9052	73.36	477.49	75.19	5128	7.78
63	7977	65.90	380.38	68.39	4200	7.64
70	7758	56.47	328.62	63.61	4011	7.72
77	7146	50.56	271.01	58.65	3852	7.78
84	6599	54.75	232.96	53.30	3380	7.65
91	5892	51.98	191.94	48.56	3141	7.75
98	5528	46.03	163.41	44.15	2970	7.85
105	5262	39.16	140.30	37.68	2807	7.81

Appendix 6.6 Rate of diffusivity from ≈3% CsCl BFS:OPC CPS in DSPW

Days	Na^+	Ca^{2+}	Cs^+	Cl^-	SO_4^{2-}	pH
			Rate of diffusivity ($\mu g/cm^2/day$)			
7	1.69	27.87	199.46	662.69	35.68	10.87
14	0.96	8.24	104.34	325.05	53.59	8.36
21	0.62	3.13	65.93	220.77	44.36	8.78
28	0.46	1.11	22.23	173.20	35.04	9.25
35	0.59	1.10	38.58	149.22	28.86	9.97
42	0.52	1.84	22.95	129.78	24.54	9.89
49	0.48	3.77	17.77	112.98	21.17	9.85
56	0.21	3.62	16.42	99.66	14.16	9.87
63	0.18	3.01	13.18	87.93	12.21	7.10
70	0.12	2.30	10.54	75.43	10.83	7.80
77	0.11	1.94	9.89	67.22	9.92	7.90
84	0.09	1.71	8.30	61.25	9.02	7.54
91	0.06	1.53	6.64	56.14	8.05	7.79
98	0.05	1.23	5.82	49.34	7.05	7.74
105	0.05	1.27	3.85	46.34	4.08	8.57

Appendix 6.7 Rate of diffusivity from ≈3% SrCO₃ BFS:OPC CPS in CSPW

Days	Na$^+$	Ca^{2+}	Sr^{2+}	Cl$^-$	SO$_4^{2-}$	pH
			Rate of diffusivity (µg/cm^2/day)			
7	10939	148.09	6.88	12713	24.14	7.55
14	6578	71.73	3.67	11355	26.22	7.62
21	4301	44.61	2.35	6670	16.98	7.79
28	3290	32.10	1.73	5272	13.82	7.81
35	2618	23.48	1.36	5145	11.76	7.92
42	1929	17.25	1.12	4811	13.86	8.65
49	1554	12.53	0.92	4291	9.83	8.78
56	1149	11.31	0.79	4387	19.86	9.3
63	906	9.04	0.69	3661	26.05	9.45
70	765	7.53	0.60	3384	15.15	9.64
77	626	6.57	0.54	3752	4.98	9.75
84	544	5.37	0.48	3626	19.27	9.72
91	484	4.58	0.43	3473	21.58	9.71
98	431	3.86	0.38	3338	23.87	9.83
105	386	3.23	0.34	3250	23.88	9.82

Appendix 6.8 Rate of diffusivity from ≈3% SrCO₃ BFS:OPC CPS in DSPW

Days	Na$^+$	Ca^{2+}	Sr^{2+}	Cl$^-$	SO$_4^{2-}$	pH
			Rate of diffusivity (µg/cm^2/day)			
7	2.79	18.55	0.08	33.77	50.38	10.02
14	3.48	7.13	0.07	23.10	29.89	10.89
21	3.97	9.11	0.06	15.08	22.62	10.95
28	3.55	6.89	0.05	9.83	16.54	11.68
35	3.36	5.63	0.04	8.46	13.19	11.81
42	3.27	4.25	0.03	7.05	10.73	11.86
49	2.92	3.58	0.02	6.13	9.60	11.89
56	2.43	2.85	0.02	5.32	8.26	11.92
63	2.81	2.35	0.02	4.86	7.43	11.91
70	3.07	2.12	0.02	4.13	6.34	11.89
77	2.68	1.89	0.01	3.82	7.51	11.93
84	2.78	1.74	0.01	3.52	7.90	11.95
91	2.63	1.72	0.01	2.99	9.25	11.95
98	2.47	1.47	0.01	2.86	6.40	11.94
105	2.34	1.21	0.01	2.71	4.95	11.95

Appendix 6.9 Rate of diffusivity from ≈0.3% SrCl₂ BFS:OPC CPS in CSPW

Days	Na$^+$	Ca^{2+}	Sr^{2+}	Cl$^-$	SO$_4^{2-}$	pH
	Rate of diffusivity (µg/cm^2/day)	
7	11605	92.39	11.02	9266	6.94	7.16
14	6291	48.04	6.17	9855	19.78	7.26
21	5200	22.77	4.47	12245	15.18	7.3
28	4385	16.19	2.93	6228	15.67	7.5
35	3704	9.18	2.42	4969	9.47	8.12
42	2927	4.63	2.00	4681	14.30	8.8
49	3050	2.76	1.73	4828	13.16	9.2
56	2318	2.22	1.21	4398	17.57	9.4
63	2183	10.96	1.05	3931	20.41	9.3
70	1937	8.74	1.32	3616	20.75	9.25
77	1800	7.35	1.13	3338	17.20	9.35
84	1401	5.58	1.01	2943	9.02	9.15
91	1217	3.87	0.83	2683	10.76	9.61
98	1090	2.92	0.70	2474	12.94	9.75
105	972	1.11	0.59	2286	14.27	9.6

Appendix 6.10 Rate of diffusivity from ≈0.3% SrCl₂ BFS:OPC CPS in DSPW

Days	Na$^+$	Ca^{2+}	Sr^{2+}	Cl$^-$	SO$_4^{2-}$	pH
	Rate of diffusivity (µg/cm^2/day)	
7	2.30	36.82	1.81	113.63	27.26	7.5
14	0.98	9.21	0.50	63.45	16.73	7.74
21	0.83	4.97	0.30	43.79	11.54	8.96
28	1.01	3.53	0.23	35.18	8.22	10.47
35	0.92	2.76	0.18	28.90	6.72	10.5
42	1.14	2.31	0.15	20.28	5.44	10.51
49	1.00	1.94	0.13	15.63	4.76	10.78
56	0.92	1.67	0.12	13.02	4.21	11.63
63	0.83	1.47	0.11	11.39	3.81	11.75
70	0.71	1.30	0.10	10.34	3.50	11.84
77	0.69	1.16	0.03	9.09	3.21	11.9
84	0.57	0.90	0.09	8.46	2.93	11.96
91	0.52	0.79	0.10	7.88	2.72	11.95
98	0.49	0.73	0.10	7.14	2.46	11.94
105	0.43	0.65	0.09	6.18	2.30	11.85

Appendix 6.11 Rate of diffusivity from ≈0.3% CsCl BFS:OPC CPS in CSPW

Days	Na$^+$	Ca^{2+}	Cs$^+$	Cl$^-$	SO$_4^{2-}$	pH
			Rate of diffusivity (µg/cm^2/day)			
7	11599	41.14	373	11418	224.97	7.18
14	6582	32.40	198	9655	219.27	7.2
21	4281	13.25	128	5331	95.70	7.46
28	3229	7.85	95	4555	104.12	7.47
35	2406	4.41	77	4209	84.67	7.52
42	2293	2.82	61	4878	73.95	7.56
49	1876	2.06	50	4038	56.57	8.12
56	1803	1.15	40	3665	4.94	8.25
63	1541	5.00	33	3423	17.08	8.53
70	1295	4.19	27	4130	29.42	8.52
77	1125	3.46	23	3858	41.69	8.55
84	1023	3.13	18	3829	46.58	8.61
91	917	2.85	16	3592	47.68	8.65
98	821	1.75	13	3407	46.60	8.8
105	711	1.55	9	3251	53.25	9.05

Appendix 6.12 Rate of diffusivity from ≈0.3% CsCl BFS:OPC CPS in DSPW

Days	Na$^+$	Ca^{2+}	Cs$^+$	Cl$^-$	SO$_4^{2-}$	pH
			Rate of diffusivity (µg/cm^2/day)			
7	2.75	9.11	3.30	64.50	26.83	7.77
14	1.68	5.14	2.48	34.13	17.99	8.03
21	1.83	3.42	1.87	22.26	13.62	8.73
28	1.66	2.57	1.44	15.82	11.35	8.96
35	1.42	4.29	1.83	12.36	10.22	9.56
42	1.26	4.24	1.86	10.05	11.50	10.82
49	1.26	4.49	1.85	8.24	11.00	10.96
56	1.24	4.28	1.64	6.88	14.18	11.66
63	1.21	3.99	1.52	5.82	15.55	11.68
70	1.13	4.28	1.52	5.00	14.66	11.77
77	1.08	3.95	1.45	4.27	13.20	11.82
84	1.09	4.04	1.43	3.81	13.23	11.96
91	1.08	3.75	1.31	3.40	11.66	11.98
98	0.94	3.72	1.23	3.13	10.53	12.01
105	0.89	3.25	1.11	2.65	9.34	11.95

Appendix 6.13 Rate of diffusivity from ≈0.3%SrCO3 BFS:OPC CPS in CSPW

Days	Na^+	Ca^{2+}	Sr^{2+}	Cl^-	SO_4^{2-}	pH
			Rate of diffusivity ($\mu g/cm^2/day$)			
7	11581	8.88	1.01	13560	675.25	7.1
14	6631	5.87	0.72	11378	338.85	7.25
21	4302	3.39	0.54	7371	235.04	7.31
28	3207	2.33	0.40	5385	176.08	7.65
35	2556	2.10	0.30	5015	139.87	7.95
42	2049	1.79	0.24	5301	122.27	9.85
49	1617	1.93	0.20	4692	88.27	9.69
56	1456	1.22	0.17	4413	54.52	9.35
63	1275	1.00	0.14	4143	32.87	9.07
70	1095	1.41	0.12	4020	16.27	8.92
77	942	0.39	0.10	4068	48.06	8.19
84	837	0.20	0.08	3979	62.38	8.66
91	744	0.68	0.08	3772	60.51	8.68
98	626	0.51	0.07	3644	59.63	8.59
105	520	0.14	0.06	3733	61.56	8.52

Appendix 6.14 Rate of diffusivity from ≈0.3%SrCO3 BFS:OPC CPS in DSPW

Days	Na^+	Ca^{2+}	Sr^{2+}	Cl^-	SO_4^{2-}	pH
			Rate of diffusivity ($\mu g/cm^2/day$)			
7	2.59	3.80	0.041	30.24	25.64	9.05
14	1.17	3.44	0.035	19.71	16.21	10.64
21	1.81	2.98	0.034	12.41	11.60	10.85
28	1.38	2.54	0.030	8.71	8.14	11.64
35	1.16	1.63	0.024	7.20	6.45	11.71
42	1.03	1.26	0.019	5.80	5.21	11.79
49	0.95	0.83	0.013	5.09	4.46	11.82
56	1.08	0.43	0.010	4.48	3.83	11.83
63	0.84	0.46	0.010	3.97	3.62	11.79
70	0.79	0.49	0.010	3.47	3.14	11.71
77	0.75	0.44	0.009	3.17	3.68	11.78
84	0.63	0.39	0.008	2.90	3.98	11.95
91	0.61	0.37	0.007	2.66	3.87	11.92
98	0.52	0.35	0.008	2.46	2.68	11.75
105	0.48	0.14	0.006	2.30	2.27	11.78

Appendix 7.1 Rate of diffusivity from control PFA:OPC CPS in CSPW

Days	Na$^+$	Ca^{2+}	Sr^{2+}	Cs$^+$	Cl$^-$	SO$_4{}^{2-}$	pH
			Rate of diffusivity (µg/cm^2/day)				
7	26	31.73	0.69	0.52	18001	124	7.81
14	11	15.50	0.28	0.35	11448	59	7.69
21	7	9.16	0.17	0.19	7690	44	8.18
28	5	6.79	0.12	0.18	3996	30	7.80
35	5	5.26	0.09	0.14	2508	25	9.10

Appendix 7.2 Rate of diffusivity from ≈3%SrCl$_2$ PFA:OPC CPS in CSPW

Days	Na$^+$	Ca^{2+}	Sr^{2+}	Cl$^-$	SO$_4{}^{2-}$	pH
			Rate of diffusivity (µg/cm^2/day)			
7	16	216	69	16536	45	7.41
14	9	161	46	16508	23	7.43
21	7	114	31	12422	14	7.52
28	5	57	17	9351	11	7.54
35	5	29	11	7336	9	7.51

Appendix 7.3 Rate of diffusivity from ≈3%CsCl PFA:OPC CPS in CSPW

Days	Na$^+$	Ca^{2+}	Cs$^+$	Cl$^-$	SO$_4{}^{2-}$	pH
			Rate of diffusivity (µg/cm^2/day)			
7	24	52	1138	18386	308	8.44
14	11	38	674	14100	158	8.14
21	7	14	345	11832	105	10.30
28	5	12	236	7017	77	10.27
35	4	14	186	4073	50	10.56

Appendix 7.4 Rate of diffusivity from ≈3%SrCO$_3$ PFA:OPC CPS in CSPW

Days	Na$^+$	Ca^{2+}	Sr^{2+}	Cl$^-$	SO$_4{}^{2-}$	pH
			Rate of diffusivity (µg/cm^2/day)			
7	28	23	3	15194	243	8.31
14	15	23	2	13656	135	9.71
21	9	15	1	11069	87	9.53
28	7	11	1	4219	77	10.00
35	5	8	1	4739	64	11.35

Appendix 8.1 Rate of diffusivity from control BFS:OPC CPS in JISS

Days	Na$^+$	Ca^{2+}	Sr^{2+}	Cs$^+$	Cl$^-$	SO$_4{}^{2-}$	pH
	Rate of diffusivity (μg/cm^2/day)						
7	16.95	16.57	0.0517	0.0034	10.96	70.34	10.74
14	9.77	11.60	0.0409	0.0258	6.14	53.42	10.86
21	7.07	7.90	0.0316	0.0152	3.79	39.41	10.99
28	5.30	5.95	0.0259	0.0144	2.67	31.41	11.02
35	4.88	5.60	0.0277	0.1343	2.20	24.38	10.89
42	3.74	4.42	0.0219	0.0124	2.07	18.83	10.73
49	2.85	3.26	0.0181	0.0005	1.35	15.41	11.20

Appendix 8.2 Rate of diffusivity from ≈3%SrCl$_2$ BFS:OPC CPS in JISS

Days	Na$^+$	Ca^{2+}	Sr^{2+}	Cl$^-$	SO$_4{}^{2-}$	pH
	Rate of diffusivity (μg/cm^2/day)					
7	32.32	141.26	38.96	598	48.36	7.42
14	21.63	94.05	27.96	334	28.58	7.29
21	14.38	61.44	19.23	223	19.73	7.70
28	10.17	42.10	13.80	163	14.72	7.60
35	7.72	34.35	12.52	222	10.41	7.90
42	6.83	29.31	10.30	196	9.07	8.09
49	4.91	20.48	7.69	156	7.18	7.70

Appendix 8.3 Rate of diffusivity from ≈3%CsCl BFS:OPC CPS in JISS

Days	Na$^+$	Ca^{2+}	Cs$^+$	Cl$^-$	SO$_4{}^{2-}$	pH
	Rate of diffusivity (μg/cm^2/day)					
7	24.70	95.75	495	558	191.83	7.11
14	16.01	57.80	296	274	98.10	6.77
21	7.37	10.62	188	169	75.63	7.20
28	7.33	21.52	130	106	61.19	7.56
35	5.79	17.93	100	132	38.82	7.80
42	4.59	12.23	73	119	33.94	7.87
49	3.63	8.70	58	85	24.75	7.58

Appendix 8.4 Rate of diffusivity from ≈3%SrCO$_3$ BFS:OPC CPS in JISS

Days	Na$^+$	Ca^{2+}	Sr^{2+}	Cl$^-$	SO$_4{}^{2-}$	pH
	Rate of diffusivity (μg/cm^2/day)					
7	16.8	49.0	1.43	9.8	317.7	7.53
14	10.2	31.3	1.34	5.2	181.6	7.66
21	7.8	17.9	0.90	3.2	109.6	7.70
28	5.3	11.2	0.65	2.3	69.6	7.78
35	5.3	8.6	0.60	7.5	45.3	7.83
42	3.5	5.9	0.45	3.1	36.2	7.93
49	2.8	4.4	0.36	2.3	26.3	7.67

Appendix 9.1 Rate of diffusivity from control PFA:OPC CPS in JISS

Days	Na⁺	Ca²⁺	Sr²⁺	Cs⁺	Cl⁻	SO₄²⁻	pH
			Rate of diffusivity (µg/cm²/day)				
7	52.47	5.61	0.033	0.050	18.66	118.21	12.15
14	32.24	2.53	0.022	0.018	10.04	64.32	12.24
21	23.11	2.12	0.017	0.013	6.10	44.90	12.23
28	16.58	1.52	0.012	0.020	5.56	35.00	12.27
35	13.63	1.44	0.013	0.018	3.67	29.02	12.25
42	11.27	1.17	0.015	0.017	3.10	23.83	12.16
49	9.07	0.97	0.009	0.012	2.43	18.13	12.11

Appendix 9.2 Rate of diffusivity from ≈3%SrCl₂ PFA:OPC CPS in JISS

Days	Na⁺	Ca²⁺	Sr²⁺	Cl⁻	SO₄²⁻	pH
			Rate of diffusivity (µg/cm²/day)			
7	129.2	420	240	4024	37.9	8.07
14	74.3	247	163	2348	21.4	8.38
21	55.0	179	124	1536	14.9	8.35
28	37.3	123	87	1100	11.0	8.29
35	26.8	88	63	780	8.1	8.41
42	20.8	66	48	591	6.4	8.42
49	18.3	52	38	89	5.1	8.47

Appendix 9.3 Rate of diffusivity from ≈3%CsCl PFA:OPC CPS in JISS

Days	Na⁺	Ca²⁺	Cs⁺	Cl⁻	SO₄²⁻	pH
			Rate of diffusivity (µg/cm²/day)			
7	45.7	12.0	861	1064	153.3	11.63
14	30.5	5.1	528	597	90.5	11.85
21	21.2	2.9	346	388	58.7	11.99
28	16.7	2.1	259	273	41.7	11.98
35	10.8	1.2	163	163	22.3	11.92
42	6.4	0.4	94	83	11.4	11.84
49	4.3	0.2	58	49	7.1	11.74

Appendix 9.4 Rate of diffusivity from ≈3%SrCO₃ PFA:OPC CPS in JISS

Days	Na⁺	Ca²⁺	Sr²⁺	Cl⁻	SO₄²⁻	pH
			Rate of diffusivity (µg/cm²/day)			
7	61.4	4.1	0.09	15.6	149.2	12.16
14	40.0	0.9	0.05	8.5	88.5	12.12
21	25.3	0.5	0.03	5.9	54.5	12.19
28	20.8	0.2	0.02	4.4	37.5	12.14
35	14.1	0.3	0.02	3.6	27.0	12.11
42	6.8	0.3	0.01	2.7	20.5	12.05
49	7.6	0.3	0.01	2.1	16.4	11.99